Untersuchungen zur Entwicklung von agpaitischen Gesteinen in der Gardar Provinz in Südgrönland

DISSERTATION

zur Erlangung des Grades eines Doktors der Naturwissenschaften

der Fakultät für Geowissenschaften
der Eberhard-Karls-Universität Tübingen

vorgelegt von
JOHANNES SCHÖNENBERGER
aus Überlingen

2008

Tag der mündlichen Prüfung: 20. Oktober 2008

Dekan: Prof. Dr. Peter Grathwohl

1. Berichterstatter: Prof. Dr. Gregor Markl

2. Berichterstatter: Prof. Dr. Wolfgang Siebel

INHALTSVERZEICHNIS

Danksagung

Gregor Markl möchte ich sehr herzlich für die Ermöglichung dieses Projektes, seiner Betreuung und kontinuierlichen Unterstützung danken. Wolfgang Siebel danke ich für die Übernahme des Zweit-Gutachtens dieser Arbeit.

Für die Unterstützung bei diversen geochemischen Untersuchungen danke ich Gabi Stoschek, Bernd Steinhilber und Elmar Reitter, die – zusammen mit Gerlind Dreibus – mit Rat und Tat beim Aufbau der Pyrohydrolyse-Anlage zur Seite standen. Barbara Meier und Norbert Walker waren bei allen denkbaren technischen Fragen stets eine große Hilfe. Ein besonderer Dank geht auch an Daniel Russ für seine Unterstützung und neuen Ideen bei jeglichen Problemen. Indra Gill-Kopp danke ich für die zügige und exzellente Präparation der untersuchten Proben. Helene Brätz gab sich viel Mühe mit den La-ICP-MS Messungen. Heiner Taubald danke ich für die Durchführung der RFA-Analysen. Die Diskussionen der Isotopenergebnisse mit Heiner Taubald und Wolfgang Siebel waren sehr hilfreich.
Gregor Markl, Adrian Finch, Ian Parsons, Julian Schilling, Jamie McCreath und Ashlyn Armour-Brown danke ich für die angenehme Zeit und Unterstützung im Gelände. Ferner möchte ich mich bei Verena Krasz für die Aufbereitung der Mineralseparate und ihre Unterstützung bei den Ionenchromatographie Messungen bedanken. An dieser Stelle seien auch Jasmin Köhler, Gabi Stoschek und Daniel Russ für die gute Zusammenarbeit bei der Perfektionierung der Ionenchromatographie-Anlage gedankt.

Bei Adrian Finch, Brian Upton und Ian Parsons möchte ich mich für viele fruchtbare Diskussionen während des Schottlandaufenthalts bedanken. Außerdem danke ich Thomas Wenzel für die Unterstützung während der Mikrosondenmessungen und die gute Zusammenarbeit. Auch Thomas Wagner hatte stets ein offenes Ohr für fachliche Diskussionen. Besonderer Dank geht an dieser Stelle auch an Frau Dagmar Dimitrovice und an die Kollegen der Arbeitsgruppe Petrologie.

Jasmin Köhler danke ich für ihre kontinuierliche Unterstützung, die vielen Diskussionen und die sehr gute Zusammenarbeit, die auch zum Gelingen dieser Arbeit beigetragen haben. Bei meinen Eltern Horst und Katja Schönenberger bedanke ich mich für ihre Unterstützung und ihr stetes, auch fachliches Interesse an dieser Arbeit.

Der Deutschen Forschungsgemeinschaft danke ich für die Finanzierung dieses Projekts sowie Angus & Ross Ltd. für die finanzielle Unterstützung der beiden Geländeaufenthalte in Grönland.

Zusammenfassung

Agpaite sind peralkaline Gesteine, die komplexe Na-Ti-Zr-Silikate wie Eudialyt anstelle von Fe-Ti-Oxiden und Zirkon enthalten, und in denen Halogene sowie Spurenelemente (HFSE, SEE) stark angereichert sind. Allerdings sind ihre genauen Bildungsprozesse noch nicht vollständig verstanden. Die 1,3 bis 1,1 Ga alte Gardar Provinz in Südgrönland eignet sich hervorragend für die Untersuchung der Agpaitbildung, da sich hier nicht nur die Typlokalität für Agpaite (Ilímaussaq Intrusion), sondern auch die miaskitische Motzfeldt Intrusion befindet, in der nur ein kleiner Teil Agpaite kristallisierte. Der Übergang von „normalen" miaskitischen zu agpaitischen Gesteinen wurde daher am Beispiel der Motzfeldt Intrusion untersucht. Eine zweite Studie sollte den Spurenelementgehalt in Fluoriden der Gardar Provinz vergleichen und Aufschluss über mögliche Anreicherungsprozesse liefern. Im dritten Teil wurden Ganggesteine auf ihren Halogengehalt untersucht. Diese gelten als Zufuhrkanäle des Magmatismus der Gardar Provinz und geben somit Einblicke in die Magmenquelle und -entwicklung.

Die miaskitischen Gesteine der Motzfeldt Intrusion sind durch Feldspat, Amphibol, Pyroxen, Nephelin, Fe-Ti Oxide, Zirkon und Fluorite gekennzeichnet. Die Agpaite enthalten Aegirin, Feldspat, Nephelin und Eudialyt. Die Gesteine zeigen eine kontinuierliche Entwicklung von Na-Ca-Fe^{2+}(-Mg)-Reichtum in den Miaskiten hin zu Na-Fe^{3+}-Dominanz in den Agpaiten. Bildungstemperaturen reichen von ca. 1000 °C in den Miaskiten bis zu 500 °C in den Agpaiten. Sauerstoff-Fugazitäten schwanken zwischen -0,5 bis -2 ΔFMQ. Die homogene Nd- und O-Isotopensignatur legt eine einheitliche Magmenquelle für beide Gesteinstypen nahe. Das Auftreten von Calcit-Kristallen in niedrigsalinaren Fluideinschlüssen (< 10 Gew.% NaCl eq.) belegt den Einfluss von CO_2 in der Entwicklung der Miaskite. In den Agpaiten hingegen treten keine Calcit-Kristalle in Fluideinschlüssen auf. Sie sind vielmehr durch signifikante Mengen von CH_4 gekennzeichnet. Die O-H-Isotopie des Fluideinschlusswassers zeigt eine meteorische Signatur, während die Kohlenstoffisotopie von CO_2 z.T. auf einen Mantelursprung schließen lässt. Der Übergang von Miaskiten zu Agpaiten kann für die Motzfeldt Intrusion durch die schematische Reaktion $8\ FeO + CO_2 + 2\ H_2O = CH_4 + Fe_2O_3$ beschrieben werden. Der Wechsel von Fe^{2+}-CO_2-dominierten Miaskiten zu Fe^{3+}-CH_4-dominierten Agpaiten wird mit abnehmender Temperatur, ansteigendem Alkali-Gehalt und den allgemein reduzierten Bedingungen in Verbindung gebracht.

Die SEE Gehalte von Fluoriden und Calciten wurden in den drei Gardar Intrusionen Ilímaussaq, Motzfeldt und Ivigtut untersucht. Alle Proben zeigen in Chondrit-normierten SEE

Mustern eine negative Eu Anomalie, die auf eine Feldspatfraktionierung zurückgeführt wird. Primär magmatische Fluorite in Motzfeldt und Ilímaussaq weisen eine nahezu identische Anreicherung der leichten SEE auf, unabhängig ob in agpaitischen oder miaskitischen Gesteinen. Dies lässt auf einen ähnlichen Bildungsprozess und ähnliche Fluorit-Schmelz-Verteilungskoeffizienten sowohl für Miaskite als auch Agpaite schließen. Hydrothermal gebildete Fluorite zeigen unterschiedliche Spurenelementcharakteristika, die auf verschiedene Phänomene wie Komplexierung, Wechselwirkung mit einem (CO_2-)F-reichen Fluid, Mobilisierung von Elementen aus dem Umgebungsgestein sowie verschiedene Fluid-Generationen hindeuten. Hydrothermale Proben des granitischen Ivigtut-Komplexes weisen flache bis schwach an schweren SEE angereicherte SEE-Muster auf. Diese Merkmale sowie der stark ausgeprägte Tetrad-Effekt sind typisch für intensive Fluid-Gesteins-Wechselwirkungen in Si-reichen, hoch-fraktionierten Systemen.

Ganggesteine der Gardar Provinz zeigen einen kontinuierlichen Fraktionierungstrend von Basalten zu Trachyten. Die variierenden, geochemischen Eigenschaften der Ganggesteine deuten auf einen Ursprung aus einem heterogenen, metasomatisch überprägten Mantel hin. Die Anreicherung von LILE, LSEE und Sr zusammen mit der Abreicherung an HFSE, Nb und Ti belegen eine Subduktions-bezogene Metasomatose, zu der es während der ketilidischen Orogenese vor ca. 1,8 Ga kam. Die hohen F-Gehalte der Gänge (< 1,2 Gew.%) deutet auf Teilschmelzung des lithosphärischen Mantels hin, in dem F-Apatit und F-Phlogopit auftreten. Cl/Br (Gewichts-) Verhältnisse der Ganggesteine liegen meist über 500 und Cl/F Verhältnisse unter 1. Dies kann auf den Verlust einer Fluidphase im Zuge der Kristallisation der Gänge zurückgeführt werden und wird durch den Vergleich mit Daten von Gesteinen und Fluiden der Ilímaussaq und Ivigtut Intrusionen unterstützt. Die Gesteine/Minerale der Intrusionen haben ähnliche Cl/Br- und Cl/F-Verhältnisse (Cl/Br > 300; Cl/F < 1) wie die Gänge. Jedoch zeigen Fluideinschlüsse komplementäre Verhältnisse: Cl/Br ~100 und Cl/F > 10. Analog zu mit experimentellen Daten verhalten sich die Halogene in der Schmelze somit zunehmend inkompatibel in der Reihenfolge F < Cl < Br.

Abstract

Apgaitic rocks are peralkaline rocks with complex Na-Ti-Zr silicates like eudialyte instead of common Fe-Ti oxides and zircon and exhibit a strong enrichment of halogens and trace elements (REE, HFSE). However, the detailed processes which form these exotic rocks are not yet fully understood. The 1.3 to 1.1 Ga old failed-rift Gardar Province in South Greenland is very well suited for the investigation of the agpaite formatione. The Province is not only the type locality of agpaitic rocks (Ilímaussaq), but also comprises the Motzfeldt intrusion where only a (volumetrically) small magmatic batch crystallised agpaitic rocks within a large occurrence of miaskitic ones. A second, comparative study of trace elements in fluorides of the Gardar Province provides insights into enrichment processes. Finally, the geochemistry and the halogen contents of primitive dyke rocks from the Gardar Province sheds light on the magmas' source region and the evolution of the halogens.

The rocks of the Motzfeldt intrusion are dominated by feldspar, amphibole, clinopyroxene, nepheline, Fe-Ti oxides, zircon and fluorite. The agpaitic rocks are characterised by aegirine, feldspar, nepheline and varying amounts of eudialyte. The rocks show a continuous evolution from Na-Ca-Fe^{2+}(-Mg) in the miaskitic to Na-Fe^{3+} enrichment in the agpaitic rocks. Formation temperatures range from ca. 1000 °C in the miaskitic rocks down to 500 °C in the agpaitic rocks. Calculated oxygen fugacities range from -0.5 to -2 ΔFMQ. The homogeneous Nd and O isotopic signatures suggest one single magma source for both rock types. The occurrence of calcite crystals in low salinity fluid inclusions (< 10 wt.% NaCl eq.) testifies the presence of CO_2 during the evolution of the miaskitic rocks. Fluid inclusions in the agpaitic rocks lack calcite crystals, however, they contain considerable amounts of methane. The isotopic composition of the inclusions' water suggests a meteoric origin whereas the carbon isotopes of inclusions' CO_2 partially reflects a mantle origin. The transition from miaskitic to agpaitic rocks in the Motzfeldt intrusion can be explained by a continuous fractionation process summarised by the redox-reaction $8\ FeO + CO_2 + 2\ H_2O = CH_4 + 4\ Fe_2O_3$. The change from Fe^{2+}-CO_2 in the miaskites to Fe^{3+}-CH_4 in the agpaites is related to decreasing temperature, increasing alkali content and the generally reduced conditions of the rocks.

The REE content of fluorides and associated minerals was investigated from three different Gardar intrusions: Ilímaussaq, Motzfeldt and Ivigtut. All investigated samples show a negative Eu anomaly in chondrite-normalised REE patterns which is attributed to feldspar fractionation in the parental magmas. The primary magmatic fluorites from the agpaitic Ilímaussaq intrusion and from the miaskitic and agpaitic parts of the Motzfeldt intrusion show

identical enrichments of LREE. This points to a common formation process and similar fluorite-melt partition coefficient irrespective of miaskitic or agpaitic evolution. REE patterns of hydrothermal fluorites reflect the influence of various processes like complexation, migration of a (CO_2-) F-rich fluid, country rock leaching and the influence of multiple fluid generations. The hydrothermal samples from the granitic Ivigtut complex show rather flat normalised pattern or a slight enrichment in heavy REE and a strong tetrad effect. These characteristics record extensive fluid-rock interaction in a Si-rich, highly fractionated system.

Dyke rocks are common throughout the Gardar Province and exhibit a continuous fractionation trend from basalts to trachytes. The dykes show a diverse geochemistry which is related to a heterogeneous, metasomatised mantle source. The enrichment of LILE, LREE and Sr together with depletion of HFSE, Nb and Ti evidence a subduction-related metasomatism during the Ketilidian orogeny some 600 Ma before the Gardar magmatism. The dykes have high fluorine contents up to 1.2 wt% F which is likely associated to partial melting of lithospheric mantle enriched in F-apatite and F-phlogopite. Cl/Br (weight) ratios are commonly > 500 while Cl/F ratios are < 1. These ratios point to a fluid degassing/separation process during the evolution of the dykes. This is supported by mineral/rock and fluid inclusion data from the Ilímaussaq and Ivigtut intrusions. The rock ratios are similar to the investigated dykes (high Cl/Br > 300; low Cl/F < 1) whereas associated fluid inclusion data have complementary low Cl/Br ~ 100 and high Cl/F > 10. Therefore, halogens show an increasing incompatibility in the Gardar melts in the order F < Cl < Br which is in accordance with published experimental data.

Einführung und Zielsetzung der Arbeit

Alkaline [(Na + K)/Al > 1] Gesteine gehören zu den höchstfraktionierten Gesteinen der Welt. Sie reichern Elemente wie U, Nb oder die Seltenenerdelemente (SEE) z.T. bis in den Prozentbereich an und können somit von ökonomischer Bedeutung sein. Alkaline Gesteine gehen durch Fraktionierungsprozesse aus primitiven Magmen hervor. Dabei ist ihre Entstehung an bestimmte tektonische Milieus gebunden, wie z.B. während des frühen Auseinanderbrechens von Kontinenten (*rifting*). Solch ein *rifting*-Ereignis fand vor ca. 1,3 bis 1,1 Ga in der Gardar Provinz im heutigen Südgrönland statt. Dabei kristallisierten große Volumina (per-)alkaliner Gesteine, wie z.B. Nephelin-Syenite oder Alkali-Granite.

Unter den alkalinen Magmatiten gibt es zahlreiche Exoten, wie z.B. die agpaitischen Gesteine. Agpaite sind peralkaline Nephelin-Syenite, die charakteristischerweise Eudialyt und andere komplexe Zr(Ti)-Silikate führen (Sørensen, 1997). Im Gegensatz dazu stehen „normale“ miaskitische Gesteine, in denen die High-Field-Strength Elemente (HFSE) wie Zr und Ti in Zirkon, Fe-Ti-Oxiden bzw. Titanit fixiert werden. Die Typlokalität der Agpaite ist die Ilímaussaq Intrusion in der Gardar Provinz in Südgrönland.

Die physiko-chemischen Bildungsbedingungen agpaitischer Gesteine sind noch nicht vollständig verstanden. Im Besonderen ist z.B. der Einfluss bzw. die Ursachen der Bildung von Methan und die Kristallisationsbedingungen der komplexen Zr(Ti)-Silikate noch nicht endgültig geklärt. Daher ist die Untersuchung der Agpait-Bildung die zentrale Fragestellung der vorliegenden Arbeit. Die Entstehung von Agpaiten wird mit einer extremen Reduziertheit eines Mantelmagmas in Verbindung gebracht, was unter anderem durch die Anwesenheit von Methan als magmatisches Fluid belegt wurde (Markl et al., 2001; Krumrei et al., 2007). Diese Reduziertheit verhindert eine Fluid-Entmischung im frühmagmatischen Stadium. Im Zuge der Bildung von Methan wird nach der Reaktion $CO_2 + 2\ H_2O = CH_4 + 2\ O_2$ Wasser verbraucht, wodurch die Schmelzen relativ wasserarm sind. Darüber hinaus sind Magmen, die Agpaite kristallisieren, durch ein langes Kristallisationsintervall bis zu Solidus-Temperaturen von 450-500 °C gekennzeichnet (Piotrowski & Edgar, 1970; Sood & Edgar, 1970; Larsen & Sørensen, 1987; Wolff, 1987). Diese extrem niedrigen Temperaturen hängen wahrscheinlich mit dem z.T. sehr hohen Fluorgehalt (per-)alkaliner und im Besonderen agpaitischer Gesteine zusammen. Dadurch weisen die Schmelzen eine sehr niedrige Viskosität auf. Elemente wie die HFSE werden somit nicht von einem Fluid mobilisiert, sondern in der Schmelze zurückgehalten und stehen zur Bildung der „exotischen“ Minerale, wie z.B. Eudialyt oder Rinkit, zur Verfügung.

Am Beispiel der Motzfeldt Intrusion in der Gardar Provinz wird im ersten Kapitel der Übergang von miaskitischen zu agpaitischen Gesteinen im Detail petrologisch, isotopengeochemisch und fluid-petrologisch untersucht. Die Motzfeldt Intrusion eignet sich besonders gut für die Charakterisierung dieses Übergangs, da sie zum größten Teil aus miaskitischen Gesteinen besteht und nur während des letzten Magmenschubs agpaitische Gesteine kristallisierten. Somit kann der Übergang genau studiert werden, was bei großen agpaitischen Intrusionen wie der Ilímaussaq Intrusion (Typlokalität für Agpaite) oder den Intrusivkomplexen auf der Kola-Halbinsel nicht ohne weiteres möglich ist.

Das zweite Kapitel dieser Arbeit ist eine Vergleichsstudie der Spurenelementgehalte von Fluoriden und Karbonaten aus miaskitischen, agpaitischen sowie granitischen Proben von Intrusionen der Gardar Provinz (Motzfeldt, Ilímaussaq und Ivigtut). In alkalinen Gesteinen sind Halogene häufig so stark angereichert, dass sie neben magmatischem Fluorit auch andere exotische Minerale wie Kryolith (Na_3AlF_6) und Villiaumit (NaF) führen können. So befindet sich z.B. in Ivigtut die weltweit einzige Kryolith-Lagerstätte (inzwischen vollständig abgebaut). Da die hohe Konzentration an Fluor und anderen Volatilen (wie z.B. Cl) einen großen Einfluss auf die Verteilung der Spurenelemente hat, lassen sich durch deren Untersuchung wichtige Einblicke in die Entwicklung dieser Gesteine gewinnen. Darüber hinaus kann die Frage diskutiert werden, ob und in welchem Maße sich die Kristallisationsbedingungen agpaitischer oder miaskitischer Gesteine auf den Spurenelementgehalt in den oben genannten Mineralen auswirken.

Auch der dritte Teil dieser Arbeit beschäftigt sich mit dem Halogengehalt von alkalinen Gesteinen Südgrönlands. Dabei wird diskutiert, welche Prozesse zur Halogenanreicherung in den Gesteinen der Gardar Provinz führten, und ob Halogene ein unterschiedliches Verhalten in der magmatischen Fraktionierung zeigen. Dafür eignen sich im Besonderen Ganggesteine, da sie die primitivsten Gesteine der Gardar Provinz repräsentieren. Außerdem können sie als Zufuhrkanäle eines Oberflächenvulkanismus gedeutet werden und stellen somit ein Bindeglied zwischen den großen Intrusionen (z.B. Motzfeldt oder Ilímaussaq) und dem Vulkanismus in der Gardar Provinz dar. Die Untersuchung des Ursprungs bzw. der Entwicklung des Halogengehalt liefert wichtige Einblicke in die allgemeine Entwicklung von alkalinen Gesteinen. Des Weiteren lassen sich Rückschlüsse auf tektonische Aktivitäten (z.B. Subduktion) sowie Einblicke in die Quellenregion der Magmen gewinnen.

Geologische Einführung

Die Gardar Provinz im Süden Grönlands ist eine „*failed rift*“ Provinz, die im Zuge des Auseinanderbrechens eines Superkontinents im Mittel-Proterozoikum entstand (Piper, 1982). Sie kann mit dem Keweenawan-Rift in Kanada korreliert (z.B. Bridgwater, 1967) und dem heutigen ostafrikanischen Rift-System verglichen werden (Fitton & Upton, 1987). Die Gesteine der Gardar Provinz bildeten sich zwischen ca. 1,3 und 1,1 Ga im Kontaktbereich zwischen dem Archaischen Kraton im Norden und dem Ketilidischen Orogen im Süden (z.B. Upton et al., 2003). Die 1,85 bis 1,80 Ga alten Ketiliden entstanden durch nordwärts-gerichtete Subduktion ozeanischer Kruste unter den Archaischen Kraton (van Breemen et al., 1974; Garde et al., 2002) und bestehen zum größten Teil aus Dioriten und I-Typ Graniten (Julianhåb Batholith; Garde et al., 2002).

Die Gardar Provinz umfasst 12 Intrusionen unterschiedlicher Größe (von < 1 km^2 Durchmesser (Ivigtut Intrusion) bis zu mehreren 100 km^2, wie z.B. die Motzfeldt oder Ilímaussaq Komplexe), deren chemische Zusammensetzung von SiO_2-gesättigten Graniten bis hin zu SiO_2-untersättigten Nephelin-Syeniten reicht. Des Weiteren kommen eine Abfolge von Sedimenten und Vulkaniten (Eriksfjord-Formation) und Gangschwärme vor. Die bis zu 800 m mächtigen Gänge werden auch als Zufuhrkanäle des Oberflächenvulkanismus gedeutet (Upton & Emeleus, 1987). Ihre Zusammensetzung reicht von Doleriten bis hin zu Rhyolithen. Sie treten oft in dichten Schwärmen auf, die (störungsgebunden) meist WSW-ENE bis SW-NE streichen. Die Gardar Gesteine entstanden im Laufe von 210 Ma (Upton et al., 2003). Aufgrund dieser langen Zeitspanne und Isotopenuntersuchungen wird von einer lithosphärischen Mantelquelle ausgegangen, die nur in geringem Maße krustaler Kontamination unterlag (z.B. Goodenough et al., 2000; 2002; Upton et al., 2003; Halama et al., 2003; 2005).

Drei Intrusionen spielen für diese Arbeit eine besondere Rolle: die Ilímaussaq , Ivigtut und Motzfeldt Intrusionen. Die 1,16 Ga (Krumrei et al. 2006) alte Ilímaussaq Intrusion ist Typlokalität agpaitischer Gesteine und weltberühmt für ihre spektakulär ausgebildete magmatische Schichtung. Der Intrusivkomplex entstand im Zuge vier aufeinander folgender Magmenschübe (Sørensen et al., 2006). Der erste besteht aus dem Augit-Syenit, der heute im Rand- und Dachbereich aufgeschlossen ist. Der zweite brachte ein kleines Volumen an Alkali-Granit hervor. Die dritten und vierten Magmenschübe waren schließlich für die Bildung der agpaitischen nephelin-syenitischen Gesteine verantwortlich, die aus Naujait sowie Kakortokit und Lujavrit bestehen (Sørensen et al., 2006). Die Naujaite werden dabei als

Dachkumulate, die Kakortokite als Bodenkumulate beschrieben. Der Lujavrit bildet den so genannten „Sandwich"-Horizont, in dem die letzte Schmelze auskristallisierte (Sørensen, 2001).

Der kleine Ivigtut Komplex (Durchmesser 350 m) besteht aus granitischen Gesteinen und beinhaltete das weltweit einzige abbauwürdige Vorkommen von Kryolith (Na_3AlF_6). Die Kryolith-Lagerstätte befindet sich in einem A-Typ Granit, der durch Fluor- und CO_2-reiche Fluide stark alteriert wurde (Pauly & Bailey, 1999; Goodenough et al., 2000). Die Kryolith-Lagerstätte entstand durch mehrere Entmischungsprozesse aus einer Fluorid- und Volatil-reichen Schmelzfraktion (Pauly & Bailey, 1999; Köhler et al., 2008). Kryolith ist häufig vergesellschaftet mit Siderit, Quarz, Fluorit, Topas und anderen Fluoriden wie Kryolithionit, Chiolith, Ralstonit oder Prosopit (Pauly & Bailey, 1999).

Eine dritte Intrusion der Gardar Provinz, die Motzfeldt Intrusion, ist für diese Arbeit von besonderer Bedeutung. Sie gehört zum größeren Igaliko Komplex im Osten der Provinz, der neben der Motzfeldt Intrusion die North- und South-Qoroq Intrusionen sowie den Igdlerfigssalik Komplex umfasst. Die Motzfeldt Intrusion kristallisierte sowohl miaskitische als auch, während des letzten Magmenschubs, agpaitische Nephelin-Syenite. Sie eignet sich daher sehr gut für die Untersuchung der Entwicklung von agpaitischen Gesteinen und wird im folgenden Kapitel im Detail beschrieben.

Erweiterte Zusammenfassung der Veröffentlichungen

Kapitel 1 – Die Magma- und Fluid-Entwicklung der Motzfeldt Intrusion

Die Motzfeldt Intrusion eignet sich sehr gut für das Studium des Übergangs von miaskitischen zu agpaitischen Gesteinen. Agpatische Gesteine treten in dieser Intrusion nur (volumenmäßig) untergeordnet im letzten Magmenschub auf (Jones, 1980). Dies steht im Gegensatz zu den großen Vorkommen von agpaitischen Gesteinen, wie z.B. der Ilímaussaq Intrusion oder auf der Kola-Halbinsel (z.B. Larsen & Sørensen, 1987; Kramm & Kogarko, 1994; Zaitsev et al., 1998; Markl et al., 2001).

Die Motzfeldt Intrusion entstand im Zuge von (mindestens) sechs aufeinander folgenden Magmenschüben (SM1 bis SM6; Emeleus & Harry, 1970; Jones, 1980). Aus ihnen kristallisierten überwiegend (Nephelin-) syenitische Gesteine, welche sich lediglich durch ihren modalen Mineralbestand unterscheiden. Die ersten fünf Magmenschübe (SM1 bis SM5) brachten eine miaskitische Mineralvergesellschaftung hervor. Diese besteht aus Alkali-Feldspat, Nephelin, Fe^{2+}-reichem Amphibol (Taramit, Katophorit, Ferro-nyböit und Arfvedsonit), augitischem Klino-Pyroxen, Fe-Ti Oxiden, Zirkon sowie untergeordnet Fluorit, Apatit, Sodalith und anderen Akzessorien. Eine spät- bis post-magmatische hydrothermale Alteration tritt häufig auf, wobei Einheit SM1 am stärksten alteriert ist. Die Alteration spiegelt sich im Auftreten von sekundärem Klinopyroxen (Aegirin), Fluorit, Calcit, Magnetit, Hämatit sowie anderer Alterationsprodukte (Cancrinit, Analcim) wider.

Die agpaitische Einheit (SM6) besteht aus idiomorphem Klinopyroxen (Aegirin), Alkali-Feldspat, Nephelin und interstitiellem Eudialyt. Vor allem Eudialyt ist häufig stark alteriert. Alterationsprodukte sind z.B. Cancrinit, Zirkon, Calcit, Pektolith und andere, SEE-reiche Minerale (z.B. Katapleiit, Zirfesit oder Pyrochlor; Jones, 1980; Jones & Larsen, 1985).

Mineralchemisch kann die Entwicklung von den miaskitischen Einheiten SM1-SM5 zur agpaitischen Einheit SM6 als ein (kontinuierlicher) Fraktionierungstrend beschrieben werden. Dabei sind früh gebildete Einheiten reich an Na-Ca-Fe^{2+}(-Mg), während die agpaitische Einheit SM6 den höchstfraktionierten, Na-K-Fe^{3+}-dominierten Teil der Intrusion darstellt (siehe auch Jones, 1980).

Intensive Parameter wie Temperatur, Sauerstoff-Fugazität (f_{O2}) und Silika-Aktivität können mithilfe koexistierender mafischer Minerale (Pyroxene, Fe-Ti Oxide, Olivin) abgeschätzt werden (z.B. Andersen & Lindsley, 1985; Andersen et al., 1993, Marks & Markl, 2001). Die Berechnungen (mit QUILF: Andersen et al., 1993; bzw. koexistierenden Fe-Ti

Oxiden: Andersen & Lindsley, 1985) für die miaskitischen Gesteine der Motzfeldt Intrusion ergeben Kristallisations-Temperaturen zwischen 800 und 600 °C bei Sauerstoff-Fugazitäten unterhalb des QFM-Puffers (ΔQFM -1 bis -2) und Silika-Aktivitäten zwischen 0,3 und 0,5. Ähnliche Temperaturen zeigen die Nephelin- (nach Hamilton, 1961) sowie Feldspatzusammensetzungen an (Jones, 1980). Da in der agpaitischen Einheit (SM6) weder primär magmatische Fe-Ti Oxide noch Olivin auftreten, konnten keine Sauerstoff-Fugazitäten abgeschätzt werden. Das Auftreten von Aegirin könnte auf eine höhere Oxidiertheit hindeuten. Hämatit als Alterationsprodukt zeigt eine f_{O2} oberhalb des Hämatit-Magnetit Puffers an. Die separate Kristallisation von zwei Feldspäten (nahezu reiner Albit und Orthoklas) weist auf sehr niedrige Kristallisationstemperaturen hin (< 500 °C; z.B. Brown & Parsons, 1989).

Isotopenuntersuchungen liefern Informationen über die Magmenherkunft und Magmenentwicklung. Amphibol- bzw. Pyroxen-Mineralseparate der unterschiedlichen miaskitischen (SM1-SM5) und agpaitischen (SM6) Magmenschübe zeigen nahezu konstante εNd(i) Werte von +0,1 bis +2,4 (berechnet für ein initiales Alter von 1,275 Ga; Upton et al., 2003). Die Sauerstoffisotopie ($\delta^{18}O$) der Minerale reicht von +4,9 bis +5,3 ‰ (relativ zu VSMOW; SM2 bis SM6). Die zwei Proben aus der am stärksten alterierten Einheit SM1 zeigen leicht niedrigere $\delta^{18}O$-Werte von +4,2 und +4,6 ‰ (VSMOW). Die homogene εNd- und $\delta^{18}O$-Isotopensignaturen lassen auf eine homogene Magmenquelle für die verschiedenen miaskitischen und agpaitischen Einheiten schließen (SM1 bis SM6). Die Übereinstimmung der Isotopen-Werte der Motzfeldt Intrusion mit anderen Gesteinen der Gardar Provinz (Ilímaussaq, Grønnedal-Ika, Puklen Intrusionen, Eriksfjord-Basalte: Halama et al., 2003; 2005; Marks et al., 2004) deutet auf einen gemeinsamen Ursprung im lithosphärische Mantel hin (z.B. Goodenough et al., 2002; Upton et al., 2003). Die Wasserstoffisotopie (δD) der Amphibolseparate aus den miaskitischen Gesteinen schwankt zwischen -97,7 und -133 ‰ (VSMOW). Diese Werte sind niedriger als typisch magmatische Werte (δD -50 bis -80 ‰: Hoefs, 1997), was sich durch eine Alteration mit meteorischem Wasser bei niedrigen Fluid-Gesteins-Verhältnissen erklären lässt. Die Menge an meteorischem Wasser reichte jedoch nicht aus, um die primär magmatische Sauerstoffisotopie zu verändern (aufgrund der höheren Konzentration von Sauerstoff gegenüber Wasserstoff im Gesamtgestein). Einen Einfluss von meteorischem Wasser zeigen auch die Isotopenzusammensetzungen von fein im Gestein verteilten Karbonaten. Deren Sauerstoffisotopie liegt meist deutlich über typischen Mantelwerten ($\delta^{18}O$ +21,9 bis 24,2 ‰ (VSMOW)) im Gegensatz zu $\delta^{18}O$-Werten zwischen +4 und +8 ‰ im Mantel (z.B. Taylor et al., 1967; Keller & Hoefs, 1995). Die

Kohlenstoffisotopie von sekundärem Calcit weist jedoch auf einen Mantelursprung hin ($\delta^{13}C$ -2,1 bis -4,4 ‰ (VPDB)). Sie ist vergleichbar mit anderen Carbonatit-/Calcit-Analysen der Gardar Provinz (z.B. Pearce et al., 1997; Coulson et al., 2003; Halama et al., 2005).

Fluideinschlüsse wurden in den Einheiten SM1, SM4, SM5 und SM6 sowohl in primär magmatischen Mineralen (Fluorit, Nephelin, Feldspat) als auch in hydrothermal gebildeten Fluoriten und Quarz untersucht. Die Fluideinschlüsse in miaskitischen Proben (Einheiten SM1, SM4 und SM5) können grob in drei Kategorien eingeteilt werden: (1a) wässrig-salinare, 2-phasige (Flüssigkeit-Gas) Fluideinschlüsse mit Salinitäten meist < 10 Gew.% (nach Bodnar, 1993); (1b) wässrig-salinare, 3-phasige Fluideinschlüsse, die neben Flüssigkeit und Gas noch einen Calcit-Kristall enthalten; (2) CO_2-haltige Einschlüsse (nur in einer Probe: JS34). Die Fluideinschlüsse der Typen (1a) und (1b) enthalten zusätzlich geringe Mengen an CO_2 und CH_4. Primäre und sekundäre Einschlüsse der Typen (1a) und (1b) treten sowohl in primär magmatischen als auch hydrothermal gebildeten Proben auf. Bei den Calcit-Kristallen handelt es sich meist um Tochterminerale, da sie in sekundären Einschlussbahnen stets in konstanten Volumenproportionen auftreten. Das Auftreten der Calcit-Kristalle sowohl in primären als auch sekundären Fluideinschlüssen belegt, dass das ursprüngliche Fluid reich an CO_2 bzw. CO_3^{2-} gewesen sein muss. Eine relative Altersabfolge der verschiedenen Einschlusstypen konnte aufgrund fehlender eindeutiger Indikatoren (z.B. sich schneidender Einschlussbahnen) nicht herausgearbeitet werden. Die für einen Bildungsdruck zwischen 1 und 2 kbar (Jones, 1980) korrigierten Homogenisierungstemperaturen schwanken zwischen 200 und 300 °C. Ionenchromatographie-Messungen zeigen, dass das Fluid Na- und Cl-dominiert ist, aber auch Ca enthält. Cl/Br (Gewichts-)Verhältnisse liegen zwischen 95 und 120 und sind mit Ergebnissen anderer Gardar Intrusionen vergleichbar (Ilímaussaq und Ivigtut; Graser et al., in press; Köhler et al., 2008). Diese niedrigen Verhältnisse können auf einen Fluidentmischungsprozess innerhalb eines Magmas zurückgeführt werden. Die relative Anreicherung von Br im Fluid führt dabei zu einem niedrigen Cl/Br-Verhältnis im Fluid (z.B. Bureau et al., 2000; Bureau & Métrich, 2003; siehe auch Anhang 3).

Primäre und sekundäre Fluideinschlüsse in Fluoriten aus den agpaitischen Gesteinen (SM6) enthalten neben NaCl und H_2O auch bedeutende Mengen an Methan. Die enge räumliche Assoziation von reinen CH_4 als auch gemischten CH_4-H_2O-NaCl Fluideinschlüssen zeigt, dass es sich ursprünglich um ein heterogenes Fluid gehandelt haben muss.

Die Isotopenzusammensetzung von H_2O, CO_2 und CH_4 der Fluideinschlüsse wurde in 10 Fluorit-Proben untersucht. Die Wasserstoff- und Sauerstoffisotopie des Fluideinschlusswassers (δD -40,7 bis -135,6 ‰, $\delta^{18}O$ -5,7 bis -20,9 ‰ VSMOW) liegt nahe

der heutigen meteorischen Wasserlinie (Craig, 1961) und deutet demnach auf einen meteorischen Ursprung hin. Nach Berechnungen mit Fraktionierungsfaktoren von Suzuoki & Epstein (1976) bzw. Graham et al. (1984) könnte die Wasserstoffisotopie der Amphibolseparate (siehe oben) bei ca. 300 °C nahezu Gleichgewichtseinstellung mit Wasserstoff (Fluideinschlusswasser) der Fluideinschlüsse widerspiegeln. Die Sauerstoffisotopie der Minerale und des Fluideinschlusswassers zeigt dagegen kein Gleichgewicht an. Dies kann wiederum durch die Wechselwirkung von meteorischem Wasser mit den Gesteinen bei einem geringen Fluid-Gesteinsverhältnis erklärt werden (siehe oben).

CO_2 in den Fluideinschlüssen konnte – außer in der agpaitischen Probe JS122 (SM6) - in allen Proben in geringen Mengen nachgewiesen werden. Die Kohlenstoffisotopie ($\delta^{13}C$ -2 bis -16 ‰ VPDB) ist vergleichbar mit Werten von Lamprophyren, Phonolithen und Karbonatiten der Motzfeldt (Igaliko) Region (Pearce & Leng, 1996). Dies deutet auf einen gemeinsamen Ursprung, Entwicklungstrend und/oder eine ähnliche Isotopenquelle hin. Die Sauerstoffisotopie des CO_2 ($\delta^{18}O$ +26,7 bis 42,7 ‰) liegt deutlich über Mantelwerten (z.B. Taylor et al., 1967). Dies hängt vermutlich mit einer Gleichgewichtseinstellung des Sauerstoffs zwischen H_2O und CO_2 der Fluideinschlüsse bei niedrigen Temperaturen zusammen (Friedmann & O'Neill, 1977; Richet et al., 1977; Köhler et al., 2008).

Die Isotopenzusammensetzung des Kohlenstoffes aus Einschluss-Methan ist relativ konstant ($\delta^{13}C$ -21 bis -31 ‰ VPDB). Es besteht kein Isotopenunterschied zwischen CH_4 aus miaskitischen und agpaitischen Einheiten. Dies könnte damit zusammenhängen, dass CH_4 aufgrund eines Respeziationsprozesses bei abnehmenden Temperaturen aus CO_2 gebildet wurde (z.B. Konnerup-Madsen et al., 1985 und Ryabchikov & Kogarko, 2006).

Übergang Miaskite-Agpaite. Der Übergang von einer miaskitischen Mineralvergesellschaftung mit Zirkon und Titanit sowie Fe^{2+}-reichen Amphibolen (SM1-SM5) hin zu einer agpaitischen Mineralvergesellschaftung mit Eudialyt und Aegirin (SM6) in der Motzfeldt Intrusion scheint auf einen kontinuierlichen Fraktionierungsprozess hinzudeuten. Die sehr ähnliche Isotopenzusammensetzung belegt eine einheitliche Quelle und Entwicklung des Magmas. Die Änderung der Mineralchemie, der Fluidzusammensetzung sowie des Alkali-Gehalts und Fe^{3+}/Fe^{2+}-Verhältnisses der Gesamtgesteine (Jones, 1980) kann demnach durch einen reinen Fraktionierungsprozess erklärt werden.

Die Kristallisation von Aegirin in den Agpaiten anstelle von Fe^{2+}-reichem Amphibol könnte von verschiedenen Parametern abhängen: 1. Erhöhung der Fe^{3+}-Konzentration (d.h. des Fe^{3+}/Fe^{2+}-Verhältnisses) führt zu einer bevorzugten Kristallisation von Aegirin. 2. Eine Erhöhung des Alkali(Na)/Fe Verhältnisses könnte ebenfalls zur Aegirin-Kristallisation führen.

In Arfvedsonit (Amphibol) ist das Na/Fe Verhältnis mit 0.6 niedriger als in Aegirin (Pyroxen; 1). Die Kristallisation von (Na-freien) Fe-Ti Oxiden könnte dabei zur Veränderung des Na/Fe-Verhältnisses beitragen. 3. Die Methan-bildende Reaktion: $CO_2 + 2\ H_2O = CH_4 + 2\ O_2$ (Gl. 1) verbraucht Wasser und könnte somit die Kristallisation von „wasserhaltigen" Mineralen wie Amphibol verhindern. Darüber hinaus führt die Bildung von CH_4 auch zu einer Erhöhung von „freiem" Sauerstoff, welcher wiederum zur Oxidation von Fe^{2+} zur Verfügung steht. Die relative Wasserarmut durch die Methanbildung (Gl. 1) könnte gleichzeitig eine (frühe) Entmischung einer Fluidphase aus dem Magma verhindern. Somit würden Halogene, Zr sowie andere HFSE in der Schmelze zurückbleiben und dort für die relativ späte Kristallisation von Eudialyt zur Verfügung stehen (z.B. Kogarko, 1974, Treuil et al., 1979, Taylor et al., 1981).

Die Veränderung der Fluidzusammensetzung von einem H_2O-HCO_3^--NaCl-$CaCl_2$ Fluid zu einem CH_4-H_2O-NaCl-$CaCl_2$(?) Fluid kann durch (einfache) Temperaturabnahme erklärt werden. Dies wurde bereits von Konnerup-Madsen (2001) sowie Ryabchikov & Kogarko (2006) gezeigt und durch theoretische Modellierungen von Huizenga (2001; 2005) bestätigt. Demnach ist bei hohen Temperaturen ein CO_2-(NaCl-)H_2O dominiertes Fluid stabil, welches bei abnehmenden Temperaturen von einem CH_4-(NaCl-)H_2O reichen Fluid abgelöst wird.

Zusammenfassend kann also der Übergang von Miaskiten zu Agpaiten in der Motzfeldt Intrusion durch eine Oxidation von Fe^{2+} zu Fe^{3+} im Gestein (Magma) einerseits und einer Reduktion des Kohlenstoffes von CO_2 zu CH_4 im Fluid andererseits beschrieben werden. Die Oxidation von Fe lief nach folgender Reaktion ab: $4\ Fe^{2+} + O_2 = 4\ Fe^{3+} + 2\ O^{2-}$ (Gl. 2). Eine Kombination der Gleichungen (1) und (2) ergibt: $8\ FeO^{melt} + CO_2 + 2\ H_2O = CH_4 + 4\ Fe_2O_3^{melt}$ (Gl. 3). Diese Gleichung (3) kann die Entwicklung der Motzfeldt Intrusion in einfacher Weise beschreiben. Die Verschiebung des Gleichgewichtes (Gl. 2 bzw. 3) ist sowohl von der Temperatur als auch vom Gesamt-Alkaligehalt der Schmelze abhängig (z.B. Kress & Carmichael, 1988; 1991; Lange & Carmichael, 1989; Gerlach et al., 1998; 1999; Rüssel & Wiedenroth, 2004). Eine Erhöhung des Alkaligehalts und eine Erniedrigung der Temperatur führt dabei jeweils zur bevorzugten Bildung von Fe^{3+}. Dies stimmt sehr gut mit den Beobachtungen in der Motzfeldt Intrusion überein (siehe auch Jones, 1980): Die früh, bei hohen Temperaturen auskristallisierten Einheiten sind eher durch Ca-Na-Fe^{2+}-reiche Minerale (Amphibole) charakterisiert. Im Zuge der Kristallisation/Fraktionierung steigt der Anteil an Na-Fe^{3+}(-K) bis hin zur agpaitischen Einheit (SM6), wo nur noch Aegirin und Alkali-reiche Minerale stabil sind (Alkali-Feldspat, Nephelin). Diese höchstfraktionierten Schmelzen, die

durch sehr niedrige (Solidus-)Temperaturen gekennzeichnet sind (ca. 450 °C), entwickelten sich schließlich kontinuierlich zu einem hydrothermalen Na-reichen Fluid (Jones & Larsen, 1985). Dieses Fluid führte dann zu der beobachteten spät- bis post-magmatischen Metasomatose bei höheren (relativen) Sauerstoff-Fugazitäten. Solch eine (Auto-) Metasomatose ist sehr typisch für peralkaline magmatische Komplexe (z.B. Salvi & Williams-Jones, 1990; Nivin et al., 2001, 2002, 2005).

Die Kristallisationsbedingungen der Motzfeldt Intrusion können gut in die Ergebnisse anderer Studien der Gardar Provinz eingeordnet werden. Generell scheinen die Magmen der Gardar Provinz aufgrund ihrer Nd- und O-Isotopenzusammensetzung aus einer gemeinsamen (lithosphärischen) Mantelquelle gebildet worden zu sein. Die T-f_{O2}-Bedingungen hatten einen entscheidenden Einfluss auf die Kristallisation von miaskitischen und/oder agpaitischen Gesteinen in der Motzfeldt Intrusion. Die Motzfeldt Intrusion nimmt in Bezug auf die f_{O2}-Bildungs-Bedingungen eine Position zwischen Intrusionen ein, die nur Miaskite umfassen (Grønnedal-Ika, Puklen; Halma et al., 2003; Marks et al., 2003) und der nahezu komplett aus agpaitischen Gesteinen bestehenden Ilímaussaq Intrusion (Markl et al., 2001). In der Motzfeldt Intrusion wurden frühmagmatische miaskitische Charakteristika (Fe^{2+}-Dominanz, Fe-Ti-Oxide, Zirkon und CO_2 im Fluid) im Zuge der Fraktionierung (und Abnahme der Kristallisationstemperatur) von einer agpaitischen Vergesellschaftung (Eudialyt, Na-Fe^{3+}-Dominanz, Methan) abgelöst. Die Reduziertheit des Fluides scheint dabei die Schlüsseleigenschaft zur Bildung von agpaitischen Gesteinen zu sein. Diese Arbeit zeigt, dass Fluideinschlüsse und im Speziellen die Speziation eines C-O-H Fluides (CO_2 oder CH_4) als sehr gute Indikatoren für Redox-Bedingungen der Schmelze verwendet werden können.

Kapitel 2 – Vergleichsstudie der SEE-Gehalte in Fluoriden und Karbonaten der Motzfeldt, Ilímaussaq und Ivigtut Intrusionen

In dieser Studie wurden Spurenelementgehalte, insbesondere die Seltenen Erd-Element sowie Y in Fluoriden, Calciten und Sideriten der Motzfeldt, Ilímaussaq und Ivigtut Intrusionen mit Kathodo-Lumineszenz (KL) sowie LA ICP-MS untersucht. Dafür wurden Proben von verschiedenen Einheiten und Entwicklungsstadien (primär magmatisch, pegmatitisch und hydrothermal) verwendet. Spurenelementuntersuchungen können nicht nur Einblicke in das Kristallisationsverhalten während den magmatischen und hydrothermalen Stadien geben, sondern auch Auskunft über Fluidentwicklung bzw. Fluid-Gesteinswechselwirkungen liefern. Als wichtigste Mechanismen zählen hierbei Komplexierung, Redox-Charakter,

kristallographisch kontrollierter Elementeinbau sowie der Einfluss bzw. die chemische Zusammensetzung eines mit der Schmelze assoziierten Fluides (z.B. Fleischer & Altschuler, 1969; Möller et al., 1976; Bau & Möller, 1992; Möller et al., 1998; Gagnon et al., 2003; Sallet et al., 2005).

Aus der Motzfeldt Intrusion wurden Fluorite und Calcite untersucht. Die Proben stammen aus den miaskitischen Einheiten SM1, SM4, SM5 sowie aus der agpaitischen Einheit SM6. Sie treten sowohl primär magmatisch in SM1 und SM6 als auch in hydrothermalen Gängen oder als Alterationsprodukte (SM1-SM5) auf. Aus der agpaitischen Ilímaussaq Intrusion wurden neben Fluoriten auch Villiaumit untersucht. Fluorit stammt hauptsächlich aus den Dach- und Bodenkumulaten (Naujaite, Kakortokite) und ist meist primär magmatisch. Villiaumit kommt im letzten Magmenschub (Lujavrite) vor. Die hydrothermal gebildeten Fluorite der beiden Intrusionen treten entweder in geringmächtigen Gängen (bis zu ca. 5 cm Mächtigkeit), pegmatitisch (bis zu 5 cm Größe) oder krustenförmig auf und zeigen stellenweise eine rhythmische Zonierung aus hellen und dunklen Bereichen. Primär magmatische Fluorite sind hypidiomorph bis xenomorph und nicht zoniert.

Die Proben der Ivigtut Intrusion stammen ausschließlich aus dem Fluorid-reichen Bereich der Lagerstätte. Es wurden Fluorit, Kryolith, Kryolithionit und Siderit untersucht. Die Minerale zeigen überwiegend eine xenomorphe Ausbildung während Fluorite im KL-Bild eine rhythmische Zonierung aus hellen und dunklen Bereichen aufweisen, sind die anderen Minerale stets unzoniert.

Die Gehalte der Seltenen Erden (SEE) wurden auf chondritische Werte normiert (McDonough & Sun, 1995). Das Pseudolanthanid Yttrium wurde nach Bau & Dulski (1995) zwischen Dysprosium und Holmium den SEE-Diagrammen hinzugefügt. Die Charakteristika der SEE-Muster können generell in zwei Kategorien eingeteilt werden: 1. Gemeinsamkeiten von primär magmatischen *und* hydrothermalen Mineralen 2. Besonderheiten, die nur in primär magmatischen *oder* hydrothermalen Mineralen vorkommen.

Gemeinsame Phänomene in primär magmatischen und hydrothermalen Mineralen

Kristallographisch kontrollierter Spurenelementeinbau. Die SEE-Konzentration hängt stark von der Ionen-Größe des Elements (z.B. Ca, Na etc.) ab, welches durch die SEE ersetzt wird. Von den untersuchten Mineralen zeigt Fluorit (und Calcit) die höchsten SEE-Konzentrationen, was durch den leichten Austausch von Ca durch die SEE erklärt werden kann. In Sideriten der Ivigtut Intrusion sind einzig die schweren SEE oberhalb der Nachweisgrenze. Dies liegt daran, dass die schweren SEE einen sehr ähnlichen Ionenradius

wie Fe^{2+} haben (z.B. Bau & Möller, 1992; Morgan & Wandless, 1980). Villiaumit (NaF) hingegen baut nahezu keine SEE ein, was durch einen erschwerten Ladungsausgleich erklärbar ist (Na^+ vs. Ca^{2+}). Kryolith (Na_3AlF_6) und Kryolithionit (Na_2LiAlF_6) bauen weniger SEE als Fluorit, aber deutlich mehr als Villiaumit ein. Dies ist mit einem einfacheren Ladungsausgleich durch Al^{3+} (im Vergleich zu Na^+ in Villiaumit) verbunden.

Hinweise auf die Zusammensetzung der Quelle (Schmelze/Fluid). Der SEE Einbau in Minerale (insbesondere Fluorit) hängt stark vom SEE-Gehalt im ursprünglichen Fluid (Schmelze) und dem chemischen (und geologischen) Milieu ab (z.B. Fleischer & Altschuler, 1969; Hill et al., 2000; Gagnon et al., 2003; Sallet et al., 2005; Schwinn & Markl, 2005). Dies stimmt mit den Beobachtungen dieser Studie überein: Demnach weisen Fluorite in alkalinen Nephelin-Syeniten (Motzfeldt und Ilímaussaq Komplexe) im Allgemeinen eine Anreicherung der leichten SEE in Frühkristallisaten auf und zeigen ähnliche Charakteristika wie das Umgebungsgestein. Die SEE-Muster und z.T. positive Eu-Anomalie in Proben aus Einheit SM5 (Motzfeldt) weisen hin auf eine deutliche Auslaugung und intensive Fluid-Interaktion mit dem Umgebungsgestein. Minerale der Ivigtut Intrusion besitzen eine leichte Anreicherung an schweren SEE, wie sie charakteristisch für Quarz-führende, pegmatitisch gebildete Minerale ist (Fleischer & Altschuler, 1969).

Ausbildung von Anomalien in normierten SEE-Mustern. Eine ausgeprägte negative Eu Anomalie tritt in (nahezu) allen Proben sowie in den Gesamtgesteinen aller drei untersuchten Intrusionen auf (Jones, 1980; Goodenough et al., 2000; Bailey et al., 2001). Diese Anomalie wird auf Plagioklas-Fraktionierung zurückgeführt, die durch große Anorthosit-Vorkommen unter der Gardar Provinz belegt ist (Halama et al., 2002). Die negative Ce Anomalie in manchen, sehr spät gebildeten Proben der Motzfeldt und Ilímaussaq Intrusionen könnte auf oxidiertere Verhältnisse, niedrigere Temperaturen oder veränderte pH-Bedingungen hinweisen (Constantopoulos, 1988; Bau & Möller, 1992; Hollings and Wyman, 2005).

Charakteristika primär magmatischer Fluorite

Die frühmagmatisch gebildeten Fluorite der Ilímaussaq und Motzfeldt Intrusionen zeigen nahezu identische, an leichten SEE angereicherte Muster. Dies deutet auf einen ähnlichen Bildungsmechanismus und/oder vergleichbare Verteilungskoeffizienten zwischen Fluorit und Schmelze hin. Dies ist bemerkenswert, da die Fluorite sowohl in miaskitischen Gesteinen (SM1 der Motzfeldt Intrusion) als auch in agpaitischen Gesteinen auftreten (SM6 – Motzfeldt; Kakortokite und Naujaite der Ilímaussaq Intrusion). Das konstante Y/Ho Verhältnis zwischen

60 und 70 deutet auf magmatische (und nicht hydrothermale) Fraktionierung hin (Bau & Dulski, 1995). Das gegenüber dem chondritischen Wert von 28 (Anders & Grevesse, 1989) deutlich erhöhte Y/Ho Verhältnis könnte mit einem erhöhten Verteilungskoeffizienten für Y im Vergleich zu Ho erklärbar sein (Veksler et al., 2005).

Die allgemeine Anreicherung von leichten SEE in primären Fluoriten, in Gesamtgesteinen der jeweiligen Intrusionen und in Gängen der Gardar Provinz (Goodenough et al., 2002; Halama et al., 2007; Köhler et al., eingereicht) deutet auf eine allgemeine Anreicherung an leichten SEE bereits in der Magmenquelle hin. Als Grund für die Anreicherung an leichten SEE (und auch Fluor und LILE) wurde von Upton & Emeleus (1987) eine metasomatische Veränderung der Magmenquelle im Zuge von Subduktionsprozessen angenommen.

Hydrothermal gebildete Fluorite und assoziierte Minerale

Fraktionierung der Fluid-Zusammensetzung. Die Verteilung bzw. der Einbau von SEE in Minerale verändert sich systematisch im Zuge der Kristallisation. Spät kristallisierte Fluorite zeigen generell geringere Konzentrationen an SEE im Vergleich zu früher kristallisierten. Frühkristallisate bauen bevorzugt leichte SEE ein, während später kristallisierende mittlere bzw. schwere SEE anreichern (z.B. Möller et al., 1976; Lüders et al., 1993; Kempe et al., 1999; Trinkler et al., 2005). Die Tb/Ca und Tb/La Verhältnisse werden häufig zur groben Einteilung von Fluoriten nach ihrem Kristallisationsstadium verwendet (pegmatitisch, hydrothermal, sedimentär; z.B. Möller et al., 1976; Gagnon et al., 2005). Analysen von primär magmatischen Fluoriten haben nahezu identische Tb/Ca und Tb/La Verhältnisse unabhängig von Intrusion oder Magmenschub und deuten auf ein pegmatitisches Milieu hin. Analysen von hydrothermalen Fluoriten aus SM1 (Motzfeldt Intrusion) zeigen stärker variierende Werte als primäre Fluorite, was auf eine Remobilisation der SEE hindeutet. Die meisten anderen Proben weisen auf hydrothermale Bildungsbedingungen hin.

Zonierungen sind häufig deutlich im KL-Bild ausgeprägt. Sie zeigen jedoch keine kontinuierliche, sondern eher abrupte Veränderungen des SEE Gehaltes an. Dies wird auf plötzliche Änderungen des SEE Gehaltes im Fluid zurückgeführt. Fluorite aus Motzfeldt zeigen oft eine komplexe, fleckenartige Zonierung (v.a. Proben aus SM1), die mit unterschiedlichen Fluorit-Generationen und/oder Überprägung durch ein (oder mehrere) Fluid(e) in Verbindung gebracht werden kann.

Im Allgemeinen spielt die **Komplexierung** von SEE eine wichtige Rolle beim Einbau von SEE in Minerale (Möller et al., 1976; Bau, 1991; Bau & Möller, 1992). Generell nimmt

die Stabilität von SEE-Komplexen mit F^-, OH^- oder CO_3^{2-} Liganden mit höherer Massenzahl (La ➔ Lu) sowie höherer Temperatur zu (Wood, 1990 a,b; Haas et al., 1995). Dies führt zur Fraktionierung der SEE: Während die leichten SEE in den kristallisierenden Mineralen angereichert werden, bleiben die schweren im Fluid zurück. Für alle drei Intrusionen wird aufgrund von Fluideinschluss-Untersuchungen angenommen, dass neben Fluorid-Komplexen, Hydroxyl-Komplexe und für die Motzfeldt und Ivigtut Intrusionen auch Karbonat-Komplexe eine Rolle spielten (Köhler et al., 2008; Graser et al., in press; Schönenberger & Markl, in press).

Der **Tetrad-Effekt** entsteht durch starke Fluid-Gesteins-Wechselwirkungen, wodurch sich die SEE nicht mehr gemäß ihres Ionenradius und Ladung verhalten (Bau, 1996; Irber, 1999). Er zeigt sich in M- oder W-förmigen Mustern in normierten SEE Diagrammen und ist von hoch fraktionierten Silikat-reichen Gesteinen (Graniten) bekannt (Irber, 1999; Zhao et al., 2002; Liu & Zhan, 2005). Einzig in Proben der granititschen Ivigtut Intrusion zeigt sich ein deutlich M-förmiges Muster. Dies belegt, dass die Lagerstätte Ivigtuts aus hoch entwickelten Schmelzen hervorging, die stark mit einem (Fluor-reichen) Fluid wechselwirkten (Pauly & Bailey, 1999).

Y/Ho Fraktionierung. Y und Ho waren im hydrothermalen Stadium der Motzfeldt und Ilímaussaq Intrusionen entkoppelt, was durch die stark schwankenden Y/Ho-Verhältnisse (< 60 bis > 1300) belegt wird. Ein Anstieg des Y/Ho-Verhältnisses im Laufe der Kristallisation kann nach Bau & Dulski (1995) in einem Fluor-reichen Milieu stattfinden. Entsprechend zeigen früh gebildete Fluorite der Ilímaussaq Intrusion ein relativ niedriges Y/Ho-Verhältnis (60 bis 70), während später gebildete stark ansteigende Verhältnisse zeigen (bis zu > 1300).

Während die heterogenen Y/Ho-Verhältnisse von Fluoriten aus SM1 der Motzfeldt Intrusion auf gekoppelte Effekte von Fluid-Interaktion, Remobilisierung und unterschiedliche Fluoritgenerationen hindeuten, zeigen die relativ konstanten Verhältnisse in SM4 homogene Bildungsbedingungen an. Die leicht niedrigeren Y/Ho-Verhältnisse der Proben aus SM5 deuten auf eine Wechselwirkung mit einer (bi)-Karbonat-reichen Lösung hin (Bau & Dulski, 1995).

Fluorite und Kryolith des Ivigtut Komplexes haben relativ niedrige Y/Ho-Verhältnisse zwischen 3 und 15 (Mittelwert 8-9), wobei der Ivigtut-Granit selbst nahezu chondritische Werte aufweist (Mittelwert bei 28). Es wird vermutet, dass die niedrigen Y/Ho-Verhältnisse in Fluoriten in Zusammenhang mit der starken Fluid-Gesteins-Interaktion vor bzw. während

der Bildung der eigentlichen Lagerstätte steht und durch eine unterschiedliche Mobilisierung von Y und Ho aus dem ursprünglichen Granit gebildet wurde.

Zusammenfassung. Diese Studie zeigt, dass der SEE-Einbau in Fluoride und assoziierte Karbonate wichtige Hinweise auf die bestimmenden Bildungsprozesse geben kann. Die Tatsache, dass primär magmatische Fluorite praktisch identische Charakteristika aufweisen, kann durch einen ähnlichen Verteilungskoeffizienten erklärt werden. Hydrothermale Fluorite zeigen auf der einen Seite multiple Fluid- und Fluorit-Generationen an, die bei unterschiedlichen physiko-chemischen Bedingungen entstanden. Auf der anderen Seite konnten auch Fluid-Wechselwirkungen mit dem umgebenden Gestein beobachtet werden (SM5, Motzfeldt; z.T. positive Eu-Anomalie). Die Proben des Ivigtut-Komplexes sind an schweren SEE angereichert bzw. zeigen relativ flache normierte SEE-Muster und spiegeln die hydrothermalen Bildungsbedingungen dieser Intrusion wider. Der SEE-Einbau wurde wohl am stärksten durch Fluor-Komplexierung gesteuert. Darüberhinaus zeigt der deutliche Tetrad-Effekt die starken Fluid-Gesteins-Wechselwirkungen in hoch entwickelten granitischen Gesteinen an.

Im Allgemeinen kann festgehalten werden, dass SiO_2-reiche, granitische Systeme (Ivigtut) schwere SEE bevorzugen, während SiO_2-untersättigte, alkaline Nephelin-Syenite der Motzfeldt und Ilímaussaq Intrusionen bevorzugt leichte SEE einbauen. Es konnte jedoch kein Unterschied zwischen Fluoriten aus miaskitischen bzw. agpaitischen Einheiten festgestellt werden. Neben der Magmenquelle (Fluid, Schmelze, Mantel?) spielt ferner die Größe und Ladung des Kations sowie die Verfügbarkeit Komplex-bildender Anionen eine Rolle beim Einbau der SEE.

Kapitel 3 – Halogen- und Spurenelement-Untersuchungen an Ganggesteinen aus der Gardar Provinz.

Halogene (Fluor, Chlor und Brom) sind nützliche Indikatoren für unterschiedliche Prozesse in plutonischen und vulkanischen Gesteinen und können insbesondere Auskunft über Fluid-bezogene Prozesse geben (z.B. Sigvaldason & Óskarsson, 1986; Kullerud, 1996; Markl & Schumacher, 1996; Bureau et al., 2000).

Die Bedeutung der Halogene für die Kristallisation der Gesteine der alkalinen Gardar Provinz in Südgrönland wurde bereits von Upton & Emeleus (1987) und Upton et al. (2006) beschrieben. In dieser Provinz treten Gesteine auf, die sehr stark an Halogenen angereichert sind. Die Ivigtut Intrusion mit der weltweit einzigartigen Kryolith- (Na_3AlF_6) Lagerstätte

sowie die Naujaite (Nephelin-Syenite) der Gardar Provinz mit ihrer sehr hohen Cl-Konzentration (in Sodalith) sind die zwei extremsten Beispiele dieser Halogenanreicherung. Diese Studie versucht, den Ursprung bzw. die Entwicklung des Halogen-Reichtums anhand von Ganggesteinen näher zu beleuchten. Die daraus gewonnenen Ergebnisse dienen zum besseren Verständnis des zeitlich und räumlich variablen Halogengehalts sowie der Eigenschaften der Magmenquelle.

Ganggesteine (Dykes) eigenen sich aus zwei Gründen besonders gut für die Untersuchung des Einflusses der Halogene auf die Gesteinsentwicklung: a) diese Gesteine spiegeln die unfraktioniertesten Gesteine der ganzen Provinz wider und b) sie können z.T. als Übergang zu den großen Intrusionen angesehen werden (Upton & Emeleus, 1987). Dykes treten in der Gardar Provinz sehr häufig auf und bildeten sich über den gesamten Zeitraum der magmatischen Aktivität (1,31 bis 1,16 Ga) (z.B. Upton et al., 2003). Die ältesten, ca. 1,28 Ga alten „Brown Dykes“ (BD 0) reichen von Lamprophyren bis hin zu (Trachy-) Doleriten und Gabbros. Die jüngeren, 1,20 Ga alten „Giant Dykes“ (GD) kommen hauptsächlich in der Gegend um Nunarssuit-Isortoq und Tugtutôq vor und erreichen Mächtigkeiten bis zu 800 m. Die GD-Gänge haben eine Augit-syenitische, Quarz-syenitische bis hin zu einer Alkali-granitischen Zusammensetzung. Die „Giant Dykes“ bestehen meist aus einem gabbroischen Rand und einem syenitischen Zentrum und zeigen magmatische Schichtung sowie Feldspat-Laminierung. Die älteren (1184 ±5 Ma) „Giant Dykes“ (OGDC) von Tugtutôq werden von den jüngeren 1,163-1,165 Ga „Giant Dykes“ (YGDC) abgelöst. Die Gänge der Ilímaussaq-Narsaq-Motzfeldt Gegend sind sehr feinkörnig, wobei es sich meist um basaltische bis trachytische Gesteine handelt. In der Ivigtut-Region kommen überwiegend basaltische, aber auch doleritische Gänge vor.

Gesamtgesteinschemismus. Im Allgemeinen haben die Gänge der Gardar Provinz stark variable, basisch bis saure Zusammensetzungen. Aufgrund des Na-Reichtums (bis zu 8 Gew.% Na_2O) handelt es sich zum Teil um Hawaiite, Mugearite und Benmoreite. Andere Gänge weisen Ähnlichkeiten zu K-angereicherten, kalk-alkalinen Gesteinen wie z.B. Shoshoniten, auf. Die Mg-Zahl (Mg/(Mg+Fe)) deutet darauf hin, dass es sich bei den Gardar Gängen um mittel bis stark entwickelte Gesteine handelt. Insgesamt unterscheiden sich die Gänge nicht nur regional, sondern auch nach ihrem Alter. Während ältere OGDC und BD 0 Gänge höher fraktioniert sind (d.h. niedrigere Mg-Zahlen), haben die YGDC primitivere Zusammensetzungen (d.h. höhere Mg-Zahlen). Es wird angenommen, dass die Gänge Produkte von Restmagmen sind, die nach (ausgeprägter) fraktionierter Kristallisation entstanden (Upton & Emeleus, 1987; Upton et al., 2003). Dies wird durch ihre niedrigen

Gehalte an Cr und Ni und einer (mäßigen) Anreicherung an inkompatiblen Elementen deutlich (z.B. Halama et al., 2007; Goodenough et al., 2000). Der Fluorgehalt liegt meist unter 2000 ppm, wobei Dykes aus der Ivigtut Region bis zu 12000 ppm Fluor enthalten. Die Gehalte an Cl und Br sind deutlich niedriger (Cl << 1000 ppm; Br < 1 ppm).

Insgesamt zeigen die analysierten Gardar Gänge klare Fraktionierungstrends, in denen inkompatible Spurenelemente negativ mit der Mg-Zahl korrelieren. Kompatible Elemente nehmen mit sinkender Mg-Zahl ebenfalls ab. Spurenelemente wie Ni, Cr, Sc, TiO_2, SEE deuten auf eine Fraktionierung von Fe-Ti-Oxiden, Klinopyroxen, Olivin, z.T. Apatit sowie Plagioklas hin.

Gänge aus der Region um Narsaq-Ilímaussaq-Motzfeldt zeigen eine Anreicherung an Übergangsmetallen (Ni, Cr, Co) in hoch *und* niedrig fraktionierten Gesteinen. Das (Kurven-) Minimum liegt bei einer Mg-Zahl von ca. 30. Bei niedrigeren und höheren Mg-Zahlen steigt der Übergangsmetallgehalt wieder an. Dies lässt sich nicht mit einfacher Fraktionierung erklären. Es wird vermutet, dass dieser Trend durch Wechselwirkungen zwischen einer Schmelze mit dem darüberliegenden Mantelkeil im Zuge von Subduktionsprozessen hervorgerufen wird. Auf der anderen Seite könnte dieser Trend auch durch Unterschiede in den Sauerstoff-Fugazitäten der Schmelzen erklärt werden. Der Einbau von Ni in Olivin hängt beispielsweise von der Sauerstoff-Fugazität ab (z.B. Morse et al., 1991). Bei niedrigen Sauerstoff-Fugazitäten nahe des Wüstit-Magnetit-Puffers tritt Ni verstärkt als Ni^0 im Magma auf und wird dann nicht in Olivin eingebaut, sondern in der Schmelze angereichert. Dies könnte zum beobachteten konkaven Trend im Diagramm (Ni vs. Mg-Zahl) führen. Die Reduziertheit der Magmen wurde sowohl in den jüngeren „Giant Dykes“ (Upton & Thomas, 1980) als auch in den Gesteinen der Ilímaussaq Intrusion beschrieben (Sauerstoff-Fugazitäten um FMQ -4; Marks & Markl, 2001).

Aufgrund der Spurenelementcharakteristika (LILE und LSEE Anreicherung; Abreicherung an schweren SEE, HFSE, Nb und Ti) wird davon ausgegangen, dass eine krustale Kontamination – falls überhaupt – nur eine sehr untergeordnete Rolle spielte. Einzig die Gänge in den Regionen um Isortoq und Nunarssuit haben wohl bis zu ca. 10% Unterkrustenmaterial assimiliert (Halama et al., 2004). Taylor & Upton (1993) zeigten jedoch mit Hilfe von Pb-Isotopen, dass der Einfluss einer krustalen Komponente im Zuge der fraktionierten Kristallisation zunimmt.

Als Mantelquelle der Gardar Gesteine wird der lithosphärische Mantel angenommen (z.B. Upton et al., 2003), was sowohl die Spurenelementcharakteristika als auch die lange Dauer des relativ einheitlichen Magmatismus (> 150 Ma) belegen. Die Gardar Magmen

bildeten sich vermutlich im Zuge einer Teilaufschmelzung des lithosphärischen Mantels, welcher bereits durch Subduktions-bezogene Fluide an LILE und inkompatiblen Elementen wie K, Ba, P und LSEE metasomatisch angereichert war. Zu dieser Anreicherung kam es durch nordwärts-gerichtete Subduktion vor ca. 1,8 Ga während der Bildung des ketilidischen Orogens (Chadwick & Garde, 1996; Garde et al., 2002). Die Beziehung der Gardar Gesteine zu früheren Subduktionsprozessen wird auch durch Nd-Modell-Alter belegt, die Alter von ca. 1850 bis 1720 Ma angeben und damit dem Alter der Ketiliden entsprechen (z.B. Schönenberger & Markl, in press; Marks et al. 2004).

Eine Mantelmetasomatose im Zuge der Subduktion kann entweder durch Fluide, die von der subduzierten Platte abgegeben werden, oder durch Aufschmelzung der subduzierten Platte hervorgerufen werden. Die relativ konstanten K/Rb Verhältnisse zusammen mit den sehr niedrigen La/Nb und Ba/Nb Verhältnissen könnten auf eine Fluid-gesteuerte Metasomatose hindeuten. Jedoch ist die endgültige Differenzierung zwischen diesen beiden Prozessen mit den hier angewendeten Methoden nicht eindeutig möglich.

Halogene. Fluor tritt im Mantel hauptsächlich in Wasser-haltigen Mineralen wie Amphibol, Phlogopit oder Apatit auf. Allerdings zeigten Experimente, dass auch nominell Volatil-freie Minerale wie Olivin, Granat oder Pyroxene relativ große Mengen an Halogenen einbauen können (bis zu 0,45 Gew.%; Bromiley & Kohn, 2007). Aufgrund der guten Korrelation der Phosphor-, Kaliumgehalte mit Fluor in den Ganggesteinen kann davon ausgegangen werden, dass Apatit und Phlogopit die Hauptquelle für Fluor in der Gardar Provinz darstellten.

Der relativ hohe Fluorgehalt der untersuchten Ganggesteine (< 12000 ppm) korelliert mit geringen Cl- (< 1000 ppm) und sehr niedrigen Br-Gehalten (< 1 ppm). Das Cl/Br (Gewichts-) Verhältnis der Gänge ist gewöhnlich > 500 und reicht von 300 bis > 1500. Es besteht weder eine Korrelation zwischen den unterschiedlichen Gang-Generationen, noch eine Abhängigkeit des Cl- und Br-Gehalts von anderen Elementen. Das Cl/Br Verhältnis scheint zudem keine bekannte Quellenregion im Erdinnern widerzuspiegeln (z.B. primitiver Mantel (Cl/Br 230); Kruste (Cl/Br 273); Dreibus et al., 1979; Jambon, 1994).

Es ist jedoch interessant, die Analysen der Ganggesteine in einen Zusammenhang mit Gesteins- und Mineral-Analysen der Ilímaussaq (und Ivigtut) Intrusion sowie Fluideinschlussuntersuchungen zu bringen. Die bisher untersuchten Fluideinschlüsse aus verschiedenen Intrusionen der Gardar Provinz zeigen generell ähnliche Cl/Br (Gewichts-) Verhältnisse um ca. 100 (Graser et al., in press; Schönenberger & Markl, in press; Köhler et al., 2008). Gesamtgesteine und Minerale (der Ilímaussaq Intrusion) zeigen deutlich höhere

Werte meist >> 500. Dieser große Unterschied zwischen Fluiden und Gesteinen könnte mit folgendem Mechanismus erklärt werden: Nach Bureau et al. (2000) und Bureau & Métrich (2003) wird Br im Vergleich zu Cl gegenüber der Schmelze stark im Fluid angereichert. Das heißt, Br verhält sich in der Schmelze inkompatibler als Cl. Eine (frühe) Entmischung eines Fluides lässt sich demnach in einem Gestein durch ein hohes Cl/Br-Verhältnis nachweisen. Dies kann auf die Ganggesteine übertragen werden: Das sehr hohe Cl/Br Verhältnis der analysierten Proben zeigt demnach, dass aus dem Stamm-Magma der Ganggesteine ein Fluid separierte. Dieses Fluid hatte relativ zu Cl einen hohen Gehalt an Br.

Auch das Cl/F Verhältnis könnte auf eine mögliche Entgasung hinweisen. Nach Villemant & Boudon (1999) zeigt Fluor eine relativ große Affinität zur Schmelze und wird demnach in der Schmelze zurückgehalten, während Cl (und noch stärker Br) ins Fluid partitionieren. Dies entspricht wiederum den Beobachtungen und Schlussfolgerungen aus Fluideinschlussuntersuchungen, die Cl/F-Verhältnisse > 10 haben und Gesamtgesteinen, die Cl/F-Verhältnisse < 1 aufweisen. Übertragen auf die Ganggesteine bestätigt diese Beobachtung die oben genannte Theorie der (frühen) Fluidentmischung.

Zusammenfassung. Diese Studie zeigte, dass die Ganggesteine der Gardar Provinz einen normalen Fraktionierungstrend beschreiben, wobei die Gänge sich sowohl nach dem Alter als auch nach ihrer räumlichen Beziehung in Gruppen einteilen lassen. Die Gänge sind allgemein an LILE und LSEE angereichert und an schweren SEE, HFSE, Nb und Ti abgereichert. Zusammen mit dem hohen Sr- und K-Gehalt weist dies auf eine Mantelmetasomatose unter der Gardar Provinz hin. Diese Metasomatose steht höchstwahrscheinlich in Zusammenhang mit Subduktionsprozessen. Die vom normalen Fraktionierungstrend abweichende Gehalte der Übergangsmetalle in Dykes der Ilímaussaq-Narsaq-Motzfeldt Gegend weisen wahrscheinlich auf niedrige Sauerstoff-Fugazitäten in den Magmen hin.

Die Ganggesteine sind relativ stark an Fluor angereichert, während die Cl- und Br-Gehalte meist niedriger sind. Als Fluorquelle kann Apatit und Phlogopit aus dem Mantel angenommen werden. Die Halogenverhältnisse (F/Cl und Cl/Br) deuten auf einen starken Entgasungsprozess eines Fluides hin, welcher zu einem Verlust der Halogene (F < Cl < Br) aus der Schmelze führt. Dies resultiert in hohen Cl/Br und niedrigen Cl/F Verhältnissen im zurückbleibenden Magma/Gestein bzw. in niedrigen Cl/Br und hohen Cl/F im entmischten Fluid. Die Halogen verhalten sich in der Schmelze zunehmend inkompatibel in der Reihenfolge F < Cl < Br.

Literatur

Anders, E., Grevesse, N., 1989. Abundances of the elements: meteoritic and solar. Geochimica et Cosmochimica Acta 53, 197-214.

Andersen, D.J., Lindsley, D.H., 1985. New (and final!) models for the Ti-magnetite/ilmenite geothermometer and oxygen barometer. Abstract AGU 1985 Spring Meeting Eos Transactions. American Geophysical Union 66, 416.

Andersen, D.J., Lindsley, D.H., Davidson, P.M., 1993. QUILF; a Pascal program to assess Equilibria among Fe-Mg-Mn-Ti oxides, pyroxenes, olivine, and quartz. Computers & Geosciences 19, 1333-1350.

Bailey, J.C., Gwozdz, R., Rose-Hansen, J., Sørensen, H., 2001: Geochemical overview of the Ilímaussaq alkaline complex, South Greenland. In: Sørensen, H. (ed.), The Ilímaussaq complex, South Greenland: status of mineralogical research with new results. Geology of Greenland Survey Bulletin 190, 35-53.

Bau, M., 1991. Rare earth element mobility during hydrothermal and metamorphic fluid-rock interaction and the significance of the oxidation state of europium. Chemical Geology 93, 219-230.

Bau, M., 1996. Controls on the fractionation of isovalent trace elements in magmatic and aqueous systems: evidence from Y/Ho, Zr/Hf, and the lanthanide tetrad effect. Contributions to Mineralogy and Petrology 123, 323-333.

Bau, M., Dulski, P., 1995. Comparative study of yttrium and rare-earth element behaviours in fluorine-rich hydrothermal fluids. Contributions to Mineralogy and Petrology 119, 213-223.

Bau, M., Möller, P., 1992. Rare Earth Element Fractionation in Metamorphogenic Hydrothermal Calcite, Magnesite and Siderite. Mineralogy and Petrology 45, 231-246.

Bodnar, R.J., 1993. Revised equation and table for determining the freezing point depression of the H2O-NaCl solutions. Geochimica et Cosmochimica Acta 57, 683-684.

Bridgwater, D. 1967. Feldspathic inclusions in the Gardar igneous rocks of South Greenland and their relevance to the formation of major Anorthosites in the Canadian Shield. Canadian Journal of Earth Sciences 4, 995-1014.

Bromiley, D.V., Kohn, S.C., 2007. Comparisons between fluoride and hydroxide incorporation in nominally anhydrous and fluorine-free mantle minerals. Geochimica et Cosmochimica Acta 71, Goldschmidt Conference Abstracts, A124.

Brown, W.L., Parsons, I., 1989. Alkali feldspars: ordering rates, phase transformations and behaviour diagrams for igneous rocks. Mineralogical Magazine 53, 25-42.

Bureau, H., Métrich, N., 2003. An experimental study of bromine behaviour in water-saturated silicic melts. Geochimica et Cosmochimica Acta 67, 1689-1697.

Bureau, H., Keppler, H., Métrich, N., 2000. Volcanic degassing of bromine and iodine: experimental fluid/melt partitioning data and applications to stratospheric chemistry. Earth and Planetary Science Letters 183, 51-60.

Chadwick, B., Garde, A.A., 1996. Palaeoproterozoic oblique plate convergence in South Greenland: a re-appraisal of the Ketilidian orogen. From: Brewer, T.S., Atkin, B.P. (eds.), Precambrian crustal evolution in the North Atlantic Region. Geological Society of London, Special Publication 112, 179-196.

Constantopoulos, J., 1988. Fluid Inclusions and Rare Earth Element Geochemistry of Fluorite from South-Central Idaho. Economic Geology 83, 626-636.

Coulson, I.M., Goodenough, K.M., Pearce, N.J.G., Leng, M.J., 2003. Carbonatites and lamprophyres of the Gardar Province-a 'window' to the Sub-Gardar Mantle? Mineralogical Magazine 67, 855–872.

Craig, H., 1961. Isotopic variations in meteoric waters. Science 133, 1702.

Dreibus, G., Spettel, B., Wanke, H., 1979. Halogens in meteorites and their primordial abundances. In: Ahrens, L.H. ed. Origin and Distribution of the Elements. Wiley, 33-38.

Emeleus, C.H., Harry, W.T., 1970. The Igaliko nepheline syenite complex; general description. Meddelelser om Grønland 186, 115 pp.

Fitton, J.G. & Upton, B.G.J. 1987: Alkaline igneous rocks: a review symposium. J. of the Geolog. Soc., London 142, 697-708.

Fleischer, M., Altschuler, Z.S., 1969. The relationship of the rare-earth composition of minerals to geological environment. Geochimica et Cosmochimia Acta 33, 725-732.

Friedman, I., O'Neil, J. R., 1977. Compilation of stable isotope fractionation factors of geochemical interest. In: Fleischer, M. (ed.), Data of geochemistry. U.S. Geological Survey Professional Paper 440-KK, 12.

Gagnon, J.E., Samson, I.M., Fryer, B.J., Williams-Jones, A.E., 2003. Compositional heterogeneity in fluorite and the genesis of fluorite deposits: insights from LA-ICP-MS analysis. Canadian Mineralogist 41, 365-382.

Garde, A.A., Hamilton, M.A., Chadwick, B., Grocott, J., McGaffrey, K.J.W., 2002. The Ketilidian orogen of South Greenland: geochronology, tectonics, magmatism, and fore arc accretion during Palaeoproterozoic oblique convergence. Canadian Journal of Earth Sciences 39, 765-793.

Gerlach, S., Claußen, O., Rüssel, C., 1998. Thermodynamics of iron in alkali-magnesia-silica glasses. Journal of Non-Crystalline Solids 238, 75–82.

Gerlach, S., Claußen, O., Rüssel, C., 1999. A voltammetric study on the thermodynamics of the Fe3+/Fe2+-equilibrium in alkali-lime-alumosilicate melts. Journal of Non-Crystalline Solids 248, 92-98.

Goodenough, K.M., Upton, B.G.J., Ellam, R.M., 2000. Geochemical evolution of the Ivigtut granite, South Greenland: a fluorine-rich "A-type" intrusion. Lithos 51, 205-221.

Goodenough, K.M., Upton, B.G.J., Ellam, R.M., 2002. Long-term memory of subduction processes in the lithospheric mantle: evidence from the geochemistry of basic dykes in the Gardar Province of South Greenland. Journal of the Geological Society, London 159, 705-714.

Graham, C.M., Harmon, R.S., Sheppard, S.M.F., 1984. Experimental hydrogen isotope studies: hydrogen isotope exchange between amphibole and water. American Mineralogist 69, 128-138.

Graser, G., Potter, J., Köhler, J., Markl, G., in press. Isotope, major, minor and trace element geochemistry of late-magmatic fluids in the peralkaline Ilímaussaq intrusion, South Greenland. Lithos.

Haas J.R., Shock E.L., Sassani D.C., 1995. Rare earth elements in hydrothermal systems: estimates of standard partial molal thermodynamic properties of aqueous complexes of the rare earth elements at high pressures and temperatures. Geochimica et Cosmochimica Acta 59, 4329–4350.

Halama, R., Waight, T., Markl, G., 2002. Geochemical and isotopic zoning patterns of plagioclase megacrysts in gabbroic dykes from the Gardar Province, South Greenland: implications for crystallisation processes in anorthositic magmas. Contributions to Mineralogy and Petrology 144, 109-127.

Halama, R., Wenzel, T., Upton, B.G.J., Siebel, W., Markl, G., 2003. A geochemical and Sr-Nd-O isotopic study of the Proterozoic Eriksfjord Basalts, Gardar Province, South Greenland: Reconstruction of an OIB signature in crustally contaminated rift-related basalts. Mineralogical Magazine 67, 831-854.

Halama, R., Marks, M., Brügmann, G., Siebel, W., Wenzel, T., Markl, G., 2004. Crustal contamination of mafic magmas; evidence from a petrological and Sr-Nd-Os-O isotopic study of the Proterozoic Isortoq dike swarm, South Greenland. Lithos 74, 3-4, 199-232.

Halama, R., Vennemann, T., Siebel, W., Markl, G., 2005. The Grønnedal-Ika carbonatite-syenite complex, South Greenland: An origin involving liquid immiscibility. Journal of Petrology 46, 191-217.

Halama, R., Joron, J.L., Villemant, B., Markl, G., Treuil, M., 2007. Trace element constraints on mantle sources druing mid-Proterozoic magmatism: evidence for a link between the Gardar (South Greenland) and Abitibi (Canadian Shield) mafic rocks. Canadian Journal of Earth Sciences 44, 1-20.

Hamilton, D.L., 1961. Nephelines as crystallisation temperature indicators. Journal of Geology 69, 321-329

Hill, G.T., Campbell, A.R., Kyle, P.R., 2000. Geochemistry of southwestern New Mexico fluorite occurrences implications for precious metals exploration in fluorite-bearing systems. Journal of Geochemical Exploration 68, 1-20.

Hoefs, J., 1997. Stable isotope geochemistry. Springer, Berlin Heidelberg

Hollings, P., Wyman, D., 2005. The geochemistry of trace elements in igneous systems: principles and examples from basaltic systems. In: Linnen, R.L., Samson, I.M. (eds.), Rare-Element Geochemistry and Mineral Deposits: Geological Association of Canada, GAC Short Course Notes 17, 1-16.

Huizenga, J.M., 2001. Thermodynamic modelling of C-O-H fluids. Lithos 55, 101-114

Huizenga, J.M., 2005. COH, an Excel spreadsheet for composition calculations in the C-O-H fluid system. Computers & Geosciences 31, 797-800.

Irber, W., 1999. The lanthanide tetrad effect and its correlation with K/Rb, Eu/Eu*, Sr/Eu, Y/Ho, and Zr/Hf of evolving peraluminous granite suites. Geochimica et Cosmochimica Acta 63, 489-508.

Jambon, A., 1994. Earth degassing and large-scale geochemical cycling of volatile elements. In: M.R. Carrol and J.R. Holloway, (eds.), Volatiles in Magmas. Mineralogical Society of America, Reviews in Mineralogy 30, 479–517.

Jones, A.P., 1980 Petrology and structure of the Motzfeldt centre, Igaliko complex, South Greenland. PhD thesis, Univ. of Durham, UK.

Jones, A.P., Larsen, L.M., 1985. Geochemistry and REE minerals of nepheline syenites from the Motzfeldt Centre, South Greenland. American Mineralogist 70, 1087-1100.

Keller, J., Hoefs, J., 1995. Stable isotope characteristics of recent natrocarbonatites from Oldoinyo Lengai. In: Bell, K., Keller, J. (eds.), Carbonatite Volcanism: Oldoinyo Lengai and the Petrogenesis of Natrocarbonatites. Berlin: Springer, 113–123.

Kempe, U., Monecke, T., Oberthür, T., Kremenetsky, A.A., 1999. Trace elements in scheelite and quartz from the Muruntau/Myutenbai gold deposit, Uzbekistan: constraints on the nature of ore-forming fluids. In: Stanley, C.J., et al. (eds.), Mineral Deposits: Processes to Processing. Balkema, Rotterdam, The Netherlands, 373-376.

Kogarko, L.N., 1974. Rôle of Volatiles. In: Sørensen, H. ed. The Alkaline Rocks. London: John Wiley & Sons, 474-487.

Köhler, J., Konnerup-Madsen, J., Markl, G., 2008. Fluid chemistry in the Ivigtut cryolite deposit, South Greenland. Lithos 103, 369-392.

Köhler, J., Schönenberger, J., Upton, B.G.J., Markl, G., submitted. Halogen and trace element geochemistry in the magmatic Gardar Province, South Greenland: evidence for subduction-related mantle metasomatism and fluid exsolution processes from alkalic melts. Lithos.

Konnerup-Madsen, J., 2001. A review of the composition and evolution of hydrocarbon gases during solidification of the Ilímaussaq alkaline complex, South Greenland. Geology of Greenland Survey Bulletin 301, 159–166.

Konnerup-Madsen, J., Dubessy, J., Rose-Hansen, J., 1985. Combined Raman microprobe spectrometry and microthermometry of fluid inclusions in minerals from igneous rocks of the Gardar province (south Greenland). Lithos 18, 271-280.

Kramm, U., Kogarko, L.N., 1994. Nd and Sr isotope signatures of the Khibina and Lovozero agpaitic centres, Kola Province, Russia. Lithos 32, 225-242.

Kress, V.C., Carmichael, I.S.E., 1988. Stoichiometry of the iron oxidation reaction in silicate melts. American Mineralogist 73, 1267-1274.

Kress, V.C., Carmichael, I.S.E., 1991. The compressibility of silicate liquids containing Fe2O3 and the effect of composition, temperature, oxygen fugacity and pressure on their redox states. Contributions to Mineralogy and Petrology 198, 82-92.

Krumrei, T.V., Villa, I.M., Marks, M., Markl, G., 2006. A 40Ar/39Ar and U/Pb isotopic study of the Ilímaussaq Complex, South Greeland; implications for the 40K decay constant and for the duration of magmatic activity in a peralkaline complex. Chemical Geology 227, 258-273.

Krumrei, T., Kaliwoda, M., Pernicka, E., Markl, G., 2007. Volatiles in a peralkaline system: Abiogenic hydrocarbons and F-Cl-Br systematics in the naujaite of the Ilimaussaq intrusion South Greenland. Lithos 95, 298-314.

Kullerud, K., 1996. Chlorine-rich amphiboles: interplay between amphibole composition and an evolving fluid. European Journal of Mineralogy 8, 355-370.

Lange, R.A., Carmichael, I.S.E., 1989. Ferric-ferrous Equilibria in Na2O-FeO-Fe2O3-SiO2 melts: Effects of analytical techniques on derived partial molar volumes. Geochimica et Cosmochimica Acta 53, 2195-2204.

Larsen, L.M., Sørensen, H., 1987. The Ilímaussaq intrusion-progressive crystallization and formation of layering in an agpaitic magma. In: Fitton, J.G., Upton, B.G.J. (eds.), Alkaline Igneous Rocks. Geological Society Special Publication

30, 473-488.
Liu, C.Q., Zhan, H., 2005. The lanthanide tetrad effect in apatite from the Altay No. 3 pegmatite, Xingjiang, China: an intrinsic feature of the the pegmatitic magma. Chemical Geology 214, 61-77.
Lüders, V., Möller, P., Dulski, P., 1993. REE Fractionation in Carbonates and Fluorite. Monograph Series on Mineral Deposits 30, 133-150.
Markl, G., Schumacher, J.C., 1996. Spatial variations in temperature and composition of greisen-forming fluids; an example from the Variscan Triberg granite complex, Germany. Economic Geology and the Bulletin of the Society of Economic Geologists 91, 576-589.
Markl, G., Marks, M., Schwinn, G., Sommer, H., 2001. Phase Equilibrium Constraints on Intensive Crystallization Parameters of the Ilímaussaq Complex, South Greenland. Journal of Petrology 42, 2231-2258.
Marks, M., Markl, G., 2001. Fractionation and assimilation processes in the alkaline augite syenite unit of the Ilimaussaq Intrusion, South Greenland, as deduced from phase equilibria. Journal of Petrology 42, 1947-1969.
Marks, M., Vennemann, T., Siebel, W. & Markl, G., 2003. Quantification of Magmatic and Hydrothermal Processes in a Peralkaline Syenite-Alkali Granite Complex Based on Textures, Phase Equilibria, and Stable and Radiogenic Isotopes. Journal of Petrology 44, 1247-1280.
Marks, M., Venemann, T., Siebel, W., Markl, G., 2004. Nd-, O-, and H-isotopic evidence for complex, closed-system fluid evolution of the peralkaline Ilímaussaq intrusion, South Greenland. Geochimica et Cosmochimica Acta 68, 3379-3395.
McDonough, W.F.M., Sun, S.S., 1995. The composition of the Earth. Chemical Geology 120, 223-253.
Möller, P., Parekh, P., Schneider, H.J., 1976. The application of Tb/Ca-Tb/La abundance ratios to problems of fluorspar genesis. Mineralium Deposita 11, 111-116.
Möller, P., Bau, M., Dulski, P., Lüders, V., 1998. REE and Y fractionation in fluorite and their bearing on fluorite formation. Proceedings of the Ninth Quadrennial IAGOD Symposium. Schweizerbart, Stuttgart, 575-592.
Morgan, J.W., Wandless, G.A., 1980. Rare earth element distribution in some hydrothermal minerals: evidence for crystallographic control. Geochmicia et Cosmochimica Acta 44, 973-980.
Morse, S.A., Rhodes, J.M., Nolan, K.M., 1991. Redox effect on the partitioning of nickel in olivine. Geochimica et Cosmochimica Acta 55, 2373-2378.
Nivin, V.A., Belov, N.I., Treloar, P.J., Timofeyev, V.V., 2001. Relationships between gas geochemistry and release rates and the geochemical state of igneous rock massifs. Tectonophysics 336, 233-244.
Nivin, V.A., Ikorskii, S.V., Treloar, P.J., 2002. Bulk gas content variations in fluid inclusions of minerals from the Khibina and Lovozero nepheline-syenite plutons (NE Baltic Shield, Russia); implication for origin of hydrocarbon gases. Abstracts of the 18th General Meeting of the International Mineralogical Association 18, 248.
Nivin, V.A., Treloar, P.J., Konopleva, N.G., Ikorsky, S.V., 2005. A review of the occurrence, form and origin of C-bearing species in the Khibiny alkaline igeneous complex, Kola Peninsula, NW Russia. Lithos 85, 93-112.
Pauly, H., Bailey, J.C., 1999. Genesis and evolution of the Ivigtut cryolite deposit, SW Greenland. Meddelelser om Grønland, Geoscience 37, 60 p.
Pearce, N.J.G., Leng, M.J., 1996. The origin of carbonatites and related rocks from the Igaliko Dyke Swarm, Gardar Province, South Greenland: field, geochemical and C–O–Sr–Nd isotope evidence. Lithos 39, 21–40.
Pearce, N.J.G., Leng, M.J., Emeleus, C.H., Bedford, C.M., 1997. The origins of carbonatites and related rocks from the Grønnedal-Ika Nepheline Syenite Complex, South Greenland: C–O–Sr isotope evidence. Mineralogical Magazine 61, 515–529.
Piotrowski, J.M., Edgar, A.D., 1970. Melting relations of undersaturated alkaline rocks from South Greenland compared to those of Africa and Canada. Meddelelser om Grønland 181.
Piper, J.D.A. 1982: The Precambrian paleomagnetic record: The case for the Proterozoic supercontinent. Earth and Planetary Science Letters 59, pp. 61-89.
Richet, P., Bottinga, Y., Javoy, A., 1977. A review of hydrogen, carbon, nitrogen, oxygen, sulphur and chlorine stable isotope fractionation among gaseous molecules. Annual Reviews Earth Planetary Science 5, 65-110.
Rüssel, C., Wiedenroth, A., 2004. The effect of glass composition on the thermodynamics of the Fe2+/Fe3+ equilibrium and the iron diffusivity in Na2O/MgO/CaO/Al2O3/SiO2 melts. Chemical Geology 213, 125-135.
Ryabchikov, I.D., Kogarko, L.N., 2006. Magnetite compositions and oxygen fugacities of the Khibina magmatic system. Lithos 91, 35-45.
Sallet, R., Moritz, R., Fontignie, D., 2005. The use of vein fluorite as probe for paleofluid REE and Sr–Nd isotope geochemistry: The Santa Catarina Fluorite District, Southern Brazil. Chemical Geology 223, 227-248.
Salvi, S., Williams-Jones, A.E., 1990. The role of hydrothermal processes in the granite hosted Zr, Y, REE deposit at Strange Lake, Quebec/Labrador: evidence from fluid inclusions. Geochimica et Cosmochimica Acta 54, 2403–2418.
Schönenberger, J., Markl, G. in press. The Magmatic and Fluid Evolution of the Motzfeldt Intrusion in South Greenland: Insights into the Formation of Agpaitic and Miaskitic Rocks. Journal of Petrology, doi: 10.1093/petrology/egn037.
Schwinn, G., Markl, G., 2005. REE systematics in hydrothermal fluorite Chemical Geology, 216, 225-248.
Sigvaldason, G.E., Óskarsson, N., 1986. Fluorine in basalts from Iceland. Contributions to Mineralogy and Petrology 94, 263-271.
Sood, M.K., Edgar, A.D., 1970. Melting relations of undersaturated alkaline rocks from the Ilímaussaq intrusion and Grønnedal-Ika complex South Greenland, under water vapour and controlled partial oxygen pressure. Meddelelser om Grønland 181.
Sørensen, H., 1997. The agpaitic rocks – a review. Mineralogical Magazine 61, 485-498.
Sørensen, H. 2001: Brief introduction to the geology of the Ilímaussaq alkaline complex, South Greenland, and its exploration history. Geology of Greenland Survey Bulletin 190, 7-23.
Sørensen, H., Bohse, H., Bailey, J.C., 2006. The origin and mode of emplacement of lujavrites in the Ilimaussaq alkaline complex, South Greenland. Lithos 91, 286-300.
Suzuoki, T., Epstein, S., 1976. Hydrogen isotope fractionation between OH-bearing minerals and water. Geochimica et Cosmochimica Acta 40, 1229-1240.

Taylor, H.P., Frechen, J. Degens, E.T., 1967. Oxygen and carbon isotope studies of carbonatites from the Laacher See District, West Germany and the Alnø District, Sweden. Geochimica et Cosmochimica Acta 31, 407–430.

Taylor, R.P., Strong, D.F., Fryer, B.J., 1981. Volatile control of contrasting trace element distributions in peralkaline granitic and volcanic rocks. Contributions to Mineralogy and Petrology 77, 267-271.

Taylor, P.N., Upton, B.G.J., 1993. Contrasting Pb isotopic compositions in two intrusive complexes of the Gardar Magmatic Province of South Greenland. Chemical Geology 104, 261-268.

Treuil, M., Joron, J.L., Jaffrezic, H., Villemant, B., Calas, G., 1979. Géochimie des elements hygromagmatophiles: Coefficients de partage minéraux/liquides et propriétés structurales de ces éléments dans les liquides magmatiques. Bullétin de Mineralogy 102, 402-409.

Trinkler, M., Monecke, T., Thomas, R., 2005. Constraints on the genesis of yellow fluorite in hydrothermal barite-fluorite veins of the Erzgebirge, Eastern Germany: Evidence from optical absorption spectroscopy, rare-earth-element data and fluid-inclusion investigations. The Canadian Mineralogist 43, 883-898.

Upton, B.G.J., Thomas, J.E., 1980. The Tugtutôq Younger Giant Dyke Complex, South Greenland; fractional crystallization of transitional olivine basalt magma. Journal of Petrology 21, 167-198.

Upton, B.G.J., Emeleus, C.H., 1987. Mid-Proterozoic alkaline magmatism in southern Greenland: the Gardar Province. In: Fitton, J.G. & Upton, B.G.J. (eds.), Alkaline Igneous Rocks, Geological Society Special Publication 30, 449-471.

Upton, B.G.J., Emeleus, C.H., Heaman, L.M., Goodenough, K.M., Finch, A.A., 2003. Magmatism of the mid-Proterozoic Gardar Province, South Greenland: chronology, petrogenesis and geological setting. Lithos 68, 43-65.

Upton, B.G.J., Craven, J.A., Kirstein, L.A., 2006. Crystallisation of mela-aillikites of the Narsaq region, Gardar alkaline province, south Greenland and relationships to other aillikitic–carbonatitic associations in the province. Lithos 92, 300-319.

van Breemen, O., Aftalion, M. & Allaart, J. H. 1974: Isotopic and geochronologic studies on granites from the Ketilidian mobile belt of South Greenland. Geological Society of America Bulletin 85, 403–412.

Veklser, I.V., Dorfman, A.M., Kamenetsky, M., Dulski, P., Dingwell, D., 2005. Partitioning of lanthanides and Y between immischible silicate and fluoride melts, fluorite and cryolite and the origin of the lanthanide tetrad effect in igneous systems. Geochimica et Cosmochimica Acta 69, 2847-2860.

Villemant, B., Boudon, G., 1999. H2O and halogen (F, Cl, Br) behaviour during shallow magma degassing processes. Earth and Planetary Science Letters 168, 271-286.

Wolff, J.A., 1987. Crystallization of nepheline syenite in a subvolcanic magma system: Tenerife, Canary Islands. Lithos 20, 207-223.

Wood, S.A., 1990a. The aqueous geochemistry of the rare-earth elements and yttrium. 1. Review of available low-temperature data for inorganic complexes and the inorganic REE speciation of natural waters. Chemical Geology 88, 159-186.

Wood, S.A., 1990b. The aqueous geochemistry of the rare-earth elements and yttrium. 2. Theoretical predictions of speciation in hydrothermal solutions to 350 °C at saturation water vapor pressure. Chemical Geology 88, 99-125.

Zaitsev, A.N., Wall, F., LeBas, M.J., 1998. REE-Sr-Ba minerals from the Khibina carbonatites, Kola Peninsula, Russia; their mineralogy, paragenesis and evolution: Mineralogical Magazine 62, 225-250.

Zhao, Z., Xiong, X., Han, X., Wang, Y., Wang, Q., Bao, Z., Jahn, B., 2002. Controls on the REE tetrad effect in granites: Evidence from the Qianlishan and Baerzhe Granites, China. Geochemical Journal 36, 527-543.

Anhang

The magmatic and fluid evolution of the Motzfeldt intrusion in South Greenland: insights into the formation of agpaitic and miaskitic rocks.

Johannes Schönenberger and Gregor Markl

Eberhard-Karls Universität Tübingen, Institut für Geowissenschaften, Wilhelmstrasse 56, 72074 Tübingen, Germany

Keywords: Agpaite; Methane; Miaskite; Nepheline Syenite; Redox Reactions

In press bei Journal of Petrology 2008: doi: 10.1093/petrology/egn037.

ABSTRACT

The 1.275 Ga old Motzfeldt intrusive complex in the Gardar failed-rift province in South Greenland formed from six successively intruding melt batches (SM1-SM6) interpreted to be derived from a common magma source at depth. Five units (SM1-SM5)crystallised an alkaline to peralkaline, miaskitic mineral assemblage of amphibole, clinopyroxene, feldspar, nepheline, Fe-Ti oxides, zircon, apatite, fluorite and rarely olivine. The last magmatic batch (SM6) is characterised by an agpaitic mineral assemblage of aegirine, nepheline, alkali-feldspar, eudialyte and rare fluorite or sodalite.

Coexisting mafic minerals constrain the crystallisation conditions of the miaskitic rocks to about 850 to 600 °C, while solidus temperatures below 500°C are indicated by coexisting alkali feldspars in the agpaitic rocks. Oxygen fugacities during the orthomagmatic stage are below the FMQ buffer (ΔFMQ -0.5 to -2.0) while late hematite provides evidence of a higher relative oxygen fugacity during late-stage alteration. The Nd and oxygen isotope compositions of amphiboles and pyroxenes are homogeneous throughout the whole complex and suggest a common, mantle-derived magma source for all six units which is comparable to other Gardar intrusions. The hydrogen isotopic composition of amphiboles (-99 to -132 ‰) indicates low-temperature fluid-rock interaction with low fluid-rock ratios.

Fluid inclusion studies indicate that H_2O-NaCl fluids present during the magmatic stages in the miaskitic units had salinities of < 10 wt.% NaCl eq. Calcite crystals in fluid inclusions within these rocks suggest that CO_2 or HCO_3^- was an important component of the original fluid phase. In contrast, the agpaitic unit is characterised by a CH_4-H_2O-NaCl fluid. The C-O-H isotope compositions of the fluid inclusions in all units are consistent with mixing between a small volume of magmatic fluid and a large volume of meteoric water.

The chemical evolution of the Motzfeldt complex is a type example of the connection of the transition from miaskitic to agpaitic mineral assemblages with redox-dependent fluid-solid equilibria. The transition from a relatively oxidized to a relatively reduced fluid is correlated with a change from a more reduced, Fe^{2+}-bearing miaskitic (taramite-arfvedsonite, zircon, SM1-SM5) to a more oxidized, Fe^{3+}-bearing agpaitic assemblage (aegirine, eudialyte, SM6). We suggest that coupled fluid-solid redox equilibria involving Fe^{2+}, Fe^{3+}, CO_2 and CH_4 in this case were simply driven by temperature decrease and an overall increase in Na (+K) in the melt. This observation sheds light on the heavily debated miaskite-agpaite-transition. The combined temperature and compositional effect stabilised Fe^{3+}, CH_4 and enhanced the solubility of Zr (possibly as Na-Zr-Si-O complexes) in the latest stage melt (SM6) resulting in the crystallisation of an agpaitic mineral assemblage. In terms of redox conditions during

crystallization, the Motzfeldt rocks represent an intermediate case in the Gardar Province between more oxidized, CO_2-dominated intrusions such as the syenite-carbonatite complex of Grønnedal-Ika and CH_4-dominated, more reduced complexes such as the peralkaline granitic Puklen and the agpaitic Ilímaussaq complex.

INTRODUCTION

Agpaitic rocks are peralkaline nepheline syenites which are characterised by the occurrence of complex Na-Zr silicates such as eudialyte instead of the more common zircon and Fe-Ti oxides in miaskitic rocks (Sørensen, 1997). They represent some of the most highly differentiated magmatic rocks worldwide, sometimes exhibiting enrichments of high field-strength elements (HFSE) such as Nb, Ta, U, Th, REE or Zr up to economic values (Sørensen, 1997). They occur as large intrusions (Ilímaussaq: Larsen & Sørensen, 1987; Markl *et al.*, 2001; Khibina and Lovozero: Kramm & Kogarko, 1994; Zaitsev *et al.*, 1998), as smaller parts of intrusions (Motzfeldt & Qoroq: Jones, 1980, 1984; Coulson, 1997; Mont St. Hilaire: Horvath & Gault, 1990; Tamazeght: Bouabdli *et al.*, 1988; Marks *et al.*, 2008) or as late-magmatic pegmatites (Crazy Mountains: Chakhmouradian & Mitchell, 2002; Oslo Rift: Brøgger, 1890, Fitou: Vitrac-Michard *et al.*, 1977; Gardiner Complex: Nielsen, 1994).

The petrogenesis of agpaitic rocks is not yet fully understood: however they clearly originate from extensively differentiated, alkalic, mantle-derived mafic magmas (alkali basalts, nephelinites or benmoreites: Kramm & Kogarko, 1994; Sørensen, 1997). They show particularly long crystallisation intervals down to temperatures < 450 °C (Piotrowski & Edgar, 1970; Sood & Edgar, 1970; Kogarko, 1977; Kogarko *et al.*, 1977; Kogarko, 1987; Larsen & Sørensen, 1987; Wolff, 1987) and can exhibit unusual melt immiscibility phenomena (Markl, 2001). The physico-chemical processes responsible for the formation of agpaitic mineral assemblages are not quantitatively understood and remain controversial. Markl *et al.* (2001) suggested and Krumrei *et al.* (2007) provided evidence for the existence of very reduced, methane-rich fluid phase at high, orthomagmatic temperatures. Both the high alkali content of the rocks and the low water activity (methane-forming reaction consumes water: $CO_2 + 2\ H_2O = CH_4 + 2\ O_2$) would effectively prevent unmixing of an NaCl-rich hydrous fluid phase. Accordingly, Kogarko (1974), Kogarko & Romanchev (1983), Wallace *et al.* (1990) and Sørensen (1997) argued that HFSE and volatile elements are kept in the melt which then gradually evolves towards silica-rich sodic aqueous solutions. Therefore, the melt would become highly enriched in alkalis and halogens compared to the differentiation products of similar parental magma compositions which exsolve a fluid phase at an earlier stage. This

could be a prerequisite for the enrichment of HFSE complexed by halogens and for the formation of Na-HFSE-(halogen) minerals such as eudialyte.

Reduced conditions seem to be important for the evolution of strongly peralkaline and especially agpaitic rocks as evidenced by the studies of Konnerup-Madsen & Rose-Hansen (1982, 1984), Markl *et al.* (2001), Ryabchikov & Kogarko (2006), and Krumrei *et al.* (2007). In particular, the evolution and influence of a CH_4-bearing fluid phase seems to be of major significance (e.g. Nivin *et al.*, 2001; 2002; 2005; Markl *et al.*, 2001; Potter *et al.*, 2004; Beeskow *et al.*, 2006; Salvi & Williams-Jones, 2006; Ryabchikov & Kogarko, 2006; Krumrei *et al.*, 2007). Several hypotheses for methane formation in peralkaline intrusive rocks have been suggested: (1) Primary magmatic methane (e.g. Markl *et al.*, 2001; Krumrei *et al.*, 2007); (2) Late-magmatic reduction of a CO_2-H_2O rich primary fluid due to closed-system cooling (e.g. Petersilie & Sørensen, 1970; Konnerup-Madsen & Rose Hansen, 1982; Konnerup-Madsen, 2001; Ryabchikov & Kogarko, 2006); (3) late- to post-magmatic Fischer-Tropsch-type reactions (Salvi & Williams-Jones, 1997; Potter & Konnerup-Madsen, 2003; Potter *et al.*, 2004). In all these scenarios, the redox-reaction

$$CO_2 + 2\ H_2O = CH_4 + 2\ O_2 \qquad \text{(eq.1)}$$

plays a key role. Investigations of the redox conditions during the crystallisation of peralkaline magmas are clearly crucial for understanding the details of the processes mentioned above.

In this respect, it is particularly useful to study the Motzfeldt intrusion in the Gardar Province of South Greenland, as its petrology is well known from the work of Jones (1980; 1984; Jones & Larsen, 1985) and it shows a transition from miaskitic to agpaitic rocks. We will show that the formation of agpaitic rocks in the Motzfeldt complex is a strong function of redox conditions.

REGIONAL GEOLOGY

The Gardar Province is a failed rift within which magmatic activity lasted from ca. 1350 to 1120 Ga (Upton *et al.*, 2003). It is characterised by 12 major intrusions (Fig. 1) which comprise carbonatites, gabbros, granites and nepheline syenites. Several intrusions including Ilímaussaq, Motzfeldt and Qoroq contain agpaitic nepheline syenites with eudialyte and other complex Na-Zr-Ti silicates instead of miaskitic zircon and Fe-Ti oxides. Numerous dyke swarms presumably served as feeders for extensive regional volcanism evidenced by the basalts of the Eriksfjord Formation (Escher & Watt, 1970; Upton *et al.*, 2003) which also includes quartzitic sandstones.

The 1.275 Ga old Motzfeldt intrusion (Upton *et al.*, 2003) forms part of to the large Igaliko complex which also includes the Qoroq and Igdlerfigssalik intrusions (Emeleus & Harry, 1970, Fig. 1). It intruded the Julianehåb batholith of the 1.8 Ga Ketilidian orogen (Garde *et al.*, 2002) at a depth of ca. 4 to 6 km (Jones, 1980). The Motzfeldt intrusion mainly comprises nepheline syenites in which a number of several hundred meter long rafts of Eriksfjord basalts are embedded (Fig. 1). The intrusion was first mapped by Emeleus & Harry (1970). Jones (1980) provided a detailed petrological investigation of the intrusive units SM1 to SM6 which he defined based on cross-cutting relationships in the field (Fig. 1). The whole-rock geochemistry and mineralogy of the main rock-forming minerals were studied in detail by Jones (1980, 1984), Jones & Peckett (1980), Jones & Larsen (1985), and Bradshaw (1988). The complex attracted economic interest during the Syduran project (Armour-Brown *et al.*, 1983; Tukiainen *et al.*, 1984) when considerable amounts of Nb were discovered, especially in the NE part of the intrusion in unit SM1. In this contribution, we use the SM1 to SM6 nomenclature of Emeleus & Harry (1970) and Jones (1980) instead of the more complex one proposed by Tukiainen *et al.* (1984) as this is better suited for addressing the transition from miaskitic to agpaitic rocks. Furthermore, it is easier to compare our data with the earlier data of Jones (1980, 1984), Jones & Peckett (1980) and Jones & Larsen (1985).

PETROGRAPHY

Samples from units SM1, SM2, SM4, SM5 and SM6 (Table 1) were studied. In general, these rocks are miaskitic to agpaitic (± nepheline) syenites, interpreted to have originated from different magmat batches (Jones, 1980). Detailed petrographic descriptions can be found in Jones (1980, 1984) and we summarise here only the most important information necessary to support our line of argument.

Miaskitic units SM1-SM5

The miaskitic units SM1, SM2, SM4 and SM5 are very uniform in terms of their mineral assemblages, but they vary in modal composition and grain size. Rock-forming minerals are amphibole, clinopyroxene, feldspar, nepheline, Fe-Ti oxides and accessory zircon, apatite, aenigmatite and pyrochlore (Jones, 1984).

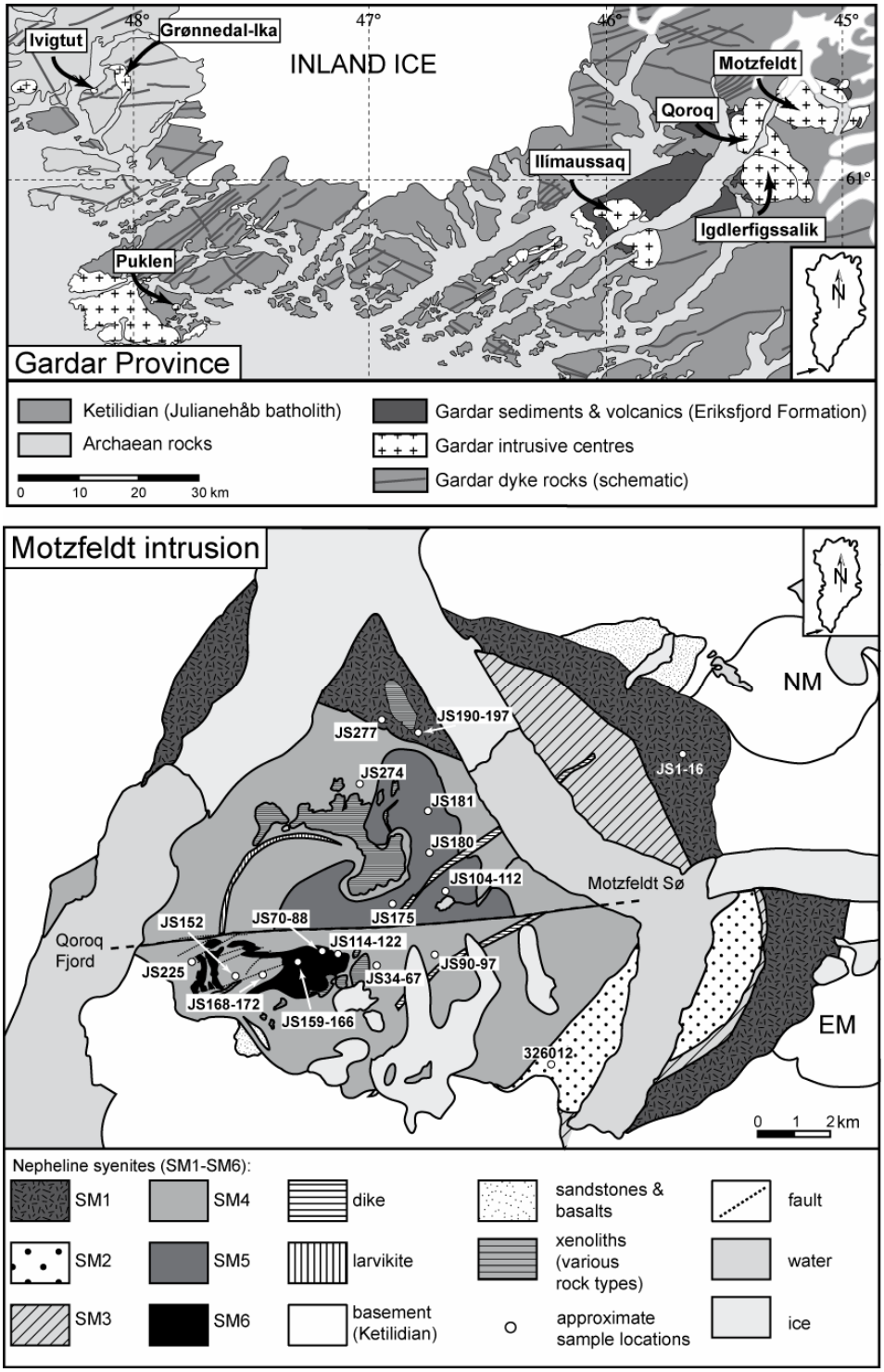

Figure 1 Top: Geological overview of the Gardar Province (modified after Upton & Emeleus, 1987). Bottom: Geological map of the Motzfeldt intrusion (modified after Emeleus & Harry, 1970 and Jones, 1980; NM, EM = North Motzfeldt and East Motzfeldt satellite intrusions).

Table 1 Investigated samples indicating the type of analyses performed.

	SM1											SM2	SM4								
JS	**1**	**3**	**6**	**9**	**10**	**16**	**190**	**195**	**196**	**197**	**277**	**326012**	**34**	**36**	**67**	**90**	**91**	**97**	**152**	**168**	**171**	**172**
m	x	x						x	x	x		x		x				x			x	x
sep									x	x		x									x	x
fl			x	x	x	x	x			x	x		x			x	x		x	x	x	x
flis			x	x		x											x					
IC			x	x		x					x								x	x		
CC															x							
	SM4		**SM5**									**SM6**										
JS	**225**	**274**	**104**	**105**	**108**	**109**	**110**	**112**	**175**	**180**	**181**	**70**	**88**	**114**	**122**	**159**	**162**	**163**	**164**	**165**	**166**	
m				x	x			x		x	x	x		x		x	x	x	x	x	x	
sep					x					x		x		x		x						
fl	x	x	x		x	x	x		x	x			x		x							
flis	x	x				x			x						x							
IC	x	x				x			x													
CC						x					x					x			x			

Note: m = microprobe, sep = O, H, Sm/Nd isotopes from mineral separates, fl = fluid inclusion analysis, flis = fluid isotopes, IC = ion chromatography, CC = carbonate isotopes

Unit SM1 consists of < 1 cm size grains, nepheline is absent and pyroxene is rare in the investigated samples. However, Jones (1980) described nepheline and/or pyroxene-bearing varieties. Some samples contain primary magmatic fluorite (JS190, JS195, JS197; Schönenberger *et al.*, 2008). SM2 (only one sample provided by H. Emeleus) consists of large, turbid feldspar laths (Fig. 2a) with interstitial brownish amphibole. The samples from unit SM4 (JS36, JS97, JS171, JS172) are relatively fine-grained (grain size < 0.5 cm). Amphibole is occasionally poikilitic (Fig. 2d). Rinkite occurs intergrown with Fe-Ti oxides (Fig. 2e). The minerals in SM5 are much coarser (< 2 cm) than in the other units. Feldspar characteristically forms several cm long laths. Occasionally, colourless to slightly green clinopyroxene occur as cores within brown amphibole (Fig. 2h). Rare sodalite forms interstitial grains.

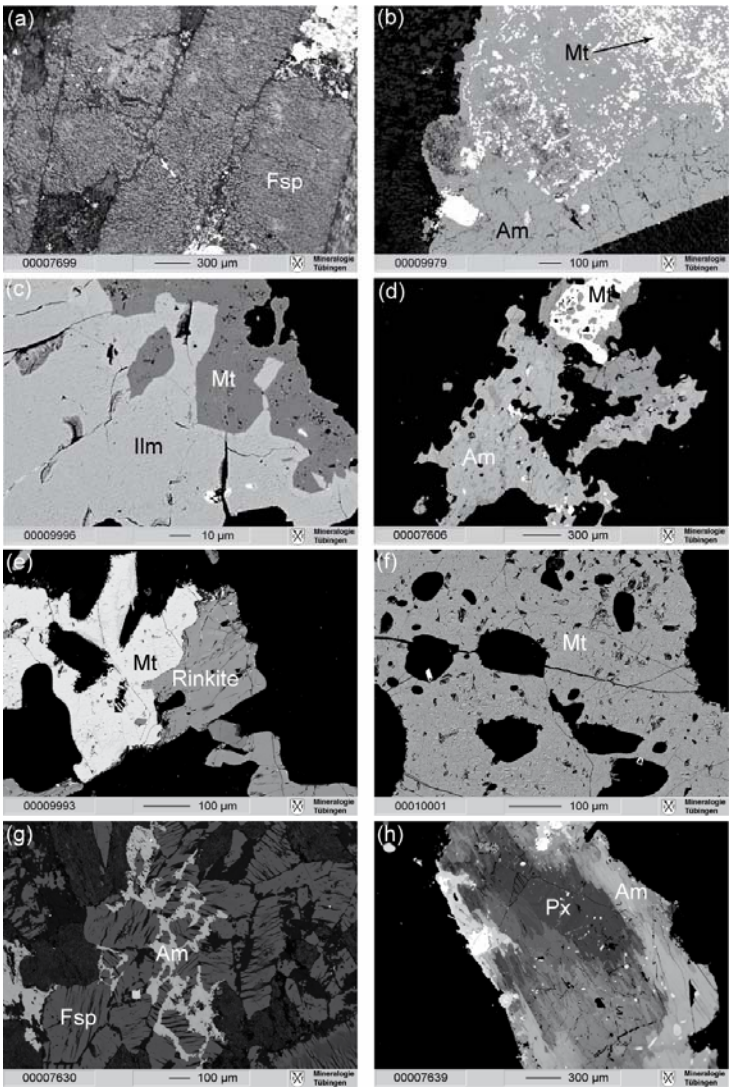

Figure 2 Textures observed in the miaskitic units (BSE images). (a) heterogeneously exsolved alkali feldspars in SM2 (326012). (b) Amphibole in unit SM1. It is altered to secondary amphibole with magnetite intergrowths. (c) Ilmenite and magnetite of SM1 (JS196) interpreted to have crystallized simultaneously. (d) Amphibole of SM4 (JS97) with inclusions of pyroxene and magnetite. (e) Magnetite and rinkite intergrown in unit SM4 (JS172). (f) Finely exsolved magnetite of SM4 (JS171). (g) Typical amphibole-feldspar association in SM5 (JS180). (h) Complex pyroxene-amphibole texture from SM5 (JS108) where a core of primary pyroxene is rimmed by secondary amphibole.

Alteration phenomena include the common turbidity of feldspars and replacement of amphibole by green pyroxene especially in units SM1, SM2 and SM5. SM1 is the most altered unit. Secondary minerals such as biotite, fluorite, quartz, titanite, and hematite are common. Calcite and cancrinite occur mainly as alteration products of nepheline, but also of feldspars in all units. Furthermore, calcite was observed in thin veinlets cutting all other rock types. Secondary veins consist of fluorite and/or quartz (SM1), fluorite ±calcite, ±aegirine (SM4) and fluorite ±feldspar (SM5). The unusual occurrence of quartz may be attributed to the assimilation of rafts of the Eriksfjord formation which contain large amounts of quartzitic sandstone.

Agpaitic unit SM6

The samples of unit SM6 are dominated by green, euhedral to hypidiomorphic clinopyroxene, large euhedral nepheline and feldspar laths together with interstitial nepheline, eudialyte and minor amounts of fluorite and sodalite (Fig. 3). Amphibole is rare (Jones, 1980, 1984) and does not occur at all in the studied samples. The nepheline syenitic rocks of unit SM6 are called "lujavrites" based on their textural similarity to rocks from the Kola peninsula, Russia, and the Ilímaussaq intrusion in the Gardar Province. Magmatic modal layering is common and three distinct varieties of rocks can be defined: white (feldspar-dominated), green (pyroxene- & nepheline-dominated) and black (pyroxene-dominated) lujavrite (c.f. Jones, 1980, 1984). The eudialyte in these rocks is especially heavily altered to complex REE-bearing phases (Fig. 3). Alteration products are cancrinite, zircon, calcite, pectolite and trace element(REE)-rich minerals such as catapleiite, zirfesite, pyrochlore and others (Jones, 1980; Jones & Larsen, 1985). Comparable alteration phenomena were investigated in detail in the nearby Qoroq intrusion (Coulson, 1997).

ANALYTICAL METHODS

All analyses were carried out at the Institut für Geowissenschaften, Universität Tübingen, Germany. A JEOL 8900 electron microprobe was used for analysing minerals for their major element contents. It was calibrated using natural and synthetic standards. The beam current was 15 nA and acceleration voltage 15 kV. Counting time on the peak positions ranged between 16s for major elements and 60s for minor elements while background counting times were half the peak time. A focused electron beam was used; however Fe-Ti oxides, feldspar and nepheline were analysed with a defocused beam (up to 20 μm beam diameter) to avoid

alkali migration and/or to obtain average compositions. The overlap of F Kα and Fe Lβ peaks was corrected and an internal ϕρZ correction (Armstrong, 1991) was applied. Analytical uncertainties are below 1 % (relative) for major elements, reaching up to around 5 % (relative) for minor elements.

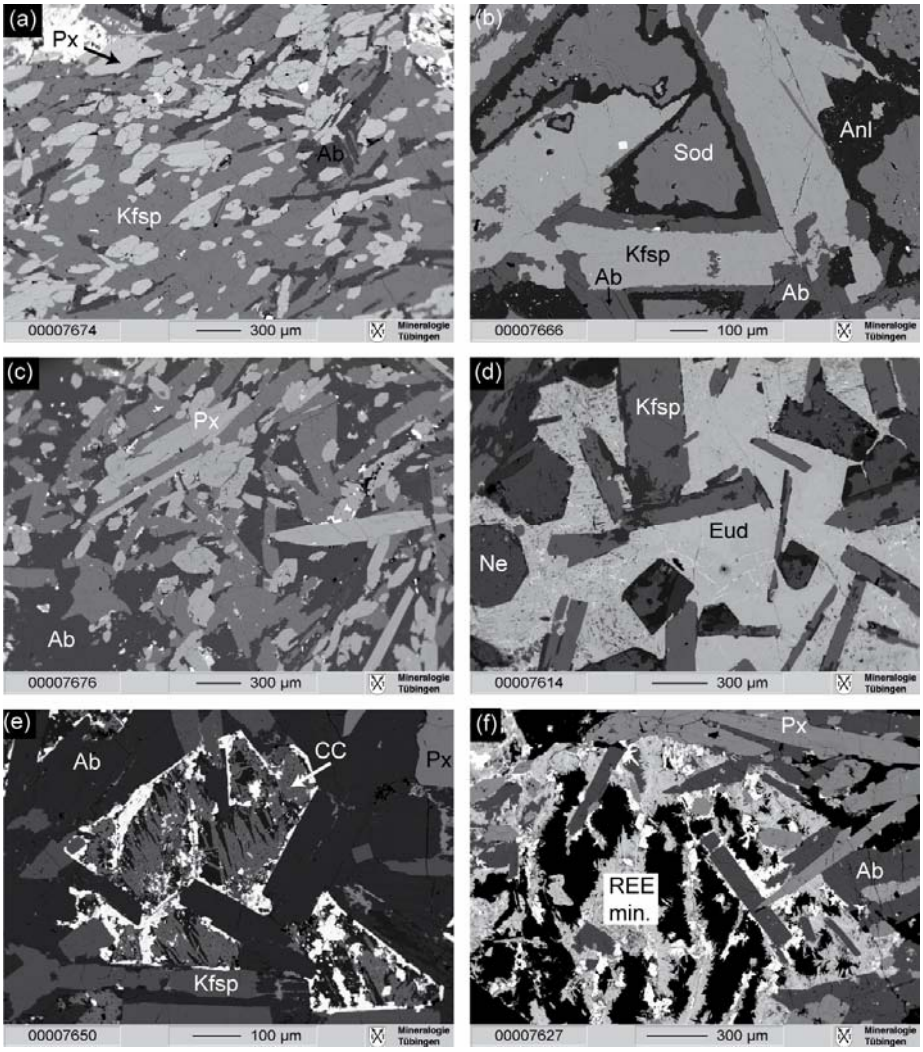

Figure 3 Textures in the agpaitic unit SM6 (BSE images). (a) Typical texture of SM6 with euhedral pyroxenes and albite laths in a matrix of K-feldspar. (b) Large K-feldspar laths rimmed by albite and interstitial sodalite with analcite reaction rim. (c) Euhedral pyroxenes with K-feldspar laths in an albite matrix. (d) Poikilitic eudialyte enclosing slightly altered K-feldspar and nepheline. (e) Typical alteration texture of what may have been eudialyte comprising calcite, albite, zircon and other REE-bearing minerals (bright colours). (f) Complex alteration texture where eudialyte is altered to secondary, complex trace element-rich minerals (REE-min) together with analcite (black).

Details of the oxygen isotope analysis techniques of ca. 10 mg handpicked pyroxene and amphibole mineral separates can be found in Marks *et al.* (2003) who followed the methods of Sharp (1990) and Rumble & Hoering (1994). The determination of the hydrogen

isotopic composition of ca. 50 mg amphibole mineral separates was performed according to the method of Vennemann & O´Neil (1993). Oxygen and hydrogen isotopic compositions were analyzed on a Finnigan MAT 252 mass spectrometer. The analytical precision of the oxygen isotope analyses of the standards (NBS-28 quartz; Valley et. al., 1995) is ± 0.1 ‰ and the precision of the in-house kaolinite standard for hydrogen isotope analyses is ± 2 ‰. All stable isotope analyses in this study are reported in permil (‰) in standard notation relative to VSMOW (oxygen and hydrogen) and VPDB (carbon).

Detailed description of the analyses of the Nd isotopic compositions of ~10 mg of hand-picked mineral separates can be found in Marks *et al.* (2003). After spiking with a ^{150}Nd-^{149}Sm tracer, the samples were dissolved in HF acid at 180 °C in poly-tetrafluor-ethylene (PTFE) reaction bombs. Sm and Nd were separated in quartz columns using 1.7 ml Teflon powder coated with HDEHP (Di-Ethyl Hexyl Phosphate) for cation exchange. A Finnigan MAT262 thermal ionization mass spectrometer (TIMS) was used. Analyses of the LaJolla standard yielded a ^{143}Nd/^{144}Nd ratio of 0.511824 ±10 (±2σ error, n = 13). The blank of the total procedure (chemistry & loading) was < 100 pg for Nd. The decay constant of Lugmair & Marti (1978) was used for ^{147}Sm ($6.54 * 10^{-12}$ a^{-1}). Present day CHUR values of 0.1967 (^{147}Sm/^{144}Nd; Jacobson & Wasserburg, 1980) and 0.512638 (^{143}Nd/^{144}Nd; Goldstein *et al.*, 1984) were applied to calculate $\varepsilon_{Nd}(t)$ values. Initial Nd isotope ratios were corrected for an age of 1.275 Ga (Upton *et al.*, 2003; McCreath, unpublished data). The uncertainty in $\varepsilon_{Nd}(t)$ ratios is < 0.5 based on analytical errors.

For fluid inclusion investigations, doubly polished, 100-300 µm thick wafers from nepheline, fluorite and quartz were analysed using a Leica DMLP microscope and a Linkam THMS 600 heating-cooling stage for fluid petrography and microthermometry. The heating-cooling stage was calibrated using synthetic CO_2 and H_2O standards. The accuracy of melting and homogenisation temperatures is ±0.2 and ±2.0 °C, respectively. Raman spectroscopy was performed on a Dilor Jobin Yvor Raman spectroscope. Fluid inclusions and the mineral matrix were analysed using a blue argon laser (488 nm) for a wave number range between 600 to 4500 cm^{-1}. Counting times varied between 10 and 60s.

Bulk chemistry of the fluid inclusions was determined using a Dionex ICS1000 ion chromatography system with a CS-12A cation column and an AS9-HC anion column. All samples were treated with concentrated (65 %) HNO_3 at 60-70 °C in a sand bath for 4 hours and washed with triple deionised water for 7 days in order to prevent any contamination from the HNO_3 washing procedure. After having ground 2 g of each sample in an agate mortar, the salts were dissolved in 10 ml triple deionised water. For anions, 5 ml were injected. 10 µl of

33 % HNO_3 were added to the remaining 5 ml to ensure a pH value between 2 and 3 required for the cation column. The run time of the samples was 30 minutes. Analytical errors are in the range of 20 % relative (Köhler *et al.*, 2008).

Fluid inclusions in fluorite samples were analysed for their C, H and O isotopic composition using the low temperature crushing method described by Friedman (1953), Craig (1961) and Vennemann & O'Neil (1993). The samples were carefully hand-picked, dried and mechanically crushed. Fluorite which was found to be finely intergrown with carbonate was treated with concentrated HNO_3 prior to analysis in order to preclude any contamination effect on the fluid inclusion content. δD, $\delta^{18}O$ and $\delta^{13}C$ values of hydrocarbons, CO_2 and H_2O were measured on a Finnigan MAT-252 mass spectrometer. The analytical error is 0.3 ‰ for oxygen and carbon and better than 6 ‰ for hydrogen.

To analyze the isotopic composition of the calcite daughter crystals, one fluorite sample (JS109) was thoroughly washed with concentrated HCl to remove possible carbonate intergrowths. This sample was heated to 1000 °C in the same analytical set-up as that used for the isotope analyses of the fluid inclusions in order to thermally decompose the calcite daughter crystals (e.g. Hollemann & Wiberg, 1995). The thermal decomposition of calcite proceeds according to the reaction $CaCO_3$ ➔ CaO (solid) + CO_2 (gas, measured; Hollemann & Wiberg, 1995). Significant fractionation of oxygen isotopes can be ruled out at the high temperatures used (ca. 1000 °C; e.g. Zheng, 1999).

The oxygen and carbon isotopic composition of carbonates were analysed according to the method described by Spötl & Vennemann (2003) with a ThermoFinnigan GasBench which is connected directly to a Finnigan MAT 252 mass spectrometer. 100% orthophosphoric acid was added to <500 mg of carbonate powder or several g of whole-rock powder to release the CO_2 from the sample. In order to remove water vapour and interfering gases, the CO_2 vapour was led via a He stream and a gas chromatograph column. Subsequently the CO_2 was passed into the mass spectrometer. The standard analytical errors are 0.1 ‰ for $\delta^{13}C$ and $\delta^{18}O$. As petrographic investigations showed that apart from carbonates, cancrinite may also be present in the samples, test measurements were performed in order to only extract the CO_2 from calcite and not from cancrinite. These measurements yielded excellent values for a reaction time of 85 min where > 98 vol.% of calcite reacted whereas only minor amounts of CO_2 from cancrinite were detected (< 2 vol.%).

RESULTS

Mineral Chemistry

Electron microprobe analyses were carried out on minerals of units SM1, SM2, SM4, SM5 and SM6. Only a brief summary of the data is given here, as Jones (1980, 1984) has already characterised the mineral chemistry of the different intrusive phases in detail.

Amphibole

The composition of the amphiboles from units SM1-SM5 (Table 2) is mainly characterised by the exchange CaAl ⇔ NaSi and ranges from Ca-dominated via Na-Ca to Na-dominated compositions including taramite, katophorite, Ferro-nyböite and arfvedsonite (Leake *et al.*, 1997). Fe^{3+} is mostly below 1 apfu. The fluorine content is around 1 wt.% (SM1, SM2, SM4) but reaches up to 3.5 wt.% (= 1.7 apfu) in unit SM1. However, amphiboles from SM5 exhibit larger variations obeying the F-Fe avoidance rule (e.g. Marks *et al.*, 2003; Schönenberger *et al.*, 2006).

Clinopyroxene

The composition of the pyroxenes varies from diopside/hedenbergite-dominated pyroxenes via aegirine-augite to almost pure aegirine-endmember pyroxenes (Table 3, Fig. 4). The diopside/hedenbergite-rich pyroxenes mainly occur in SM4 and SM5 as cores which are overgrown by aegirine-augite. Jones (1980) also described such pyroxenes from units SM1 and SM2 (Fig. 4). Unit SM6 only crystallised almost pure aegirine. The jadeite content increases with increasing $NaFe^{3+}$ content, but does not exceed 8 mol%. ZrO_2 reaches up to 1.2 wt.% in our samples, but has been reported to attain up to 6.96 wt.% (Jones, 1980; Jones & Peckett, 1980).

Table 2 Representative microprobe analyses of Motzfeldt amphiboles.

JS	195	197	326012	97	171	105	108
wt %	SM1	SM1	SM2	SM4	SM4	SM5	SM5
SiO_2	43.86	47.56	39.30	41.96	42.50	44.02	45.14
TiO_2	1.81	0.99	1.55	1.69	1.38	2.78	1.77
Al_2O_3	5.54	3.00	8.68	6.78	6.01	7.04	5.21
FeO	27.91	27.39	31.59	31.09	28.86	19.02	22.87
MnO	1.06	1.12	1.51	1.44	1.68	0.94	1.46
MgO	4.23	5.17	1.11	1.36	3.01	9.14	7.03
CaO	6.89	3.59	8.57	7.21	6.99	9.97	7.68
Na_2O	5.10	6.90	4.05	4.72	5.00	3.76	5.05
K_2O	1.53	1.35	1.61	1.75	1.71	1.55	1.61
ZrO_2	0.32	0.33	0.36	0.29	0.32	0.12	0.38
Cl	0.00	0.03	0.05	0.01	0.02	0.02	0.01
F	0.98	1.65	0.23	0.18	0.68	1.74	1.28
Total	99.23	99.08	98.61	98.48	98.16	100.1	99.49
formula based on 16 cations and 23 anions							
Si	6.90	7.42	6.33	6.73	6.79	6.72	6.96
Al	1.03	0.55	1.65	1.28	1.13	1.27	0.95
Ti	0.21	0.12	0.19	0.20	0.17	0.32	0.21
Fe^{3+}	0.55	0.67	0.85	0.63	0.81	0.04	0.48
Mg	0.99	1.20	0.27	0.32	0.72	2.08	1.62
Fe	3.12	2.90	3.40	3.55	3.04	2.39	2.47
Mn	0.14	0.15	0.21	0.20	0.23	0.12	0.19
Ca	1.16	0.60	1.48	1.24	1.20	1.63	1.27
Na	1.56	2.09	1.27	1.47	1.55	1.11	1.51
K	0.31	0.27	0.33	0.36	0.35	0.30	0.32
Zr	0.02	0.03	0.03	0.02	0.02	0.01	0.03
Cl	0.00	0.01	0.01	0.00	0.00	0.00	0.00
F	0.49	0.81	0.12	0.09	0.34	0.84	0.62
Sum	16.00	16.00	16.00	16.00	16.00	16.00	16.00

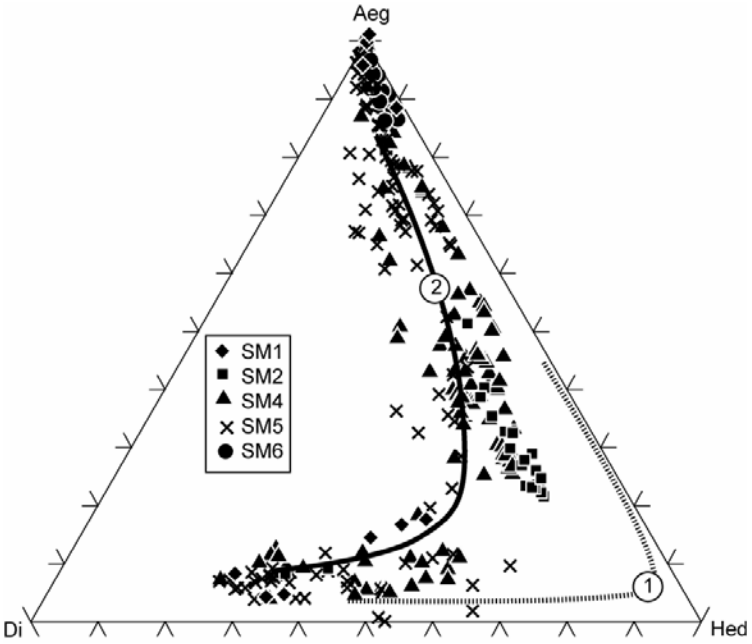

Figure 4 Evolution of pyroxene composition in the diopside-hedenbergite-aegirine triangle (data from this study and Jones, 1980). For comparison: Stippled curve 1 = general trend of clinopyroxene evolution in the Ilímaussaq intrusion (Larsen, 1976). Solid curve 2 = general trend of clinopyroxene evolution in the Grønnedal-Ika intrusion (Halama *et al*., 2005).

Fe-Ti oxides

The Fe-Ti oxides from units SM1, SM4, SM5 and SM6 (Table 4) are titanomagnetites which are commonly heterogeneously exsolved to magnetite with lamellae of the hematite-ilmenite-pyrophanite solid solution series. In unit SM1, textures suggest that ilmenite ($Ilm_{77-85}Hm_{3-7}Pyr_{10-19}$) and titanomagnetite ($Mt_{56-74}Usp_{44-36}$) crystallised as (primarily) separate grains (Fig. 2). Finely exsolved titanomagnetite from SM4 (Fig. 2) shows reintegrated average compositions of $Mt_{69-78}Usp_{31-22}$. Reintegrated titanomagnetites from SM5 usually show compositions of $Mt_{50-56}Usp_{50-44}$ while few compositions reach extreme values of $Mt_{37}Usp_{63}$. Magnetites occurring as alteration products of amphibole (e.g. sample JS180, SM5; but also in other samples from SM1, SM4) commonly have a composition of $Mt_{>90}Usp_{<10}$. In SM6, no primary Fe-Ti oxide phase is present but almost pure hematite ($Hm_{94-99}Ilm_{0-5}Pyr_{0-2}$) occurs as an alteration product of aegirine.

Table 3 Representative microprobe analyses of Motzfeldt clinopyroxenes.

JS	1	326012	97	171	171	172	108	180	180	114	166
wt %	SM1	SM2	SM4	SM4	SM4	SM4	SM5	SM5	SM5	SM6	SM6
SiO_2	52.77	49.01	49.41	49.50	50.90	48.69	50.06	50.75	52.98	52.10	51.80
TiO_2	2.69	0.30	0.75	0.23	0.22	0.32	0.38	0.56	1.29	0.35	0.37
Al_2O_3	0.80	0.87	2.06	0.86	0.90	0.86	0.77	1.18	1.79	0.95	1.10
FeO	27.58	25.20	17.84	24.47	24.76	24.91	23.03	13.55	27.08	28.55	28.27
MnO	0.02	1.86	0.93	1.41	0.95	1.42	1.52	0.94	0.50	0.29	0.38
MgO	0.04	1.11	6.88	1.76	1.89	1.55	2.74	9.91	0.27	0.10	0.12
ZrO_2	0.06	0.31	0.09	0.37	0.41	0.31	0.88	0.12	0.15	0.72	0.42
CaO	0.04	18.17	22.17	15.56	9.87	18.10	16.62	22.49	0.67	1.79	2.22
Na_2O	13.91	2.82	0.71	4.68	8.26	3.22	3.69	0.95	13.44	12.79	12.58
Total	97.91	99.65	100.84	98.84	98.16	99.38	99.69	100.45	98.17	97.64	97.26
					formula based on 6 oxygens and 4 cations						
Si	1.99	1.97	1.91	1.96	1.97	1.95	1.98	1.92	1.99	1.99	1.98
Al	0.04	0.04	0.09	0.04	0.04	0.04	0.04	0.05	0.08	0.04	0.05
Ti	0.08	0.01	0.02	0.01	0.01	0.01	0.01	0.02	0.04	0.01	0.01
Cr	0.00	0.00	0.00	0.00	0.00	0.00	0.00	0.00	0.00	0.00	0.00
Fe^{3+}	0.85	0.23	0.10	0.38	0.62	0.30	0.27	0.14	0.85	0.91	0.90
Mg	0.00	0.07	0.40	0.10	0.11	0.09	0.16	0.56	0.02	0.01	0.01
Fe	0.02	0.62	0.48	0.43	0.18	0.53	0.49	0.29	0.01	0.00	0.01
Mn	0.00	0.06	0.03	0.05	0.03	0.05	0.05	0.03	0.02	0.01	0.01
Zr	0.00	0.01	0.00	0.01	0.01	0.01	0.02	0.00	0.00	0.01	0.01
Ca	0.00	0.78	0.92	0.66	0.41	0.77	0.70	0.91	0.03	0.07	0.09
Na	1.02	0.22	0.05	0.36	0.62	0.25	0.28	0.07	0.98	0.95	0.93
Sum	4.00	4.00	4.00	4.00	4.00	4.00	4.00	4.00	4.00	4.00	4.00

Table 4 Representative microprobe analyses of Fe-Ti oxides.

JS	196	196	196	171	172	172	108	180	180	180	181	164	166
	SM1	SM1	SM1	SM4	SM4	SM4	SM5	SM5	SM5	SM5	SM5	SM6	SM6
wt. %	Ilm	Mt	Mt	Mt	Mt	Hm	Mt	Mt	Ilm	Ilm	Mt	Hm	Hm
TiO_2	51.10	12.12	1.88	8.01	9.32	0.08	16.00	22.19	51.11	51.23	19.69	0.62	2.80
Al_2O_3	0.02	0.11	0.09	0.18	0.19	0.10	0.13	0.06	0.01	0.00	0.08	0.05	0.36
FeO	40.80	81.41	90.45	84.94	83.61	90.37	76.76	71.85	38.45	41.06	74.37	89.27	86.14
MnO	8.30	2.13	0.37	1.72	1.68	0.06	2.98	3.09	10.68	7.44	2.37	0.36	0.35
MgO	0.00	0.00	0.00	0.02	0.00	0.01	0.00	0.00	0.00	0.00	0.03	0.00	0.00
Total	100.22	95.77	92.79	94.87	94.80	90.62	95.87	97.19	100.25	99.73	96.54	90.30	89.65
formula based on 2 (3) cations and 3 (4) anions for ilmenite (Ilm)and hematite (Hm) (magnetite)													
Al	0.00	0.00	0.00	0.01	0.01	0.00	0.01	0.00	0.00	0.00	0.00	0.00	0.01
Ti	0.97	0.35	0.05	0.23	0.27	0.00	0.46	0.63	0.96	0.97	0.56	0.01	0.06
Fe^{3+}	0.07	1.30	1.88	1.53	1.45	1.98	1.08	0.74	0.07	0.05	0.87	1.97	1.84
Mg	0.00	0.00	0.00	0.00	0.00	0.00	0.00	0.00	0.00	0.00	0.00	0.00	0.00
Fe	0.79	1.28	1.04	1.17	1.21	0.01	1.36	1.53	0.74	0.81	1.48	0.01	0.06
Mn	0.18	0.07	0.01	0.06	0.05	0.00	0.10	0.10	0.23	0.16	0.08	0.01	0.01
Sum	2.00	3.00	3.00	3.00	3.00	2.00	3.00	3.00	2.00	2.00	3.00	2.00	2.00

Feldspars

Feldspars commonly exhibit coarse perthitic exsolution textures (Fig. 2, SM1-SM5). The composition of the reintegrated feldspar grains is: SM1 $Ab_{57-73}Or_{27-43}$; SM2 $Ab_{47-65}Or_{45-53}$; SM4 and SM5 $Ab_{37-52}Or_{48-63}$. This corresponds to an increase in the Or component from SM1 to SM5. The anorthite content of the feldspars is always < An_1. In SM6 two separate feldspars of almost endmember composition ($Ab_{>98}Or_{<2}$ and $Ab_{<5}Or_{>95}$) crystallized as noted by Jones (1980) and Jones & Larsen (1985).

Nepheline

Because of the strong alteration of nepheline within our samples from units SM1 and SM2, nepheline was analysed in units SM4 to SM6 only. Its composition ranges from $Ne_{74}Ks_{16}Qz_{10}$ to $Ne_{76}Ks_{22.6}Qz_{0.4}$ (Fig. 5). Jones (1980) and Jones & Larsen (1985) report nephelines from other units with similar compositions.

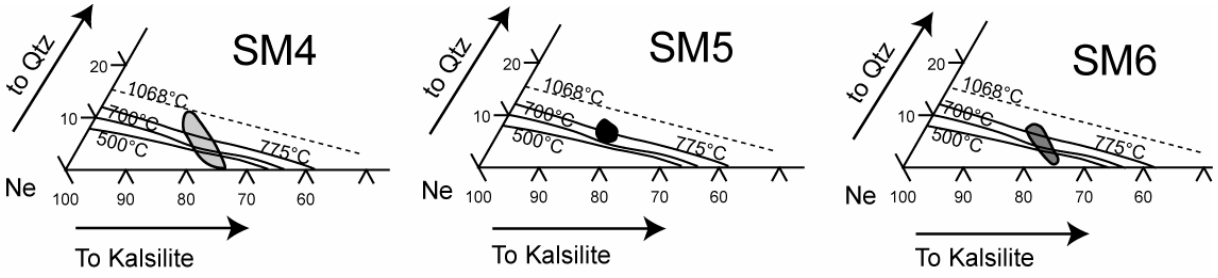

Figure 5 Composition of nepheline analysed in this study with isotherms from Hamilton (1961). The compositions are very similar to those reported by Jones (1980).

Isotopic composition of mineral separates

The isotopic composition (O, H, Nd, Table 5) of amphibole was determined from SM1 (JS195, 196), SM2 (326012), SM4 (JS171, JS172) and SM5 (JS108, JS181) and of pyroxenes from SM6 (JS70, JS114, JS159).

The $\delta^{18}O$ values range from +4.2 to +5.3 ‰ (VSMOW, Fig. 6). Samples from SM1 have the lowest values (+4.2 and +4.6 ‰). The δD of amphibole varies between -98 and -132 ‰ (VSMOW) with SM1 and SM2 having the lowest values of -120.1, -127.6 and -132.3 ‰, respectively.

Initial $\varepsilon_{Nd}(t)$ values (T = 1.275 Ga; Upton *et al.*, 2003; McCreath, pers. comm. 2007) for the mineral separates range from +0.1 to +2.4. SM1 and SM2 have the lowest values while SM4 and SM5 are similar to the values from SM6 (+0.9 to +2.4, Fig. 6).

Carbon and oxygen isotope compositions of carbonates were analysed for three whole-rocks from units SM5 and SM6 (JS159, JS164, JS181, Table 6) which contain finely disseminated calcite occurring as alteration products and/or in very small veinlets. $\delta^{13}C$ values range from -2.1 to -3.2 ‰ (VPDB, Fig. 7). The oxygen isotopic compositions of these samples varies from +21.9 to +24.2 ‰ (VSMOW). Additionally, calcite from one calcite vein within SM4 (JS67, Table 6) yielded a $\delta^{13}C$ value of -4.4 ‰ (VPDB) and a $\delta^{18}O$ of +7.8 ‰ (VSMOW). Calcite crystals from fluid inclusions analyzed in one sample (JS109,Table 6) have $\delta^{13}C$ and $\delta^{18}O$ values of -3.9 ‰ and +8.1 ‰, respectively.

Table 5 Nd, O and H isotopic compositions of mineral separates. $\varepsilon_{Nd}(i)$ was corrected to the time of emplacement at about 1.275 Ga (Upton et al., 2003); $\delta^{18}O$ and δD in ‰ (VSMOW). T_{DM} (Ga) Nd model ages relative to the depleted mantle (Liew *&* Hofman, 1987).

sample	unit	min	Sm (ppm)	Nd (ppm)	$^{147}Sm/^{144}Nd$	$^{143}Nd/^{144}Nd$		$\varepsilon Nd_{(i)}$	T_{DM} (Ga)	$\delta^{18}O$	δD
JS195	SM1	Am	48.52	286.06	0.1026	0.511857	±6	0.14	1.77	4.2	-120.1
JS196	SM1	Am	35.29	208.78	0.1022	0.511877	±8	0.60	1.74	4.6	-127.6
326012	SM2	Am	84.23	526.96	0.0966	0.511818	±9	0.36	1.73	5.3	-132.3
JS171	SM4	Am	20.98	141.91	0.0894	0.511799	±9	1.17	1.65	4.8	-111.5
JS172	SM4	Am	31.39	202.50	0.0937	0.511842	±7	1.30	1.66	4.7	-109.7
JS108	SM5	Am	14.73	90.50	0.0984	0.511898	±10	1.63	1.65	5	-119.1
JS180	SM5	Am	28.28	169.84	0.1007	0.511923	±9	1.74	1.65	5	-98.5
JS70	SM6	Px	4.14	19.16	0.1307	0.512131	±8	0.90	1.86	5.1	n.a.
JS114	SM6	Px	1.70	12.70	0.0811	0.511793	±9	2.40	1.56	4.9	n.a.
JS159	SM6	Px	3.80	18.13	0.1267	0.512123	±10	1.40	1.79	4.9	n.a.

sample	unit	type	$\delta^{13}C$	$\delta^{18}O$
JS67	SM4	vein	-4.4	7.8
JS109	SM5	cryst.	-3.9	8.1
JS181	SM5	wr	-3.2	24.2
JS159	SM6	wr	-2.2	21.9
JS164	SM6	wr	-2.1	21.9

Table 6 $\delta^{13}C$ and $\delta^{18}O$ (in ‰ VPDB and VSMOW) isotopic composition of Motzfeldt samples. vein = calcite vein; cryst. = calcite crystals in fluid inclusions; wr = whole rock samples. See text for discussion.

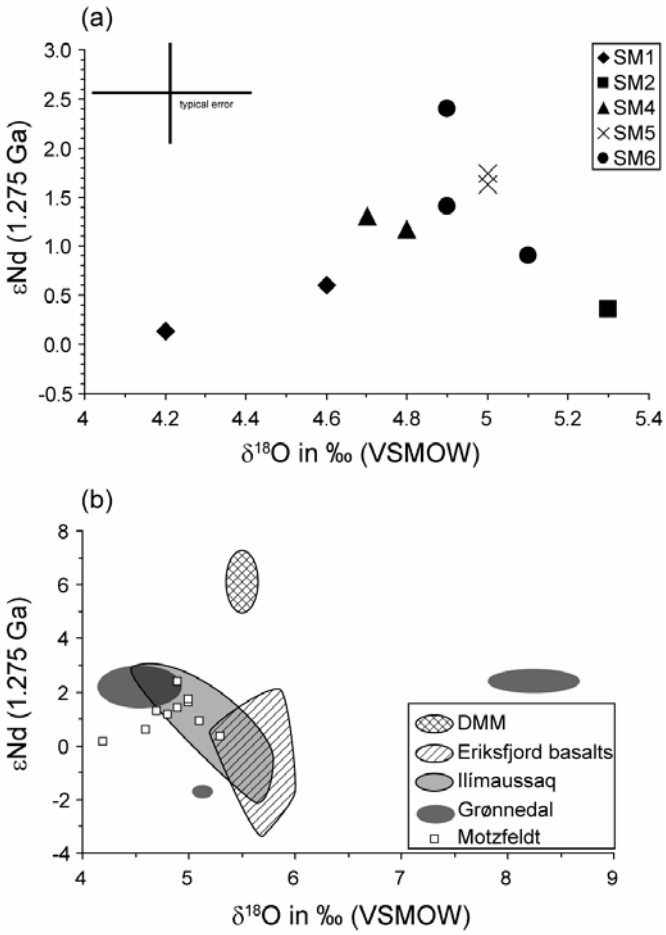

Figure 6 (a) Initial ε_{Nd} (at t=1.275 Ga) vs. $\delta^{18}O$ in ‰ (VSMOW) of amphibole (SM1-SM5) and pyroxene (SM6) mineral separates. (b) Comparison of data obtained in this study with values from the depleted MORB mantle (DMM according to DePaolo, 1981, Goldstein *et al.*, 1984 and Eiler *et al.*, 2000) and other Gardar rocks (Coulson *et al.*, 2003; Halama *et al.*, 2003; 2005; Marks *et al.*, 2004).

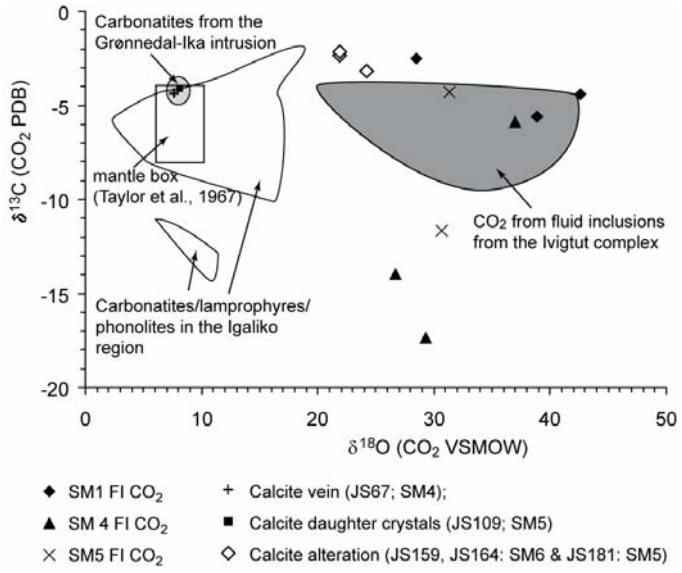

Figure 7 Isotopic composition of CO_2 from fluid inclusions, calcite from veins and altered samples compared with reference data from other Gardar rocks/fluids (Igaliko region: Pearce & Leng, 1996; Coulson *et al.*, 2003; Ivigtut complex: Köhler *et al.*, 2008; Grønnedal-Ika intrusion: Halama *et al.*, 2005).

Fluid inclusion investigations

Petrography and microthermometry

Fluid inclusions were analysed from magmatic fluorites of SM1 (JS190, 197) and SM6 (JS88, JS122; Schönenberger *et al.*, 2008) and magmatic nepheline and feldspar of SM4 and SM5 (JS171, JS172, JS104, JS108, JS180, Fig. 8). Hydrothermal fluorites were studied from units SM1, SM4 and SM5 (Table 1) and secondary hydrothermal quartz in unit SM1 (JS10, JS277). Four different types of fluid inclusions can be distinguished: (1a) saline-aqueous two-phase (liquid-vapour l-v) inclusions; (1b) saline-aqueous three-phase inclusions (liquid-vapour-solid l-v-s); (2) pure CO_2 two-phase (liquid-vapour l-v) inclusions (only in sample JS34); (3) aqueous-CH_4 one or two-phase inclusions. The last fluid inclusion type is unique to the agpaitic unit SM6 whereas the first three types (1a, 1b and 2) only occur in the miaskitic units SM1 to SM5. Inclusions of type (1) also contain trace amounts of CO_2 and CH_4 (detected only during isotope analyses). For the saline-aqueous fluid inclusions, salinities (wt.% NaCl eq.) were calculated according to Bodnar (1993; Table 7, Fig. 9).

(1a) Saline-aqueous two-phase inclusions. These fluid inclusions are the dominant type in the investigated samples. In primary magmatic fluorite of SM1 (Fig. 8a), they mainly occur along (pseudo)secondary trails, have an irregular to rounded shape and reach sizes up to 40 µm. They have salinities of < 3.5 wt.% NaCl eq. and filling ratios of 0.85 to 0.95. The fluid inclusions in magmatic nepheline (units SM4 and SM5) are rectangular and generally < 20 µm in size. They show negative crystal shapes and occur as isolated inclusions or in groups but also in pseudo-secondary trails and have filling ratios between 0.80 and 0.95. The isolated fluid inclusions are interpreted to be of primary origin (Sheperd et al., 1985). Fluid inclusions from SM4 (JS171, JS172) typically have salinities < 2-5 wt.% NaCl eq., but some reach 6 to 7 wt.% NaCl eq. In nephelines from samples of SM5 (JS104, JS108, JS180), most fluid inclusions (80 %) vary in salinity between 4 and 6 wt.% NaCl eq.

Hydrothermally formed (secondary) fluorites of units SM1, SM4 and SM5 mainly contain trails of secondary fluid inclusions and only a few isolated ones. They are commonly of irregular shape, but also rounded to angular (Fig. 8b). The size of fluid inclusions varies from < 5 µm up to 100 µm (Fig. 8). Necking-down was occasionally observed but these fluid inclusions were not further analysed. Filling ratios commonly range from 0.80 to 0.95, but are rather constant within single trails.

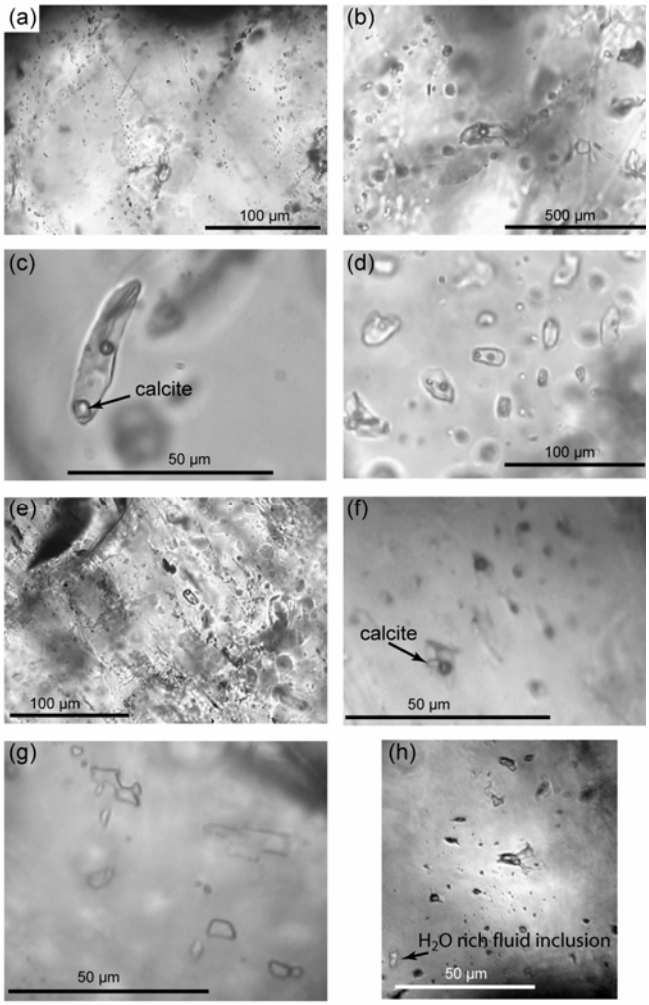

Figure 8 Typical fluid inclusions (FI). (a) Secondary and pseudo-secondary fluid inclusions (FI type (1a)) from JS197 (SM1). (b) Secondary fluid inclusions (FI type (1a)) in SM4 (JS168). (c) Fluid inclusion (FI) with large calcite crystal (FI type (1b); SM1, JS16). (d) Secondary fluid inclusions with calcite crystals (FI type (1b)) in primary magmatic fluorite from SM1 (JS197). (e) Primary fluid inclusion (in the centre of photograph) with large calcite crystal (FI type (1b)) in JS172 (nepheline, SM4). (f) Secondary fluid inclusion with calcite crystals (FI type (1b)) in nepheline (JS180, SM5). (g) Irregular, pure methane fluid inclusions (FI type (3)) in JS88 (SM6). (h) Irregular, pure methane fluid inclusions (FI type (3)) in JS122 (SM6; visible bubble because photograph was taken at -110 °C) in close association with H_2O-rich fluid inclusion.

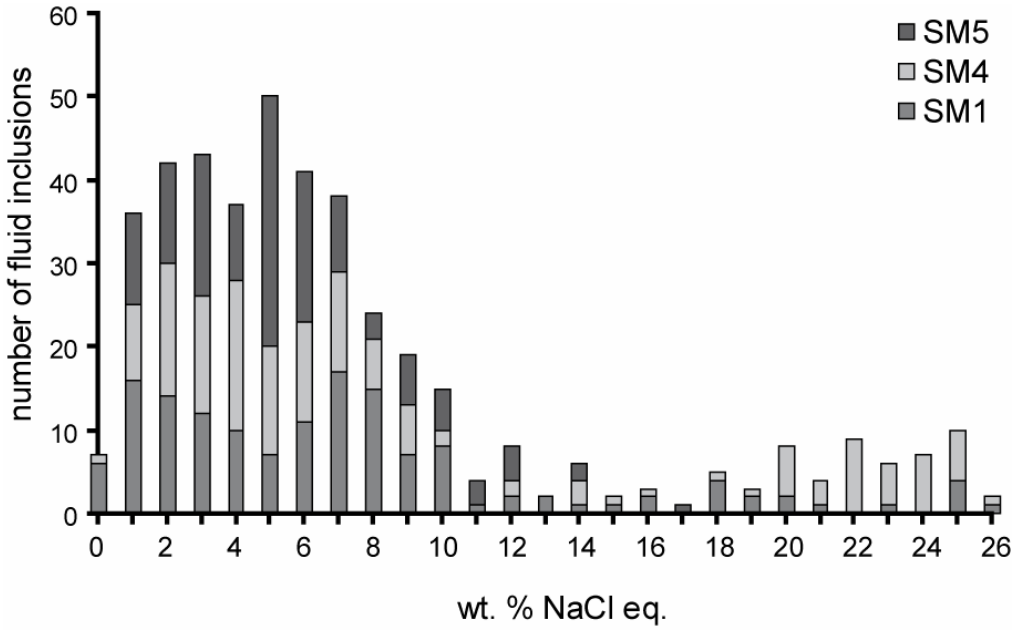

Figure 9 Histogram of wt.% NaCl eq. (calculated after Bodnar, 1993) of all investigated fluid inclusions in the miaskitic units (fluid inclusion types (1a) and (1b)). See text for further discussion.

Table 7 Microthermometric data of Motzfeldt fluid inclusions. All values in °C (except salinity; # = number of fluid inclusions analysed; T(me): eutectic melting; T(m)H_2O: final melting of ice; T(h)H_2O: total homogensation temperature to the liquid. Fluids analysed in: fl-sec: hydrothermal fluorite; qtz-sec: hydrothermal quartz; fl-prim: primary magmatic fluorite; fsp-prim: primary magmatic feldspar; ne-prim: primary magmatic nepheline. Fluid type: l-v: liquid vapour two-phase inclusions; l-v-s: liquid-vapour-solid three phase inclusions; CO_2: Pure CO_2-bearing fluid inclusions; aq. CH_4: mixed aqeous-CH_4 bearing inclusions; pure CH_4: pure CH_4 inclusions. T(m) Clathrate: Measured CH_4-clathrate (CH_4*5.75H_2O) melting temperatures in mixed aqueous-CH_4-bearing fluid inclusions in JS88 and JS122.

JS	unit	mineral	type	#	T(me)	T(m) H_2O	T(h) H_2O	Salinity (wt.% NaCl eq.)
6	SM1	fl-sec	(1a) l-v	9	-25 to -48	-1.7 to -14.2	107 to 284	2.9 to 18.0
9	SM1	fl-sec	(1a) l-v	7	-28 to -32	-0.6 to -5.8	106 to 245	1.1 to 9.0
9	SM1	fl-sec	(1b) l-v-s	2		-2.3 to -7.2		3.9 to 10.8
10	SM1	qtz-sec	(1a) l-v	34	-20 to -40	-3.8 to -14.1	99 to 264	6.2 to 17.9
16	SM1	fl-sec	(1a) l-v	34	-35 to -75	-0.8 to -24.1	111 to 288	1.4 to 25.0
16	SM1	fl-sec	(1b) l-v-s	13		-1.0 to -13.2		1.8 to 17.1
190	SM1	fl-prim	(1a) l-v	14	-	0.0 to -3.1	78 to 246	0.0 to 5.1
190	SM1	fl-prim	(1b) l-v-s	5		-0.3 to -1.2		0.5 to 2.1
197	SM1	fl-prim	(1a) l-v	22	-30 to -40	-0.4 to -6.2	104 to 362	0.7 to 9.5
197	SM1	fl-prim	(1b) l-v-s	4		-0.6 to -1.3		1.0 to 2.2
34	SM4	fl-sec	(1a) l-v	20	-20 to -35	-0.7 to -21.7	94 to 310	1.2 to 23.5
34	SM4	fl-sec	(1b) l-v-s	9		-3.1 to -5.0		5.2 to 7.9
34	SM4	fl-sec	2 CO_2	15	T(m) CO2 -56.8 to -57.9, T(h) CO2 28.4 to 33.5			
90	SM4	fl-sec	(1a) l-v	21	-27 to -38	-1.2 to -6.5	116 to 256	2.1 to 9.9
90	SM4	fl-sec	(1b) l-v-s	1		-2.1		3.6
91	SM4	fl-sec	(1a) l-v	7	-30	-0.3 to -4.1	133 to 328	0.5 to 6.6
91	SM4	fl-sec	(1b) l-v-s	3		-2.1 to -4.0		3.6 to 6.5
152	SM4	fl-sec	(1a) l-v	9	-28 to -43	-0.5 to -23.1	119 to 319	0.9 to 24.4
152	SM4	fl-sec	(1b) l-v-s	4		-2.1 to -21.5		3.5 to 23.4
168	SM4	fl-sec	(1a) l-v	10	-30 to -53	-0.5 to -18.6	103 to 165	0.9 to 21.4
171	SM4	fsp-prim	(1a) l-v	5	-	-2.7 to -4.7	156 to 203	4.5 to 7.4
172	SM4	ne-prim	(1a) l-v	15	-	-0.7 to -4.3	137 to 198	1.2 to 6.9
172	SM4	ne-prim	(1b) l-v-s	9		-0.8 to -2.2		1.4 to 3.7
225	SM4	fl-sec	(1a) l-v	33	-30 to -50	-0.4 to -24.6	94 to 193	0.7 to 25.3
274	SM4	fl-sec	(1a) l-v	10	-28 to -60	-0.5 to -23.1	112 to 153	0.9 to 24.4
274	SM4	fl-sec	(1b) l-v-s	1		-3.3		5.5
104	SM5	ne-prim	(1a) l-v	19	-40	-1.9 to -13.1	171 to 192	3.2 to 17.0
104	SM5	ne-prim	(1b) l-v-s	1		-2.9		4.8
108	SM5	ne-prim	(1a) l-v	10	-25 to -35	-1.7 to -9.8	115 to 185	2.9 to 13.7
108	SM5	ne-prim	(1b) l-v-s	2		-3.1 to -3.8		5.1 to 6.2
109	SM5	fl-sec	(1a) l-v	17	-30 to -47	-0.2 to -7.5	91 to 216	0.4 to 11.1
109	SM5	fl-sec	(1b) l-v-s	13		-0.3 to -4.8		0.5 to 7.6
110	SM5	fl-sec	(1a) l-v	26	-35	-0.4 to -6.9	105 to 343	0.7 to 10.4
110	SM5	fl-sec	(1b) l-v-s	4		-0.5 to -2.5		0.9 to 4.2
175	SM5	fl-sec	(1a) l-v	6	-28 to -29	-0.3 to -3.4	105 to 163	0.5 to 5.6
175	SM5	fl-sec	(1b) l-v-s	1		-0.3		0.5
180	SM5	ne-prim	(1a) l-v	22	-	-2.1 to -3.3	136 to 250	3.5 to 5.4
180	SM5	ne-prim	(1b) l-v-s	9		-2.7 to -3.2		4.5 to 5.3
88	SM6	fl-prim	(3) aq. CH4	5	-40 to -45	-8.0 to -13.9	143 to 190	11.7 to 17.7
88	SM6	fl-prim	(3) pure CH4	3	T(m) Clathrate 5.4 to 13.0, T(h) CH4 -77.2 to -85.3			
122	SM6	fl-prim	(3) aq. CH4	17	-35 to -45	-1.9 to -13.8	93 to 283	3.2 to 17.6
122	SM6	fl-prim	(3) pure CH4	17	T(m) Clathrate 3.0 to 21.2, T(h) CH4 -74.7 to -92.5			

Fluid inclusions in hydrothermal fluorite samples of SM1 are typically characterised by a salinity of < 5 wt.% NaCl eq. Sample JS16 has two different types of fluid inclusion, one with high salinity > 15 wt.% NaCl eq. and another with < 10 wt.% NaCl eq. Quartz sample JS10 is dominated by secondary fluid inclusions with salinities varying from 6 to 9 wt.% NaCl eq. Fluid inclusions in quartz from JS277 were either too small for microthermometry or showed metastable melting. Therefore, a mean salinity of 8.6 wt.% NaCl eq. was used for calculating the ion content (see crush leach results below). In fluorite samples from SM4, fluid inclusions with low salinities < 5 wt.% NaCl eq. predominate. Higher salinity fluid inclusions (up to 25 wt.% NaCl eq.) commonly show brownish ice colours. Hydrothermally formed fluorites from SM5 (JS110, JS175, JS109) show two different types of salinities: < 5 wt.% NaCl eq. and those ranging from 7 to 11 wt.% NaCl eq.

Eutectic melting temperatures (T_{me}) generally range from -40 to -28 °C. The low T_{me} around -40 °C and the brownish ice colour of the higher salinity fluid inclusions indicate that salts other than NaCl are present in the fluid (e.g. Ca_2Cl, $FeCl_2$, $MgCl_2$ etc., see below; Sheperd *et al.*, 1985; Davis *et al.*, 1989; Borovikov *et al.*, 2001). In addition, trace amounts of CO_2 and CH_4 were detected during isotope analyses.

All fluid inclusions homogenise to the liquid usually between 110 and 230 °C. The dominant low salinity fluid inclusions scatter over the whole temperature range independent of sample or unit. However, the higher salinity fluid inclusions (> 10 wt.% NaCl eq.) tend to have lower homogenisation temperatures and may be interpreted as a later fluid phase present at lower temperatures, but still related to the same magmatic event (as later tectonic, metamorphic or magmatic events in the area are unknown; Upton & Emeleus, 1987).

(1b) Saline-aqueous three-phase inclusions. In contrast to the previously described fluid-vapour (two-phase inclusions), three-phase fluid inclusions additionally contain a solid phase (calcite; determined by Raman spectroscopic analyses; Fig. 8c-f). In general they have a similar shape and size to the two-phase inclusions. The three-phase fluid inclusions not only occur as primary inclusions in nepheline (SM4, SM5), but also along secondary trails in hydrothermal fluorite. In these trails, the phase proportions of calcite-fluid-vapour are rather constant (Fig. 8). In a few of the "fluid" inclusions (sample JS109) the calcite minerals are very large and the inclusions contain up to 65 wt.% calcite (recalculated using the densities of calcite and fluid). These "fluid" inclusions may be better referred to as carbonatite melt inclusions. In general, the fluid inclusions containing calcite show a melting behaviour very similar to fluid inclusions of type (1a). However, the calcite predominantly occurs in

inclusions with low salinities (Table 7). During heating experiments up to 450 °C (at which temperature most inclusions decrepitated), the calcite never dissolved.

(2) Pure CO_2 fluid inclusions. Apart from types (1a/b), one fluorite sample (JS34) contain rounded to elongated (< 50 μm) fluid inclusions of pure CO_2. These inclusions either occur in groups or within secondary trails together with aqueous fluid inclusions. Their melting temperatures range from -56.8 to -57.9 °C and they homogenise to the vapour at temperatures between +28 and +34 °C.

(3) aqeous-CH_4 fluid inclusions. Magmatic fluorite from the agpaitic unit SM6 (JS88 & JS122) contains one- or two-phase fluid (CH_4-bearing) inclusions (Fig. 8g-h). They either occur along (pseudo-)secondary trails or (rarely) as isolated groups in which case they may be interpreted to be of primary origin. The fluid inclusions generally have a rounded to irregular shape reaching up to 40 μm. They range from pure methane with homogenisation temperatures between -75 and -93 °C to mixed aqueous-methane inclusions. The aqueous-methane proportions vary considerably as methane clathrate does not always form during the heating-freezing experiments. The final ice melting temperatures of the inclusions scatter between -14 and -2 °C and are not constant within single trails. Methane clathrate melts between +3 and +21 °C. No higher hydrocarbons or any other components were detected by Raman spectroscopy.

Ion chromatographic analyses

Ion chromatographic analyses of fluid inclusions were performed on fluorites and one quartz sample from SM1, SM4 and SM5. For samples finely intergrown with feldspar, no cation contents are reported due to contamination effects during the analysis/preparation procedure. The absolute ion concentration was calculated using the average salinity of the respective sample (Table 8). The calculations were performed using a Cl-factor which was calculated according to the following equation:

Cl = (atom weight Cl / atom weight NaCl) * 10000 * salinity (wt.% NaCl eq.)

Chlorine reaches up to 10 wt.% and is by far the most abundant anion in the analysed samples. Nitrate is below 5000 ppm but reaches up to 1.1 and 2.0 wt.% in samples JS109 and JS152, respectively. The significance of these values and the nitrogen species originally present in the fluid before sample preparation is not clear and we do not suggest that the fluid contained magmatic nitrate. The sulphate concentration is very low (< 170 ppm). Bromine reaches up to 820 ppm and averages around 400 ppm. The Cl/Br (weight) ratio is between 88 and 124 with two values at 268 and 356 (which is close to modern seawater).

The dominant cation is Na reaching up to 10.7 wt.%. The second most abundant cation is K with up to 9000, but usually below 4000 ppm. Mg ranges from 34 to 4558 ppm averaging around 900 ppm. Ba is very low with values < 200 ppm while Sr is mostly masked by overlapping Ca but is below 130 ppm in the two analysed samples.

The anion-cation charge balance is always > 1 because Ca and F were not quantified during the analyses due to their abundance in the host mineral (fluorite). However, a fluorine-free charge balance allows calculation of the minimum amount of Ca in the fluid. This estimation indicates that Ca is the second most abundant cation ranging from 0.2 to 2.5 wt.% with a mean Na/Ca ratio of 4.5 (except JS6). This is in agreement with the one analysed quartz sample (JS277, Table 8) which gave a anion-cation ratio of 1.06 and a Na/Ca ratio of 4.0.

Isotopic composition of the fluid inclusions in fluorite

The δD of the inclusion water varies between -40.7 and -135.6 ‰ (VSMOW, Table 9, Fig. 10). $\delta^{18}O$ values range from -5.7 to -20.9 ‰ (VSMOW). The $\delta^{13}C$ and $\delta^{18}O$ of inclusion CO_2 ranges from -2.5 to -17.4 ‰ (VPDB) and from +26.7 to +42.7 ‰ (VSMOW), respectively (Fig. 7). The $\delta^{13}C$ of inclusion methane could be determined in all samples and ranges from -27.2 to -30.9 ‰ (VPDB, Fig. 11). The hydrogen isotopic composition of methane could not be determined in all of the samples, as the recovered amount of hydrogen was too small to be analysed in some cases. However, where possible, $\delta D_{methane}$ values of -174 to -195 ‰ (VSMOW) were obtained which are in the range of values measured in samples from other nepheline syenitic intrusions (e.g. Potter & Konnerup-Madsen, 2003, Graser *et al.*, in prep.).

Table 8 Results of ion chromatography analyses of fluid inclusion content. All values in ppm except for sal., Cl/Br and a/c ratios.

sample	unit	min.	sal.	F^-	Cl^-(a)	Br^-	NO_3^-	SO_4^{2-}	Cl/Br	Na^+	K^+	Li^+	Mg^{2+}	Sr^{2+}	Ba^{2+}	Ca^{2+}	Ca^{2+}**	a/c
JS6	SM1	fl	5.7	n.a.	34472	278	666	49	124	45670	1454	26	80	b.d.	58	n.a.	2096	1.15
JS9	SM1	fl	5.3	n.a.	31751	258	3313	156	123	27839	1998	6	209	b.d.	59	n.a.	7924	1.86
JS16	SM1	fl	11.2	n.a.	67704	190	2884	165	356	56724	3015	38	1115	128	194	n.a.	13350	1.69
JS277	SM1	qtz	8.6*	1353	51897	590	770	65	88	40473	1478	84	1003	57	22	10106	-	1.06
JS152	SM4	fl	14.7	n.a.	88513	489	19832	b.d.	181	107341	4046	18	4558	b.d.	125	n.a.	18803	1.53
JS168	SM4	fl	1.9	n.a.	11497	107	151	5	108	9570	398	1	34	b.d.	b.d.	n.a.	2401	1.80
JS225	SM4	fl	16.3	n.a.	98590	828	635	b.d.	119	67182	3260	13	289	b.d.	45	n.a.	23758	2.12
JS274	SM4	fl	7.9	n.a.	47459	475	3722	31	100	44008	8667	b.d.	1317	b.d.	b.d.	n.a.	6798	1.38
JS109	SM5	fl	5.3	n.a.	31751	311	11029	135	102	n.a.	n.a.	n.a.	n.a.	b.d.	n.a.	n.a.	n.a.	-
JS175	SM5	fl	3.2	n.a.	19469	73	4713	b.d.	268	n.a.	n.a.	n.a.	n.a.	b.d.	n.a.	n.a.	n.a.	-

Note: *average salinity of all analyzed samples; **calculated Ca^{2+} content assuming balanced uncharged fluid, a/c = 1
min. = host mineral of fluid inclusions; sal. = average salinity of fluid inclusions of respective sample in wt.% NaCl eq.; Cl (a) = calculated chlorine content; a/c = calculated anion-cation balance (molar), n.a. not quantified; b.d. below detection limit

Table 9 Isotopic composition of fluid inclusions (H_2O, CO_2, CH_4).

	unit	δD_{H2O}	$\delta^{18}O_{H2O}$	$\delta^{18}C_{CH4}$	δD_{CH4}	$\delta^{13}C_{CO2}$	$\delta^{18}O_{CO2}$	$T_{(eq.\ H2O-CO2)}$	$T_{(eq.\ CO2-CH4)}$	$\Delta_{H2O-CO2}$ ($\delta^{18}O$)
JS6	SM1	-95.8	-16.49	-27.21	n.a.	-5.49	38.87	10.0	342.5	55.36
JS9	SM1	-52.4	-9.56	-29.95	-174.1	-2.48	28.50	81.2	260.5	38.06
JS16	SM1	-91.5	-7.55	-28.15	-195.1	-4.46	42.70	26.5	311.0	50.25
JS91	SM4	-135.6	-20.80	-30.85	n.a.	-17.38	29.40	24.0	537.5	50.20
JS225	SM4	-40.7	-5.69	-28.60	-189.9	-5.82	36.87	59.0	325.0	42.56
JS274	SM4	-78.7	-13.96	-29.66	n.a.	-14.03	26.67	66.9	472.5	40.63
JS109	SM5	-76.3	-14.74	-28.18	n.a.	-11.63	30.63	44.5	449.0	45.37
JS175	SM5	-83.2	-12.97	-27.38	n.a.	-4.36	31.34	49.5	321.5	44.32
JS122	SM6	-132.7	-20.86	-29.56	-185.2	n.a.	n.a.			

Note: All values in ‰ VSMOW (for D and O isotopes) and in ‰ VPDB (for C isotopes); $T_{(eq.\ H2O-CO2)}$, $T_{(eq.\ CO2-CH4)}$ = equilibration temperatures between O and C, respectively, in °C and $\Delta_{H2O-CO2}$ = fractionation water-CO_2 ($\delta^{18}O$).

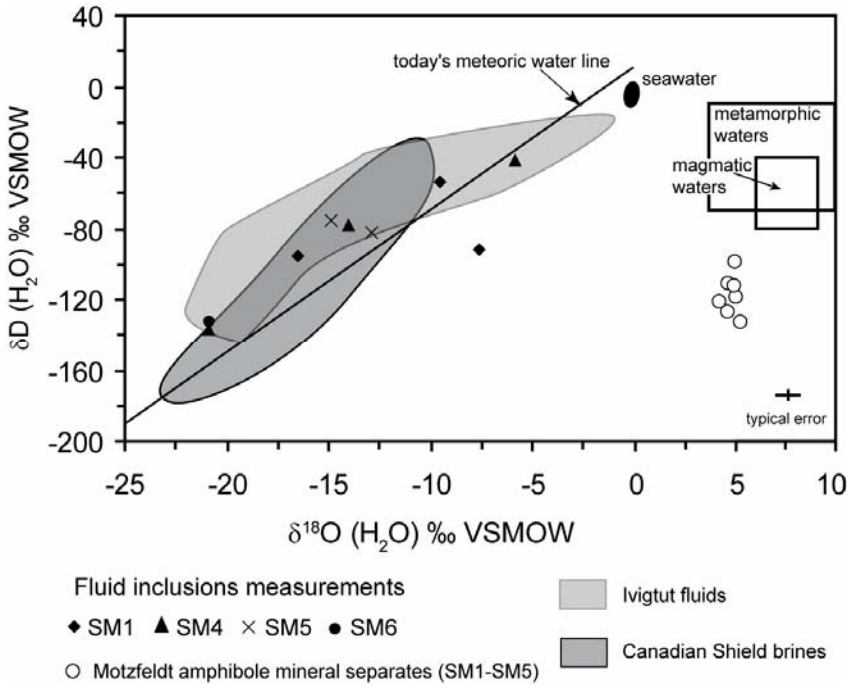

Figure 10 Isotopic composition of fluid inclusion water. Note the good agreement with data from the Ivigtut complex fluids (Köhler *et al*. 2008) and Canadian Shield brines (Frape & Fritz, 1982; Frape *et al*., 1984, and Bottomley *et al*., 1994). Reference data for magmatic, metamorphic and meteoric waters from Sheppard (1986).

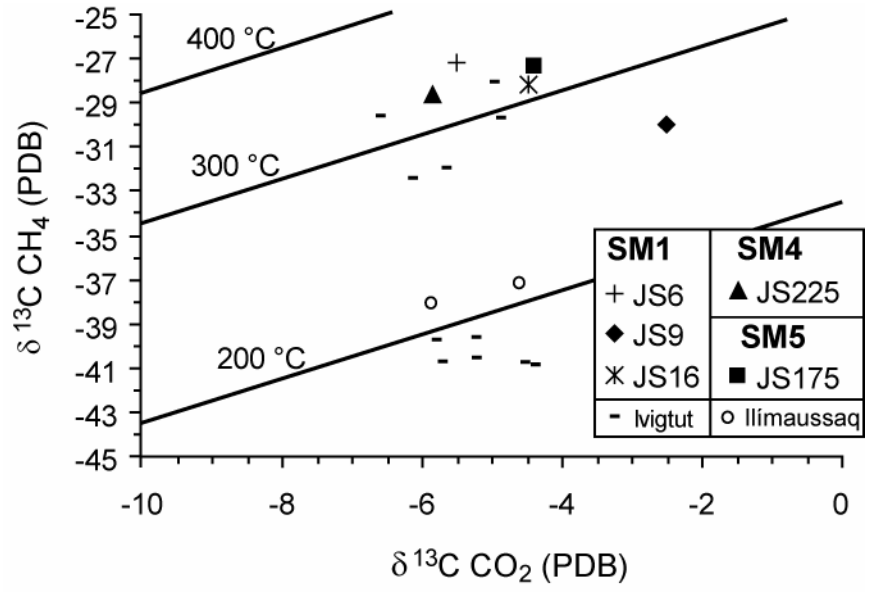

Figure 11 $\delta^{13}C$ (CH_4) vs. $\delta^{13}C$ (CO_2). Equilibration temperatures according to Richet *et al*. (1977). Reference data for Ivigtut and Ilímaussaq from Köhler *et al.* (2008) and Graser *et al*. (in prep.), respectively.

DISCUSSION

Estimation of crystallisation temperatures and oxygen fugacity of the Motzfeldt rocks

Both nepheline and feldspar compositions can provide an estimate of the crystallisation temperatures of the Motzfeldt rocks. Hamilton (1961; Fig. 5) calibrated the nepheline compositions so that they could be used as a temperature indicator. Based on the maximum values recorded (= crystallisation temperatures), the nephelines of the Motzfeldt units SM4, SM5 and SM6 gave the following temperatures: SM4 ~1000 °C; SM5 ~850 °C; SM6 ~800 °C which are in good agreement to the data of Jones (1980) and Jones & Larsen (1985).

Jones (1980) assumed that the feldspars from SM1 to SM5 crystallised at hypersolvus conditions and constrained the minimum temperature of formation of these feldspars to the range 650 to 800 °C. These temperatures are slightly lower than the temperature estimates based on nepheline and may reflect solidus rather than liquidus temperatures. The crystallisation of two separate feldspars (albite and orthoclase, Fig. 3) in the agpaitic unit SM6 suggests lower crystallisation temperatures below the feldspar solvus (e.g. McDowell, 1986; Brown & Parsons, 1989). The very pure end-member compositions indicate temperatures as low as 500 °C.

For the miaskitic units, coexisting olivine, clinopyroxene and Fe-Ti oxides can be used to constrain crystallisation temperatures, oxygen fugacities and silica activities using two different approaches. Temperature and oxygen fugacities can be obtained for samples containing the coexisting Fe-Ti oxide minerals magnetite and ilmenite provided that they crystallised in equilibrium as assumed for samples JS195-JS197 in SM1 (Fig. 2). Calculations according to Andersen & Lindsley (1985) using the spreadsheet of Lepage (2003) gave temperatures of 640 to 690 °C at f_{O2} values below the FMQ buffer (ΔFMQ -0.8 to -1.3). However, two-oxide thermometry is strictly only valid for quenched (volcanic) rocks as Fe, Ti and Mg may re-equilibrate at subsolidus conditions. Therefore, the calculated temperatures and oxygen fugacities have to be interpreted with care. However, the results give an approximate indication of the T-f_{O2} conditions which prevailed during the evolution of the Motzfeldt complex.

In order to at least partially overcome the problem of fast (subsolidus) reequilibration of the coexisting Fe-Ti oxides, the QUILF approach was used (see Frost & Lindsley 1992, Lindsley & Frost, 1992, Andersen et al., 1993, for the theoretical background). The QUILF method (software package by Andersen et al., 1993) uses olivine-pyroxene-Fe-Ti oxide equilibria to calculate T-f_{O2} conditions. The temperature is calculated based on Fe, Mg and Ca

exchange between clinopyroxene and olivine. Oxygen fugacities and silica activities are calculated using equilibria between Fe-Mg silicates and Fe-Ti oxides. Marks & Markl (2001) give details of the approach for application to syenitic rocks.

Due to the lack of fresh olivine in our samples (it is rare and altered to iddingsite), we used the olivine and pyroxene compositional data from Jones (1980, 1984). This is justified, as Jones' pyroxene analyses are identical to those in our study (Fig. 4). Hence, we combined his analyses with the Fe-Ti oxide analyses as these were not analysed by Jones. Obviously, in doing this, we assume that our Fe-Ti oxide compositions of samples JS181, JS180 and JS108 (from SM5) were in equilibrium with olivine and pyroxene with similar compositions to those reported by Jones (1980, 1984; pyroxene core compositions with high diopside content). With respect to the uncertainty as to whether the minerals really crystallised in equilibrium, the results have to be regarded as rough estimates of T and f_{O2} only. Calculations yielded temperatures from ca. 600 to 800 °C at f_{O2} conditions below the FMQ buffer (ΔFMQ -0.5 to -2) at a_{SiO2} between 0.3 and 0.5. These calculations are in good agreement with the data obtained by two-oxide thermometry and temperature constraints based on nepheline and feldspar compositions. The temperatures have to be regarded as solidus temperatures (e. g., Marks & Markl, 2001). The calculated T-f_{O2} conditions of the miaskitic rocks lie in a region where a CO_2-fluid is stable and only slightly above the CH_4-stability field (Huizenga, 2001; 2005; see discussion below).

Due to the lack of suitable mineral assemblages, the oxygen fugacity for SM6 could not be estimated. However, the high Fe^{3+}/Fe_{total} ratio (Fig. 12, Jones, 1980) and the occurrence of aegirine instead of titanomagnetite and Fe^{2+}-rich amphibole may indicate a higher oxidation state than in the earlier pulses (which does not necessarily mean a higher f_{O2} because of the strong temperature dependence of the f_{O2}-buffer reactions). The late-magmatic alteration to hematite clearly indicates f_{O2} conditions above the hematite-magnetite buffer.

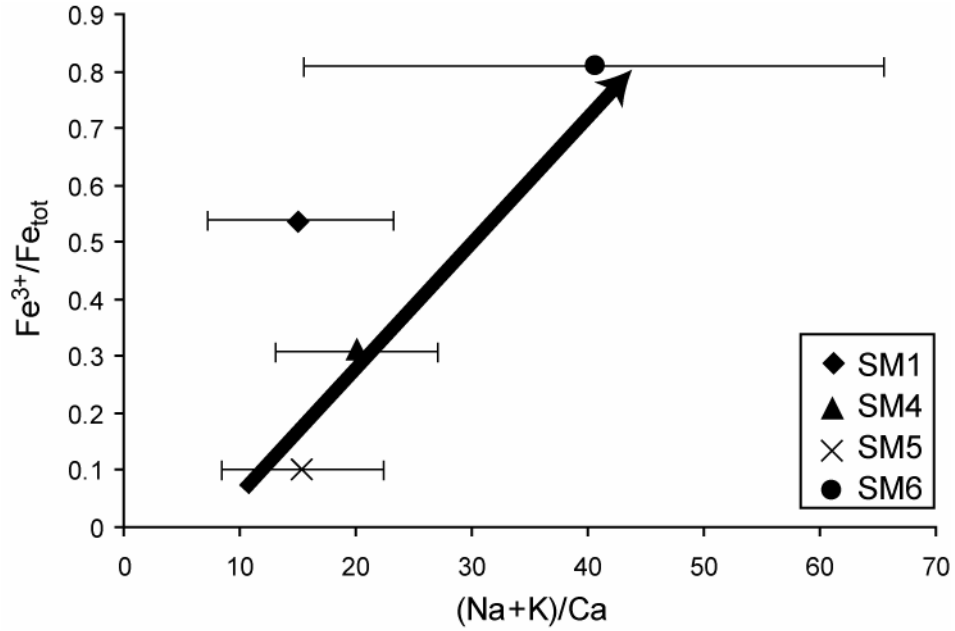

Figure 12 Fe^{3+}/Fe^{total} vs. (Na+K)/Ca for whole-rock data from Jones (1980). The increase in (Na+K)/Ca equals a fractionation increase. As shown by several authors, the arrow may indicate a temperature decrease (= increase in Fe^{3+} and (Na+K)). The high whole-rock Fe^{3+} content of SM1 is related to the formation of secondary Fe^{3+}-rich minerals. See text for further discussion.

Isotopic constraints derived from mineral separates

The initial ε_{Nd} values (corrected for an age of 1.275 Ga; Upton *et al.*, 2003) are relatively homogeneous varying by only ±2.3 ε_{Nd} units. The similarity to the Ilímaussaq (Marks *et al.*, 2004) and Grønnedal-Ika intrusions (Halama *et al.*, 2005), the basalts of the Eriksfjord formation (Halama *et al.*, 2003) and Igaliko/Quassiarsuk lamprophyres and carbonatites (Coulson *et al.*, 2003; Fig. 6) suggests that these intrusions/rocks formed from similar mantle sources. The Nd model ages of 1.5 to 1.8 Ga relative to the depleted mantle (Liew & Hofmann, 1987) are most probably related to the Ketilidian orogeny at this time (Garde *et al.*, 2002) and fall into the range of other model ages for rocks from the Gardar Province (e.g. Marks *et al.*, 2004). Hence, we are dealing with a large magmatic province that is fed from a similar source over a large spatial and temporal interval.

Similar to the Nd isotopic values, the $\delta^{18}O$ values of the minerals define a narrow range (between +4.2 and +5.3 ‰) and suggest an isotopically rather homogeneous melt throughout the different units. The $\delta^{18}O$ of a nepheline-syenitic melt in equilibrium with the analysed minerals can be constrained using the approach of Zheng (1993a, b) and Zhao & Zheng (2003) as shown by Halama *et al.* (2005). Assuming an equilibration temperature of ca. 800 °C, the fractionation between amphibole(hornblende) and melt is -1.6 ‰ and aegirine-

melt -0.3 ‰. Thus the original melt would have a $\delta^{18}O$ between 5.2 and 6.9 ‰. These values are not only typical mantle values (e.g. Kyser, 1986; Eiler, 2001; Marks *et al.*, 2004), but also $\delta^{18}O$ values characteristic of other syenitic intrusions (e.g. Taylor & Sheppard, 1986; Harris, 1995; Dallai *et al.*, 2003; Marks *et al.*, 2004). The two samples from SM1 show slightly lower $\delta^{18}O$ amphibole values of +4.2 and +4.6 ‰. Such lower values are usually attributed to interaction with low-$\delta^{18}O$ meteoric fluids (c.f. O isotopic composition of the fluid inclusions of this study; Marks *et al.*, 2003). The locally intense alteration, the turbidity of feldspars and the occurrence of hydrothermal alteration minerals (e.g. hematite, fluorite, calcite etc.), especially in unit SM1, support such an interpretation.

The δD values are lower than "normal" magmatic values which are usually between -50 and -80 ‰ (c.f. Hoefs, 1997). The most likely process to explain the unusual hydrogen isotopic composition may be post-magmatic interaction with a meteoric fluid as the hydrogen isotopic composition reacts very easily to the infiltration of an H_2O-rich fluid phase. This is due to its low concentration in minerals compared to oxygen (e.g. Taylor, 1974; 1977). Using the mineral-water fractionation factors for arfvedsonite (at 400 °C; Graham *et al.*, 1984) and for hornblende (at 450-800 °C; Suzuoki & Epstein, 1976), a coexisting fluid would have a δD of ca. -60 to -110 ‰. These values are in good agreement with our isotope analyses of water from fluid inclusions which ranges from -40 to -135 ‰. If indeed the hydrogen isotopic composition reflects late- to post-magmatic alteration by a meteoric fluid phase, the fluid-rock ratio which caused this shift must have been low, because otherwise, it should also be visible in the O isotope compositions.

Other processes which could also cause depleted δD values include extreme degassing of magmatic fluids, assimilation of organic-rich sediments and oxidation of magmatic methane (c.f. Marks *et al.,* 2004). However, no signs of extreme degassing of magmatic fluids, such as the presence of large contact aureole around the intrusion, are observed and no organic-rich sediments have been described anywhere in the vicinity of the Motzfeldt intrusion or in the Gardar Province as a whole (Marks *et al.*, 2004). Our fluid inclusion study suggests that CO_2 and not CH_4 was the dominant carbon species in the fluid during most of the differentiation history of the Motzfeldt magmas (see below).

The isotopic composition of the calcite from a calcite/fluorite vein lies within the mantle box of Taylor *et al.* (1967; see also Kyser *et al.*, 1982; Des Marais & Moore, 1984; Deines, 1989; Clarke *et al.*, 1993; Keller & Hoefs, 1995; $\delta^{18}O$ 7.8 ‰; $\delta^{13}C$ -4.4 ‰). The values are in accordance with analyses by Pearce & Leng (1996), Pearce *et al.* (1997), Goodenough (1997), Coulson *et al.* (2003), Taubald *et al.* (2004) and Halama *et al.* (2005)

from various carbonate or carbonatite localities in the Gardar Province, suggesting a common mantle source of the carbonates.

Three whole-rock powders (JS159, JS164 from SM6 and JS181 from SM5) containing considerable amounts of calcite veinlets and/or calcite as an alteration product of feldspar and eudialyte (e.g. Fig. 3) were also analysed for their C and O isotopic composition. The $\delta^{18}O$ values range from +21.9 to +24.2 ‰ and $\delta^{13}C$ from -2.1 to -3.2 ‰ (Fig. 7). Similar values for samples from SM1 and SM4 were obtained by McCreath (pers. comm. 2007). The results are comparable to those obtained by Pearce & Leng (1996) and Coulson *et al.* (2003) from the area around the Motzfeldt intrusion (i.e. Igaliko region). The $\delta^{13}C$ values lie near those reported for mantle rocks (Taylor *et al.*, 1967; Keller & Hoefs, 1995) and therefore possibly suggest mantle derivation. The oxygen isotope values are considerably enriched in ^{18}O with regard to mantle rocks and are more typical of secondary and/or low temperature alteration of calcite (Deines, 1989; Demenéy *et al.*, 1998). The slight enrichment of $\delta^{13}C$ and variably enriched $\delta^{18}O$ might be explained by the model of Deines (1989) who stated that $\delta^{18}O$ increases with fractionation and with a decreasing carbonate:silicate ratio (see also Worley *et al.*, 1995). Furthermore, Tichomirowa *et al.* (2006) assumed that increasing $\delta^{18}O$ values could be explained by interaction with water-rich fluids, which is the most likely explanation for the observed heavy oxygen isotopic composition (see below). Hence, only the C isotope signature would likely preserve the mantle record during hydrous alteration if the C concentration of the infiltrating fluid is low. Köhler *et al.* (2008) used a similar explanation for the observed change in $\delta^{18}O$ at constant $\delta^{13}C$ of CO_2 for fluid inclusions from another Gardar intrusion, the Ivigtut complex (see discussion of fluid inclusion results).

Discussion of fluid inclusion results

The fluid inclusions present in primary minerals of the miaskitic units SM1, SM4 and SM5 are of both primary and secondary origin. Their salinities are commonly < 6 wt.% NaCl eq. The few higher salinity fluid inclusions possibly represent a different (low-temperature) fluid generation.

Regarding the commonly observed calcite crystals in the low-salinity fluid inclusions, we may ask whether these minerals are “true” daughter minerals or if they are just accidentally trapped solid crystals. The fact that in certain secondary fluid inclusion trails, each fluid inclusion contains a calcite crystal in constant phase proportions (Fig. 8) suggests that these are indeed daughter minerals. They crystallised after entrapment from a fluid

originally undersaturated in calcite. However, accidental trapping cannot be completely ruled out for samples in which only few inclusions contain calcite.

The fact that both two-phase (liquid-vapour) and three-phase (liquid-vapour-solid) fluid inclusions occur in the miaskitic rocks provides evidence that during their evolution the fluid was characterised by H_2O and NaCl with variable amounts of CO_2 (or HCO_3^-). Unfortunately, the sample material did not allow us to decipher the exact relative chronologies of entrapment of the two types of fluid inclusions due to the lack of adequate cross-cutting relationships.

In contrast to the H_2O-NaCl-CO_2 fluid in the miaskitic rocks, fluid inclusions in magmatic fluorite from the agpaitic rocks (SM6) are characterised by H_2O-NaCl-CH_4 without any calcite. The close association of pure methane, mixed H_2O-NaCl-CH_4 and (almost) pure H_2O-NaCl inclusions suggest that they formed from a heterogeneous, but definitely reduced fluid displaying immiscibility.

Based on stratigraphic reconstructions, pressure conditions during emplacement of the Motzfeldt intrusion were probably between 1 and 2 kbar as suggested by Jones (1980). Similar conditions were obtained for the Ilímaussaq intrusion (Konnerup-Madsen & Rose-Hansen, 1984). Accordingly, a pressure correction of 50 to 100°C has to be applied to the homogenisation temperatures. The corrected homogenisation temperatures range from 78 to 343 °C (Table 7) with the majority lying between 100 and 200 °C. Accordingly, formation temperatures between 150 and 300 °C can be assumed (Bakker, 2003; not applicable to fluid inclusions from SM6 as they are assumed to be trapped from a heterogeneous fluid). No isochores could be calculated for inclusions containing calcite as no total homogenisation temperature could be determined. Not even partial dissolution of the daughter minerals was observed and it is unclear to us whether the dissolution of the daughter minerals was kinetically inhibited or because the formation temperatures were much higher than the decrepitating ones.

The results of our crush-leach analyses support our microthermometric results indicating that the fluid is, in addition to H_2O, dominated by Na, Cl and minor amounts of Ca. Other ions are only of minor importance. The Cl/Br ratios (by weight) of our samples mostly lie between 95 and 120. The high Cl/Br ratio in sample JS16 may be attributed to either a mixture of a high and a low salinity fluid and/or to another fluid generation (higher proportion of higher salinity fluid inclusions in this sample). The predominant low Cl/Br ratios are comparable to those of other peralkaline Gardar intrusions (Graser *et al.*, in prep.; Köhler *et al.*, 2008). This similarity across the Gardar Province suggests a common halogen source

which is in agreement with the Nd isotope-based assumption of a common mantle source of the magmas in general and a common evolution process of the fluid phase. The Cl/Br values of about 100 suggest that unmixing/exsolution of a fluid phase preferentially partitions Br into the fluid relative to the melt and early crystallising minerals, as suggested by the experiments of Bureau *et al.* (2000) and Bureau & Métrich (2003).

Isotopic composition of inclusion H_2O

In terms of H and O isotopic composition, the water within the inclusions closely follows the present-day meteoric water line (MWL, Craig, 1961) and falls within the published data array for the Ivigtut complex (Köhler *et al.*, 2008) and Canadian Shield brines (Fig. 10; Frape & Fritz, 1982; Frape *et al.*, 1984; Bottomley *et al.*, 1994). However, the isotopic composition of the inclusion water is slightly shifted to the left of the MWL. This may be either attributed to equilibration with CO_2 (Richet *et al.*, 1977; Cartwright *et al.*, 2000; Köhler *et al.*, 2008) or to low-temperature isotopic equilibration with the host-rocks at low water/rock ratios (Frape & Fritz, 1982; Kelly *et al.*, 1986; Sheppard, 1989). A mixing process with a fluid of unknown origin cannot explain the displacement of the data to the left of the MWL as all known "reservoirs" lie to the right of the MWL (e.g. magmatic or metamorphic waters, Hoefs, 1997). We prefer the second explanation, as the volume of CO_2 in the fluid inclusions is negligible compared to the dominant water-salt mixture (up to 95 mol%). Furthermore, the available fractionation factors between amphibole and water (Suzuoki & Epstein, 1976; Graham *et al.*, 1984) suggest that the hydrogen isotope composition of the inclusion water (-40 to -100 ‰) could represent equilibrium values. The low oxygen isotope values (-5 to -25 ‰) of the inclusion water, however, are not in equilibrium with the analysed oxygen isotope compositions of the mineral separates (+4.2 to +5.3 ‰). This again points to interaction of a low proportion of meteoric water with the rocks (low fluid-rock ratio; see above, discussion of isotopic composition of mineral separates).

Isotopic composition of inclusion CO_2

In all analysed samples (except for JS122, SM6), trace amounts of CO_2 were detected during the isotope analyses. The $\delta^{13}C$ values of the CO_2 define two different groups (Fig. 7) which may be explained in the following way: $\delta^{13}C$ values between -2 and -6‰ (VDPB) resemble primary magmatic and/or mantle values (Taylor *et al.*, 1967; Keller & Hoefs, 1995). The second group is defined by lower $\delta^{13}C$ values ranging from -10 to -17‰. These lower values are commonly explained by contamination with organic-rich material, which is, however,

unknown in the Gardar Province (e. g. Marks *et al.*, 2004). Calcite daughter crystals were observed in (almost) all studied samples irrespective of carbon isotopic composition. Therefore, there seems to be no influence from these crystals on the isotopic composition. However, the fluorite-samples with low $\delta^{13}C$ values are very finely intergrown with carbonates. The fractionation of carbon between calcite and CO_2(aq) based on the fractionation factors of Ohmoto & Goldhaber (1997) is 8 ‰ at low temperatures (20 to 50 °C). Such a fractionation could account for the difference in carbon isotopes between the two groups (even regarding the fact that calcite intergrowths were removed by treating the samples with acid prior to analysis). However, the geological significance of this process remains enigmatic.

The very similar range of $\delta^{13}C$ values of -4 to -14.1‰ obtained for lamprophyres, phonolites and carbonatites from the Motzfeldt (Igaliko) region (Fig. 7; Pearce & Leng, 1996) points to a common carbon isotopic source and evolution in the whole region and in different rock types, inviting speculation about CO_2 metasomatism in the mantle source region.

The $\delta^{18}O$ value of inclusion CO_2 ranges from +26.7 to +42.7‰ (VSMOW). The inclusion CO_2 is considerably enriched in ^{18}O and is much higher than normal carbonatitic mantle values (Fig. 7; e.g. Taylor *et al.*, 1967; Halama *et al.*, 2005). We follow the argumentation of Köhler *et al.* (2008) who pointed out the similarity in isotopic composition to CO_2 vesicles in MORB (Pineau & Javoy, 1983). They explain these high values by low temperature isotopic exchange with oxygen from the inclusion water. Using the fractionation factors of Friedmann & O'Neill (1977), the fractionation of oxygen between CO_2 and H_2O(aq) is around -40 ‰ at low temperatures (10 to 100 °C). This is in accordance with the work of Richet *et al.* (1977) who reported a fractionation of between -41.2 and -44.1 ‰, which may even be increased by the presence of dissolved salts in the fluid inclusions (Pineau & Javoy, 1983). The fractionation for the samples from the Motzfeldt intrusion ranges between 38.1 and 55.4 ‰, with a mean of 46.3 ‰, comparable to the data of Richet *et al.* (1977) and Köhler *et al.* (2008).

Isotopic composition of inclusion CH_4

The carbon isotopic composition of CH_4 in the inclusions is fairly constant ($\delta^{13}C$ -27 to -31‰ VPDB). Even the isotopic composition of CH_4 from fluorite in the agpaitic unit is in the range of the samples from the miaskitic rocks. Calculating the C isotopic equilibration temperatures between methane and CO_2 using the fractionation factors of Richet *et al.* (1977) results in values of 300 to 350 °C (only $\delta^{13}C$ values of CO_2 from samples in which the CO_2 has a

mantle-like carbon isotopic composition were used, see above). These temperatures are only slightly higher than those deduced from the pressure-corrected fluid inclusion temperatures.

As no sign of organic material is found within the Gardar province, the low $\delta^{13}C$ values of CH_4 in the inclusion cannot be attributed to a thermogenic origin due to the thermal decomposition of organic material (Schoell, 1988). However, Konnerup-Madsen *et al.* (1985) and Ryabchikov & Kogarko (2006) have suggested that the formation of methane may be explained by the respeciation of an originally CO_2-H_2O rich fluid upon temperature decrease (c.f. Figs. 13 & 14). Given the calculated equilibration temperatures, this mechanism appears plausible also for our samples.

The transition from miaskitic to agpaitic rocks

The transition from the miaskitic units SM1-SM5 to the agpaitic SM6 can be observed in the change in mineralogy, fluid composition, whole-rock alkali content and Fe^{3+}/Fe^{2+}. These changes should be related to a common process.

Mineralogical Change

The change from miaskitic to agpaitic mineral assemblages (zircon and titanite to eudialyte) and from (Fe^{2+}-rich) amphibole- to (Fe^{3+}-rich) aegirine-dominated mafic minerals in very late-stage magmatic rocks may be related to several partly interrelated causes:

- change in oxidation state: a dominance of Fe^{3+} over Fe^{2+} in the melt would effectively inhibit the crystallisation of amphibole which commonly has a rather low Fe^{3+} content ($Fe^{3+}/Fe^{2+}<0.4$ in Ilímaussaq, Marks *et al.*, 2007; see also Leake *et al.*, 1997). Crystallization of aegirine would be a direct consequence of a change in oxidation state.
- a change of the melt's alkali(Na)/iron ratio: arfvedsonite has an alkali(Na)/Fe ratio of 0.6, while aegirine has a ratio of 1; increasing alkalis relative to iron could drive a melt towards aegirine crystallization irrespective of redox conditions. Although nominally unrelated to redox conditions, crystallization of Fe-Ti oxides would effectively increase this ratio. Their crystallization, however, is again highly redox-dependent.
- The formation of a water-deficient fluid resulting from the methane-producing reaction:

$$CO_2 + 2\ H_2O = CH_4 + 2\ O_2 \qquad \text{(eq. 1)}$$

Apart from consuming water and possibly inhibiting the formation of "water-rich" amphibole, this reaction could be responsible for an increase of "free" oxygen which in turn could further oxidize the iron in the melt.

- The formation of eudialyte may be mainly related to the increased solubility of Zr (and possibly other HFSE; e.g. Kogarko, 1974; Watson, 1979; Watson & Harrison, 1983; Farges *et al.*, 1991; Hanchar & Watson, 2003) in peralkaline melts because a high alkali/Al ratio inhibits crystallisation of zircon or baddeleyite (Nicholls & Carmichael, 1969; Hoskin & Schaltegger, 2003). Finally and very importantly, the early exsolution of a hydrous fluid phase is inhibited due to the high alkalinity and low water activity (see eq. 3). This retains Na, halogens and consequently also Zr and other HFSE elements in the melt (Kogarko, 1974; Treuil *et al.*, 1979; Taylor *et al.*, 1981). Therefore, the formation of eudialyte can be assumed to be a consequence of the high concentration of alkalis, the long crystallisation interval and the inhibited exsolution of a fluid phase associated with the reduced conditions.

Change in fluid composition

The change in fluid composition from an H_2O-HCO_3^--NaCl-$CaCl_2$ to a CH_4-H_2O-NaCl-$CaCl_2$(?) fluid can be explained by combining the temperature-f_{O2} data detailed above with theoretical calculations by Huizenga (2001, 2005) who used fugacity coefficients from Shi & Saxena (1992). Figure 13 shows that a CO_2-H_2O dominated fluid at high temperatures generally evolves to a fluid dominated by CH_4-H_2O at lower temperatures at constant relative oxygen fugacities (expressed as ΔQFM in Fig. 13; c.f. Ryabchikov & Kogarko, 2006; Konnerup-Madsen, 2001 and Fig. 14) if f_{O2} is buffered by a mineral assemblage such as olivine-spinel-clinopyroxene-feldspar, in which clinopyroxene and feldspar buffer a_{SiO2} due to Ca-tschermakite- or jadeite-involving equilibria. This is in accordance with calculations using thermodynamic data from Robie & Hemingway (1995) assuming ideal gas behaviour, a C:H ratio of 0.5 and a pressure of 1 kbar with variable $f(CH_4)/f(CO_2)$ ratios (Halama *et al.*, 2005; Fig. 14). Additionally, the H/O ratio of the fluid may also be important for equilibrium (1) as a high H/O ratio favours hydrocarbons and a low ratio carbon dioxide (e.g. Huizenga, 2001, 2005). Figure 14 shows that the calculated T-f_{O2} conditions for the miaskitic rocks from the Motzfeldt intrusion lie within the CO_2-H_2O stability field, just slightly above the transition curve relating a CO_2-H_2O with a CH_4-H_2O fluid. The evolution to lower temperatures at a constant relative oxygen fugacity may explain the observed change of the composition to a CH_4-H_2O dominated fluid in the agpaitic rocks. Obviously, only a slight decrease in oxygen

fugacity due to e.g. the increase in the melts alkali content may also influence the carbon speciation in the fluid (see discussion below).

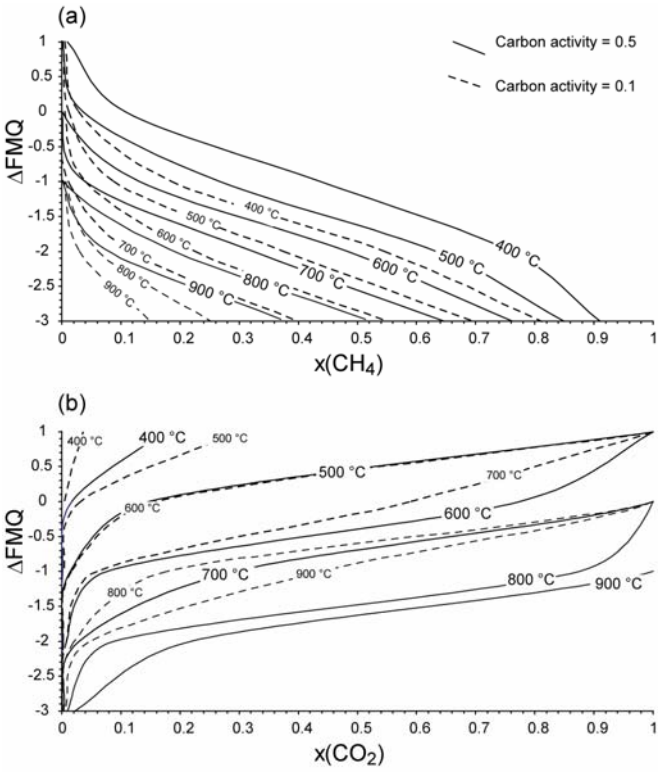

Figure 13 (a) $x(CH_4)/(x(CH_4)+x(CO_2)+x(H_2O))$ vs. oxygen fugacity in the relevant T-f_{O2} range (oxygen fugacity given as ΔQFM). Different modelled curves represent $x(CH_4)$ in the fluid for different temperatures and carbon activities at 1 kbar calculated according to Huizenga (2001, 2005). At a constant relative oxygen fugacity (i.e. constant ΔFMQ), the CH_4 content increases with decreasing temperature. (b) Same as (a) but with $x(CO_2)/(x(CH_4)+x(CO_2)+x(H_2O))$ vs. oxygen fugacity given as ΔQFM. At constant relative oxygen fugacity (i.e. constant ΔFMQ), the CO_2 content in the fluid decreases with decreasing temperature.

Fischer-Tropsch (F-T) type reactions (e.g. Salvi & Williams-Jones, 1997; 2006) are not believed to be important as no sign of higher hydrocarbons and/or H_2 was found in the fluid inclusions, nor are the CH_4-bearing fluid inclusions associated with the breakdown of hydrous minerals which would be necessary to trigger F-T-type reactions (e.g. Salvi & Williams-Jones, 2006; Nivin *et al.*, 2005). A mixing process involving meteoric and magmatic water, which may be important for the formation of methane as suggested by Potter *et al.* (1999) and Nivin *et al.* (2005), is questionable for the Motzfeldt intrusion as no CH_4-bearing fluid inclusions were found in samples from the miaskitic rocks. The trace amounts of methane found during isotope analyses in the fluid inclusions may be more easily explained by the proposed respeciation model (Konnerup-Madsen *et al.*, 1985; Ryabchikov & Kogarko, 2006).

The change in mineralogy ($Fe^{2+} \rightarrow Fe^{3+}$ bearing mafic minerals) is closely linked to the change in fluid composition ($CO_2 \rightarrow CH_4$), but it is very important to note that they work in different directions. While the first requires oxidation, the second requires reduction.

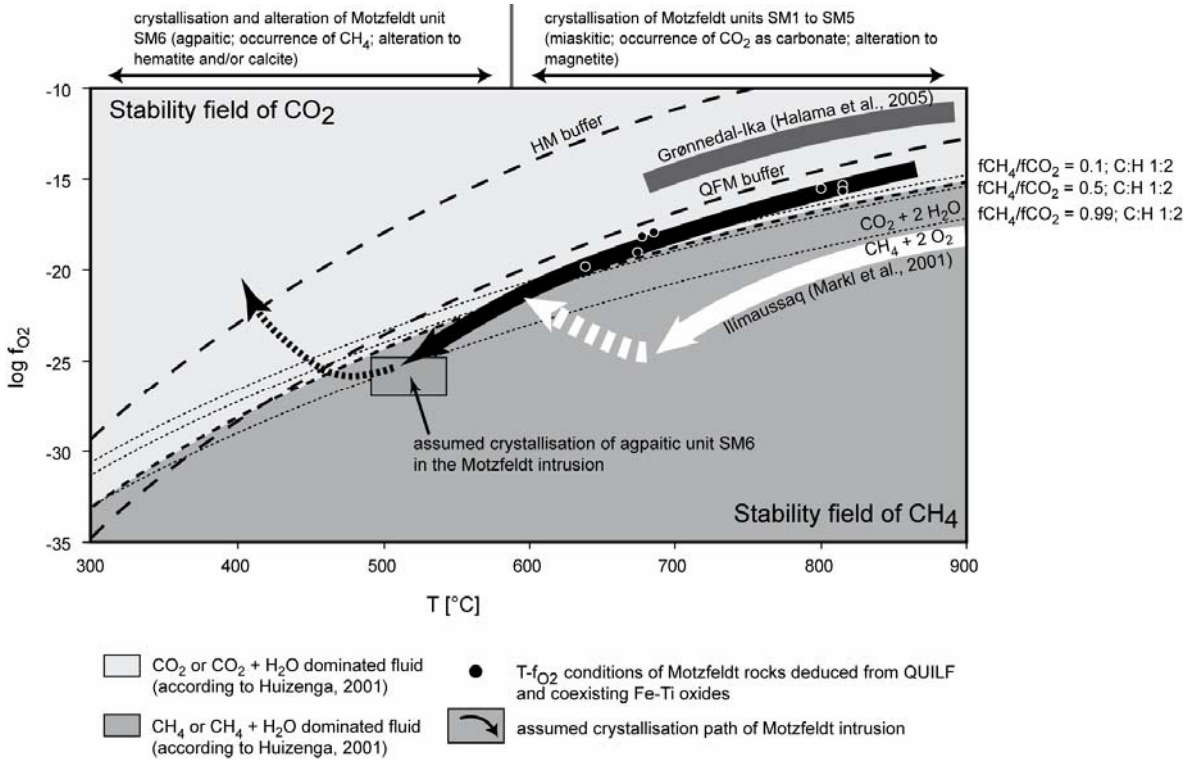

Figure 14 Assumed crystallisation path of the Motzfeldt intrusion (thick black line). The miaskitic rocks formed at high temperatures within the stability field of CO_2 (calculated according to Huizenga, 2001 and using thermodynamic data of Robie & Hemingway, 1996; thin dotted lines represent varying CH_4/CO_2 fugacities). In the course of crystallisation and due to a temperature decrease, the Motzfeldt magma entered the stability field of CH_4 which lead to the crystallisation of the agpaitic unit SM6. The final increase in oxygen fugacity is evidenced by post-magmatic hematite and/or calcite. Compared to other Gardar intrusions, the Motzfeldt intrusion has an intermediate position between the oxidized and CO_2-(calcite)-dominated miaskitic Grønnedal-Ika intrusion (dark grey line: Halama *et al.*, 2005) and the CH_4-dominated reduced agpaitic Ilímaussaq complex (white line: Markl *et al.*, 2001).

The whole-rock compositional change from Fe^{2+}- to Fe^{3+}-dominated linked to alkali content and C-O-H speciation

Generally, the speciation of a C-O-H fluid as well as the oxidation state of Fe is closely linked to the oxidation state of the magma (Bezos & Humler, 2005). Assuming fractional crystallisation in a system closed with respect to oxygen (Byers *et al.*, 1984), the Fe^{3+}/Fe_{total} ratio commonly increases (Bezos & Humler, 2005). As it is difficult to envisage how a magmatic system can be closed to oxygen diffusion, Bezos and Humler (2005) suggested that the Fe^{3+}/Fe^{2+} ratio of a basaltic melt increases due to the highly compatible behaviour of Fe^{2+} in olivine and the strong incompatibility of Fe^{3+} in olivine and plagioclase. Although we are obviously not dealing with an olivine-fractionating system, the preferred uptake of Fe^{2+} by

e.g. amphibole, ulvöspinel-rich titanomagnetite or ilmenite would explain the increasing Fe^{3+}/Fe^{2+} in the Motzfeldt melt.

In magmatic systems, ferric and ferrous iron concentrations are related by the following equilibrium (e.g. Rüssel & Wiedenroth, 2004):

$$4\ Fe^{3+} + 2\ O^{2-} \Leftrightarrow 4\ Fe^{2+} + O_2 \qquad \text{(eq. 2)}$$

It has been shown by a number of authors (Kress & Carmichael, 1988; Gerlach *et al.*, 1998; 1999; Rüssel & Wiedenroth, 2004; Lange & Carmichael, 1989) that equilibrium (2) is shifted to the left with decreasing temperature and increasing Na and K content of the melt (e.g. Kress & Carmichael, 1991; Rüssel & Wiedenroth, 2004), which fits with the observations at Motzfeldt (Fig. 12; Jones, 1980). Accordingly, the peralkalinity of a melt and the degree of oxidation of iron (i.e. the stability of Fe^{2+} vs. Fe^{3+}) are strongly related (Sack *et al.*, 1981; Kilinic *et al.*, 1983; Lange & Carmichael, 1989; Kress & Carmichael, 1989; 1991; Gerlach *et al.*, 1999; Rüssel & Wiedenroth, 2004). Using the empirical equation of Kress & Carmichael (1991) to calculate the oxygen fugacity in silicate liquids, an increase in the peralkalinity index (molar (Na+K)/Al) from 0.9 to 1.3 can lead to a decrease in oxygen fugacity by 0.5 log f_{O2} units (at constant Fe^{2+}/Fe^{3+} ratio). Furthermore, there is the petrographic observation that agpaitic mineral assemblages are confined to very highly differentiated, extremely alkaline rocks (e.g. Khomyakov, 1995; Sørensen, 1997; Markl *et al.*, 2001) which commonly have a high Fe^{3+}/Fe^{2+} ratio.

A related reaction equation can be easily derived by combining reactions 1 and 2:

$$8\ FeO^{melt} + CO_2 + 2\ H_2O \Leftrightarrow CH_4 + 4\ Fe_2O_3{}^{melt} \qquad \text{(eq. 3)}$$

This reaction describes the magmatic evolution of the Motzfeldt intrusion in a simple way. It takes into account the observed change from an Fe^{2+}-dominated miaskitic mineral assemblage in Motzfeldt units SM1 to SM5 to the Fe^{3+}-dominated agpaitic rocks of SM6. Furthermore it also includes the observed transition in the fluid phase from (H_2O-NaCl-) CO_2 in the miaskitic rocks to (H_2O-NaCl-) CH_4 in the agpaitic rocks.

Late-stage alteration phenomena involving peralkaline fluids

In general, late- to post-magmatic metasomatism involving a Na-rich fluid at higher relative oxidation state is typical of peralkaline magmatic complexes (Salvi & Williams-Jones, 1990; Nivin *et al.*, 2001; 2002; 2005; Marks *et al.*, 2003; 2004; Potter *et al.*, 2004; Halama *et al.*, 2005; Schönenberger *et al.*, 2006; Beeskow *et al.*, 2006; Fig. 14). For Motzfeldt Jones & Larsen (1985) suggested that there was a continuous evolution from a low-T, peralkaline,

volatile-rich melt which formed the agpaitic rocks (SM6) to a hydrothermal solution containing excess sodium (e.g. Tuttle & Bowen, 1958, Khomyakov, 1995). This fluid would be efficient for metasomatism, especially in the roof zone of the intrusion (Jones & Larsen, 1985). The action of such a fluid is evidenced, especially in SM1, by the presence of secondary aegirine-augite or aegirine and the common occurrence of late-stage calcite/cancrinite which records a Na- and HCO_3^--bearing fluid. Jones & Larsen (1985) assumed that these alteration fluids had trace element characteristics similar to those of the lujavritic melts and therefore enriched the altered syenites with some trace elements up to sub-economic values.

In the agpaitic rocks, fluid metasomatism led to destabilisation of the agpaitic assemblage (eudialyte, aegirine, CH_4) and sodalite was replaced by analcime and nepheline by sodalite + analcime, comparable to the reactions described by Markl *et al.* (2001) for the Ilímaussaq intrusion. The alteration of eudialyte resembles the textures described from the nearby North Qoroq intrusion (Coulson, 1997), stabilising miaskitic minerals such as zircon, allanite-(Ce), natrolite, hematite and calcite (Fig. 3). Mitchell & Liferovich (2006) suggested that this alteration of a primary magmatic agpaitic to a miaskitic assemblage may be explained by changing pH (c.f. Khomyakov, 1995; Markl & Baumgartner, 2002).

SUMMARY AND CONCLUSIONS

Magmatic and fluid evolution of the Motzfeldt intrusion

The chemical evolution of the different magmatic units of the Motzfeldt intrusion suggests one continuous crystallization sequence. Fe^{2+}-rich miaskitic mineral assemblages are followed by a late-stage Fe^{3+}-rich agpaitic mineral assemblage. Based on the Nd and O isotopic composition of mineral separates, both the miaskitic and the agpaitic rocks in the Motzfeldt intrusion appear to have been derived from the same magma source and show minimal signs of crustal contamination. Hence, their different mineralogical and geochemical evolution must be explained in terms of fluid-melt partitioning and/or magmatic differentiation processes. The Motzfeldt rocks formed at oxygen fugacities below the FMQ buffer; however, the presence of late-stage alteration products such as hematite suggest higher oxygen fugacities above the HM buffer during the waning stages of magmatism.

Studies of fluid inclusions in fluorite, nepheline and quartz have revealed the presence of a Na- and Cl- dominated fluid with a salinity of < 10 wt.% NaCl eq. All the miaskitic units show evidence of oxidised fluid compositions and the presence of calcite points to

considerable amounts of HCO_3^- in the system. In contrast, the agpaitic unit SM6 contains reduced H_2O-NaCl-CH_4 fluid inclusions. It is interesting to note that the T-f_{O2} conditions derived for the miaskitic units only barely lie in the field of CO_2-dominance in the fluid (Fig. 14). Accordingly, a small change in any parameter related to f_{O2} can push the fluid and thereby the whole system into the CH_4 stability field and may thereby cause agpaitic assemblages to form. The similar fluid isotopic composition of the miaskites and agpaites indicates that not only the minerals/rocks but also all the Motzfeldt fluids were derived from a similar source. Combining the carbon isotopic composition, which partially reflects a mantle origin, with the hydrogen and oxygen isotope compositions of the inclusion water, which imply a meteoric origin, a fluid mixing model best explains the fluid assemblage observed in the Motzfeldt rocks. This seems to be similar to the case of the South Greenlandic Ivigtut Complex (Köhler *et al.*, 2008) and at least the late-stage hydrothermal fluids in the Ilímaussaq intrusion (Graser *et al*., in prep.).

We suggest that the association of a reduced mineral assemblage (Fe^{2+}-dominated minerals) and an oxidised fluid (CO_2, calcite) progressively changes during magmatic differentiation to an oxidised mineral assemblage (Fe^{3+}-bearing; aegirine) and a reduced fluid (CH_4) in the last crystallising rock unit (SM6). These changes are probably mainly driven by respeciation during temperature decrease and the increasing alkali content of the melt. The lujavrites in the Motzfeldt intrusion formed from these very highly fractionated, late-stage melts.

Comparison to other intrusions

On the basis of Nd and O isotope data, the source of the Motzfeldt magmas seems to be similar to that of the other Gardar intrusions (Ilímaussaq: Marks *et al*., 2004; Puklen: Marks *et al*., 2003; Grønnedal-Ika: Halama *et al*., 2005). Therefore, comparing the T-f_{O2} conditions of the Motzfeldt rocks to those of other Gardar intrusions can reveal underlying mechanisms of alkaline to peralkaline magmatic differentiation (Fig. 14). The syenites in the Grønnedal-Ika complex crystallised at higher oxygen fugacities (~ΔFMQ +3 to +4; 700-900 °C, Halama *et al.*, 2005) where only CO_2-bearing phases are stable (carbonates, cancrinite). In contrast, Markl *et al.* (2001) showed that the Ilímaussaq intrusion (the type locality of agpaitic rocks) crystallised under very reduced conditions (~ΔFMQ -3 to -4); consequently, the stable high-temperature fluid phase was methane-dominated (Krumrei *et al.*, 2007) and carbonates are absent at orthomagmatic conditions. Marks *et al.* (2003) showed that the granitic to syenitic Puklen intrusion crystallised at ~ΔFMQ -0.8 to -2 and ca. 800 °C. Consequently, Puklen

contains carbonate as a late-stage (alteration) product (Marks *et al.*, 2003). No evidence of CO_2 was found in the fluid inclusions (Köhler, 2004). However, in syenitic samples which crystallised at oxygen fugacities of ΔFMQ -0.8 to -2.3 (Marks *et al.*, 2003), Köhler (2004) detected subordinate amounts of methane. In samples from the Puklen alkali granite which formed at higher f_{O2}, only methane-free H_2O-NaCl fluid inclusions were observed. Grønnedal-Ika and Puklen lack any sign of agpaitic minerals such as eudialyte.

Globally, agpaitic rocks occur from early magmatic as in the Ilímaussaq intrusion or Lovozero and Khibina, Kramm & Kogarko, 1994; Zaitsev *et al.*, 1998) to hydrothermal stages of crystallisation (agpaitic pegmatites, e.g. in Langesundfjord, Tamazeght and Mont St. Hilaire; Brøgger, 1890; Bouabdli *et al.*, 1988; Horvath & Gault, 1990; Marks *et al.*, 2008). We propose that these differences may be related to the T-f_{O2} evolution of the respective intrusions. In this respect, it is interesting to note that in terms of f_{O2} evolution during magmatic differentiation, Motzfeldt is similar to but slightly more reduced than the Puklen intrusion; this may be related to the stronger contamination effects detected in the Puklen melts (Marks *et al.*, 2003). This slight change in redox (and crustal contamination) conditions to the more reducing side is just enough to allow the melt to enter the field of agpaitic mineral stability in the very last magmatic stage SM6. In the highly reduced Ilímaussaq intrusion, in contrast, eudialyte is found as an early-crystallizing liquidus phase which may be attributed to the reduced character.

This contribution demonstrates that fluid inclusion chemistry, particularly the speciation of a C-O-H fluid (CO_2 or CH_4), may serve as an excellent tracers for the redox conditions of the melt and help to understand the transition from miaskitic to agpaitic rocks. The transition from miaskitic to agpaitic rocks can be explained in terms of a continuous magmatic differentiation sequence in peralkaline systems. Several features are common to all agpaitic intrusions: (1) an extreme peralkaline composition which causes the high solubility of trace elements such as Zr and other HFSE. These elements are complexed with Na and Si, forming the precursor species to the complex minerals of agpaites (eudialyte, rinkite). (2) an extremely long crystallisation interval down to temperatures as low as 450 °C. (3) Redox reactions involving the speciation of Fe (Fe^{2+}/Fe^{3+}) and C (CO_2/CH_4). (4) no (or very late) exsolution of a characteristically methane-bearing fluid phase.

ACKNOWLEDGMENTS

Adrian Finch, Ian Parsons and Julian Schilling are thanked for their help during the field work. Angus & Ross and their Greenland Team (especially Ashlyn Armour-Brown and Jamie

McCreath) are thanked for the pleasant time in the field as well as giving the possibility to do a second field season. Henry Emeleus kindly provided one sample of SM2. Valuable discussions with Adrian Finch, Ian Parsons, Wolfgang Siebel, Heiner Taubald and Thomas Wagner helped to improve the interpretations of this study. Ralf Halama is thanked for his help with the calculations of the CO_2-CH_4 reaction curves and Verena Krasz for carefully hand picking the mineral separates. Thomas Wenzel provided assistance with microprobe measurements which is greatly acknowledged. Gabi Stoschek, Bernd Steinhilber & Elmar Reitter are thanked for their help with the isotope analysis. Jasmin Köhler's help to improve an earlier version of this manuscript is greatly acknowledged. The careful reviews and suggestions of Tom Andersen, Stefano Salvi and an anonymous reviewer and the editorial handling of Marjorie Wilson helped to improve the manuscript significantly. Financial support by the German Science Foundation is greatly acknowledged.

REFERENCES

Andersen, D. J. & Lindsley, D. H. (1985). New (and final!) models for the Ti-magnetite/ilmenite geothermometer and oxygen barometer. Abstract AGU 1985 Spring Meeting Eos Transactions. *American Geophysical Union* **66**, 416.

Andersen, D. J., Lindsley, D. H. & Davidson, P. M. (1993). QUILF; a Pascal program to assess Equilibria among Fe-Mg-Mn-Ti oxides, pyroxenes, olivine, and quartz. *Computers & Geosciences* **19**, 1333-1350.

Armour-Brown, A., Tukiainen, T., Wallin, B., Bradshaw, C. & Emeleus, C. H. (1983). Uranium exploration in South Greenland. **115**, 68-75.

Armstrong, J. T. (1991). *Quantitative elemental analysis of individual microparticles with electron beam instruments.* In: Heinrich, K. F. J., Newbury, D. E. (eds.) *Electron Probe Quantitation*. Plenum Press, New York and London, 261-315.

Bakker, R. J. (2003). Package FLUIDS 1. Computer programs for analysis of fluid inclusion data and for modelling bulk fluid properties. *Chemical Geology* **194**, 3-23.

Beeskow, B., Treloar, P. J., Rankin, A. H., Vennemann, T. W. & Spangenberg, J. (2006). A reassessment of models for hydrocarbons generation in the Khibiny nepheline syenite complex, Kola Peninsual, Russia. *Lithos* **91**, 1-18.

Bezos, A. & Humler, E. (2005). The Fe3+/ΣFe ratios of MORB glasses and their implications for mantle melting. *Geochimica et Cosmochimica Acta* **69**, 711-725.

Bodnar, R. J. (1993). Revised equation and table for determining the freezing point depression of the H_2O-NaCl solutions. *Geochimica et Cosmochimica Acta* **57**, 683-684.

Bottomley, D. J., Gregoire, D. C. & Raven, K. G. (1994). Saline Groundwaters and brines in the Canadian Shield: geochemical and isotopic evidence for a a residual evaporite brine component. *Geochimica et Cosmochimica Acta* **58**, 1483-1498.

Borovikov, A. A., Gushchina, L. N. & Borisekno, A. S. (2001). Specific features of FeCl2 and FeCl3 solution behaviour at low temperatures (cryometry of fluid inclusions). *XVI ECROFI European Current Research On Fluid Incluions, Faculdade de Ciências do Porto, Departamento de Geologia, Memória* **7**, 61–63.

Bouabdli, A., Dupuy, C. & Dostal, J. (1988). Geochemistry of Mesozoic alkaline lamprophyres and related rocks from the Tamezeght massif, High Atlas, Morocco. *Lithos* **22**, 43-58.

Bradshaw, C. (1988). A Petrographic, Structural and Geochemical study of the Alkaline Igneous rocks of the Motzfeldt centre, South Greenland. *Ph.D. thesis*, University of Durham.

Brøgger, W. V. (1890). Die Mineralien der Syenitpegmatitgänge der Südnorwegischen Augit- und Nephelinsyenite.

Zeitschrift für Kristallographie - Mineralogie **16**, 1-235 and 1-663.

Brown, W. L. & Parsons, I. (1989). Alkali feldspars: ordering rates, phase transformations and behaviour diagrams for igneous rocks. *Mineralogical Magazine* **53**, 25-42.

Bureau, H. & Métrich, N. (2003). An experimental study of bromine behaviour in water-saturated silicic melts. *Geochimica et Cosmochimica Acta* **67**, 1689-1697.

Bureau, H., Keppler, H. & Métrich, N. (2000). Volcanic degassing of bromine and iodine: experimental fluid/melt partitioning data and applications to stratospheric chemistry. *Earth and Planetary Science Letters* **183**, 51-60.

Byers, C. D., Christie, D. M., Muenow, D. W., Sinton, J. M. (1984). Volatile contents and ferric-ferrous ratios of basalt, ferrobasalt , andesite and rhyodacite glasses from the Galapagos 95.5°W propagating rift. *Geochimica et Cosmochimica Acta* **48**, 2239-2245.

Cartwright, I., Weaver, T., Tweed, S., Ahearne, D., Cooper, M., Czapnik, C. & Tranter, J. (2000). O, H, C isotope geochemistry of carbonated mineral springs in central Victoria, Australia: sources of gas and water-rock interaction during dying basaltic volcanism. *Journal of Geochemical Exploration* **69-70**, 257-261.

Chakhmouradian, A. R. & Mitchell, R. H. (2002). The mineralogy of Ba- and Zr-rich alkaline pegmatites from Gordon Butte, Crazy Mountains (Montana, USA): comparisons between potassic and sodic agpaitic pegmatites. *Contributions to Mineralogy and Petrology* **143**, 93-114.

Clarke, L. B., Le Bas, M. J. & Spiro, B. (1993). Rare Earth, trace elements and stable isotope fractionation of carbonatites at Kruidfontein, Transvaal, South Africa. *Proc. 5th Kimberlite Conference 1, Kimberlite, Related Rocks and Mantle Xenoliths. CPRM, Brasilia,* 236-251.

Coulson, I. M. (1997). Post-magmatic alteration in eudialyte from the North Qoroq centre, South Greenland. *Mineralogical Magazine* **61**, 99 – 109.

Coulson, I. M., Goodenough, K. M., Pearce, N. J. G. & Leng, M. J. (2003). Carbonatites and lamprophyres of the Gardar Province-a 'window' to the Sub-Gardar Mantle? *Mineralogical Magazine* **67**, 855–872.

Craig, H. (1961). Isotopic variations in meteoric waters. *Science* **133**, 1702.

Dallai, L., Ghezzo, C. & Sharp, Z. D. (2003). Oxygen isotope evidence for crustal assimilation and magma mixing in the Granite Harbour intrusives, Northern Victoria Land, Antarctica. *Lithos* **67**, 135-151.

Davis, W. D., Lowenstein, T. K. & Spencer, R. J. (1989). Melting behaviour of fluid inclusions in laboratory-grown halite crystals in the systems NaCl–H2O, NaCl–KCl–H2O, NaCl–MgCl2–H2O and NaCl-CaCl2-H2O. *Geochimica et Cosmochimica Acta* **54**, 591-601.

Deines, P. (1989). *Stable isotope variations in carbonatites.* In: Bell, K. (ed.) *Carbonatites: Genesis and evolution*. Unwin Hyman, London, Boston, Sydney, Wellington, 301-359.

Deméney, A., Ahijado, A., Casillas, R. & Vennemann, T. W. (1998). Crustal contamination and fluid/rock interaction in the carbonatites of Fuerteventura (Canary Islands, Spain): a C, O, H isotope study. *Lithos* **44**, 101-115.

DePaolo, D. J. (1981). Neodymium isotopes in the Colorado Front Range and crust-mantle evolution in the Proterozoic. *Nature* **291**, 193-196.

Des Marais, D. J. & Moore, J. G. (1984). Carbon and its isotopes in mid-oceanic basalt glasses. *Earth and Planetary Science Letters* **69**, 43-57.

Eiler, J. M. (2001). *Oxygen isotope variations of basaltic lavas and upper mantle rocks.* In: Valley, J.W. and Cole, D.R. (eds.) *Stable Isotope Geochemistry. Reviews in Mineralogy.* Washington: Mineral. Soc. America. **43**, 319-364.

Eiler, J. M., Schiano, P., Kitchen, N. & Stolper, E. M. (2000). Oxygen-isotope evidence for recycled crust in the sources of mid-ocean-ridge basalts. *Nature* **403**, 530-534.

Emeleus, C. H. & Harry, W. T. (1970). The Igaliko nepheline syenite complex; general description. *Meddelelser om Grønland* **186**, 115 pp.

Escher, A. & Watt, W. S. (1970). Geology of Greenland. Copenhagen: *Geological Survey of Greenland*. 603 pp.

Farges, F., Ponader, C. W. & Brown, Jr., G. E. (1991). Structural environments of incompatible elements in silicate glass/melts systems, I. Zr at trace levels. *Geochimica et Cosmochimica Acta* **55.** 1563-1574.

Frape, S. K. & Fritz, P. (1982). The chemistry and isotopic composition of saline groundwaters from the Sudbury Basin, Ontario. *Canadian Journal of Earth Sciences* **19**, 645-661.

Frape, S. K., Fritz, P., McNutt, R. H. (1984). Water-rock interaction and chemistry of groundwaters from the Canadian Shield. *Geochimica et Cosmochimica Acta* **48**, 1617-1627.

Friedman, I. (1953). Deuterium content of natural waters and other substances. *Geochimica et Cosmochimica Acta* **4**, 89-103.

Friedman, I. & O'Neil, J. R. (1977). *Compilation of stable isotope fractionation factors of geochemical interest.* In: Fleischer, M. (ed.) *Data of geochemistry.* U.S. Geological Survey Professional Paper 440-KK, 12.

Frost, B. R. & Lindsley, D. H. (1992). Equilibria among Fe-Ti-oxides, pyroxenes, olivine, and quartz: Part II. *Application. American Mineralogist* **77,** 1004-1020.

Garde, A. A., Hamilton, M. A., Chadwick, B., Grocott, J. & McGaffrey, K. J. W. (2002). The Ketilidian orogen of South Greenland: geochronology, tectonics, magmatism, and fore arc accretion during Palaeoproterozoic oblique convergence. *Canadian Journal of Earth Sciences* **39**, 765-793.

Gerlach, S., Claußen, O. & Rüssel, C. (1998). Thermodynamics of iron in alkali-magnesia-silica glasses. *Journal of Non-Crystalline Solids* **238**, 75–82.

Gerlach, S., Claußen, O. & Rüssel, C. (1999). A voltammetric study on the thermodynamics of the Fe^{3+}/Fe^{2+}-equilibrium in alkali-lime-alumosilicate melts. *Journal of Non-Crystalline Solids* **248**, 92-98.

Goldstein, S. L., O´Nions, R. K. & Hamilton, P. J. (1984). A Sm-Nd isotopic study of the atmospheric dust and particulates from major river systems. *Earth and Planetary Science Letters* **70**, 221-236.

Goodenough, K. M. (1997). Geochemistry of gardar intrusions in the Ivigtut Area, South Greenland. *Ph.D. thesis*, University of Edinburgh.

Graham, C. M., Harmon, R. S. & Sheppard, S. M. F. (1984). Experimental hydrogen isotope studies: hydrogen isotope exchange between amphibole and water. *American Mineralogist* **69**, 128-138.

Graser, G., Potter, J., Köhler, J. & Markl, G. (in press). Isotope, major, minor and trace element geochemistry of late-magmatic fluids in the peralkaline Ilímaussaq intrusion, South Greenland. *Lithos.*

Halama, R., Wenzel, T., Upton, B. G. J., Siebel, W. & Markl, G. (2003). A geochemical and Sr-Nd-O isotopic study of the Proterozoic Eriksfjord Basalts, Gardar Province, South Greenland: Reconstruction of an OIB signature in crustally contaminated rift-related basalts. *Mineralogical Magazine* **67**, 831-854.

Halama, R., Vennemann, T., Siebel, W. & Markl, G. (2005). The Grønnedal-Ika carbonatite-syenite complex, South Greenland: An origin involving liquid immiscibility. *Journal of Petrology* **46**, 191-217.

Hamilton, D. L. (1961). Nephelines as crystallisation temperature indicators. *Journal of Geology* **69**, 321-329

Hanchar, J. M. & Watson, E. B. (2003). *Zircon saturation thermometry.* In: Hanchar, J. M., Hoskin, P. W. O. (eds.) *Zircon. Reviews in Mineralogy and Geochemistry* **53**, 89-112.

Harris, C. (1995). Oxygen isotope geochemistry of the Mesozoic anorogenic complexes of Damaraland, northwest Namibia: evidence for crustal contamination and its effects on silica saturation. *Contributions to Mineralogy and Petrology* **122**, 308-321.

Hoefs, J. (1997). *Stable isotope geochemistry.* Springer, Berlin Heidelberg

Hollemann, A. F. & Wiberg, E. 1995. *Lehrbuch der anorganischen Chemie.* De Gruyter, Berlin, New York, 101.

Horvath, L. & Gault, R. A. (1990). The Mineralogy of Mont Saint-Hilaire, Quebec. *Mineralogical Record* **21**, 284-359.

Hoskin, P. W. O. & Schaltegger, U. (2003). *The composition of zircon and igneous and metamorphic petrogenesis.* In:

Huizenga, J. M. (2001). Thermodynamic modelling of C-O-H fluids. *Lithos* **55**, 101-114

Huizenga, J. M. (2005). COH, an Excel spreadsheet for composition calculations in the C-O-H fluid system. *Computers & Geosciences* **31**, 797-800.

Jacobson, S. B. & Wasserburg, G. J. (1980). Sm-Nd isotopic evolution of chondrites. *Earth and Planetary Science Letters* **50**, 139-155.

Jones, A. P. (1980) Petrology and structure of the Motzfeldt centre, Igaliko complex, South Greenland. *PhD thesis*, Univ. of Durham, UK.

Jones, A. P. (1984). Mafic silicates from the nepheline syenites of the Motzfeldt centre, south Greenland. *Mineralogical Magazine* **48**, 1-12.

Jones, A. P. & Larsen, L. M. (1985). Geochemistry and REE minerals of nepheline syenites from the Motzfeldt Centre, South Greenland. *American Mineralogist* **70**, 1087-1100.

Jones, A. P. & Peckett, A. (1980). Zirconium-bearing aegirines from Motzfeldt, South Greenland. *Contributions to Mineralogy and Petrology* **75**, 251-255.

Keller, J. & Hoefs, J. (1995). *Stable isotope characteristics of recent natrocarbonatites from Oldoinyo Lengai.* In: Bell, K. & Keller, J. (eds.) *Carbonatite Volcanism: Oldoinyo Lengai and the Petrogenesis of Natrocarbonatites.* Berlin: Springer, 113–123.

Kelly, W. C., Rye, R. O. & Livnat, A. (1986). Saline minewaters of the Keweenaw Peninsula, Northern Michigan: Their natural origin and relation to similar deep waters in the Precambrian crystalline rocks of the Canadian Shield. *American Journal of Science* **286**, 281-308.

Khomyakov, A. P. (1995). *Mineralogy of Hyperagpaitic Alkaline Rocks.* Oxford science publications. Clarendon Press.

Kilinc, A., Carmichael, I.S.E., Rivers, M.L. & Sack, R.O. (1983). The ferric–ferrous ratio of natural silicate liquids equilibrated in air. *Contributions to Mineralogy and Petrology* **83**, 136–141.

Kogarko, L. N. (1974). *Rôle of Volatiles.* In: Sørensen, H. (ed.) *The Alkaline Rocks*. London: John Wiley & Sons, 474-487.

Kogarko L. N. (1987) *Alkaline rocks of the eastern part of the Baltic Shield (Kola Peninsula).* In: Fitton, J. G. & Upton, B. G. J. (eds.) *Alkaline Igneous Rocks*, Geological Society Special Publication **30**, 531-544.

Kogarko L. N., Burnham C. W. & Shettle D. (1977) Water regime in alkalic magmas. *Geochemistry International* **14**, 1-8.

Kogarko, L. N. & Romanchev, B. P. (1983). Phase equilibria in alkaline melts. *International Geological Reviews* **25**, 534-46.

Kogarko L. N., Kosztolanyi C. & Ryabchikov I. D. (1987) Geochemistry of the reduced fluid in alkali magmas. *Geochemistry International* **24**, 20-27.

Köhler, J. (2004). Petrologische und Geochemische Untersuchungen von Fluideinschlüssen in Gesteinen der Puklen Intrusion, Südgrönland. *Master thesis*. Univ. Tübingen.

Köhler, J., Konnerup-Madsen, J. & Markl, G. (2008). Fluid chemistry in the Ivigtut cryolite deposit, South Greenland. *Lithos* **103**, 369-392.

Konnerup-Madsen, J. (2001). A review of the composition and evolution of hydrocarbon gases during solidification of the Ilímaussaq alkaline complex, South Greenland. *Geology of Greenland Survey Bulletin* **301**, 159–166.

Konnerup-Madsen, J. & Rose-Hansen, J. (1982). Volatiles associated with alkaline igneous rift activity: fluid inclusions in the Ilímaussaq intrusion and the Gardar granite complexes. *Chemical Geology* **37,** 79 -93.

Konnerup-Madsen, J. & Rose-Hansen, J. (1984). Composition and significance of fluid inclusions in the Ilímaussaq peralkaline granite, South Greenland. *Bulletin de Minéralogie* **107**, 317-326.

Konnerup-Madsen, J., Dubessy, J. & Rose-Hansen, J. (1985). Combined Raman microprobe spectrometry and microthermometry of fluid inclusions in minerals from igneous rocks of the Gardar province (south Greenland). *Lithos* **18**, 271-280.

Kramm, U. & Kogarko, L. N. (1994). Nd and Sr isotope signatures of the Khibina and Lovozero agpaitic centres, Kola Province, Russia. *Lithos* **32**, 225-242.

Kress, V. C. & Carmichael, I. S. E. (1988). Stoichiometry of the iron oxidation reaction in silicate melts. *American Mineralogist* **73**, 1267-1274.

Kress, V. C. & Carmichael, I. S. E. (1989). The lime-iron-silicate melt system: Redox and volume systematics. *Geochimica et Cosmochimica Acta* **53**, 2883-2892.

Kress, V. C. & Carmichael, I.S.E. (1991). The compressibility of silicate liquids containing Fe_2O_3 and the effect of composition, temperature, oxygen fugacity and pressure on their redox states. *Contributions to Mineralogy and Petrology* **198**, 82-92.

Krumrei, T., Kaliwoda, M., Pernicka, E. & Markl, G. (2007). Volatiles in a peralkaline system: Abiogenic hydrocarbons and F-Cl-Br systematics in the naujaite of the Ilimaussaq intrusion South Greenland. *Lithos* **95**, 298-314.

Kyser, T. K. (1986). *Stable Isotope variations in the mantle.* In: Valley, J. W., Taylor, H. P. & O'Neil, J. R. (eds.) *Stable Isotopes in High Temperature Geological Processes.* Reviews in Mineralogy **16**, 141-164.

Kyser, T. K., O'Neil, J. R. & Carmichael. I. S. E. (1982). Genetic relations among basic lavas and ultramafic nodules: evidence from oxygen isotope compositions. *Contributions to Mineralogy and Petrology* **81,** 88-102.

Lange, R. A. & Carmichael, I. S. E. (1989). Ferric-ferrous Equilibria in Na_2O-FeO-Fe_2O_3-SiO_2 melts: Effects of analytical techniques on derived partial molar volumes. *Geochimica et Cosmochimica Acta* **53**, 2195-2204.

Larsen, L. M. & Sørensen, H. (1987). *The Ilímaussaq intrusion-progressive crystallization and formation of layering in an agpaitic magma.* In: Fitton, J. G. & Upton, B. G. J. (eds.) *Alkaline Igneous Rocks*. Geological Society Special Publication **30**, 473-488.

Leake, B. E. (Chairman) (1997). Nomenclature of amphiboles. Report of the Subcommittee on Amphiboles of the International Mineralogical Association Commission on New Minerals and Mineral Names. *European Journal of Mineralogy* **9**, 623-651.

Lepage, L. D. (2003). ILMAT: an Excel worksheet for ilmenite-magnetite geothermometry and geobarometry. *Computers & Geosciences* **29**, 673-678.

Liew, T. C. & Hofmann, A. W. (1988). Precambrian crustal components, plutonic associations, plate environment of the Hercynian Fold Belt of central Europe: Indications from a Nd and Sr isotopic study. *Contributions to Mineralogy and Petrology* **98**, 129-138.

Lindsley, D. H. & Frost, B. R. (1992). Equilibria among Fe-Ti-oxides, pyroxenes, olivine, and quartz: Part I. Theory. *American Mineralogist* **77**, 987-1003.

Lugmair, G. W. & Marti, K. (1978). Lunar initial 143Nd/144Nd: differential evolution of the lunar crust and mantle. *Earth and Planetary Science Letters* **39**, 349-357.

Markl, G. (2001). A new type of silicate liquid immiscibility macroscopically visible in Proterozoic peralkaline rocks from Ilímaussaq, South Greenland. *Contributions to Mineralogy and Petrology* **141**, 458-472.

Markl, G. & Baumgartner, L. (2002). pH changes in peralkaline late-magmatic fluids. *Contributions to Mineralogy and Petrology* **144**, 331-346.

Markl, G., Marks, M., Schwinn, G. & Sommer, H. (2001). Phase equilibrium constraints on intensive crystallization parameters of the Ilímaussaq Complex, South Greenland. *Journal of Petrology* **42**, 2231-2258.

Marks, M., Vennemann, T., Siebel, W. & Markl, G. (2003). Quantification of Magmatic and Hydrothermal Processes in a Peralkaline Syenite-Alkali Granite Complex Based on Textures, Phase Equilibria, and Stable and Radiogenic Isotopes. *Journal of Petrology* **44**, 1247-1280.

Marks, M., Venemann, T., Siebel, W. & Markl, G. (2004). Nd-, O-, and H-isotopic evidence for complex, closed-system fluid evolution of the peralkaline Ilímaussaq intrusion, South Greenland. *Geochimica et Cosmochimica Acta* **68**, 3379-3395.

Marks, M., Rudnick, R. L., McCammon, C., Vennemann, T. & Markl, G. (2007). Arrested kinetic Li isotopic fractionation at the margin of the Ilímaussaq complex, South Greenland: evidence for open-system processes during final cooling of peralkaline igneous rocks*. Chemical Geology* **246**, 207-230.

Marks, M., Schilling, J., Coulson, I., Wenzel, T. & Markl, G. (2008). The Alkaline-PeralkalineTamazeght Complex, High Atlas Mountains, Morocco: Mineral Chemistry and Petrological Constraints for Derivation from a Compositionally Heterogeneous Mantle Source. *Journal of Petrology* **49**, 1097-1131.

Marks, M. & Markl, G. (2001). Fractionation and assimilation processes in the alkaline augite syenite unit of the Ilimaussaq Intrusion, South Greenland, as deduced from phase equilibria. *Journal of Petrology* **42**, 1947-1969.

McDowell, S. D. (1986). Composition and structural state of coexisting feldspars, Salton Sea geothermal field. *Mineralogical Magazine* **50**, 75-84.

Mitchell, R. H. & Liferovich, R. P. (2006). Subsolidus deuteric/hydrothermal alteration of eudialyte in lujavrite from the Pilansberg alkaline complex, South Africa. *Lithos* **91**, 352-372.

Nicholls, J. & Carmichael, I. S. E. (1969). Peralkaline acid liquids: a petrological study. *Contributions to Mineralogy and Petrology* **20**, 268–294.

Nielsen, T. F. D. (1994). Alkaline dike swarms of the Gardiner complex and the origin of ultramafic alkaline complexes. *Geochemistry International* **31**, 37-56.

Nivin, V. A., Belov, N. I., Treloar, P. J. & Timofeyev, V. V. (2001). Relationships between gas geochemistry and release rates and the geochemical state of igneous rock massifs. *Tectonophysics* **336**, 233-244.

Nivin, V. A., Ikorskii, S. V. & Treloar, P. J. (2002). Bulk gas content variations in fluid inclusions of minerals from the Khibina and Lovozero nepheline-syenite plutons (NE Baltic Shield, Russia); implication for origin of hydrocarbon gases. *Abstracts of the 18th General Meeting of the International Mineralogical Association* **18**, 248.

Nivin, V. A., Treloar, P. J., Konopleva, N. G. & Ikorsky, S. V. (2005). A review of the occurrence, form and origin of C-bearing species in the Khibiny alkaline igeneous complex, Kola Peninsula, NW Russia. *Lithos* **85**, 93-112.

Ohmoto, H. & Goldhaber, M. B. (1997). *Sulfur and carbon isotopes*. In: Barnes, H.L. (ed.) *Geochemistry of hydrothermal ore deposits.* 3rd ed., Wiley, New York, 517-611.

Pearce, N. J. G. & Leng, M. J. (1996). The origin of carbonatites and related rocks from the Igaliko Dyke Swarm, Gardar Province, South Greenland: field, geochemical and C–O–Sr–Nd isotope evidence. *Lithos* **39**, 21–40.

Pearce, N. J. G., Leng, M. J., Emeleus, C. H. & Bedford, C. M. (1997). The origins of carbonatites and related rocks from the Grønnedal-Ika Nepheline Syenite Complex, South Greenland: C–O–Sr isotope evidence. *Mineralogical Magazine* **61**, 515–529.

Petersilie, I. A. & Sørensen, H. (1970). Hydrocarbon gases and bituminous substances in rocks from the Ilímaussaq alkaline intrusion, South Greenland. *Lithos* **3**, 59-76.

Pineau, F. & Javoy, M. (1983). Carbon isotopes and concentrations in mid-oceanic ridge basalts. *Earth and Planetary Science Letters* **62**, 239-257.

Piotrowski, J. M. & Edgar, A. D. (1970). Melting relations of undersaturated alkaline rocks from South Greenland compared to those of Africa and Canada. *Meddelelser om Grønland* **181**.

Potter, J., Rankin, A. H. & Treloar, P. J. (1999). *The relationship between CH4 and CO2 inclusions and Fe–O–S mineralization in intrusions of the Kola Alkaline Province.* In: Stanley, C. J., et al. (eds.) *Mineral Deposits: Processes to Processing 1.* Balkema, Rotterdam, 87– 90.

Potter, J. & Konnerup-Madsen, J. (2003). *A review of the occurrence and origin 1 of abiogenic hydrocarbons in igneous rocks.* In: Petford, N. & McCaffrey K. J. W. (eds.) *Hydrocarbons in Crystalline Rocks.* Geological Society, London, Special Publications **214**, 151-173.

Potter, J., Rankin, A. H. & Treloar, P. J. (2004). Abiogenic Fischer-Tropsch synthesis of hydrocarbons in alkaline igneous rocks; fluid inclusion, textural and isotopic evidence from the Lovozero Complex, N.W. Russia. *Lithos* **75**, 311-330.

Richet, P., Bottinga, Y. & Javoy, A. (1977). A review of hydrogen, carbon, nitrogen, oxygen, sulphur and chlorine stable isotope fractionation among gaseous molecules. *Annual Reviews Earth Planetary Science* **5**, 65-110.

Robie, R. A. & Hemingway, B. S. (1995). Thermodynamic properties of minerals and related substances at 298_15K and 1 bar (105 Pascals) pressure and at higher temperatures. *US Geological Survey, Bulletin* **2131**, 461 pp.

Rumble, D. & Hoering, T. C. (1994). Analysis of oxygen and sulfur isotope ratios in oxide and sulfide minerals by spot heating with a carbon dioxide laser in a fluorine atmosphrere. *Accounts of Chemical Research* **27**, 237-241.

Rüssel, C. & Wiedenroth, A. (2004). The effect of glass composition on the thermodynamics of the Fe2+/Fe3+ equilibrium and the iron diffusivity in $Na_2O/MgO/CaO/Al_2O_3/SiO_2$ melts. *Chemical Geology* **213**, 125-135.

Ryabchikov, I. D. & Kogarko, L. N. (2006). Magnetite compositions and oxygen fugacities of the Khibina magmatic system. *Lithos* **91**, 35-45.

Sack, R. O., Carmichael, I. S. E., Rivers, M. & Ghiorso M.S. (1981). Ferric–ferrous equilibria in natural silicate liquids at 1 bar. *Contributions to Mineralogy and Petrology* **75**, 369–377.

Salvi, S. & Williams-Jones, A. E. (1990). The role of hydrothermal processes in the granite hosted Zr, Y, REE deposit at Strange Lake, Quebec/Labrador: evidence from fluid inclusions. *Geochimica et Cosmochimica Acta* **54**, 2403–2418.

Salvi, S. & Williams-Jones, A. E. (1997). Fischer-Tropsch synthesis of hydrocarbons during sub-solidus alteration of the Strange Lake peralkaline granite, Quebec / Labrador, Canada. *Geochimica et Cosmochimica Acta* **61**, 83-99.

Salvi, S. & Williams-Jones, A. E. (2006). Alteration, HFSE mineralisation and hydrocarbon formation in peralkaline igneous systems: Insights from the Strang Lake Pluton, Canada. *Lithos* **91**, 19-34.

Schoell, M. (1988). Multiple origins of methane in the Earth. *Chemical Geology* **71**, 1-10.

Schönenberger, J., Marks, M., Wagner, T. & Markl, G. (2006). Fluid-rock interaction in autoliths of agpaitic nepheline syenites in the Ilimaussaq intrusion, South Greenland. *Lithos* **91**, 331-351.

Schönenberger, J., Köhler, J. & Markl, G. (2008). REE systematics of fluorides, calcite and siderite in peralkaline plutonic rocks from the Gardar Province, South Greenland. *Chemical Geology* **247**, 16-37.

Sharp. Z. D. (1990). A laser-based microanalytical method for the in-situ determination of oxygen isotope ratios of silicates and oxides. *Geochimica et Cosmochimica Acta* **54,** 1353-1357.

Shepherd, T. J., Rankin, A. H. & Alderton, D. H. M. (1985). *A practical guide to fluid inclusion studies.* Glasgow, Blackie.

Sheppard, S. M. F. (1986). *Characterization and isotopic variations in natural waters.* In: Valley, J.W., Taylor, H.P.Jr and O´Neil, J.R. (eds.) *Stable Isotopes.* Reviews in Mineralogy. Washington: Mineral. Soc. America. **16**, 165-181.

Sheppard, S. M. F. (1989). The isotopic characterization of aqueous and leucogranitic crustal fluids. *NATO ASI Series, Series C: Mathematical and Physical Sciences* **281**, 245-63.

Shi, P. & Saxena, S. K. (1992). Thermodynamic modelling of the C-O-H-S fluid system. *American Mineralogist* **77**, 1038-1044.

Sood, M. K. & Edgar, A. D. (1970). Melting relations of undersaturated alkaline rocks from the Ilímaussaq intrusion and Grønnedal-Ìka complex South Greenland, under water vapour and controlled partial oxygen pressure. *Meddelelser om Grønland* **181**.

Sørensen, H. (1997). The agpaitic rocks - an overview. *Mineralogical Magazine* **61**, 485-498.

Spötl, C. & Vennemann, T. W. (2003). Continuous-flow isotope ratio mass spectrometric analysis of carbonate minerals. *Rapid Communications in Mass Spectrometry* **17**, 1004–1006.

Suzuoki, T. & Epstein, S. (1976). Hydrogen isotope fractionation between OH-bearing minerals and water. *Geochimica et Cosmochimica Acta* **40**, 1229-1240.

Taubald, H., Morteani, G. & Satir, M. (2004). Geochemical and isotopic (Sr, C, O) data from the alkaline complex of Grønnedal-Ika (South Greenland): evidence for unmixing and crustal contamination. *International Journal of Earth Sciences* **93**, 348–360.

Taylor, H. P. (1974). The application of oxygen and hydrogen isotope studies to problems of hydrothermal alteration and ore deposition. *Economic Geology* **69**, 843-883.

Taylor, H. P. (1977). Water/rock interactions and the origin of H2O in granitic batholiths. *Journal of the Geological Society, London* **133**, 509–558.

Taylor, H. P., Frechen, J. & Degens, E. T. (1967). Oxygen and carbon isotope studies of carbonatites from the Laacher See District, West Germany and the Aln€o District, Sweden. *Geochimica et Cosmochimica Acta* **31**, 407–430.

Taylor, H. P. Jr & Sheppard, S. M. F. (1986). *Igneous rocks: I. Processes of isotopic fractionation and isotope systematics.* In: Valley, J. W., Taylor, H. P. Jr and O´Neil, J. R. (eds.) *Stable Isotopes. Reviews in Mineralogy.* Washington: Mineralogical Society America. **16**, 227-269.

Taylor, R. P., Strong, D. F. & Fryer, B. J. (1981). Volatile control of contrasting trace element distributions in peralkaline granitic and volcanic rocks. *Contributions to Mineralogy and Petrology* **77**, 267-271.

Tichomirowa, M., Grosche, G., Götze, J., Belyatsky, B. V., Savva, E. V., Keller, J. & Todt, W. (2006). The mineral isotope composition of two Precambrian carbonatite complexes from the Kola Alkaline Province – Alteration versus primary magmatic signatures. *Lithos* **91**, 229-249.

Treuil, M., Joron, J. L., Jaffrezic, H., Villemant, B. & Calas, G. (1979). Géochimie des elements hygromagmatophiles: Coefficients de partage minéraux/liquides et propriétés structurales de ces éléments dans les liquides magmatiques. *Bullétin de Mineralogy* **102**, 402-409.

Tukiainen, T., Bradshaw, C. & Emeleus, C. H. (1984). Geological and radiometric mapping of the Motzfeldt Centre of the Igaliko Complex, South Greenland. *Grønlands Geologiske Undersøgelse* **120**, 78-83.

Tuttle, O. F. & Bowen, N. L. (1958). Origin of granite in the light of experimental studies in the system $NaAlSi_3O_8$-$KAlSi_3O_8$-SiO_2-H_2O. *Geological Society of America Memoirs* **74**.

Upton, B. G. J. & Emeleus, C. H. (1987). *Mid-Proterozoic alkaline magmatism in southern Greenland: the Gardar Province.* In: Fitton, J. G. & Upton, B. G. J. (eds.) *Alkaline Igneous Rocks,* Geological Society Special Publication **30**, 449-471.

Upton, B. G. J., Emeleus, C. H., Heaman, L. M., Goodenough, K. M. & Finch, A. A. (2003). Magmatism of the mid-Proterozoic Gardar Province, South Greenland: chronology, petrogenesis and geological setting. *Lithos* **68**, 43-65.

Valley J. W., Kitchen, N., Kohn, M. J., Niendorf, C. R. & Spicuzza, M. J. (1995). UWG-2, a garnet standard for oxygen isotope ratios: strategies for high precision and accuracy with laser heating. *Geochimica et Cosmochimica Acta* **59,** 5223-5231.

Vennemann, T. W., O´Neil, J. R. (1993). A simple and inexpensive method of hydrogen isotope and water analyses of minerals and rocks based on zinc reagent. *Chemical Geology* **103,** 227-234.

Vitrac-Michard, A. Albarede & Azambre, B. (1977). Age Rb-Sr et 39Ar/40Ar de la syénite néphélinique de Fitou (Corbières orientales). *Bullétin de la Societé francaise de Minéralogie et Cristallographie* **100**, 251-254.

Wallace, G. M., Whalen, J. B. & Martin, R. F. (1990). Agpaitic and miaskitic nepheline syenites of the McGerricle plutonic Complex, Gaspé, Quebec: An unusual petrological association. *Canadian Mineralogist* **28**, 251-266.

Watson, E. B. (1979). Zircon saturation in felsic liquids: Experimental results and applications to trace element geochemistry. *Contributions to Mineralogy and Petrology* **70**, 407-4 19.

Watson, E. B. & Harrison, T. M. (1983). Zircon saturation revisited: temperature and composition effects in a variety of crustal magma types. *Earth and Planetary Science Letters* **64**, 295–304.

Wolff, J. A. (1987). Crystallization of nepheline syenite in a subvolcanic magma system: Tenerife, Canary Islands. *Lithos* **20**, 207-223.

Worley, B. A., Cooper, A. F. & Hall, C. E. (1995). Petrogenesis of carbonate-bearing nepheline syenites and carbonatites from Southern Victoria Land, Antarctica: origin of carbon and the effects of calcite-graphite equilibrium. *Lithos* **35**, 183-199.

Zaitsev, A. N., Wall, F. & LeBas, M. J. (1998). REE-Sr-Ba minerals from the Khibina carbonatites, Kola Peninsula, Russia; their mineralogy, paragenesis and evolution: *Mineralogical Magazine* **62**, 225-250.

Zhao, Z. F. & Zheng, Y. F. (2003). Calculation of oxygen isotope fractionation in magmatic rocks. *Chemical Geology* **193**, 59–80.

Zheng, Y. G., (1993a). Calculation of oxygen isotope fractionation in anhydrous silicate minerals. *Geochimica et Cosmochimica Acta* **57**, 1079-1091.

Zheng, Y. F. (1993b). Calculation of oxygen isotope fractionation in hydroxyl-bearing silicates. *Earth and Planetary Science Letters* **120**, 247-263.

Zheng, Y. F. (1999). Oxygen isotope fractionation in carbonate and sulfate minerals. *Geochemical Journal* **33**, 109-126.

REE-systematics of fluorides, calcite and siderite in peralkaline plutonic rocks from the Gardar Province, South Greenland[1].

Johannes Schönenberger, Jasmin Köhler, and Gregor Markl

Eberhard-Karls-Universität, Institut für Geowissenschaften, Wilhelmstrasse 56, 72074 Tübingen, Germany

Keywords: Gardar; Fluorite; REE; Fractionation; Alkaline

[1]Contributions to the Mineralogy of Ilímaussaq # 140

Erschienen 2008 in Chemical Geology 247, 16-35.

Abstract

The Gardar failed-rift Province is world-famous for its (per-)alkaline plutonic rocks. Elevated contents of F in the mantle source and F-enrichment in the parental melts have been suggested to account for the peculiarities of the Gardar rocks (e.g. their rare mineralogy extreme enrichment of HFSE elements, Be or REE in the Ilímaussaq agpaites, and the formation of the unique Ivigtut cryolite deposit). To constrain the formation and chemical evolution of F-bearing melts and fluids, fluorides (fluorite, cryolite, viliaumite, cryolithionite), calcite and siderite from the Ilímaussaq, Motzfeldt and Ivigtut complexes were analysed for their trace element content focusing on the rare earth elements and yttrium (REE).

The various generations of fluorite occurring in the granitic Ivigtut, agpaitic Ilímaussaq and miaskitic to agpaitic Motzfeldt intrusions all share a negative Eu anomaly which is attributed to (earlier) feldspar fractionation in the parental alkali basaltic melts. This interpretation is supported by the abundance of anorthositic xenoliths in many Gardar plutonic rocks.

The primary magmatic fluorites from Ilímaussaq and Motzfeldt display very similar REE patterns suggesting a formation from closely related parental melts under similar conditions. Hydrothermal fluorites from these intrusions were used to constrain the multiple effects responsible for the incorporation of trace elements into fluorides: temperature dependence, fluid migration/interaction and complexation resulting in REE fractionation. Generally, the REE patterns of Gardar fluorides reflect the evolution and migration of a F/CO_2-rich fluid leading to the formation of fluorite and fluorite/calcite veins. In certain units, this fluid inherited the REE patterns of altered host rocks. In addition, there is evidence of an even younger fluid of high REE abundance which resulted in highly variable REE concentrations (up to three orders of magnitude) within one sample of hydrothermal fluorite.

The REE patterns of the granitic Ivigtut intrusion show flat to slightly heavy-REE-enriched patterns characterised by a strong tetrad effect. This effect is interpreted to record extensive fluid- rock interaction in highly fractionated, Si-rich systems.

Interestingly, the fluorides appear to record different source REE patterns, as the spatially close Motzfeldt and Ilímaussaq intrusions show strong similarities and contrast with the Ivigtut intrusion located 100 km NE. These variations may be attributed to differences in the tectonic position of the intrusions or mantle heterogeneities.

Keywords: Gardar, fluorite, REE, fractionation, alkaline

1. Introduction

Fluorine plays a crucial role in the crystallisation of magmas, as it drastically reduces the melting temperature and the melt's viscosity/density (Webster, 1990; Manning, 1981; Dingwell, 1988). In magmatic processes, fluorine-rich fluids are capable of transporting and enriching elements like HFSE, the rare earth elements and yttrium (REE) to economic amounts (Stähle et al., 1987; Rubin et al., 1993; Pan and Fleet, 1996; Rudnick et al., 2000; Salvi et al., 2000; Williams-Jones et al., 2000; Tagirov et al., 2002). Nowadays, fluorite is widely used as a geochemical exploration tool (e.g. Hill et al., 2000; Eppinger & Closs, 1990) as it is often associated with economically important elements like Pb, Zn, Ag and Au in hydrothermal deposits.

The study of REE incorporation into fluorite and associated minerals (e.g. calcite, siderite, cryolite and villiaumite) of different intrusions and evolutionary stages (e.g. primary magmatic, pegmatitic or hydrothermal; e.g. Möller et al., 1976; Kempe et al., 1999; Trinkler et al., 2005) can provide insight into fluid evolution, fluid-rock interaction and element behaviour in highly fractionated rocks during ortho- to late-magmatic processes (e.g. Gagnon et al., 2003). These mechanisms include chemical complexation, redox characteristics, mineral/rock leaching, chemical composition of the precipitating melt/fluid (e.g. Ekambaram et al., 1986; Bau, 1991; Bau & Möller, 1992; Liu et al., 2005).

Furthermore, melts and fluids can become considerably enriched in fluorine during fractionation processes leading to the crystallisation of fluorite and minerals like topaz and cryolite (Scaillet & MacDonald, 2004, Dolejš & Baker, 2007 a, b). Scaillet & Macdonald (2001; 2004) summarised the stability of magmatic fluorite in peralkaline rhyolitic melts. They stated that even in very low Ca, highly peralkaline melts, fluorite can be stabilised by high F activities.

The Gardar failed-rift Province in South Greenland comprises numerous alkaline igneous complexes (Upton et al., 2003) of which the Motzfeldt, Ilímaussaq and Ivigtut intrusions are the focus of this study. Their common rift-related origin, but their very different evolutionary paths (Ivigtut: A-type granites, Motzfeldt: miaskitic nepheline syenites, Ilímaussaq: agpaitic nepheline syenites) and the extensive literature on their petrology and geochemistry make these intrusions ideal study objects for the systematics of trace elements. The province's overall high abundance in fluorine led to the crystallisation of considerable amounts of fluorite and other fluorides (e.g. Upton & Emeleus, 1987; Pauly & Bailey, 1999; Petersen, 2001). They do not occur in all, but are associated only with certain magmatic

complexes and/or are typical of distinct crystallisation sequences. The comparison of various generations of fluorides of the Gardar Province provides insight into the different processes governing the incorporation mechanisms of trace elements into these minerals. The combination of highly resolving analytical methods (e.g. CL & LA ICP-MS) help to reveal those mechanisms.

2. Regional Geology

The 1.35 – 1.14 Ga old Gardar Province in South Greenland is considered as a failed rift system (Upton et al., 2003; Fig. 1) and is characterised by 12 major (per-) alkaline intrusive complexes along with numerous (giant) dyke swarms and a succession of volcanic-sedimentary rocks.

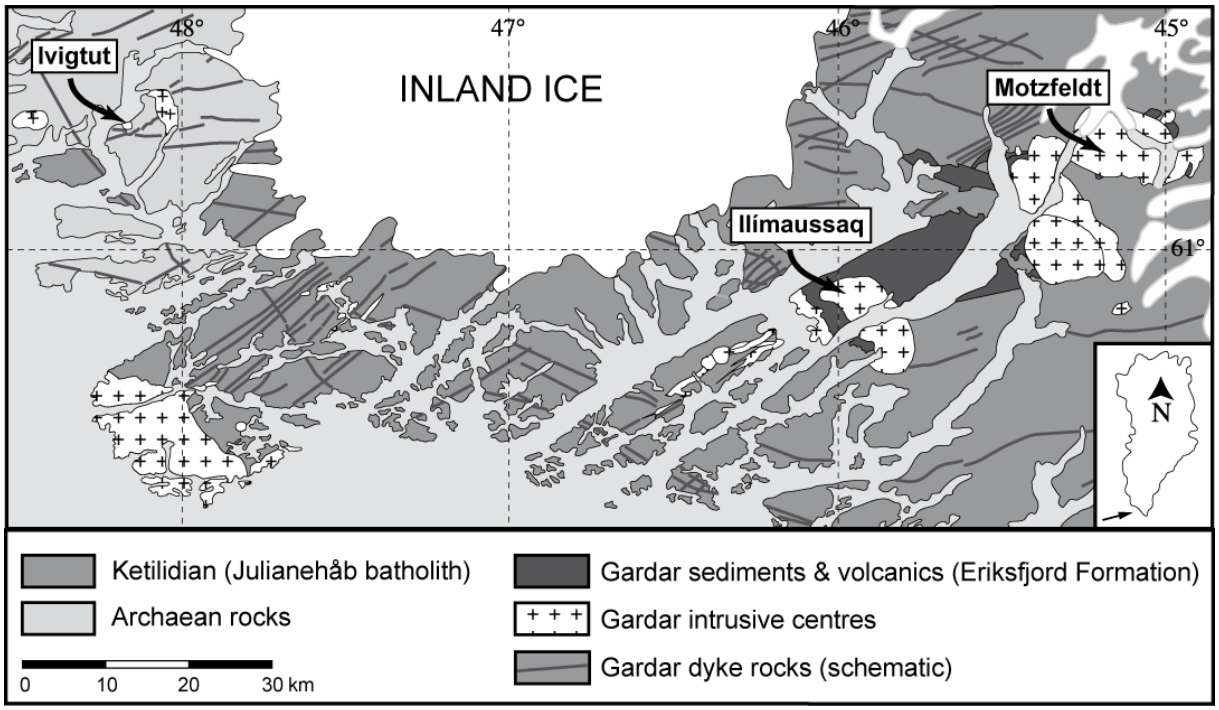

Fig. 1: Overview of the Gardar Province with the investigated intrusions Motzfeldt, Ilímaussaq and Ivigtut. Modified after Escher & Watt (1976).

The composition of the Gardar intrusions ranges from silica-over- to silica-undersaturated rocks. The province is world-famous for the type locality of agpaitic rocks in the Ilímaussaq intrusion and for the unique cryolite [Na_3AlF_6] deposit at Ivigtut. Agpaitic rocks are defined as peralkaline nepheline syenites which crystallised complex Na-Zr-Ti minerals like eudialyte instead of "normal" miaskitic rocks which comprise Fe-Ti oxides and zircon (Sørensen, 1997). These two intrusions, together with a third intrusion, the Motzfeldt complex, represent most of the compositional range of highly evolved silicate rocks occurring

in the Gardar Province. The Ilímaussaq and Motzfeldt complexes intruded the 1.8 Ga old Julianehåb batholith of the Ketilidian orogen (Garde et al., 2002) whereas the Ivigtut intrusion was emplaced in the Archaean craton (Fig. 1). Detailed descriptions of the crystallisation of the three intrusions can be found in e.g. Sørensen et al. (2006), Markl et al. (2001), Goodenough et al. (2000), Pauly & Bailey (1999), Larsen & Sørensen (1987), Jones (1984), Jones (1980), Köhler et al. (2008) and are very briefly summarised below.

Motzfeldt

The Motzfeldt intrusion can be divided into six different intrusive phases (SM1 to SM6, Emeleus & Harry, 1970; Jones, 1980; 1984). SM1 to SM5 are (per-)alkaline, miaskitic rocks, whereas SM6 is of agpaitic composition (occurrence of eudialyte; Sørensen, 1997). Since four phases (SM1, SM4-6) comprise the whole crystallisation sequence (Jones, 1984), we focused on samples from these units. The rocks mainly consist of feldspar, nepheline, Ca-Na amphiboles, augitic to aegirine-augitic pyroxene and Fe-Ti oxides (Jones, 1984). SM6 only crystallised aegirine and neither amphibole nor Fe-Ti oxides, while zircon is replaced by eudialyte. Fluorite occurs as a primary phase in SM1 and SM6, whereas late- to post-magmatic fluorite ± calcite veins are very common in SM1, SM4 and SM5.

Ilímaussaq

The Ilímaussaq intrusion developed from four magmatic batches consisting of miaskitic augite syenite and alkali granite followed by a succession of agpaitic rocks including roof cumulates (naujaites), floor cumulates (kakortokites) and a "sandwich" horizon (lujavrites; Sørensen et al., 2006). The agpaitic rocks consist of arfvedsonite, aegirine, sodalite, eudialyte, feldspar and nepheline in variable modal compositions. Fluorite and villiaumite occur as magmatic phases in the naujaites (Markl et al., 2001), but also crystallised in pegmatites and occur as late-stage and hydrothermal alteration products.

Ivigtut

The Ivigtut (Ivittuut) complex is situated in the northwest of the Gardar Province (Fig. 1). It is about 350 m across and world-famous for its unique cryolite [Na_3AlF_6] deposit that is now mined out. The deposit itself is situated within an A-type granite stock which was intensely metasomatised by F- and CO_2-rich fluids (Goodenough et al., 2000). According to Pauly & Bailey (1999), these fluids became enriched in Na, Al and Si during the breakup of feldspars and subsequently formed an aluminofluoride-rich melt which later exsolved into a silicate-

and a fluoride-rich melt at 500-600 °C. With decreasing temperature, i.e. at hydrothermal conditions, the siliceous melt led to the formation of the large (siderite-)quartz layer in the lower part of the deposit while the cryolite body itself originated from the fluoride-rich melt. It is suggested that this volatile-, F-rich melt gradually evolved to a solute-rich fluid at around and below 450 °C (Pauly & Bailey, 1999; Köhler et al., 2008). Within the deposit, cryolite is mainly associated with siderite, quartz, fluorite, topaz and fluorides such as cryolithionite [$Na_3Li_3Al_2F_{12}$], chiolite, ralstonite, pachnolite, prosopite and others (Pauly & Bailey, 1999).

3. Sample preparation and analytical procedures

Polished sections of fluorite, cryolite, calcite, cryolithionite, siderite and villiaumite samples were studied by conventional microscopy, cathodoluminescence (CL) and laser ablation ICP-MS. CL imagery was performed on a CITL CCL 8200 stage at the University of Tübingen, Germany, with the CL chamber being mounted on a Zeiss microscope. Beam current was 300 μA and acceleration voltage 14.5 kV. Exposure times were usually 3 to 6 seconds.

The laser ablation ICP-MS measurements were performed at the University of Würzburg, Germany. A Merchantek 266 LUV, 266 nm laser at 10 Hz and 0.71-0.84 mJ pulse energy for a spot size of 50 μm and an Agilent 7500i quadrupole mass spectrometer were used. ^{44}Ca for fluorite and calcite,^{27}Al for cryolite and crylithionite, ^{57}Fe for siderite and ^{23}Na for villiaumite served as internal standards. The NIST SRM 614 was used as an external standard (Pearce et al., 1997) and was measured frequently during the course of the analyses. Deduced from multiple measurements of the NIST SRM 614 standard, the precision (1 σ level) is usually better than 10 rel.%. However, errors may be larger for analyses with very low REE contents. Minimum detection limits generally lie below 50 ppb.

4. Petrography and Results

We chose 48 samples (Table 1) for detailed study according to distinct generations within one intrusion, their association with other minerals, their different CL colours and zonations. The analysed REE contents were normalised to chondrite (McDonough & Sun, 1995). The pseudo-lanthanide yttrium was added between Dy and Ho because of its trivalent oxidation state and its geochemical similarity to the REE (Bau & Dulski, 1995). Representative REE analyses can be found in Table 2. The whole data set can be found online (see Appendix A).

Table 1: Samples analysed in this study. P and s represent fluorites which are interpreted as primary magmatic (p) or secondary/late stage, hydrothermal (s); columns "Eu" and "Y" refer to the respective anomalies. All samples from Ivigtut are of hydrothermal origin.

Intrusion	unit	mineral	p/s	samples	characteristics	Eu	Y	tetrad
Ilímaussaq	Naujaite	fluorite	p	Ilm133, Ilm225, Ilm259, Ilm260	LREE enriched	neg.	pos.	none
60°56' N	Kakortokite	fluorite	p	XL30	LREE enriched	neg.	pos.	none
45°56' W	Naujaite	fluorite	s	Ilm77, Ilm99, Ilm325	low REE concentration	neg.	pos.	none
	Naujaite	villiaumite	p	villiaumite	REE below det. limit	neg.	pos.	none
Motzfeldt	SM1	fluorite	p	JS193, JS195, JS197	LREE enriched	neg.	pos.	none
61°08' N 45°06' W	SM1	fluorite	s	JS2, JS4, JS6, JS10, JS16	variably LREE enriched	neg.	pos.	none
	SM1	fluorite	s	JS9, JS10	low REE concentration	neg.	pos.	none
	SM4	fluorite	s	JS34, JS38, JS67, JS86, JS90, JS91, JS152, JS168, JS225, JS226	MREE enriched	neg.	pos.	none
	SM4	calcite	s	JS67, JS152, JS226	flat to MREE enriched	neg.	pos.	none
	SM5	fluorite	s	JS109, JS110, JS175, JS183	LREE enriched, anomalies less pronounced	neg.	pos.	none
	SM6	fluorite	p	JS88, JS122	LREE enriched	neg.	pos.	none
Ivigtut		siderite	s	IV-CPH, IV1475, IV-Sid	HREE enriched	neg.	neg.	not quant.
61°12' N 48°10' W		cryolithionite	s	IV30	flat REE pattern, low concentration	neg.	neg.	not quant.
		cryolite	s	IV20, IV30, IV33, IV35, IV-K1, IV-K4	flat REE pattern, low concentration	neg.	neg.	strong
		fluorite	s	IV31, IV 32	low REE concentration	neg.	neg.	strong
		fluorite	s	IV80, IV79a, IV1479, IV33	slightly HREE enriched	neg.	neg.	strong
		fluorite	s	IV30, IV20	flat REE pattern	neg.	neg.	strong

Table 2: Representative REE analyses of fluorides, siderite and calcite (in ppm except Y/Ho and Y/Y*) and three standard analyses (one from the lab at Würzburg and two from the literature (Horn et al., 1997; Lahaye et al., 1997) for comparison).

Ivigtut	# 9001	# 9002	# 9009	# 9012A	# 9032	# 9033	# 5026	# 5020
Sample	IV30	IV30	IV30	IV30	IV80	IV80	1479	1479
Mineral	Fluorite	Fluorite	Cryolite	Cryolithion.	Fluorite	Fluorite	Fluorite	Fluorite
La	1541	335	5.75	0.018	2.52	1.76	0.798	0.327
Ce	3772	1076	15.2	0.038	13.4	9.25	8.42	1.24
Pr	559	141	2.54	<0.01	2.98	1.99	3.06	0.236
Nd	2019	463	7.93	<0.03	18.5	9.42	18.6	1.07
Sm	1119	228	4.12	<0.02	47.7	13.9	22.4	0.676
Eu	94.8	33.3	0.604	<0.01	1.42	0.47	0.798	0.021
Gd	1129	126	4.06	0.044	57.7	17.6	22.7	0.734
Tb	280	32.7	0.817	0.011	22.6	6.79	8.32	0.287
Dy	1826	208	5.58	<0.02	177	61.3	67.8	2.62
Y	4620	291	7.53	0.054	225	102	106	9.68
Ho	286	25.1	0.784	<0.01	30.2	12.6	11.8	0.641
Er	804	76.7	2.37	<0.02	88.8	37.7	33.9	1.94
Tm	127	16.9	0.466	0.007	13.9	5.98	5.26	0.315
Yb	901	133	3.17	0.045	82.4	33.7	33.2	2.12
Lu	91.8	13.6	0.318	<0.01	7.19	3.16	2.43	0.228
Sr	5798	3544	230	0.281	502	842	576	8342
Y/Ho	16.2	11.6	9.6	-	7.5	8.1	9	15.1
Y/Y*	0.5	0.3	0.3	-	0.2	0.3	0.3	0.6

unit			SM1					
Ivigtut	BA0014	**Motzfeldt**	# 2002	# 1012	# 3010	# 3016	# 8017	# 8013
Sample	Sid		JS195	JS193	JS10	JS9	JS6	JS6
Mineral	Siderite		Fluorite	Fluorite	Fluorite	Fluorite	Fluorite	Fluorite
La	<0.02		255	209	3.63	1.24	378	50.5
Ce	0.014		454	353	1.74	3.4	771	81.3
Pr	<0.01		58.6	47.1	0.797	0.728	122	9.79
Nd	<0.08		269	212	3.37	3.34	590	39.5
Sm	<0.06		62.5	51.0	1.66	2.06	116	8.42
Eu	<0.03		6.79	4.14	0.201	0.388	8.44	0.976
Gd	0.094		66.5	56.7	3.79	2.42	98.3	11.2
Tb	0.026		9.86	9.18	0.653	0.653	10.3	1.33
Dy	0.145		66.5	59.3	3.88	4.04	51.4	6.84
Y	0.261		820	774	93.3	34.5	681	152
Ho	0.056		13.8	11.9	0.579	0.698	8.71	1.29
Er	0.158		34.1	32.4	1.16	1.77	15.8	2.61
Tm	0.036		4.2	3.67	0.106	0.227	1.32	0.282
Yb	0.528		22.6	20.6	0.469	2.08	7.57	1.47
Lu	0.058		2.52	2.26	0.05	0.186	0.669	0.152
Sr	0.019		751	430	142	300	1432	955
Y/Ho	4.7		59.4	65	161	49	78.2	117.8
Y/Y*	0.21		2	2.2	4.6	1.5	2.4	3.8

Table 2 continued

unit	SM4	SM4		SM5		SM6		Naujaite
Motzfeldt	# 8003	# 7019	# 7016	# 1027	# 1028	# 1015	**Ilímaussaq**	# 6002
Sample	JS168	JS152	JS152	JS175	JS109	JS122		ILM225
Mineral	Fluorite	Calcite	Fluorite	Fluorite	Fluorite	Fluorite		Fluorite
La	30.7	322	18.4	46.8	13.4	182		163
Ce	87.2	833	57.5	108	33.3	377		327
Pr	17.1	128	13	16.5	4.97	58.2		52.5
Nd	95.5	610	84	85.5	20.4	305		275
Sm	26.3	186	30.4	17	4.94	66.4		55.7
Eu	2.28	15.7	3.09	1.89	1.83	4.88		4.9
Gd	34.3	224	43.5	14.6	3.81	63.4		56.5
Tb	4.97	41.4	6.65	1.67	0.481	7.3		6.43
Dy	32.8	293	42.6	8.71	2.68	42.5		34.8
Y	372	2371	795	108	10.7	470		430
Ho	6.19	58.8	8.48	1.36	0.283	7.24		6.17
Er	15	177	20.7	2.48	0.753	15.8		13
Tm	1.77	26	2.22	0.245	0.055	1.49		1.28
Yb	8.77	162	12.4	1	0.259	6.49		5.88
Lu	0.965	20.4	1.24	0.126	0.017	0.613		0.618
Sr	495	1127	905	498	95	1066		124
Y/Ho	60.1	40	94	79	37.8	64.9		69.7
Y/Y*	1.9	1.3	3.1	2.3	0.9	2		2.2

	Naujaite			Kakortokite		**Standards**		
Ilímaussaq	# 6661	# 5007	# 5003	# 3003		NIST-614	NIST-614	NIST-614
Sample	ILM259	ILM99	ILM77	XL30		Würzburg	Horn et al. (1997)	Lahaye et al. (1997)
Mineral	Fluorite	Fluorite	Fluorite	Fluorite				
La	120	3.88	0.005	217		0.70	0.74	0.72
Ce	243	5.56	0.01	426		0.76	0.79	0.82
Pr	36.9	1.02	<0.01	75.2		0.70	0.78	0.75
Nd	200	3.81	0.027	385		0.78	0.75	0.74
Sm	47.2	0.894	0.039	78.7		0.74	0.77	0.74
Eu	4.63	0.081	<0.01	7.21		0.74	0.77	0.77
Gd	52.6	0.919	0.071	80.1		0.68	0.73	0.75
Tb	7.42	0.111	0.009	8.27		0.70	0.77	0.69
Dy	39.5	0.806	0.086	46.6		0.69	0.76	0.69
Y	423	14.9	16.7	582		0.74	0.79	0.75
Ho	7.47	0.144	0.018	7.75		0.74	0.78	0.71
Er	18.1	0.385	0.058	17.7		0.65	0.78	0.70
Tm	1.85	0.04	<0.01	1.66		0.71	0.77	0.67
Yb	9.03	0.248	<0.03	8.85		0.76	0.76	0.70
Lu	0.958	0.022	<0.01	0.792		0.73	0.78	0.69
Sr	70.5	19.9	54.1	636		43.80	45.50	48.58
Y/Ho	56.6	103	928	75.1				
Y/Y*	1.8	3.2	31.3	2.3				

Motzfeldt

The primary magmatic fluorites occur in SM1 and SM6 (Figs. 2 & 3). In SM1 samples (JS193, JS195, JS197; Table 1), fluorite forms interstitial grains with a diameter up to 1 mm within the feldspar matrix. They have a rounded to subhedral shape (Fig. 2 a) and are interpreted to be of primary origin. Their colour varies from light blue to white. Purple fluorite occurs as small (up to 1 mm) interstitial grains in JS88 and JS122 of unit SM6 and are similar to primary magmatic fluorite grains from SM1. They are intergrown with feldspar and aegirine and reach sizes of up to 0.5 cm. The REE patterns of all primary magmatic fluorites are characterised by an enrichment in LREE, a negative Eu and a positive Y anomaly. Fluorite from SM1 has slightly lower HREE (Fig. 3) than fluorite from SM6.

Hydrothermal fluorites either occur as patchy fluorite or in veins which show rhythmic zonation of darker and lighter parts. Patchy fluorite does not exhibit any zonation, but has randomly oriented lighter CL parts. The observed REE patterns can be divided into groups according to the different intrusive units.

Hydrothermal fluorites from SM1 developed in different textures (Fig. 2c, d). They occur as small, up to 2 cm thick veins cutting through SM1 (JS10, JS16) or as large fluorite crystals up to 10 cm (JS9). Furthermore, some fluorites up to 2 cm are irregularly associated with feldspar and/or amphibole (JS2, JS4, JS6). Their colour in hand specimen is mostly bluish/purple with some colourless parts (e.g. JS6). The hydrothermal fluorites are characterised by an enrichment of the LREE, a negative Eu anomaly and a positive Y anomaly which varies in size within the same sample (e.g. Fig. 3). Two samples (JS9 and JS10) are enriched in MREE and one (JS10) additionally has a pronounced negative Ce anomaly. Lighter CL parts tend to be more enriched in REE compared to the darker ones.

In unit SM4, fluorite mostly occurs as small veins (Fig. 2f) some of which comprise aegirine and fluorite (JS90, JS91). In these veins, fluorite occurs as 1 to 2 cm large crystals in an aegirine matrix. Other veins consist of fluorite and calcite intergrowths (JS67, JS152, JS226; Fig. 2e). Furthermore, there are large (< 5 cm) pegmatitic crystals which are not associated with veins (JS168, JS225). In fine-grained parts of SM4, fluorite is disseminated (JS38) or forms very thin veinlets (< 0.5 cm; JS34, JS86). The colour of the fluorites ranges from purple/blue to colourless. Fluorites from SM4 incorporate less REE than fluorite from SM1 (Figure 4). The patterns are either flat (e.g. JS152) or exhibit enrichments in MREE (e.g. JS168, 225). Calcite solely occurs in three samples from SM4 and is intergrown with fluorite. Its REE patterns are very similar to the patterns of the associated fluorite.

Bluish fluorites from SM5 occur in up to several cm thick veins commonnly intergrown with white alkali feldspar (JS109, JS110, JS175). In some samples, fluorite only forms a thin layer. JS183 originates from a feldspar- and biotite-rich sample which occured in close association with supracrustal basaltic rocks within unit SM5. In this sample, the fluorite is interstitial and surrounded by (albitic) feldspar. The fluorite patterns of SM5 are characterised by an enrichment of LREE or flat to slightly MREE enriched. The Eu and Y anomalies are not as pronounced as in samples from other units, and few analyses even show a positive Eu anomaly (Fig. 4).

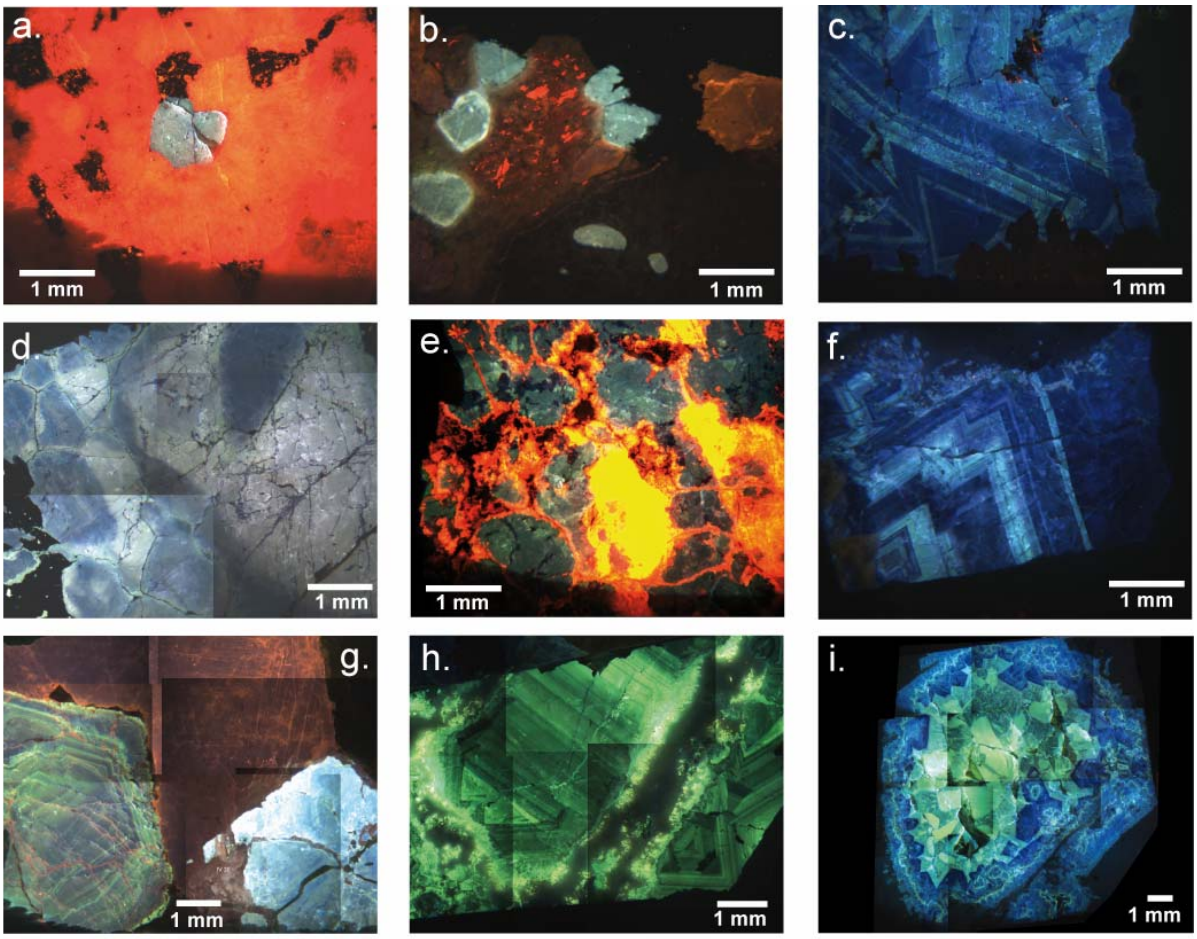

Fig. 2: Cathodoluminescence images of some of the studied samples. a) and b) primary amphiboles from Motzfeldt and Ilímaussaq, respectively, which are associated with feldspar; c) zoned fluorite from the Motzfeldt intrusion (SM1; JS10); d) patchy-grown fluorite from SM1 (JS6); e) fluorite intergrown with calcite from SM4 (JS152); f) strongly zoned fluorite from SM5 (JS175); g) zoned, euhedral fluorite (lower left), cryolite (top) and cryolithionite (lower right) from the Ivigtut deposit (IV 30); h) strongly zoned fluorite from Ivigtut (IV 80) rimmed by cryptocrystalline topaz; i) zoned fluorite from Ivigtut (IV 1479) with a green core and blue rim (CL colours).

Whole rock data from Jones (1980) and Bradshaw (1988) are similar to the REE patterns of primary magmatic fluorite (Fig. 3) regarding the overall enrichment in LREE and the negative Eu anomaly. While primary magmatic SM1 fluorite has more REE than the whole rocks, primary SM6 fluorite is equally enriched. This is attributed to the occurrence of REE-enriched minerals (i.e. eudialyte of SM6) which lead to overall high REE concentrations in the bulk rock. Mineral REE patterns of eudialyte (Fig. 3) or rinkite (Jones, 1980) also show an enrichment of LREE similar to the fluorites.

Whole rock data of unit SM5 partially show a positive Eu anomaly which is in agreement with REE patterns of fluorite from this unit. These fluorites (samples JS109 & JS175) are the only ones which do not exhibit a pronounced negative Eu anomaly, but partially a slightly positive one. All in all, the fluorites show REE patterns very similar to their immediate host rocks and to other REE-enriched minerals such as eudialyte.

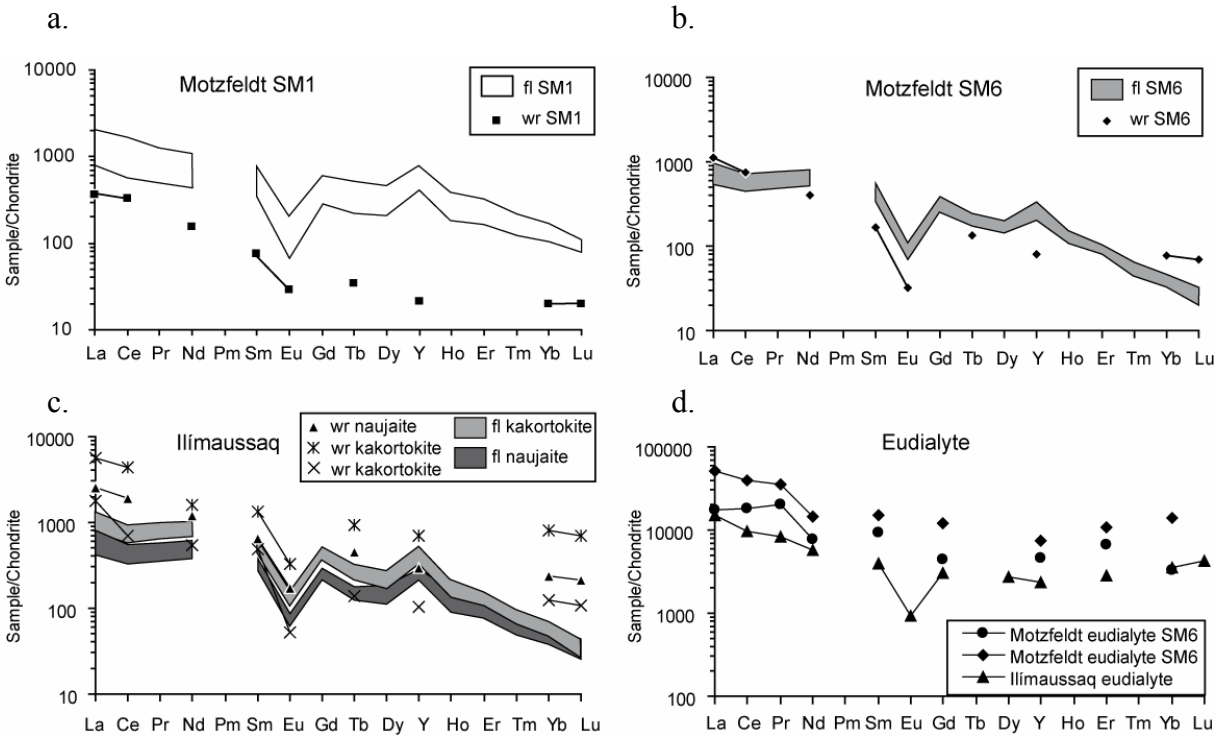

Fig. 3: Representative REE patterns of primary fluorites from Motzfeldt (a. & b.) and Ilímaussaq (c.) compared with whole rock data from Jones (1980), Bradshaw (1988) & Bailey et al. (2001) along with REE mineral data from eudialyte (d.) from Motzfeldt (SM6) and Ilímaussaq (Jones, 1980; Fryer & Edgar, 1977). wr = whole rock, fl = fluorite.

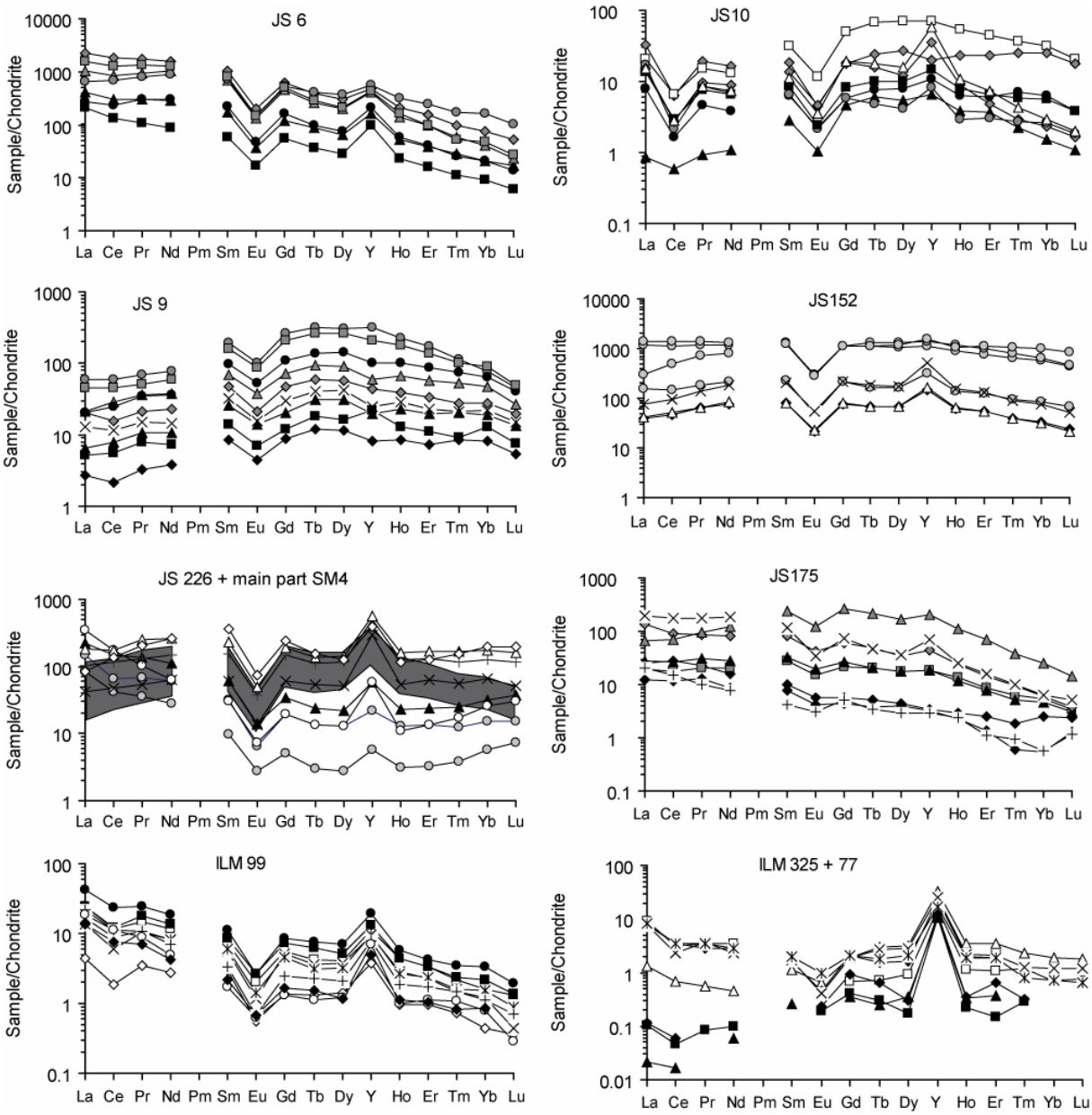

Fig. 4: REE patterns of hydrothermal fluorites from Motzfeldt (SM1: JS6, JS9 & JS10; SM4: JS152; JS226; grey shaded field: JS34, JS38, JS90, JS91, JS168, JS225; SM5: JS 175) and Ilímaussaq (Ilm 77, Ilm99, Ilm325).

Ilímaussaq

The Ilímaussaq fluorites Ilm133, Ilm225, Ilm259 and Ilm260 are subhedral to euhedral and form up to 1 mm large grains in the feldspar matrix of the naujaitic rocks (roof cumulate; Fig. 2b). Fluorites from similar samples were interpreted to be early crystallising phases (Markl et al., 2001). XL30 is the only sample from the kakortokites (floor cumulates) which occurs in a pegmatite. This pegmatite consists of fluorite, arfvedsonite, feldspar and aegirine as main crystallisation phases. Sample XL30 was described in detail by Müller-Lorch et al. (2007)

who suggested that fluorite was the first crystallising mineral. These primary magmatic fluorites are enriched in LREE, have a negative Eu and a positive Y anomaly and are very similar to fluorite patterns in units SM1 and SM6 from Motzfeldt (Fig. 3).

The samples Ilm77, Ilm99 and Ilm325 are derived from the naujaitic part (roof cumulates) of the intrusion and occur in heavily altered samples or as secondary crusts. In sample Ilm99, white albite and purple to black fluorite are finely intergrown. The few single crystals are approximately 2-3 mm. Ilm77 is a heavily altered, vuggy sample in which small (< 5 mm), deep purple fluorite grains are associated with alkali feldspar. The fluorite of Ilm325 forms a crust on altered, fine-grained, feldspar-rich rock. These secondary fluorites show no or only a slight zonation in CL. Generally, secondary fluorites have a considerably lower REE concentration than the primary magmatic ones. The chondrite-normalised REE patterns exhibit a slightly negative Ce anomaly and pronounced negative Eu and positive Y anomalies (Fig. 4). Ilm99 is characterised by an enrichment of LREE whereas Ilm325 shows flatter patterns and Ilm77 is enriched in MREE to HREE. The overall concentration of REE decreases in the order Ilm99 > Ilm325 > Ilm77. Villiaumite occurs as 3 to 4 mm large red crystals and is derived from the lujavritic part (sandwich horizon) of the intrusion. This late-stage, hydrothermal villiaumite (NaF) has REE contents mostly below the detection limits.

Whole rock Ilímaussaq REE patterns from the naujaites (Bailey et al., 2001) and eudialyte data from Fryer & Edgar (1977) are similar to fluorite. All analyses exhibit an enrichment in LREE and a negative Eu anomaly (Fig. 3). The whole rock analyses are generally more enriched in REE than the fluorites which reflects the high modal abundance of REE-bearing minerals (eudialyte) in the bulk samples which control their absolute amount of REE.

Ivigtut

The association of cryolite *or* topaz decides whether the fluorite samples are derived from the fluorite-cryolite zone or from the fluorite-topaz unit underneath. Fluorites in samples IV32, IV79a, IV80 and IV1479 (Table 1) are all finely intergrown with cryptocrystalline, bluish or green topaz. Their colours range from lightgreen (IV79a) and whitish/purple (IV32) to dark green (IV80). In sample IV1479, fluorite is ~ 1 cm across and has a brown core with a purple rim. Fluorites in association with cryolite are generally deep purple except for U-Th-rich (this study; Pauly & Bailey, 1999), red-brown fluorite in sample IV30.

The fluorites display rather smooth REE patterns with some showing a slight enrichment of HREE (Fig. 5). CL images of fluorites generally show strong zonations (Fig. 2

g,h,i) even if fluorite is finely intergrown with cryolite. Zones with bright CL-colours are more enriched in REE than the darker parts. Generally, the fluorites are 2 to 4 orders of magnitude enriched relative to chondrite (Fig. 5). The most REE-enriched sample is a U-Th-rich fluorite (IV30; cf. Pauly & Bailey, 1999; Fig. 5). Light brownish and green fluorites incorporate approximately the same amount of REE whereas purple fluorite is slightly more depleted (Fig. 5). Sample IV31 is a thin fluorite crust possibly formed from a gel-like liquid and has very low concentrations of YREE.

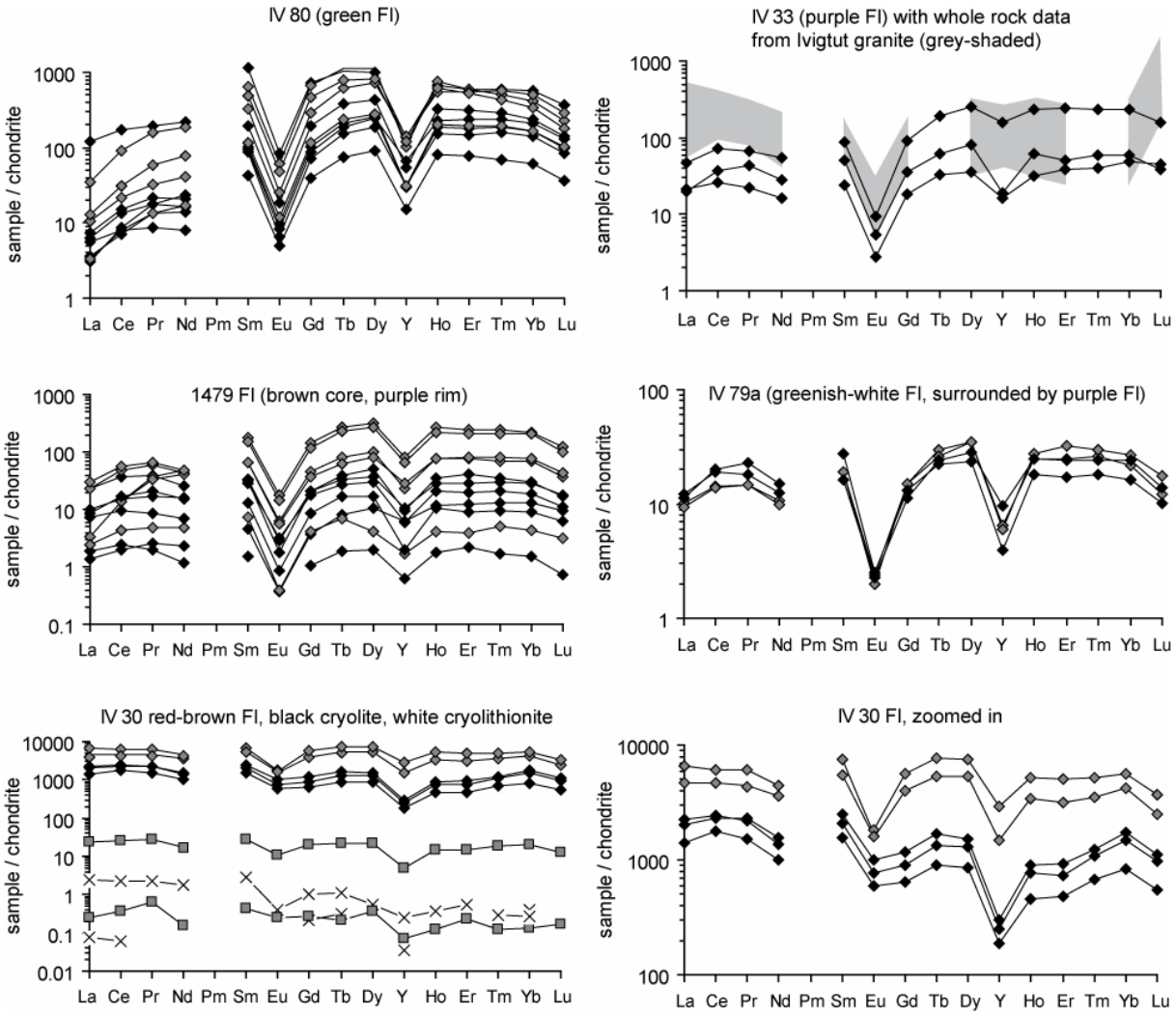

Fig. 5: REE patterns of fluorides from the Ivigtut intrusion; grey-shaded field: comparative whole rock data from the Ivigtut granite from Goodenough et al. (2000). Symbols: rhomb = fluorite; square = cryolite; cross = cryolithionite.

The typical colour of cryolite varies from white to brown. In sample IV30, however, cryolite is black due to radioactive damage of neighbouring U-Th-rich fluorite (Pauly & Bailey, 1999). Both minerals are associated with white cryolithionite. White to light brown

cryolite from samples K4 and K1, respectively, forms various cm-sized masses and comes from the deposit's pure cryolite mass. IV35 is a transparent single cryolite crystal of pseudocubic shape of about 0.5-0.7 cm. Light brown cryolite has lower REE concentrations than white or black cryolite and is mostly 1 or 2 orders of magnitude depleted relative to chondrite. In contrast, white or black cryolite is 10 to 100 times enriched relative to chondrite. Similar to fluorite, the REE patterns in cryolite are very flat and exhibit negative Eu and Y anomalies.

In all samples, siderite is reddish-brown and forms cm-large crystals. In sample IV1475, it is associated with quartz and dark-brown cryolite. The three minerals form a vein which is a few cm wide. Bailey (pers. comm., 2007) suggested sample IV Sid to be derived from the eastern extension of the cryolite deposit. The same may apply to IV CPH, but it could also be derived from the siderite-cryolite unit. Siderite very depleted in REE and exhibits a negative Y anomaly. Concentrations in siderite are sub-chondritic and in many samples below the detection limit.

The analysed cryolithionite occurs in close association with reddish-brown fluorite and black cryolite (IV30). The REE are even more depleted than in cryolite, but similar regarding the slight Eu and Y anomalies and comparable to siderite.

In summary, the chondrite-normalised patterns from the Ivigtut deposit are all very much alike and only differ in their absolute REE concentrations. Fluorite is always more enriched in REE than cryolite whereas siderite and cryolithionite hardly incorporate any REE. All minerals show strong negative Eu and negative Y anomalies which is in contrast to the positive Y anomaly in minerals from Motzfeldt and Ilímaussaq.

Whole rock analyses of the Ivigtut granite (Goodenough et al., 2000) and whole rock data of peralkaline granites from China (Jahn et al., 2001; Zhao et al., 2002; Fig. 5) are as enriched in REE as the Ivigtut fluorites and exhibit a similarly pronounced Eu anomaly. In contrast to the distinctive negative Y anomaly in fluorite and cryolite from Ivigtut, only few whole rock samples of the Ivigtut granite have a slightly negative one. The Chinese and Ivigtut granites display rather smooth patterns with the latter showing a strong enrichment in Yb and Lu. Even though the analysed fluorites and cryolites are generally enriched in HREE, their concentration gradually decreases from Yb to Lu.

6. Discussion

The REE patterns do not only differ among the three intrusive complexes, but also vary systematically within one intrusion. Generally, the patterns of different intrusive units and different evolutionary stages can be roughly grouped (Table 1). There are various processes and mechanisms which account for the large diversity of the REE patterns. These include crystallographic control, sorption on mineral surfaces, source-related effects, formation of anomalies, fractionation during crystallisation and complexation.

6.1 Common features

The characteristics discussed in this section apply to both magmatic as well as hydrothermal fluorites or fluorides. Specific aspects typical of magmatic fluorites or hydrothermal fluorides will be discussed in chapters 6.3 and 6.4.

6.1.1 Crystallographic control

In fluorite (and calcite), REE replace Ca according to the following schematic substitutions in which □ is a vacancy (e.g. Möller et al., 1998):

$2\ REE^{3+} + \square \Leftrightarrow 3\ Ca^{2+}$; $REE^{3+} + Na^{+} \Leftrightarrow 2\ Ca^{2+}$; $REE^{3+} + F^{-} \Leftrightarrow Ca^{2+}$

The substitution involving Na^{+} may be crucial as the molar Na^{+} content generally balances the REE^{3+} content even considering the fact that error of the Na^{+} measurements is very high (2 σ up to 50 %).

The enrichment of HREE in siderite from the Ivigtut intrusion can be explained by differences in the ionic size of Ca^{2+} and Fe^{2+} as pointed out by Bau & Möller (1992) and by Morgan & Wandless (1980). Due to the smaller size and higher charge/volume ratio, the HREE are incorporated into the siderite crystal lattice more easily than the LREE according to the following substitution: $2\ REE^{3+} + \square \Leftrightarrow 3\ Fe^{2+}$.

The analyses of REE in villiaumite (NaF) from the Ilímaussaq intrusion are mostly below the detection limit. Although Na^{+} (1.02 Å) has a similar ionic radius compared to the REE^{3+} (1.16 – 0.98 Å), the REE do not fit into the crystal lattice of villiaumite. This is most probably due to charge balance effects as the trivalent REE would require simultaneous formation of two vacancies for each REE cation.

Cryolite [Na_3AlF_6] and cryolithionite [$Na_3Li_3Al_2F_{12}$] incorporate more REE than villiaumite but less REE than fluorite (Fig. 5). This may be due to the different charges of Na (univalent) and Ca (divalent) compared to the REE even though they have similar ionic radii (1.02 and 1.00 Å, respectively). However, due to the presence of trivalent Al in cryolite and

cryolithionite, the charge balance can be achieved more easily than in villiaumite where only univalent Na is present. The lower amount of REE in cryolithionite compared to cryolite (Fig. 5) might be explained by the substitution of Na by small Li (radius 0.76 Å) which renders the incorporation of the larger REE more difficult.

6.1.2 Fluorite reflecting source (fluid/melt) composition

Fleischer & Altschuler (1969) stated that the geological environment (i.e. chemistry of the rocks) control the distribution of REE. This is in agreement with our fluorides which closely match the REE abundance of their host rocks. Fluorites in alkaline nepheline syenites from Motzfeldt and Ilímaussaq generally display an enrichment in LREE in early crystallisation products. Minerals in the granitic Ivigtut intrusion, however, have a (slight) enrichment in HREE representative of the quartz-saturated, pegmatitic character of the deposit.

The amount of trace elements incorporated into fluorides largely depends on their availability in the melt/fluid. Therefore, REE patterns and trace element contents reflect the source (i.e. fluid or melt) from which they crystallised or precipitated (e.g. Sallet et al., 2005) and REE in fluorites are often used to trace the REE content of an associated hydrothermal fluid (e.g. Gagnon et al., 2003; Schwinn & Markl, 2005; Hill et al., 2000 and references therein). The REE distribution in some analysed samples is potentially governed by the trace element content of the surrounding rocks, the precipitation or breakdown of minerals or the abundance of REE in the fluid (Bau, 1991). The fluorites from SM5 (Motzfeldt) are unique as they have no pronounced negative Eu anomalies (JS109 & 175) comparable to the whole rock data (Jones, 1980). An intensive interaction of the fluid with the surrounding rocks from unit SM5 can be assumed for the origin of the REE pattern in these fluorites. Therefore, it is suggested that the fluid, from which these fluorites precipitated, had leached parts of the feldspar-rich unit SM5. Subsequently, it was fixed in the fluorite/feldspar veins at low hydrothermal temperatures and/or high oxygen fugacities (Hill et al., 2000).

6.1.3 Formation of anomalies

The negative Eu anomaly is typical of all analysed samples irrespective of mineral type, intrusion, unit or evolution stage and also occurs in whole rock analyses from the investigated intrusions (Figs. 3 to 5). The Eu anomaly can be attributed to early magmatic plagioclase fractionation, i.e. the large occurrence of anorthositic rocks underlying the Gardar Province (e.g. Halama et al., 2002).

The negative Ce anomaly in JS10 and JS9 from Motzfeldt and in ILM77, ILM99 and ILM325 from Ilímaussaq may indicate more oxidised conditions and low temperatures

(Hollings & Wyman, 2005; Bau & Möller, 1992; Constantopoulos, 1988) or changes in pH (e.g. Bau & Möller, 1992) during the evolution of the fluid from which these fluorites precipitated. The more oxidised conditions during the late stages are well documented for the Ilímaussaq intrusion (Markl et al., 2001) where hematite and aegirine are common (Marks et al., 2003). The same applies to the Motzfeldt intrusion where large parts of SM1 are heavily altered and contain large amounts of hematite along with aegirine and secondary fluorite.
The pronounced Y anomaly will be discussed in further detail below.

6.2 Primary magmatic fluorites

Deducing from the textures, the early fluorites were derived from a magma, because they are closely related to other magmatic phases and do not show any sign of (hydrothermal) alteration. Sallet et al. (2000) observed that primary magmatic fluorites associated with a granite have similar REE patterns as the host rock. The same applies to fluorites from this study which are not only similar to each other but also to the associated whole rock patterns. Therefore, they are interpreted to be of early magmatic origin. The distribution of REE in the primary magmatic fluorites seems to be closely controlled by the overall availability of REE within the whole rock (e.g. Fig. 3) and hence in the magma. This suggests that the distribution coefficient is similar for all REE and thus show similar patterns. The primary magmatic fluorites from the Motzfeldt (units SM1 and SM6) and Ilímaussaq intrusions (naujaites and kakortokites; roof & floor cumulates) define a very narrow range in the Tb/Ca-Tb/La diagram (Möller et al., 1976; Fig. 7) within the pegmatitic field which reflects similar REE contents of the fluorites (cf. Figs. 3-5) suggesting similar formation processes.

All primary magmatic fluorites have Y/Ho ratios between 60 and 70 (average Y/Ho SM1 = 63, SM6 = 68, Ilm = 64) which is in contrast to the chondritic Y/Ho ratios of 28. The constant values argue for similar crystallisation conditions (Bau & Dulski, 1995). Furthermore, Bau & Dulski (1995) observed that the Y/Ho ratio does not change during magmatic fractionation processes which is evidenced by the constant Y/Ho ratios of the studied samples. Veksler et al. (2005) and Marshall et al. (1998) showed that the distribution coefficient (K_d Fluorite-melt) for Y is higher than that for Ho which would result in a positive Y anomaly in the normalised REE pattern. This could explain the high Y content of the fluorites. On the other hand, Bau & Dulski (1995) suggested that the Y/Ho ratio may reflect source values. According to that, the magma source of the Ilímaussaq and Motzfeldt complexes must have been already either Y-enriched and/or Ho-depleted due to the high Y/Ho ratio.

The primary magmatic fluorites, the whole rock data from Motzfeldt and Ilímaussaq and REE data from dykes all over the Gardar Province (Goodenough et al., 2002; Halama et al., 2007; Köhler et al., submitted) show an enrichment of LREE implying the source of the Gardar magmas must already have been enriched in LREE. Upton & Emeleus (1987) suggested that the mantle beneath the Gardar Province was metasomatised and enriched in fluorine, LREE and LILE. It is believed that this happened during subduction processes leading to the Ketilidian orogen (Garde et al., 2002; Goodenough et al., 2002; Upton & Emeleus, 1987). A metasomatic exchange associated with the mobilisation of LREE and other trace elements is common in arc related magmas (e.g. You et al., 1996; Drummond et al., 1996) and was also demonstrated experimentally (You et al., 1996; Kessel et al., 2005).

Despite the similar REE patterns which argue for the same processes during crystallisation from a magma, there are differences in the fluorite composition. This is evidenced e.g. in the variable Sr-content of the different magmatic fluorites from Motzfeldt and Ilímaussaq. Even though they have identical amounts of REE, the Sr content is higher in Motzfeldt than in Ilímaussaq (Fig. 6). This indicates different availability of Sr in the magma.

6.3 Hydrothermal (secondary) fluorites and associated minerals

Hydrothermal fluorites are the predominant samples in this study and either occur in veins or as secondary alteration products. Apart from the effects outlined in chapters 6.1-6.3, some additional processes can govern the REE distribution:

According to Bau (1991), sorption of REE on mineral surfaces is an important process in the incorporation of REE into minerals during fluid-rock interactions. He stated that sorption and complexation are opponent mechanisms: whereas the latter increases the content of REE in the fluid, sorption leads to the incorporation of REE into minerals. The effect of sorption generally leads to a preferred incorporation of HREE into the crystal lattice (Bau, 1991). However, the chemical environment in which the studied samples formed suggests that ligands like F^-, CO_3^{2-} and OH^- were highly concentrated. Therefore, sorption processes are assumed to be of minor importance compared to chemical complexation (of the REE; Bau & Möller, 1992). Additionally, as the fluorides of this study are rather large crystals, it can be assumed that they would only offer a small reactive specific surface area for sorption.

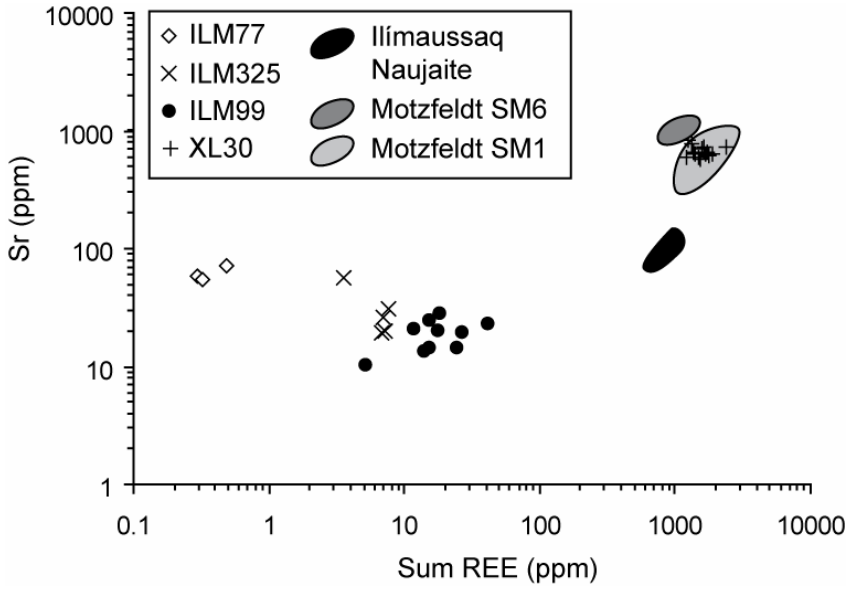

Fig. 6: Sr (ppm) vs. total REE content (ppm) of primary and hydrothermal Ilímaussaq and primary Motzfeldt fluorites.

6.3.1 Evidence for a changing fluid composition

The distribution of REE into minerals changes systematically in the course of crystallisation. It is suggested that early crystallising phases preferentially incorporate LREE whereas later formed ones are more MREE and particularly HREE enriched (Lüders et al., 1993; Schwinn & Markl, 2005; Kempe et al., 1999; Trinkler et al., 2005; Wagner & Erzinger, 2001; Möller et al., 1976). Early primary magmatic fluorites (JS193, JS195, JS197) are enriched in LREE whereas the patterns of hydrothermal vein fluorites are generally flatter (e.g. JS175) or become enriched in MREE (e.g. samples from SM4, JS10). Very late fluorites which form thin crusts or are alteration products even show a (slight) enrichment in HREE (Ilm325, Ilm77, IV31). Additionally, later fluorites commonly show decreasing REE contents indicating that the fluid or melt became depleted in REE in the course of the crystallisation or fluid migration, respectively (c.f. fluorites from Ilímaussaq, Fig. 6).

Möller et al. (1976) proposed the Tb/Ca-Tb/La diagram (Fig. 7) in order to distinguish fluorites of pegmatitic from hydrothermal or sedimentary origin. For this diagram, fluorite was assumed to be stoichiometrically composed of calcium and fluorine. The small amount of trace elements incorporated into fluorite does not change the overall position of data points in the diagram as discussed by Gagnon et al. (2003).

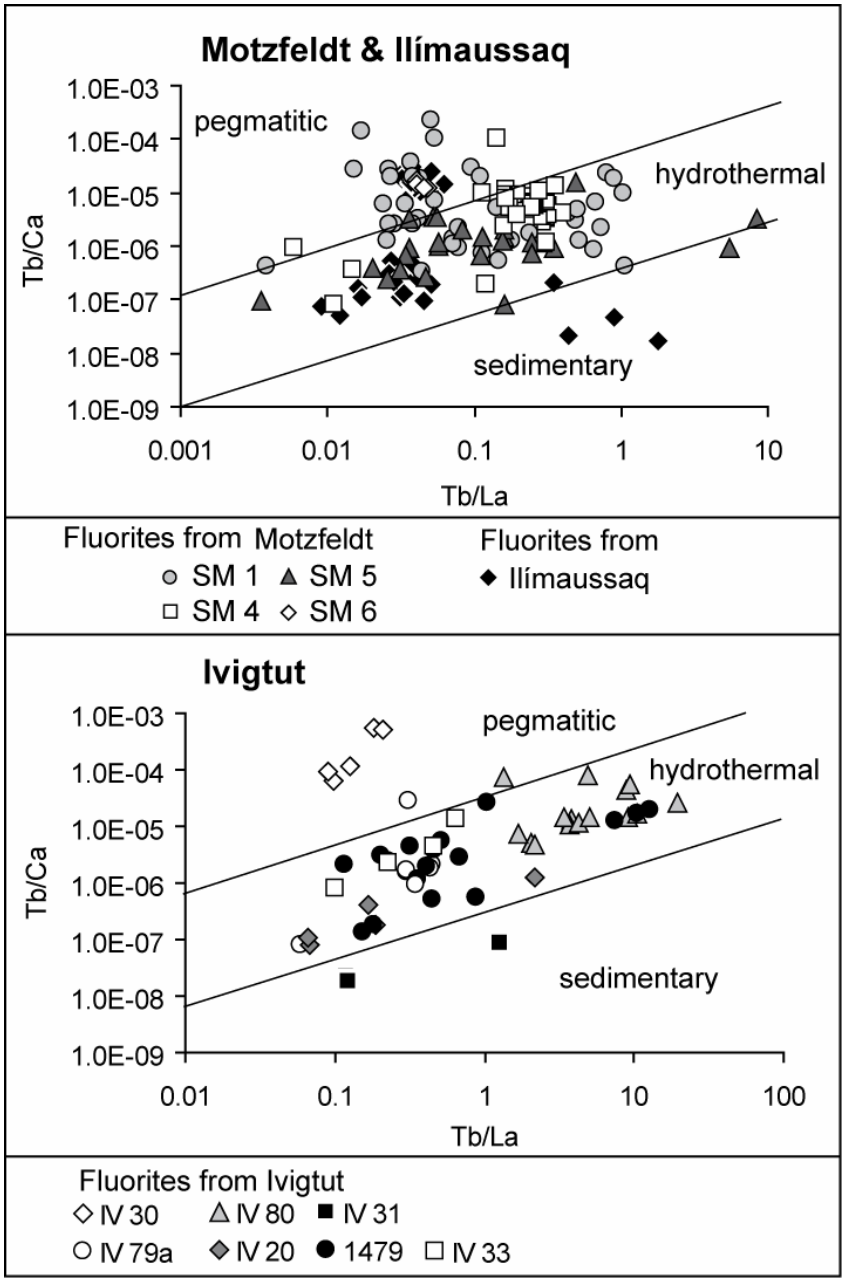

Fig. 7: Tb/Ca-Tb/La diagram (after Möller et al., 1976) of fluorites from Motzfeldt, Ilímaussaq and Ivigtut. The fields which distinguish pegmatitic, hydrothermal and sedimentary formation conditions are more gradual than sharp and "sedimentary" may be better referred to as "low temperature".

The hydrothermal fluorites of the Motzfeldt intrusion are heterogeneously distributed in Fig. 7. Two samples from SM1 (JS9 and JS10) fall into the hydrothermal field whereas almost all other hydrothermal fluorites from SM1 scatter around the field of the primary magmatic ones (Fig. 7, see above). This clearly shows that the Tb/Ca-Tb/La diagram must be used with care as analyses plotting in a particular field do not necessarily reflect those

formation conditions. It is important that the textural relationships as well as any precursor material/rocks are also taken into account (for a further discussion see Gagnon et al., 2003). Fluorites from SM4 and SM5 define fields in the Tb/Ca-Tb/La diagram and do not show any clear correlations within one sample. SM4 fluorites plot between the pegmatitic and hydrothermal fields whereas fluorites from SM5 appear to have formed hydrothermally. The secondary Ilímaussaq fluorite samples Ilm99 and Ilm325 fall into the hydrothermal field. Ilm77 is the only sample which lies within the sedimentary field indicating a very late, low-temperature formation which is in agreement with the occurrence of that fluorite in a heavily altered, vuggy sample.

Fluorites from Ivigtut (Fig. 7) are mostly of hydrothermal origin with sample IV30 being the only one that suggests a pegmatitic derivation. The thin fluorite crust of sample IV31 falls into the sedimentary field. All fluorites from Ivigtut describe a positive trend in the Tb/Ca-Tb/La diagram suggesting REE-fractionation during mineralisation. However, the lower points do not necessarily represent the fluorite cores. They are rather characteristic of the dark CL colours while the higher points generally reflect the bright areas in the CL images. This agrees well with the highly variable REE concentrations in the different colour zones.

6.3.2 Grainscale variations (zonations)

If a fluid progressively changed its composition, this fractionation should be observed in continuously evolving REE profiles (e.g. Schwinn & Markl, 2005). In this study, however, differences in REE patterns are rather typical of distinct units and/or intrusions and do not occur within one sample. The zonation of lighter and darker CL zones seen in some fluorite samples from Motzfeldt and Ivigtut most likely formed by abrupt changes of the REE content in the fluid.

Fluorite grains of SM1 from Motzfeldt partly show strong variations in their REE content within one sample. Their concentration varies by two orders of magnitude even over a short distance (< 1 mm). The CL images show that these samples consist of bright, REE-enriched parts whereas the dark ones are depleted in REE (Fig. 2d). Multiple fluorite generations are believed to account for this texture and the variable patterns. This can be clearly seen in Figure 2d where the white (earlier) parts are replaced by later-formed, darker parts. Accordingly, there must have been an overprint of these fluorites by a fluid which transported less REE. However, there are other samples which show an opposite evolution,

suggesting the presence of variably REE-enriched, late-stage fluids in these peralkaline intrusions.

6.3.3 Complexation

The complexation of REE with various ligands is a crucial mechanism that strongly controls the distribution of the REE (Möller et al., 1976; Bau, 1991; Bau & Möller, 1992). Apart from complexes involving Cl^-, the stability of REE complexes with F^-, OH^- and CO_3^{2-} increases from La to Lu and with increasing temperature (e.g. Möller et al., 1976; Ekambaran et al., 1986; Luo & Byrne, 2004; Wood, 1990 a,b; Haas et al., 1995). The continuous change in the relative complex stabilities eventually leads to REE fractionation in aqueous solutions and results in LREE-enriched patterns in the precipitating mineral and a progressive enrichment of HREE in the fluid. The importance of complexes involving F^-, CO_3^{2-}, hydroxide and Cl^- can be inferred from distinct REE characteristics and fluid inclusion data.

Complexation with fluoride may be an important mechanism in the transport of REE (e.g. Pan & Fleet, 1996; Salvi et al., 2000; Tagirov et al., 2002). Bau (1996) suggested Y-F complexes to be more stable than Ho-F ones. Therefore, the Y/Ho ratio increases during migration of F-rich hydrothermal fluids (Bau & Dulski, 1995). This is in agreement with Veksler et al. (2005) who demonstrated that in the presence of F-rich liquids, Y is more enriched than Ho and the Y/Ho ratio is greater than the chondritic one of 28 (Anders & Grevesse, 1989; McDonough & Sun, 1995; Irber, 1999). These findings are in accordance with Y/Ho ratios in fluorites from Motzfeldt and Ilímaussaq which reach up to 1375 (Ilm77; see below). However, they do not hold for fluorite and cryolite from Ivigtut whose Y/Ho ratios vary between 3 and 15 with a mean at 8-9. However, this does not necessarily preclude the effect of F-complexation at Ivigtut, because Irber (1996) showed that A-type granites (as in the case of the Ivigtut granite) normally have Y/Ho ratios below 28. Furthermore, crush leach analyses of fluid inclusions revealed the predominance of F.

In addition to fluoride complexes, carbonate ones may also play an important role in Motzfeldt and Ivigtut. The latter is dominated by abundant siderite and CO_2-rich fluid inclusions (Pauly & Bailey, 1999; Köhler et al., 2008) while in the Motzfeldt intrusion, not only calcite in veins, but also calcite daughter minerals in fluid inclusions are common (Schönenberger & Markl, in press). In contrast, carbonates or CO_2-bearing fluid inclusions are rare or absent in Ilímaussaq (Graser et al., in press) and therefore, REE complexation by (bi)carbonate seems highly unlikely.

Apart from the aforementioned processes in 6.3, the negative Ce anomaly (JS9, JS10, Ilm77, ILM325) may also be due to complexation with hydroxides. The stability of $Ce(OH)_3^0$

complexes are higher than those with other REE (Haas et al., 1995). This would lead to an increase in the solubility in the fluid and a negative Ce anomaly in the precipitating mineral. In Ivigtut, hydroxide complexation may have also influenced the distribution of REE, because fluid inclusions predominantly consist of an F-rich, CO_2-H_2O solution (Köhler et al., 2008). Additionally, various (late-stage) OH-bearing minerals like gearksutite, jarlite, pachnolite, ralstonite occur in the cryolite deposit (Pauly & Bailey, 1999).

Chloride complexes do not play an important role in the formation of complexes with "hard" ions (Pearson, 1963) at 25 °C (Wood, 1990a; Haas et al., 1995). However, they are important in more acidic fluid compositions. This may be the case at Ivigtut since thermodynamic modelling has shown that cryolite is stabilised under more acidic conditions (Köhler et al., 2008; Prokof'ev et al., 1991).

It must be noted, however, that the current data on complex stability constants of the REE with various ligands are from theoretical pressure-temperature extrapolations by Haas et al. (1995) and Wood (1990). New data on the stability of Nd and Er complexes with Cl^-, F^- and SO_4^{2-} were recently published by Migdisov & Williams-Jones (2002), Migdisov et al. (2006) and Migdisov & Williams-Jones (2007). Their results suggest that particularly at higher temperatures, Cl^- complexation may be more important than assumed by Haas et al. (1995) and Wood (1990).

To conclude, it is assumed that the REE patterns of the Motzfeldt and Ivigtut intrusions are most likely controlled by F^-, CO_3^{2-} and OH^- complexation in the fluid phase whereas for the Ilímaussaq intrusion only F^- and OH^- are suggested to have played a significant role.

6.3.4 Tetrad effect

The tetrad effect typically occurs in highly evolved silicate magmas (i.e. granites) and is attributed to strong fluid-rock interaction. It becomes visible in chondrite-normalised REE patterns. Masuda et al. (1987) classified the four tetrads as: T1 = La-Nd, T2 = (Pm)Sm-Gd, T3 = Gd-Ho and T4 = Er-Lu which can be either M- or W-shaped. The quantification of the tetrad effect in our samples was carried out after the method proposed by Monecke et al. (2002) excluding the second tetrad (Pm does not occur in nature) and considering the Ce-anomaly.

The tetrad effect does not play any role in the Motzfeldt and Ilímaussaq intrusions since its values are usually well below 0.2 which is below statistical significance (Monecke et al., 2002). In Ivigtut, however, fluorite and cryolite constantly display pronounced tetrad

effects with values as high as 1 (Fig. 8). In all analysed samples, the tetrad effect describes a convex, M-shaped pattern. However, Veksler et al. (2005) concluded from tetrad patterns involving the distribution coefficient that only silicate melts produce M-shaped patterns. The conjugate fluoride liquid, however, should have a W-shape which is not in accordance with the studied samples.

The pronounced tetrad effect in the Ivigtut deposit implies that it formed from highly evolved (granitic) melts which strongly interacted with a (F-rich) fluid (Irber, 1999; Zhao et al., 2002; Liu et al., 2005). The tetrad effect cannot be explained by fractionation of REE-rich accessory minerals (monazite, xenotime, garnet, eudialyte etc.; c.f. Liu et al., 2005; Irber, 1999) as no significant tetrad effect was observed in the unaltered Ivigtut granite surrounding the Ivigtut deposit. The fluid-rock interaction which is evidenced by the strong metasomatism of the host granite (Pauly & Bailey, 1999) is the most likely explanation for the REE distribution found in the fluorides from the Ivigtut cryolite deposit.

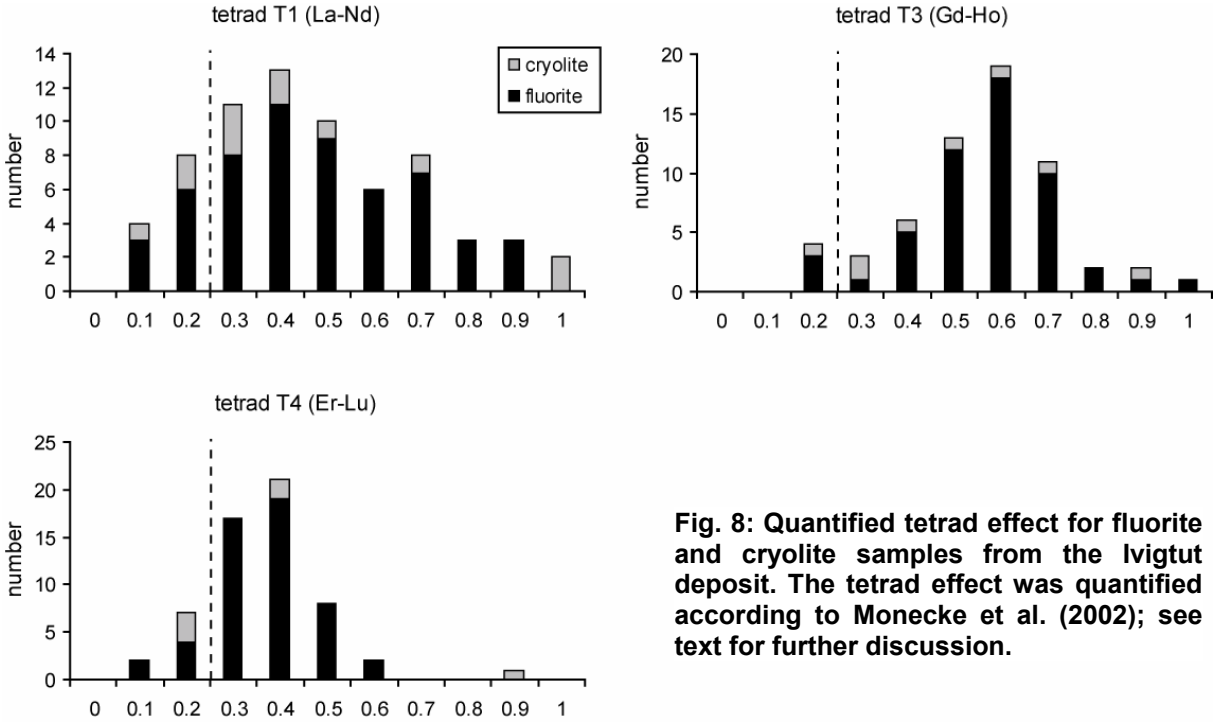

Fig. 8: Quantified tetrad effect for fluorite and cryolite samples from the Ivigtut deposit. The tetrad effect was quantified according to Monecke et al. (2002); see text for further discussion.

6.3.5 Y/Ho fractionation

Hydrothermal fluorites from Motzfeldt and Ilímaussaq

In Ilímaussaq and Motzfeldt, the hydrothermal fluorites are variable in their Y/Ho ratios that can reach up to 1370 (Ilm77). This argues for a decoupling of Y from Ho during the hydrothermal stage during which these fluorites formed. Bau & Dulski (1995) suggested that in fluorine-rich environments, the Y/Ho ratio and the positive Y anomaly increase during the migration and interaction of a fluorine-rich aqueous fluid. This is the most likely explanation for the increasing Y/Ho ratios of hydrothermal fluorites from the Ilímaussaq intrusion with ratios > 1300 (Fig. 9 & 10). Fluorites which are interpreted to have formed at a later stage (i.e. at lower temperatures) show a decreasing content of REE coupled with an increasing Y anomaly (e.g. very late formed Ilm77).

The fluorites from Motzfeldt and Ilímaussaq define steep trends in the Y against Ho diagram with slopes between 50 and 80 (R^2 = 0.7 to 0.9; Fig. 10). The Y/Ho ratios of fluorites from SM1 are widely scattered suggesting the influence of coupled effects of fluid interaction, remobilisation and/or various generations of fluorite. Additionally, the highly varying Y/Ho and La/Ho ratios may further indicate that these fluorites are not cogenetic (Bau & Dulski, 1995). It is obvious that the Y/Ho ratio decreases with increasing REE content in certain samples from SM1 (Fig. 2, JS6; JS16, JS4). This could be related to different origins of the different fluorite parts. Another hypothesis suggests that Y was complexed with F and therefore was retained in the fluid whereas the REE were incorporated in the fluorites. A migrating fluid would then show an increasing Y anomaly with decreasing REE content (Bau & Dulski, 1995).

The Y/Ho and La/Ho ratios of most fluorites from unit SM4 (Motzfeldt) have similar values implying precipitation from a similar hydrothermal fluid (Bau & Dulski, 1995). SM5 shows slightly lower Y/Ho and higher La/Ho ratios. The slightly decreasing Y/Ho ratio from SM4 to SM5 (Motzfeldt) could account for interaction with a (bi)carbonate-rich solution (Bau & Dulski, 1995). This is further supported by vein fluorites associated with carbonates and calcite daughter minerals in fluid inclusions of the Motzfeldt intrusion (Schönenberger & Markl, in press).

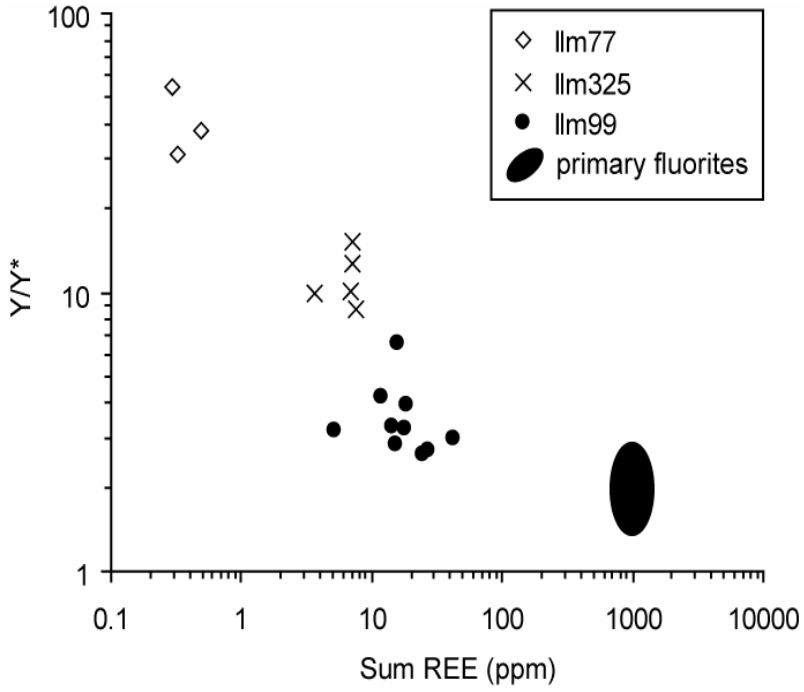

Fig. 9: Y anomaly (Y/Y* with Y* = $(Dy_n * Ho_n)^{0.5}$) vs. total REE content (ppm) of the Ilímaussaq fluorites. Primary fluorites show the highest REE content whereas the Y anomaly increases in the order primary fluorites < Ilm 99 < Ilm 325 < Ilm 77.

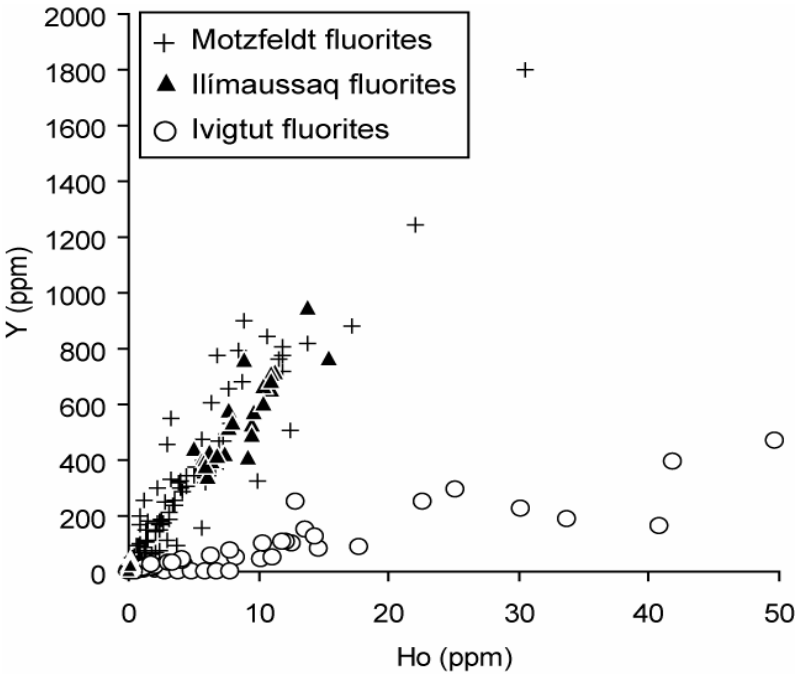

Fig. 10: Y (ppm) vs. Ho (ppm) of Motzfeldt, Ilímaussaq and Ivigtut fluorites. The Motzfeldt and Ilímaussaq fluorites describe a much steeper trend than the Ivigtut fluorites.

Hydrothermal fluorites from the Ivigtut deposit

The low Y/Ho ratio in samples from Ivigtut is in strong contrast to the rather high ratios in fluorites from Motzfeldt and Ilímaussaq. In Ivigtut, the Y/Ho ratios of cryolite and fluorite are below the chondritic value of 28 and vary between 3 and 15 with a mean at 8-9. In the Y-Ho diagram, the data points define a flat slope of about 8 (R^2 = 0.91; Fig. 10). Veksler et al. (2005) observed a decoupling of Y from Ho and a strong Y/Ho anomaly in cryolite which they ascribed not only to the influence of F itself, but rather to REE-aluminofluoride complexes. However, they also pointed out that fluoride liquids are more enriched in Y than in Ho. This is not in agreement with samples from Ivigtut, because if the analysed cryolite samples precipitated from such a fluoride liquid, much higher Y/Ho ratios would be expected. The low Y/Ho ratios could be explained by an abnormally low Y content in the fluid. Strikingly, however, bulk rock analyses from the Ivigtut granite exhibit near-chondritic Y/Ho ratios from 16 to 40 with a mean at 28 (Goodenough et al., 2000). The fact that the unaltered Ivigtut granite does have chondritic Y/Ho ratios, but fluorite and cryolite from the deposit do not, may be explained with experimental results by Veksler et al. (2005). They showed that the cryolite/fluoride or silicate melt D_Y is lower than that of Ho. This may explain the low Y/Ho ratio in cryolite, but not the low ratio in fluorite which is commonly below 10. It may be possible that some change in the Y-Ho content took place before/during the deposit's formation. Pauly & Bailey (1999) suggested that the granite had already been solidified when greisenisation and metasomatism led to its alteration. These altering fluids formed an aluminofluoride melt which later unmixed into a silica- and a fluorine-rich melt. It may be possible that during greisenisation, Y and Ho were decoupled. Y was most likely retained in the granite whereas Ho was preferably leached leading to the low Y/Ho ratios of the deposit.

7. Conclusions

In the present study, REE patterns of fluorides from three plutonic complexes in a magmatic province record distinct conditions of formation. The fluorites from the Motzfeldt and Ilímaussaq intrusions appear to have formed in a similar environment and from a similar source. Primary magmatic fluorites have (almost) identical characteristics regarding their Y/Ho ratios, REE content and patterns irrespective of their association with an agpaitic or miaskitic mineral assemblage. The most likely process having led to these comparable LREE

enriched patterns is the similar K_D and/or the whole-rock control. The latter also accounted for the LREE enriched peralkaline magmatic rocks from Motzfeldt and Ilímaussaq.

The CL imagery and REE patterns of hydrothermal fluorites from Motzfeldt suggest multiple fluorite generations within one unit (SM1). Furthermore, different physico-chemical formation conditions are reflected by low REE contents and a negative Ce anomaly indicating more oxidised conditions. Fluorites from SM5 show evidence of fluid interaction with the surrounding rocks from which they appear to have partly inherited the positive Eu anomaly.

The HREE-enriched or smooth patterns in minerals from the Ivigtut deposit are very different from Motzfeldt and Ilímaussaq and appear to reflect hydrothermal formation conditions. The incorporation of REE into fluorides from Ivigtut seems to be mostly driven by F-complexation resulting in the tetrad effect. This effect typically reflects strong interaction of a fluid with highly evolved granitic rocks. In contrast, the tetrad effect is not seen in highly evolved, Si-undersaturated rocks like those from Motzfeldt and Ilímaussaq.

These observations lead to the conclusion that the abundance and distribution of REE is strongly source-dependent. The heterogeneous mantle source assumed beneath the Gardar Province may be an important factor controlling the distribution of trace elements. Additionally, silica-rich, granitic systems like Ivigtut favour HREE whereas the low-Si, alkaline nepheline-syenites from Motzfeldt and Ilímaussaq appear to preferentially incorporate LREE. Apart from source features, it is the size and charge of the cation and the availability of complexing agents in the fluid that govern the incorporation of REE into minerals.

Acknowledgments

Financial support by the German Science Foundation (DFG) and the Graduiertenförderung des Landes Baden-Württemberg is gratefully acknowledged. Helene Brätz is thanked for performing the LA-ICP MS measurements in Würzburg. Ole V. Petersen kindly provided rock samples from Ivigtut from the Geological Musuem of Copenhagen, Denmark. Gesa Graser and Thomas Krumrei are thanked for providing samples from the Ilímaussaq intrusion. Adrian Finch is thanked for fruitful discussions. Thomas Wagner kindly helped to improve an earlier version of the manuscript. The useful comments and suggestions of two anonymous reviewer are greatly acknowledged.

Appendix A. Supplementary data

Supplementary data associated with this article can be found in the online version.

References

Anders, E., Grevesse, N., 1989. Abundances of the elements: meteoritic and solar. Geochimica et Cosmochimica Acta 53, 197-214.

Bailey, J.C., Gwozdz, R., Rose-Hansen, J. & Sørensen, H., 2001: Geochemical overview of the Ilímaussaq alkaline complex, South Greenland. In: Sørensen, H. (Ed.), The Ilímaussaq complex, South Greenland: status of mineralogical research with new results. Geology of Greenland Survey Bulletin 190, 35-53.

Bau, M., 1991. Rare earth element mobility during hydrothermal and metamorphic fluid-rock interaction and the significance of the oxidation state of europium. Chemical Geology 93, 219-230.

Bau, M., 1996. Controls on the fractionation of isovalent trace elements in magmatic and aqueous systems: evidence from Y/Ho, Zr/Hf, and the lanthanide tetrad effect. Contributions to Mineralogy and Petrology 123, 323-333.

Bau, M., 1997. The lanthanide tetrad effect in highly evolved felsic igneous rocks—a reply to the comment by Y. Pan. Contrib. Mineral. Petrol. 128, 409– 412.

Bau, M., Dulski, P., 1995. Comparative study of yttrium and rare-earth element behaviours in fluorine-rich hydrothermal fluids. Contributions to Mineralogy and Petrology 119, 213-223.

Bau, M., Möller, P., 1992. Rare Earth Element Fractionation in Metamorphogenic Hydrothermal Calcite, Magnesite and Siderite. Mineralogy and Petrology 45, 231-246.

Bradshaw, C., 1988. A Petrographic, Structural and Geochemical study of the Alkaline Igneous rocks of the Motzfeldt centre, South Greenland. PhD thesis, Univ. of Durham, UK.

Constantopoulos, J., 1988. Fluid Inclusions and Rare Earth Element Geochemistry of Fluorite from South-Central Idaho. Economic Geology 83, 626-636.

Dingwell, D.B., 1988. The structures and properties of fluorine-rich magmas: a review of experimental studies. CIM Special Volume 39, 1-12.

Dolejs, D., Baker, D.R., 2007a. Liquidus Equilibria in the System K_2O-Na_2O-Al_2O_3-SiO_2-F_2O_{-1}-H_2O to100MPa: I. Silicate-Fluoride Liquid Immiscibility in Anhydrous Systems. Journal of Petrology 48, 785-806.

Dolejs, D., Baker, D.R., 2007b. Liquidus Equilibria in the System K_2O-Na_2O-Al_2O_3-SiO_2-F_2O_{-1}-H_2O to100 MPa: II. Differentiation Paths of Fluorosilicic Magmas in Hydrous Systems. Journal of Petrology 48, 807-828.

Drummond, M.S., Defant, M.J., Kepezhinskas, P.K., 1996. Petrogenesis of slab-derived trondhjemite-tonalite-dacite/adakite magmas. Transactions of the Royal Society of Edinburgh: Earth Sciences 87, 205-215.

Ekambaram, V., Brookins, D.G., Rosenberg, P.E., Emanuel, K.M., 1986. Rare-Earth Element Geochemistry of fluorite-carbonate deposits in western Montana, USA. Chemical Geology 54, 319-331.

Emeleus, C.H., Harry, W.T., 1970. The Igaliko nepheline syenite complex; general description. Meddelelser om Grønland, 186, 115.

Eppinger, R.C., Closs, L.G., 1990. Variation of trace elements and rare earth elements in fluorite: A possible tool for exploration. Economic Geology 85, 1896-1907.

Escher, A., Watt, W.S., 1976. Geology of Greenland. Geological Survey of Greenland, Copenhagen, 603 p.

Fleischer, M., Altschuler, Z.S., 1969. The relationship of the rare-earth composition of minerals to geological environment. Geochimica et Cosmochimia Acta 33, 725-732.

Fryer, B.J., Edgar, A.D., 1977. Significance of rare earth distributions in coexisting minerals of peralkaline undersaturated rocks. Contributions to Mineralogy and Petrology 61, 35-48.

Gagnon, J.E., Samson, I.M., Fryer, B.J., Williams-Jones, A.E., 2003. Compositional heterogeneity in fluorite and the genesis of fluorite deposits: insights from LA-ICP-MS analysis. Canadian Mineralogist 41, 365-382.

Garde, A.A., Hamilton, M.A., Chadwick, B., Grocott, J., McGaffrey, K.J.W., 2002. The Ketilidian orogen of South Greenland: geochronology, tectonics, magmatism, and fore-arc accretion during Palaeoproterozoic oblique convergence. Canadian Journal of Earth Sciences 39, 765-793.

Goodenough, K.M., Upton, B.G.J., Ellam, R.M., 2000. Geochemical evolution of the Ivigtut granite, South Greenland: a fluorine-rich "A-type" intrusion. Lithos 51, 205-221.

Goodenough, K.M., Upton, B.G.J., Ellam, R.M., 2002. Long-term memory of subduction processes in the lithospheric mantle: evidence from the geochemistry of basic dykes in the Gardar Province of South Greenland. Journal of the Geological Society, London 159, 705-714.

Graser, G., Potter, J., Köhler, J., Markl, G., in press. Isotopic, major, minor and trace element geochemistry of late-stage fluids in the peralkaline Ilímaussq intrusion, South Greenland. Lithos.

Haas J.R., Shock E.L., and Sassani D.C., 1995. Rare earth elements in hydrothermal systems: estimates of standard partial molal thermodynamic properties of aqueous complexes of the rare earth elements at high pressures and temperatures. Geochim. Cosmochim. Acta 59, 4329–4350.

Halama, R., Waight, T., Markl, G., 2002. Geochemical and isotopic zoning patterns of plagioclase megacrysts in gabbroic dykes from the Gardar Province, South Greenland: implications for crystallisation processes in anorthositic magmas. Contributions to Mineralogy and Petrology 144, 109-127.

Halama, R., Joron, J.L., Villemant, B., Markl, G., Treuil, M., 2007. Trace element constraints on mantle sources druing mid-Proterozoic magmatism: evidence for a link between the Gardar (South Greenland) and Abitibi (Canadian Shield) mafic rocks. Canadian Journal of Earth Sciences 44, 1-20.

Hill, G.T., Campbell, A.R., Kyle, P.R., 2000. Geochemistry of southwestern New Mexico fluorite occurrences implications for precious metals exploration in fluorite-bearing systems. Journal of Geochemical Exploration 68, 1-20.

Hollings, P., Wyman, D., 2005. The geochemistry of trace elements in igneous systems: principles and examples from basaltic systems. In: Linnen, R.L., Samson, I.M. (Eds.), Rare-Element Geochemistry and Mineral Deposits: Geological Association of Canada, GAC Short Course Notes 17, 1-16.

Horn, I., Hinton, R.W., Jackson, S.E., Longerich, H.P., 1997. Ultra-trace element analysis of NIST SRM 616 and 614 using laser ablation microprobe-inductively coupled plasma-mass spectrometry (LAM-ICP-MS); a comparison with secondary ion mass spectrometry (SIMS). Geostandards Newsletter 21, 191-203.

Irber, W., 1996. Laugungsexperimente an peralumischen Graniten als Sonde für Alterationsprozesse im finalen Stadium der Granitkristallisation mit Anwendung auf das Rb-Sr-Isotopensystem. Ph.D. dissertation (German with English abstract), FU Berlin.

Irber, W., 1999. The lanthanide tetrad effect and its correlation with K/Rb, Eu/Eu*, Sr/Eu, Y/Ho, and Zr/Hf of evolving peraluminous granite suites. Geochimica et Cosmochimica Acta 63, 489-508.

Jahn, B., Wu, F., Capdevila, R., Martineau, F., Zhao, Z., Wang, Y., 2001. Highly evolved juvenile granites with tetrad REE patterns: the Woduhe and Baerzhe granites from the Great Xing'an Mountains in NE China. Lithos 59, 171-198.

Jones, A.P., 1980. Petrology and structure of the Motzfeldt centre, Igaliko complex, South Greenland. PhD thesis, Univ. of Durham, UK.

Jones, A.P., 1984. Mafic silicates from the nepheline syenites of the Motzfeldt centre, south Greenland. Mineralogical Magazine, 48, 1-12.

Kempe, U., Monecke, T., Oberthür, T., Kremenetsky, A.A., 1999. Trace elements in scheelite and quartz from the Muruntau/Myutenbai gold deposit, Uzbekistan: constraints on the nature of ore-forming fluids. In: Stanley, C.J., et al. (eds). Mineral Deposits: Processes to Processing. Balkema, Rotterdam, The Netherlands, 373-376.

Kessel, R., Schmidt, M.W., Ulmer, P., Pettke, T., 2005. Trace element signature of subduction-zone fluids, melts and supercritical liquids at 120-180 km depth. Nature 437, 724-727.

Köhler, J., Konnerup-Madsen, J., Markl, G., 2008. Fluid geochemistry in the Ivigtut cryolite deposit, South Greenland. Lithos 103, 369-392.

Lahaye, Y., Lamber, D., Walters, S., 1997. Ultraviolet laser sampling and high-resolution inductively coupled plasma mass spectrometry of NIST and BCR-2G glass reference materials. Geostandards Newsletter 21, 205-214.

Larsen, L.M., Sørensen, H., 1987: The Ilímaussaq intrusion . progressive crystallization and formation of layering in an agpaitic magma. In Fitton, J. G., Upton, B. G. J. (eds.), Alkaline Igneous Rocks, Geol. Soc. Spec. Pub. 30, 473-488.

Liu, C.Q., Zhan, H., 2005. The lanthanide tetrad effect in apatite from the Altay No. 3 pegmatite, Xingjiang, China: an intrinsic feature of the the pegmatitic magma. Chemical Geology 214, 61-77.

Lüders, V., Möller, P., Dulski, P., 1993. REE Fractionation in Carbonates and Fluorite. Monograph Series on Mineral Deposits 30, 133-150.

Luo, Y.-R., Byrne, R.H., 2004. Carbonate Complexation of Yttrium and the Rare Earth Elements in Natural Waters. Geochimica et Cosmochimica Acta 68, 691-699.

Manning, D.A.C., 1981. The effect of fluorine on liquidus phase relationships in the system Qz-Ab-Or with excess water at 1 kb. Contributions to Mineralogy and Petrology 104, 424-438.

Markl, G., Marks, M., Schwinn, G., Sommer, H., 2001. Phase Equilibrium Constraints on Intensive Crystallization Parameters of the Ilímaussaq Complex, South Greenland. Journal of Petrology 42, 2231-2258.

Marks, M., Vennemann, T., Siebel, W., Markl, G., 2003. Quantification of Magmatic and Hydrothermal Processes in a Peralkaline Syenite-Alkali Granite Complex Based on Textures, Phase Equilibria, And Stable and Radiogenic Isotopes. Journal of Petrology 44, 1247-1280.

Marshall, A.S., Hinton, R.W., MacDonald, R., 1998. Phenocrystic fluorite in peralkaline rhyolites, Olkaria, Kenya Rift Valley. Mineralogical Magazine 62, 477-486.

Masuda, A., Kawakami, O., Dohmoto, Y., Takenaka, T., 1987. Lanthanide tetrad effect in nature: two mutually opposite types, W and M. Geochemical Journal 21, 119-124.

McDonough, W.F.M., Sun, S.S., 1995. The composition of the Earth. Chemical Geology 120, 223-253.

Migdisov A.A., Williams-Jones A.E., 2002. A spectrophotometric study of neodymium(III) complexation in chloride solutions. Geochimica et Cosmochimica Acta 66, 4311–4323.

Migdisov A.A., Reukov V.V., Williams-Jones A.E., 2006. A spectrophotometric study of neodymium(III) complexation in sulfate solutions at elevated temperatures. Geochimica et Cosmochimica Acta 70, 983–992.

Migdisov, A.A., Williams-Jones, A.E., 2007. An experimental study of the solubility and speciation of neodymium (III) fluoride in F-bearing aqueous solutions. Geochimica et Cosmochimica Acta 71, 3056-3069.

Möller, P., Parekh, P., Schneider, H.-J., 1976. The application of Tb/Ca-Tb/La abundance ratios to problems of fluorspar genesis. Mineralium Deposita 11, 111-116.

Möller, P., Bau, M., Dulski, P., Lüders, V., 1998. REE and Y fractionation in fluorite and their bearing on fluorite formation. Proceedings of the Ninth Quadrennial IAGOD Symposium. Schweizerbart, Stuttgart, 575-592.

Monecke, T., Kempe, U., Monecke, J., Sala, M., Wolf, D., 2002. Tetrad effect in rare earth element distribution patterns: A method of quantification with application to rock an mineral samples from granite-related rare metal deposits. Geochimica et Cosmochimica Acta 66, 1185-1196.

Morgan, J.W., Wandless, G.A., 1980. Rare earth element distribution in some hydrothermal minerals: evidence for crystallographic control. Geochmicia et Cosmochimica Acta 44, 973-980.

Müller-Lorch, D., Marks, M.A.W., Markl, G., 2007. Na and K distribution in agpaitic pegmatites. Lithos 95, 315-330.

Pan, Y., Fleet, M.E., 1996. Rare element mobility during prograde granulite facies metamorphism: significance of fluorine. Contributions to Mineralogy and Petrology 123, 251-262.

Pauly, H., Bailey, J.C., 1999. Genesis and evolution of the Ivigtut cryolite deposit, SW Greenland. Meddelelser om Grønland, Geoscience 37, 60.

Pearce N.J.G., Perkins W.T., Westgate J.A., Gorton M.P., Jackson S.E, Neal C.R, Chenery S.P., 1997. A compilation of new and published major and trace element data for NIST SRM 610 and NIST SRM 612 glass reference materials. Geostandards Newsletter 21, 115-144.

Pearson, R.G., 1963. Hard and soft acids and bases. Journal of the American Chemical Society 85, 3533-3539.

Petersen, O.V., 2001: List of minerals identified in the Ilimaussaq alkaline complex, South Greenland. Geology of Greenland Survey Bulletin 190, 25-33.

Prokof'ev, V.B., Naumov, V.B., Ivanova, G.F., Savel'eva, N.I., 1991. Fluid inclusion studies in cryolite and siderite of the Ivigtut deposit (Greenland). Neues Jahrbuch für Mineralogie, Monatshefte 1, 32-38.

Rubin, J.N., Henry, C.D., Price, J.G., 1993. The mobility of zirconium and other "immobile" elements during hydrothermal alteration. Chemical Geology 110, 29-47.

Rudnick, R.L., Barth, M., Horn, I., McDonough, W.F., 2000. Rutile-bearing refractory eclogites: missing link between continents and depleted mantle. Science 287, 278-281.

Sallet, R., Moritz, R., Fontignie, D., 2000. Fluorite $^{87}Sr/^{86}Sr$ and REE constraints on fluid-melt relations, crystallization time span and bulk D^{Sr} of evolved high-silica granites, Tabuleiro granites, Santa Catarina, Brazil. Chemical Geology 164, 81-92.

Sallet, R., Moritz, R., Fontignie, D., 2005. The use of vein fluorite as probe for paleofluid REE and Sr–Nd isotope geochemistry: The Santa Catarina Fluorite District, Southern Brazil. Chemical Geology 223, 227-248.

Salvi, S., Fontan, F., Monchoux, P., Williams-Jones, A.E., Moine, B., 2000. Hydrothermal Mobilization of High Field Strength Elements in Alkaline Igneous Systems: Evidence from the Tamazeght Complex (Morocco). Economomic Geology 95, 559-576.

Scaillet, B., Macdonald, R., 2004. Fluorite stability in silicic magmas. Contributions to Mineralogy and Petrology 147, 319-329.

Scaillet, B., Macdonald, R., 2001. Phase Relations of Peralkaline Silicic Magmas and Petrogenetic Implications. Journal of Petrology 42, 825-845.

Schönenberger, J., Markl, G. in press. The Magmatic and Fluid Evolution of the Motzfeldt Intrusion in South Greenland: Insights into the Formation of Agpaitic and Miaskitic Rocks. Journal of Petrology, doi: 10.1093/petrology/egn037.

Schwinn, G., Markl, G., 2005. REE systematics in hydrothermal fluorite Chemical Geology, 216, 225-248.

Sørensen, H., 1997. The agpaitic rocks – a review. Mineralogical Magazine 61, 485-498.

Sørensen, H., Bohse, H., Bailey, J.C., 2006. The origin and mode of emplacement of lujavrites in the Ilímaussaq alkaline complex, South Greenland. Lithos 91, 286-300.

Stähle, H.J., Raith, M., Hoernes, S., Delfs, A., 1987. Element mobility during incipient granulite formation at Kabbadurga, Southern India. Journal of Petrolgy 28, 803-834.

Tagirov, B., Schott, J., Harrichourry, J.C., Salvi, S., 2002. Experimental study of aluminum speciation in fluoride-rich supercritical fluids. Geochimica et Cosmochimica Acta 66, 2013-2024.

Trinkler, M., Monecke, T., Thomas, R., 2005. Constraints on the genesis of yellow fluorite in hydrothermal barite-fluorite veins of the Erzgebirge, Eastern Germany: Evidence from optical absorption spectroscopy, rare-earth-element data and fluid-inclusion investigations. The Canadian Mineralogist 43, 883-898.

Upton, B.G.J., Emeleus, C.H., Heaman, L.M., Goodenough, K.M, Finch, A.A., 2003. Magmatism of the mid-Proterozoic Gardar Province, South Greenland: chronology, petrogenesis and geological setting. Lithos 68, 43-65.

Upton, B.G.J., Emeleus, C.H., 1987. Mid-Proterozoic alkaline magmatism in southern Greenland: the Gardar Province. In: Fitton, J.G. & Upton, B.G.J. (Eds.), Alkaline Igneous Rocks, Geological Society Special Publication 30, 449-471.

Veklser, I.V., Dorfman, A.M., Kamenetsky, M., Dulski, P., Dingwell, D., 2005. Partitioning of lanthanides and Y between immischible silicate and fluoride melts, fluorite and cryolite and the origin of the lanthanide tetrad effect in igneous systems. Geochimica et Cosmochimica Acta 69, 2847-2860.

Wagner, T., Erzinger, J., 2001. REE geochemistry of fluid-rock interaction processes related to Alpine-type fissure vein mineralisation, Rheinisches Schiefergebirge, Germany. In: Piestrzynski, A. et al. (Eds.), Mineral deposits at the beginning of the 21st century. Proc. joint 6th biennial SGA-SEG meeting, Krakow, 929-932. Society for Geology Applied to Mineral Deposits (SGA).

Webster, J.D., 1990. Partition of F between H_2O and CO_2 fluids and topaz rhyolite melt. Contrib. Mineral. Petrol. 104, 424–438.

Williams-Jones, A.E., Samson, I.M., Olivio, G.R., 2000. The genesis of hydrothermal fluorite-REE deposits in the Gallinas Mountains, New Mexico. Economic Geology and the Bulletin of the Society of Economic Geologists 95, 327-341.

Wood, S.A., 1990a. The aqueous geochemistry of the rare-earth elements and yttrium. 1. Review of available low-temperature data for inorganic complexes and the inorganic REE speciation of natural waters. Chemical Geology 88, 159-186.

Wood, S.A., 1990b. The aqueous geochemistry of the rare-earth elements and yttrium. 2. Theoretical predictions of speciation in hydrothermal solutions to 350 °C at saturation water vapor pressure. Chemical Geology 88, 99-125.

You, C.F., Castillo, P.R., Gieskes, J.M., Chan, L.H., Spivack, A.J., 1996. Trace element behavior in hydrothermal experiments: Implications for fluid processes at shallow depths in subduction zones. Earth and Planetary Science Letters 140, 41-52.

Zhao, Z., Xiong, X., Han, X., Wang, Y., Wang, Q., Bao, Z., Jahn, B., 2002. Controls on the REE tetrad effect in granites: Evidence from the Qianlishan and Baerzhe Granites, China. Geochemical Journal 36, 527-543.

Halogen and trace element geochemistry in the magmatic Gardar Province, South Greenland: evidence for subduction-related mantle metasomatism and fluid exsolution processes from alkalic melts

---

Jasmin Köhler[1], Johannes Schönenberger[1], Brian Upton[2] and Gregor Markl[1]

[1]Eberhard-Karls Universität Tübingen, Institut für Geowissenschaften, Wilhelmstraße 56, 72074 Tübingen, Germany

[2]School of GeoSciences, Grant Institute, University of Edinburgh, West Mains Road, Edinburgh EH9 3JW, UK

Keywords: Gardar; Dyke; Halogen; Fluorine; Subduction; Mantle Metasomatism

Eingereicht bei Lithos.

Abstract

XRF analyses of 152 magmatic dyke samples from a broad area (150 x 60 km) of the Gardar Province in Southern Greenland span the time 1280 to 1163 Ma and represent a wide compositional range (transitional olivine basalts to trachytes, alkalinity index of 0.3 to 1.5). Among those, 16 dyke samples were additionally analysed for Cl and Br.

Generally, the dykes represent a continuous fractionation trend from unfractionated basalts to more highly fractionated trachytes. Dykes from different areas exhibit a diverse geochemistry suggesting a heterogeneous and metasomatised mantle source. Enrichment in LILE, LREE and Sr and depletion in HFSE, Nb and Ti suggest that some of the metasomatism may have been associated with subduction processes pre-dating Gardar activity by some 600 Ma (Ketilidian orogeny).

The dykes are characterised by high fluorine contents up to 1.2 wt% F, particularly in the vicinity of the Ivigtut fluoride deposit. Fluorine probably was derived from partial melting of lithospheric mantle enriched in F-apatite and F-phlogopite. High Cl/Br (> 500) and low Cl/F (< 1) ratios of the dykes point to a fluid degassing/separation process which is supported by mineral/rock and fluid inclusion data from the Ilímaussaq and Ivigtut intrusions. There, the analysed rocks and minerals generally show high Cl/Br (> 300) and low Cl/F (< 1) weight ratios whereas the fluid inclusions have complementary low ratios (±100). Our investigations are in accordance with experimental data which show that fluorine is preferentially enriched in the melt whereas chlorine and especially bromine are lost with the fluid phase. Accordingly, the halogens show an increase in incompatible behaviour in the order F < Cl < Br.

Introduction

Halogens (F, Cl, Br) are useful geochemical tools and can provide constraints on the genesis of plutonic and volcanic rocks and their fluid evolution (Sigvaldason & Óskarsson, 1986; Kullerud, 1996; Markl & Schumacher, 1996; Bureau et al., 2000). Among the halogens, fluorine is most soluble in (alumino)silicate melts (>10 wt%) (Webster, 1990; Carroll & Webster, 1994) and generally remains in the residual magma and eventually enters hydroxyl-bearing minerals (Candela, 1986; Edgar et al., 1996). Of all rock types, alkaline rocks have the highest F content which increases with increasing peralkalinity index [molar (Na+K)/Al] (Bailey, 1977). In alkaline magmas, F forms bonds with alkali elements rather than with Si or Al (Kogarko, 1974; Kogarko & Ryabchikov, 1978) and may even generate fluoridic alkaline melts which show immiscibility with a silicate melt (Bailey, 1977; Veksler, 2004; Dolejš & Baker, 2007 a,b). In addition, F may play a crucial role in complexation processes in fluids and in the transport of ore-forming elements such as Li, Be, Sn and HFSE (Pan and Fleet, 1996; Salvi et al., 2000; Williams-Jones et al., 2000; Tagirov et al., 2002; Wood, 2003).

Chlorine can be highly concentrated in melts but especially in fluids (e.g. Carmichael et al., 1974; Metrich & Rutherford, 1992; Lowenstern, 1994; Bailey et al., 2001). Cl solubilities in aluminosilicate melts vary from a few thousand ppm to more than 2 wt% in peralkaline systems (Métrich & Rutherford, 1992; Bailey et al., 2001). Cl is commonly lost from magmas either through degassing or partitioning into aqueous fluids (Nijland et al., 1993; Carroll & Webster, 1994). During late magmatic stages, a Cl-rich aqueous phase or even a salt melt may separate (Carmichael et al., 1974; Lowenstern, 1994).

Br data may be used to constrain magmatic degassing (e.g. Villemant et al., 2008; Bureau & Métrich, 2003). The high potential solubility of Br in silicate melts makes it a sensitive tracer of the interaction of a magma with seawater or other Br-rich material (Bureau & Métrich, 2003).

Finally, the combination of these halogens, i.e. using their ratios (Cl/Br; Cl/F), allows to investigate the relation of samples to certain reservoirs in detail (primitive mantle, crust, sea water; Dreibus et al., 1979; Bottomley et al., 2005) and can provide helpful constraints on the unmixing of a fluid phase from a magma, fluid-fluid or fluid-rock interactions (e.g. Villemant and Boudon, 1999; Bureau et al., 2000; Bureau & Métrich, 2003). However, until now, very few data especially on the Br concentration in rocks exist.

Therefore, this study combines halogen data from whole rock samples as well as fluid inclusion data from the literature in order to obtain information on magmatic- and fluid-evolution processes in natural samples.

For these purposes, rocks from the Gardar Province are particularly suited for a detailed halogen analysis. The Gardar Province hosts (or hosted, prior to its exploitation) the world's largest fluoride deposit at Ivigtut (Pauly & Bailey, 1999), the importance of fluorine in the petrogenesis of the Gardar magmas has been highlighted by Upton and Emeleus (1987) and Upton et al. (2006) and recent publications provide first insights into the halogen contents of the Gardar rocks and fluids (Bailey et al., 2001; Krumrei et al., 2007; Köhler et al., 2008; Graser et al., in review; Schönenberger & Markl, in press). In order to provide more quantitative data on the subject of halogens in the Gardar magmas, 152 samples of dykes were investigated. The majority of these are of relatively unfractionated basaltic dykes, sufficiently fine-grained as to reflect compositions of the host magmas. Furthermore, the majority of the dykes crystallised under pressures sufficiently high to prevent vesiculation.

The results help to understand the timing, distribution, source and significance of halogen enrichment and distribution in the Gardar rocks and their sources, particularly the sub-continental mantle.

Geology

The Gardar Province in South Greenland is situated between the Archaean craton in the north and the Ketilidian mobile belt in the south (Fig. 1). The Gardar Province represents a failed rift structure where magmatic activity lasted from 1350 to 1160 Ma (Blaxland et al., 1978). The country rocks mainly consist of the calc-alkaline, 1855-1795 Ma old Julianehåb batholith (Garde et al., 2002) which was intruded by 12 major alkaline igenous complexes. Among the earliest Gardar rocks are those of the syn-rift Eriksfjord Formation (>1280 Ma) comprising clastic sediments and lavas.

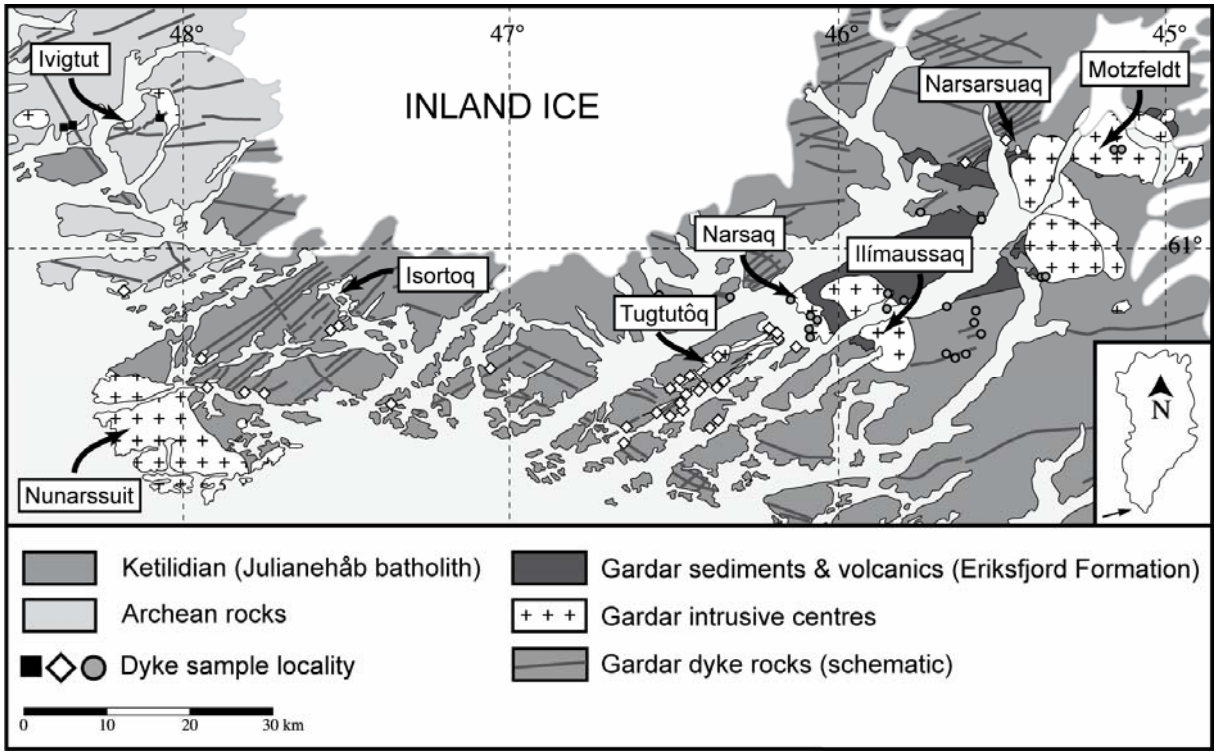

Figure 1 Overview of the Gardar Province and the localities of the analysed dykes (except for Ivigtut) with respect to the different intrusive complexes. Map modified after Escher & Watt (1976).

All over the province, numerous dyke swarms of different ages and highly variable chemical composition traverse the basement rocks. The oldest, WNW-ESE trending dykes are called "Brown Dykes" (BD 0) due to their brown alteration colour. Their composition ranges from lamprophyric to (trachy)doleritic and gabbroic (Upton & Emeleus, 1987; Goodenough, 1997). The BD 0 have an average U-Pb age of 1280 Ma and are succeeded by the "Giant Dykes" (GD) which are younger than 1200 Ma (Upton et al., 2003). The GD follow an ENE-WSW trend, have a width of 200-800 m and are mainly concentrated in the area around Nunarssuit-Isortoq and on Tugtutôq. The latter comprises the Older and Younger Giant Dyke Complexes (OGDC and YGDC, respectively; Upton, 1962; Upton & Thomas, 1980; Martin, 1985). The OGDC has an age of 1184 ± 5 Ma and acted as a precursor to the larger, 1163-1166 Ma old YGDC (Upton et al., 2003). Generally, the GD are composed of augite syenite, quartz syenite and alkali granite. Where they are composite, the dykes have a mafic (gabbroic) margin and a salic centre (Upton & Emeleus, 1987; Halama et al., 2004). Due to their broadness, the GD can be regarded as the transitional link between the dykes and the igneous complexes (Upton & Emeleus, 1987).

It has been known for a long time, that halogens were important components of the Gardar magmas. The extraordinary concentration of fluorine at Ivigtut in the western part of the Province has been apparent since Hans Giesecke's investigations some two hundred years ago. A small, A-type, granite stock, ~350m in diameter, hosted a zoned pegmatite deposit largely composed of about 12 million tons of cryolite (Na_3AlF_6) and siderite (Pauly & Bailey, 1999; Goodenough et al., 2002; Köhler et al., 2008) before it was mined out by 1962. In the eastern part of the province, the Ilímaussaq intrusion hosts nepheline syenites containing both orthomagmatic and late-stage hydrothermal villiaumite (NaF) in considerable quantities (refs). Both these and many observations on smaller scales provide ample evidence of halogen enrichment and their participation in various magmatic to hydrothermal processes.

Analytical methods

Whole-rock X-ray fluorescence analyses (XRF) were carried out on a Bruker S4 Pioneer machine at the Institut für Geowissenschaften, Universtität Tübingen, and on a Philips PW-1450 XRF at the School of Geosciences, University of Edinburgh, respectively. USGS, CRPG and international rock standards were used for calibration. Detection limits vary between 1 to 10 ppm depending on (trace) element and instrument.

For major elements, the powdered sample was fused to produce glass discs whereas pressed powder pellets were used for trace element analyses. Loss on ignition (LOI) was usually positive, with the majority varying between 0 and +1.5 %. Only two samples had a negative LOI (-0.77 and -0.18 %, respectively) indicating a mass increase upon oxidation from FeO to Fe_2O_3. XRF data from dykes of the Ivigtut area are from the archive of the Geological Survey of Denmark/Greenland (GEUS). The Ivigtut dyke samples are from drill cores, analysed by the Outokumpu OY Exploration & Mining Services/Finland during 1985-1987. The XRF whole-rock analyses were carried out at the company's Geoanalytical Laboratory on a Philips PW-1400 using the correction program "Leco". Carbon and sulphur were analysed by a Leco analyser and fluorine by a fusion procedure and selective ion electrode.

Additional halogen analyses in order to detect Cl and Br (together with F) were performed using a pyrohydrolysis extraction line in combination with ion chromatography at the Institut für Geowissenschaften, Universität Tübingen. The pyrohydrolysis extraction line was set up according to the method outlined by Dreibus et al. (1979). 10 to 120 mg sample powder washed with triple deionized water was thoroughly mixed with at least twice the amount of

V_2O_5. Subsequently, the mixture was filled into small quartz-glass vessels and heated to 1100 °C in the extraction line. The released halogens were dissolved in a 0.02 mol NaOH solution. A second halogen trap was installed after the main trap in order to avoid any loss of halogens. The total time of the experiment was 20 min with 10 to 20 ml of solution being collected. Subsequently, this solution was analysed with a Dionex ICS-1000 ion chromatograph using an IonPac AS9-HC 2-mm anion column. The ion chromatography (solution) analyses (in ppb) were recalculated to yield the halogen content in the original sample. Blank runs were performed after every analysis in order to check for possible contamination. The blanks yielded values for F and Cl of below 30 ppb and Br below detection limit. The reproducibility of the measurements was regularly checked with reference materials (Govindaraju, 1994; Michel et al., 2003; Table 1; see also Jochum et al., 2005) and is above 90 %, even when triple deionised water was used instead of a NaOH halogen trap. A maximum total error of 20 % (relative) can be assumed for the extraction/measurement process. For rock samples, detection limits are about 10 ppm for F and Cl and < 0.7 ppm for Br.

Table 1 Pyrohydrolysis-Ion-Chromatography standard analyses. All values in ppm. Columns F, Cl and Br: Values from this study. F-, Cl- and Br-published: published range mainly from Govindaraju, 1994; Michel et al., 2003; see also Jochum et al., 2005 (GeoRem database).

Standard measurements	F	Cl	Br	F-published	Cl-published	Br-published
ANG	136.9	241.3	3.4	100-131	197-330	1.9-3.18
GH	3785.5	70.5	< 0.7	3300-3696	100-120	< 0.3
GS-N	1256.4	448.3	3.5	919-1050	350-450	2.5
GS-N	1133.3	397.4	2.0	919-1050	350-450	2.5
BE-N	1260.3	186.2	< 0.7	1000-1100	179-200	0.6-2.2
UB-N	126.0	841.5	4.2	95.0	800.0	5.0
UB-N	108.6	822.9	4.4	95.0	800.0	5.0
Mica-Fe	14995.8	579.7	< 0.7	12500-16000	500-918	0.15
AC-E	2114.6	214.9	< 0.7	1677-2100	98-226	0.5-0.67
AC-E	2228.1	206.0	< 0.7	1677-2100	98-226	0.5-0.67

Results

Petrography

Giant Dykes occur on the island of Tugtutôq and around Isortoq. They are generally composite and show signs of rhythmic layering and/or feldspar lamination (Upton, 1962). Their chilled gabbroic margin is mainly composed of olivine and primary zoned plagioclase, alkali feldspar and anhedral olivine with interstitial clinopyroxene, titanomagnetite, ilmenite and abundant apatite (Halama et al., 2004). Towards the syenitic centre, amphibole becomes abundant whereas plagioclase and olivine disappear. The syenitic centre itself consists of

greyish-white, antiperthitic alkali feldspar, greenish-grey, euhedral pyroxene, sector-zoned epidote, titanite and biotite (Upton, 1962; Halama et al., 2004). The older giant dyke complex (OGDC) from Tugtutôq is made up of augite-syenite which grades into peralkaline nepheline-syenites (foyaites; Upton & Emeleus, 1987), whereas the younger giant dike complex (YGDC) mainly consists of plagioclase-olivine rocks that comprise calcic pyroxene, ilmenite, titanomagnetite, apatite and biotite as a minor component. Quartz occurs interstitially in the syenitic parts with primary calcite (Upton & Thomas, 1980).

The rather salic dykes from the Ilímaussaq-Narsaq-Motzfeldt area (Fig. 2) are holocrystalline and very fine-grained. Alkali feldspar up to 1 cm phenocrysts occur in a matrix of feldspar, aggregates of green pyroxene, altered biotite and opaque oxides. Interstitial quartz, fluorite and apatite occasionally occur. In the Ivigtut region, olivine dolerite dykes (i.e. Brown Dykes) consist of early olivine and plagioclase in an ophitic texture involving plagioclase and augite with subordinate Fe-Ti-oxides and apatite. Younger, basaltic dykes around Ivigtut comprise plagioclase phenocrysts in a fine-grained, olivine-free matrix of augite and andesine (Goodenough et al., 2002).

Whole-rock geochemistry

XRF whole-rock data are summarised in Table 2. In the TAS-diagram (Fig. 2; Le Maitre et al., 1989), the Gardar dykes span a wide compositional range from ultrabasic to intermediate/acid. The dykes around Tugtutôq-Isortoq-Nunarssuit-Narsarsuaq are confined to (ultra)basic compositions whereas most other dykes are more fractionated. Due to the predominance of Na over K, some dykes can be referred to as hawaiites, mugearites and benmoreites, respectively (Fig. 3).

Some of the dykes are compositionally similar to high-K calc-alkaline rocks, particularly to shoshonites. Their average Al_2O_3 content of 15 wt%, K_2O/Na_2O ratio (0.3-1.4) and overall high alkali content (Na_2O+K_2O >4 wt%) are typical of shoshonites (Le Maitre et al., 1989). The K_2O content of the Gardar dykes is generally > 2 wt% (Fig. 4). Na_2O contents of 3 - 8 wt% (mean, 4.4 wt%) and the high Sr contents (>400 ppm; Fig. 6 h) are similar to those of adakites (Defant & Drummond, 1990; Martin et al., 2005). Although the La/Yb (<< 21) and Sr/Y ratios (mean at 23) of the dykes are lower than those of adakites (50-72 and 21-39, respectively; Defant & Drummond, 1990).

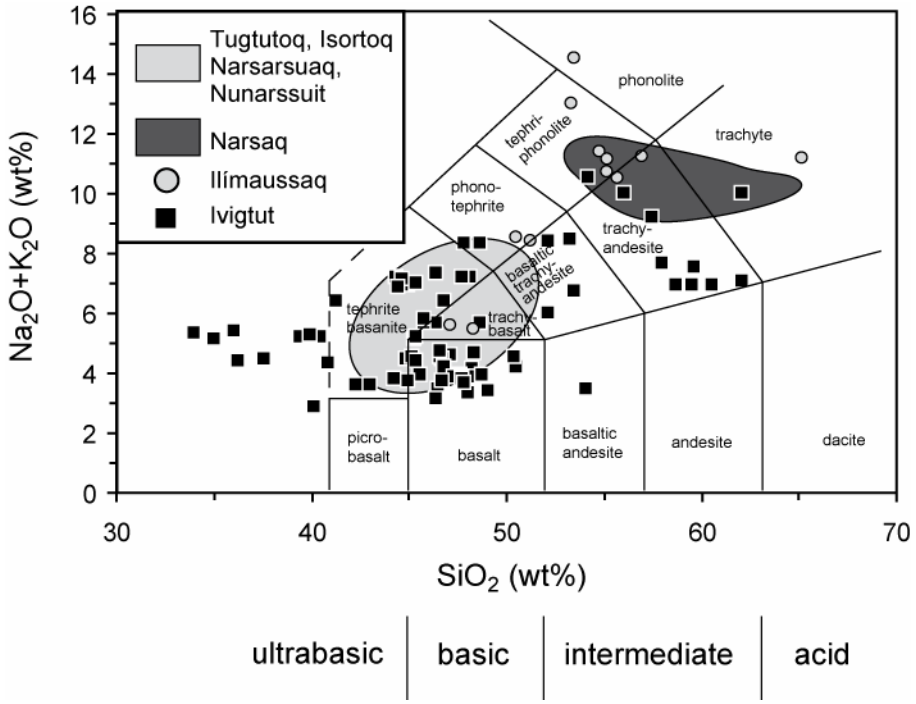

Figure 2 TAS Diagram after Le Maitre et al. (1989). The Gardar dykes cover a wide compositional range with the majority of dykes being restricted to (ultra)basic rocks.

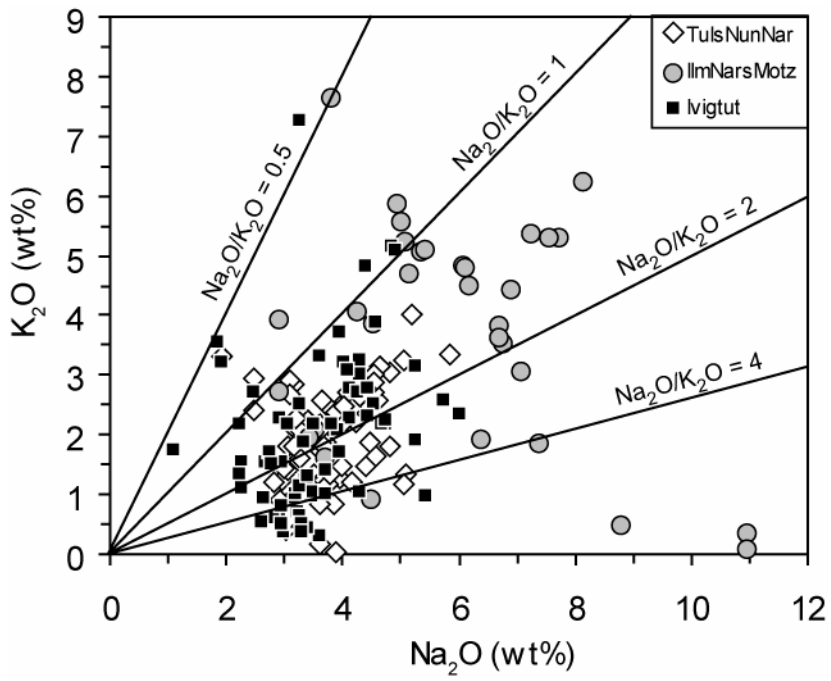

Figure 3 Na_2O (wt%) vs. K_2O (wt%). Due to the predominance of Na_2O over K_2O, some dykes can be referred to as hawaiites, mugearites or benmoreites, respectively. [TulsNunNar = Tugtutôq-Isortoq-Nunarssuit-Narsarsuaq; IlmNarsMotz = Ilímaussaq-Narsaq-Motzfeldt]

Table 2. Representative XRF whole rock data from dykes in the Gardar Province.

Locality	Tugtutôq	Tugtutôq	Tugtutôq	Tugtutôq	Tugtutôq	Tugtutôq	Isortoq	Isortoq	Isortoq	Nunarssuit	Nunarssuit
Sample	40455	86101	40583	40488	85997	86041	101337	101363	101438	101338B	101390
Dyke Generation	YGDC	OGDC	YGDC	YGDC	OGDC	OGDC					
Rock type	basalt	trachy-basalt	basalt	trachy-basalt	tephrite/ basanite	basaltic trachy-andesite	basalt	phono-tephrite	basalt	basalt	hawaiite
Fe_2O_3/FeO	0.20	0.30	0.20	0.30	0.25	0.35	0.20	0.35	0.20	0.20	0.30
Major elements (wt.%)											
SiO_2	45.5	45.17	46.43	45.04	44.37	50.63	49.34	49.38	48.67	46.41	49.67
TiO_2	2.77	3.88	2.41	3.44	4.59	2.66	1.87	2.98	3.15	1.73	1.41
Al_2O_3	16.28	14.75	17.98	15.56	14.01	15.09	16.36	14.38	13.58	17.48	18.32
$Fe_2O_{3\ total}$	15.67	16.29	14.4	16.65	16.28	13.25	13.47	13.65	15.44	14.14	10.71
FeO_{total}											
MnO	0.19	0.23	0.17	0.23	0.2	0.19	0.18	0.19	0.21	0.19	0.16
MgO	6.4	4.15	5.77	5.1	4.51	2.37	5.43	3.05	4.2	7.53	5.14
CaO	8.01	7.84	7.93	7.76	7.14	6.42	7.89	6.76	7.41	9.1	7.72
Na_2O	3.28	4.03	3.62	3.6	3.62	4.65	3.85	4.54	3.18	3.01	3.79
K_2O	1.60	2.27	1.19	1.73	2.16	3.14	0.85	2.89	1.80	0.39	1.35
P_2O_5	0.97	2.66	0.56	1.21	2.26	1.1	0.41	1.51	0.75	0.23	0.24
LOI (%)	-	-	-	-	-	-	-	-	-	-	-
Mg# **	49	40	49	44	41	32	49	37	39	56	55
Alkalinity Index	0.44	0.62	0.40	0.50	0.59	0.73	0.44	0.74	0.53	0.31	0.42
Trace elements (ppm)											
Sc	18	19	14	22	18	30	20	18	28	21	22
V	134	110	191	165	166	35	270	66	214	158	175
Cr	22	7	43	18	6	6	65	3	60	41	170
Co	-	-	-	-	-	-	-	-	-	-	-
Ni	55	6	45	34	14	4	66	5	39	82	49
Cu	70	89	58	87	51	60	87	54	70	72	91
Zn	93	96	86	90	94	99	112	88	139	87	114
Ga	21	19	20	21	17	22	19	22	23	19	21
Rb	23	37	17	24	38	58	19	38	72	6	46
Sr	859	876	1002	769	818	753	798	379	424	429	506
Y	32	40	20	38	38	43	26	52	46	25	23
Zr	171	221	122	202	208	291	105	253	323	112	94
Nb	25	37	17	30	39	47	6	16	15	7	6
Ba	1166	1898	914	1357	2220	2554	1264	1440	783	245	539
Pb	4	8	5	6	8	10	3	9	7	3	3
La	50	53	36	51	60	65	17	42	34	6	14
Ce	67	129	48	86	123	129	36	101	77	18	23
Pr	0	13	0	0	12	13	0	13	0	0	0
Nd	36	68	24	46	66	59	23	59	40	12	15
Sm											
Eu	-	-	-	-	-	-	-	-	-	-	-
Gd	0	0	0	0	0	8	0	9	0	0	0
Dy	18	28	8	34	18	9	16	16	31	16	14
Yb	-	-	-	-	-	-	-	-	-	-	-
Lu	0.5	0.7	0.4	0.6	0.9	0.9	0.7	0.9	0.8	0.4	0.5
As	0	0	0	0	0	0	0	0	0	0	0
Hf	0	2.7	0	1.7	2.7	5.1	0	8.8	9.8	3.7	1.2
Ta	0	0	0	0	0	0	0	0	0	0	0
Th	0	0	0	0	0	0	0	0	0	0	0
U	2.8	1.1	0	5.3	0.0	5.6	5.6	9.3	8.1	2	6.9
Sn	2.7	3.9	1.6	2.5	3.0	4.8	2.9	3.1	3.3	1.6	2.7
Cs	0	0	0	0	0	4	4	0	0	0	3
S	855	149	710	1261	310	756	712	1825	711	690	334
Cl	110*	195	76*	224	341	280	148*	352	83*	198	459
F	1181*	2506	734*	974	2206	1380	692*	3025	1037*	302	529
La_{cn}/Lu_{cn}	10.4	7.9	9.3	8.8	6.9	7.5	2.5	4.8	4.4	1.6	2.9
Eu/Eu* ***	-	-	-	-	-	-	-	-	-	-	-

* Cl and F contents analysed with pryohydrolysis
** Mg# = $100[Mg/(Mg+Fe^{2+})]$ - = not detected
*** Eu/Eu* with Eu* = $(Sm*Gd)^{0.5}$

Table 2 continued.

Locality	Nunarssuit	Narsarsuaq	Narsarsuaq	Ilímaussaq	Ilímaussaq	Ilímaussaq	Ilímaussaq	Narsaq	Narsaq	Narsaq	Narsaq
Sample	101374	101249	101250	GD22	GD23b	GD26	GD31a	GD5	GD7	GD5	GD7
Dyke Generation											
Rock type	trachy-basalt	trachy-basalt	hawaiite	trachy-andesite	tephri-phonolite	hawaiite	phonolite	tephrite/ basanite	ben-moreite	tephrite/ basanite	ben-moreite
Fe_2O_3/FeO	0.30	0.30	0.30	0.40	0.40	0.30	0.50	0.25	0.40	0.25	0.40
Major elements (wt.%)											
SiO_2	45.43	45.62	48.04	55.49	54.94	47.10	53.30	43.64	57.48	43.64	57.48
TiO_2	2.04	2.99	3.21	1.53	1.23	2.80	0.56	3.48	0.77	3.48	0.77
Al_2O_3	16.08	15.21	13.94	17.37	17.08	15.05	19.32	15.07	15.08	15.07	15.08
$Fe_2O_{3\ total}$	14.18	15.64	13.54	8.28	7.29	14.36	7.13	15.70	10.11	15.70	10.11
FeO_{total}											
MnO	0.18	0.19	0.21	0.17	0.20	0.18	0.27	0.19	0.25	0.19	0.25
MgO	6.73	5.28	3.64	1.39	0.94	4.47	0.54	4.68	0.44	4.68	0.44
CaO	8.98	7.74	7.37	3.40	3.08	7.16	1.80	6.72	2.66	6.72	2.66
Na_2O	1.94	3.13	4.82	5.08	4.96	4.50	8.16	2.92	6.76	2.92	6.76
K_2O	3.32	2.15	1.79	5.22	5.84	0.91	6.23	3.92	3.51	3.92	3.51
P_2O_5	0.37	1.06	1.7	0.56	0.42	0.54	0.17	1.14	0.16	1.14	0.16
LOI (%)	-	-	-	0.47	2.93	1.69	1.46	1.44	1.40	1.44	1.40
Mg# **	55	47	41	32	26	45	18	42	11	42	11
Alkalinity Index	0.42	0.49	0.71	0.80	0.85	0.56	1.04	0.60	0.99	0.60	0.99
Trace elements (ppm)											
Sc	26	25	20	13	22	22	3	24	8	24	8
V	226	235	139	25	12	236	6	215	9	215	9
Cr	77	41	4	0	3	73	8	42	11	42	11
Co	-	-	-	7	0	39	3	42	6	42	6
Ni	91	37	4	42	47	92	126	91	174	91	174
Cu	108	88	59	73	66	87	91	97	96	97	96
Zn	103	109	156	95	129	139	168	146	238	146	238
Ga	21	20	23	24	27	26	41	25	46	25	46
Rb	66	137	38	92	121	27	186	154	86	154	86
Sr	299	865	608	648	333	520	42	644	158	644	158
Y	29	31	43	42	40	46	91	40	184	40	184
Zr	117	139	218	312	343	249	984	201	1532	201	1532
Nb	7	23	32	76	78	20	261	34	246	34	246
Ba	975	1189	1378	2812	1830	715	54	1128	207	1128	207
Pb	2	3	9	22	7	6	41	7	59	7	59
La	11	32	62	31	36	24	138	0	223	0	223
Ce	20	65	139	121	122	77	289	56	446	56	446
Pr	0	0	16	14	17	0	30	0	45	0	45
Nd	15	37	74	58	67	51	112	50	184	50	184
Sm				8	10	8	20	8	30	8	30
Eu	-	-	-	2	2	2	2	2	3	2	3
Gd	0	0	11	11	12	0	21	0	27	0	27
Dy	47	27	9	145	8	34	329	36	53	36	53
Yb	-	-	-	3.2	3.0	3.6	6.7	3.1	14.2	3.1	14.2
Lu	0.8	0.9	0.9	0.7	0.7	0.8	1.3	0.8	2.0	0.8	2.0
As	0	0	0	0	0	0	13.6	0	26.7	0	26.7
Hf	5.0	0.0	4.4	6.6	12.8	4.4	36.0	2.5	51.1	2.5	51.1
Ta	0	0	0	8.0	0	0	24.3	0	24.4	0	24.4
Th	0	0	0	0.0	0	0	21.1	0	36.1	0	36.1
U	8.0	6.1	9.3	188.0	13.6	12.6	267.6	9.7	36.5	9.7	36.5
Sn	2.3	4.7	5.3	4.0	5.6	4.8	8.5	5.1	14.1	5.1	14.1
Cs	3	8	2	3	12	6	19	8	21	8	21
S	18	1371	39	56	0	435	103	538	39	538	39
Cl	184	262	241*	291	281	300	1058*	359	159*	359	159*
F	570	1260	1983*	543	520	520	2819*	1728	3928*	1728	3928*
La_{cn}/Lu_{cn}	1.4	3.7	7.2	4.5	5.4	3.1	11.0	0.0	11.6	0.0	11.6
Eu/Eu* ***	-	-	-	0.7	0.4	n.d.	0.3	0.0	0.3	0.0	0.3

Table 2 continued.

Locality	Narsaq	Narsaq	Motzfeldt	Ivigtut	Ivigtut	Ivigtut	Ivigtut	Ivigtut	Ivigtut	Ivigtut	Ivigtut
Sample	GD9	GD13	JS89	BB 8	BB 11	BB 15	BB 16	BB 23	101414	101408	101419
Dyke Generation											
Rock type	trachyte	tephri-phonolite	phonolite	phono-tephrite	ben-moreite	trachyte	trachy-andesite	basalt	basaltic andesite	basalt	basalt
Fe_2O_3/FeO	0.50	0.40	0.50	0.35	0.40	0.50	0.40	0.20	0.3	0.2	0.2
Major elements (wt.%)											
SiO_2	59.85	53.91	55.42	48.2	59.5	62.1	57.5	50.2	54.09	46.58	48.79
TiO_2	0.90	0.85	0.54	1.94	0.67	0.542	0.619	1.08	1	3.02	1.91
Al_2O_3	14.36	18.12	16.57	15.6	16.4	14.8	14.5	12	13.3	14.7	15.65
$Fe_2O_{3\ total}$	8.43	8.44	8.91						11.13	16.88	14.49
FeO_{total}				11.6	5.28	6.7	6.07	12.2			
MnO	0.21	0.35	0.24	0.181	0.091	0.157	0.111	0.19	0.14	0.22	0.19
MgO	0.50	0.46	0.34	2.09	2.46	0	0.33	4.14	8.44	4.93	5.93
CaO	2.03	2.56	2.06	5.68	5.06	2.17	3.08	8.84	7.54	7.55	8.72
Na_2O	6.07	3.80	7.25	4.01	4.75	4.85	4.4	3.21	2.97	3.4	3.17
K_2O	4.81	7.62	5.36	3.21	2.18	5.14	4.81	1.02	0.5	1.32	0.77
P_2O_5	0.18	0.13	0.11	1.26	0.239	0.093	0.113	0.15	0.11	0.48	0.32
LOI (%)	1.43	1.88	1.66	-	-	-	-				
Mg# **	15	13	9	30	54	0	12	52	66	41	49
Alkalinity Index	1.06	0.80	1.07	0.65	0.62	0.92	0.86	0.50	0.41	0.48	0.39
Trace elements (ppm)											
Sc	13	0	8	-	-	-	-	-	22	26	29
V	6	4	5	-	-	-	-	-	167	207	227
Cr	14	0	15	9	70	9	9	21	414	54	68
Co	4	1	3	-	-	-	-	-	-	-	-
Ni	60	0	103	-	-	-	-	-	205	42	66
Cu	58	82	91	59	18	68	< 5	62	42	51	59
Zn	169	252	199	880	87	188	< 5	158	101	89	106
Ga	32	25	40	-	-	-	-	-	-	-	-
Rb	106	99	180	170	126	180	188	52	14	53	17
Sr	32	2913	3	905	423	863	364	668	319	366	406
Y	76	72	101	18	26	50	< 10	26	13	41	29
Zr	527	871	857	318	370	518	5256	104	47	246	143
Nb	94	403	194	91	96	233	182	32	5	16	8
Ba	131	3339	9	1908	770	439	690	242	153	588	498
Pb	26	43	54	60	67	100	< 5	94	8	5	6
La	101	300	141	-	-	-	-	-	8	29	17
Ce	212	474	289	58	69	191	166	24	5	65	38
Pr	27	31	37	-	-	-	-	-	-	-	-
Nd	97	153	116	-	-	-	-	-	4	35	23
Sm	16	27	19	-	-	-	-	-	-	-	-
Eu	2	8	2	-	-	-	-	-	-	-	-
Gd	15	16	26	-	-	-	-	-	-	-	-
Dy	21	11	483	-	-	-	-	-	-	-	-
Yb	6.2	4.6	8.0	-	-	-	-	-	-	-	-
Lu	1.0	1.0	1.6	-	-	-	-	-	-	-	-
As	0	0	0	-	-	-	-	-	-	-	-
Hf	20.8	10.0	38.0	-	-	-	-	-	-	-	-
Ta	6.5	40.4	16.8	-	-	-	-	-	-	-	-
Th	14.0	0.0	20.5	-	-	-	-	-	2	0	1
U	15.7	20.9	290	-	-	-	-	-	-	-	-
Sn	7.8	9.6	10.4	< 10	< 10	< 10	< 10	< 10	-	-	-
Cs	10	3	21	-	-	-	-	-	-	-	-
S	148	160	429	1100	100	400	1700	300	-	-	-
Cl	300	143*	1279*	-	-	-	-	-	-	-	-
F	1258	3536*	2468*	6600	3400	5400	12000	3700	-	-	-
La_{cn}/Lu_{cn}	10.5	31.1	9.1	-	-	-	-	-	-	-	-
Eu/Eu* ***	0.3	1.1	0.2	-	-	-	-	-	-	-	-

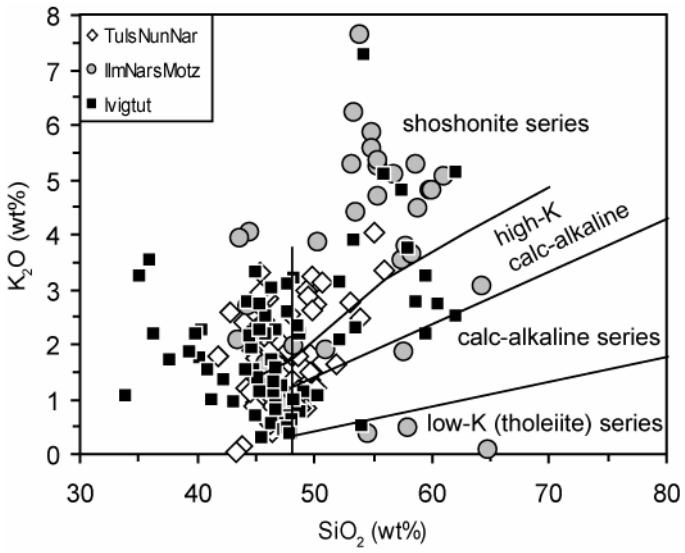

Figure 4 SiO_2-K_2O discrimination diagram for K-rich magmas after Le Maitre et al. (1989). Most dykes with SiO_2 > 48 % can be referred to as shoshonites suggesting their derivation from a subduction-related, metasomatised mantle [TulsNunNar = Tugtutôq-Isortoq-Nunarssuit-Narsarsuaq; IlmNarsMotz = Ilímaussaq-Narsaq-Motzfeldt].

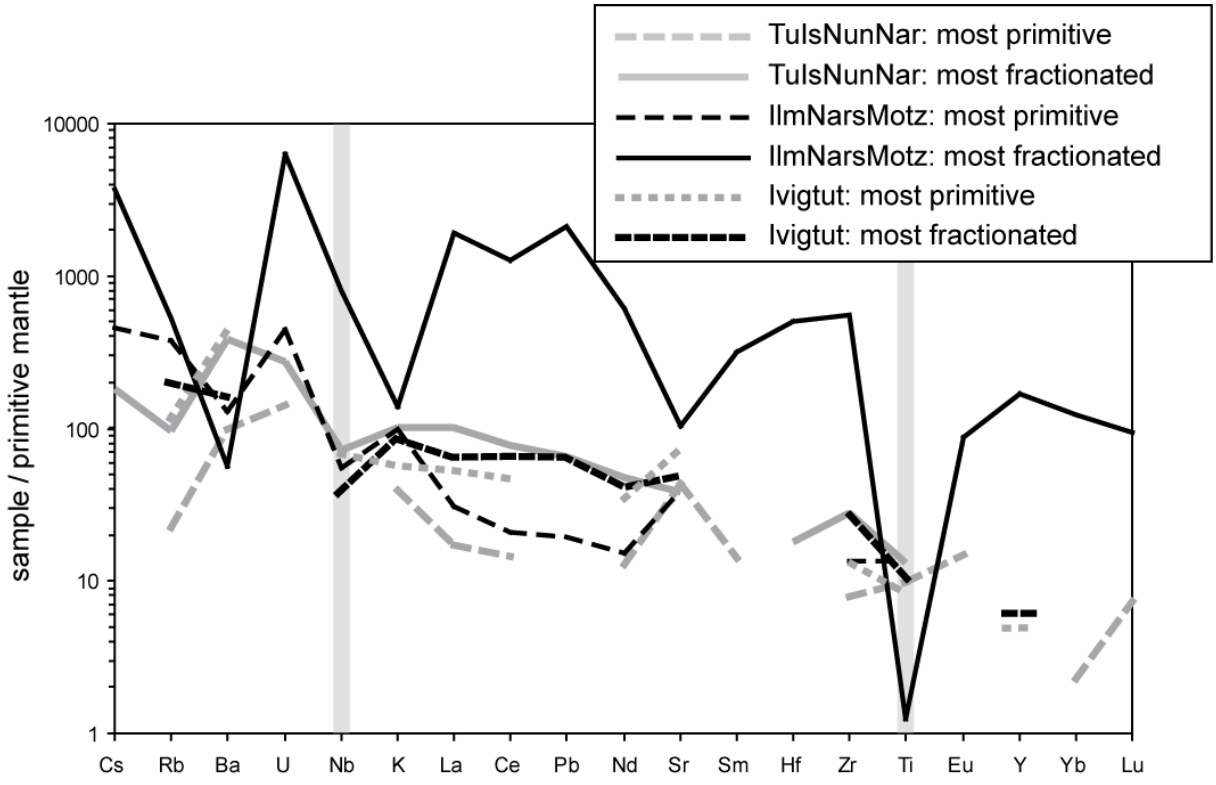

Figure 5 Primitive mantle-normalised (McDonough & Sun, 1995) trace element diagram for Gardar dykes. The ranges are given for the most primitive and most highly fractionated rocks, respectively.

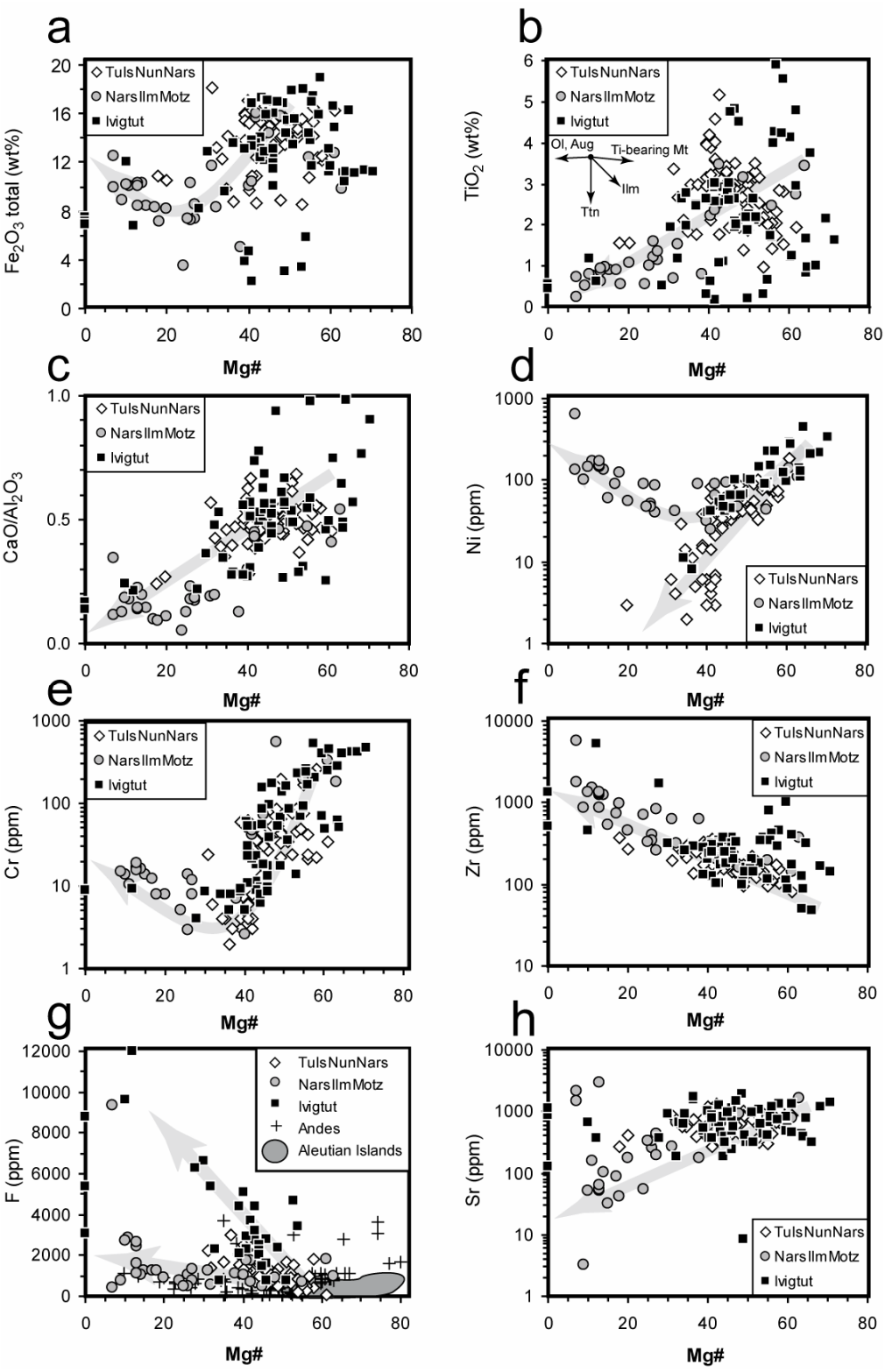

Figure 6 a-h. Whole rock variation diagrams for Gardar dykes with Mg# = Mg/(Mg+Fe^{2+}) as fractionation index. Comparative data for Andean rocks from Morgan et al. (1989) and Halter et al. (2004) and for Aleutian Islands from Coats (1953), Coats et al. (1959), Drewes et al. (1961) and Nye & Turner (1990). See text for further discussion.

Whole-rock trace element data for the dykes were normalised to primitive mantle (McDonough & Sun, 1995; Fig. 5). The incompatible trace element content tends to increase with degree of fractionation. The most primitive dykes in the Tugtutôq-Isortoq-Nunarssuit-Narsarsuaq area exhibit pronounced positive Sr anomalies which diminish in the more evolved dykes. The Ba anomaly, however, increases with fractionation as do negative Ti and positive Zr anomalies. The more primitive dykes of the Ilímaussaq-Narsaq-Motzfeldt region are distinguished by positive U anomalies and negative Ba, Nb and Ti anomalies. Whilst in the more evolved dykes these anomalies become more pronounced, the positive K and Sr anomalies turn into negative ones.

Compositional variation and possible fractionation trends are shown with respect to the Mg-number (Fig. 6). Mg-numbers [Mg# = 100*Mg/(Mg+Fe^{2+}) atomic] were calculated using different Fe_2O_3/FeO ratios from 0.15 to 0.50 for the various rock types according to Middlemost (1989). Generally, the Gardar dykes are moderately to highly evolved and have been regarded as products of magmas residual after extensive fractional crystallisation within or beneath the crust (Upton & Emeleus, 1987; Upton et al., 2003). This is indicated by their low Cr and Ni content (mostly <100 ppm) and the relative enrichment of incompatible elements like Zr (100 to >1000 ppm; Fig. 6 d, e, f) and La (10-300 ppm). Incompatible elements are especially concentrated in the dykes around Motzfeldt, Ilímaussaq and Narsaq.

The F content of the dykes does not exceed 2000 ppm except in some from the Ivigtut area (Fig. 6 g), in which F correlates negatively with Mg# and reaches up to 12,000 ppm in the most fractionated, commonly trachytic, samples. Two trends can be observed in Fig. 6 g: the first one is rather steep and comprises F-rich dykes from the Ivigtut area whereas the other Gardar dykes describe a much flatter trend with maximum F contents of about 2000 ppm. The two trends are comparable to those recognised in rocks from recent subduction zones such as the Andes (e.g. Morgan et al., 1998; Halter et al., 2004), but not in Aleutian rocks (Coats, 1953; Coats et al., 1959; Drewes et al., 1961; Nye & Turner, 1990).

The dykes in the Gardar Province do not only vary regionally, but also differ regarding their temporal appearance/age. The BD_0 dykes and the OGDC display large similarities in terms of their evolved composition. In contrast, the YGDC are more primitive which is evidenced by their higher Mg# and higher contents of compatible elements (Cr, Ni; Fig. 7 a). Incompatible elements like Rb, Ba, Zr, F and the alkalis describe negative correlations with Mg# and are more abundant in the OGDC (Fig. 7 b, c). The fact that the magmas which formed the older dykes are more highly fractionated than the younger ones is in accordance with results by Upton et al. (1985). Upton & Thomas (1980) found that the F content in the chilled margin of

the OGDC is higher than in the YGDC, in agreement with results from this study. Whole-rock analyses of basaltic OGDC rocks mostly have a F content > 2000 ppm whereas F in the basaltic YGDC commonly does not exceed 950 ppm (Fig. 7 d).

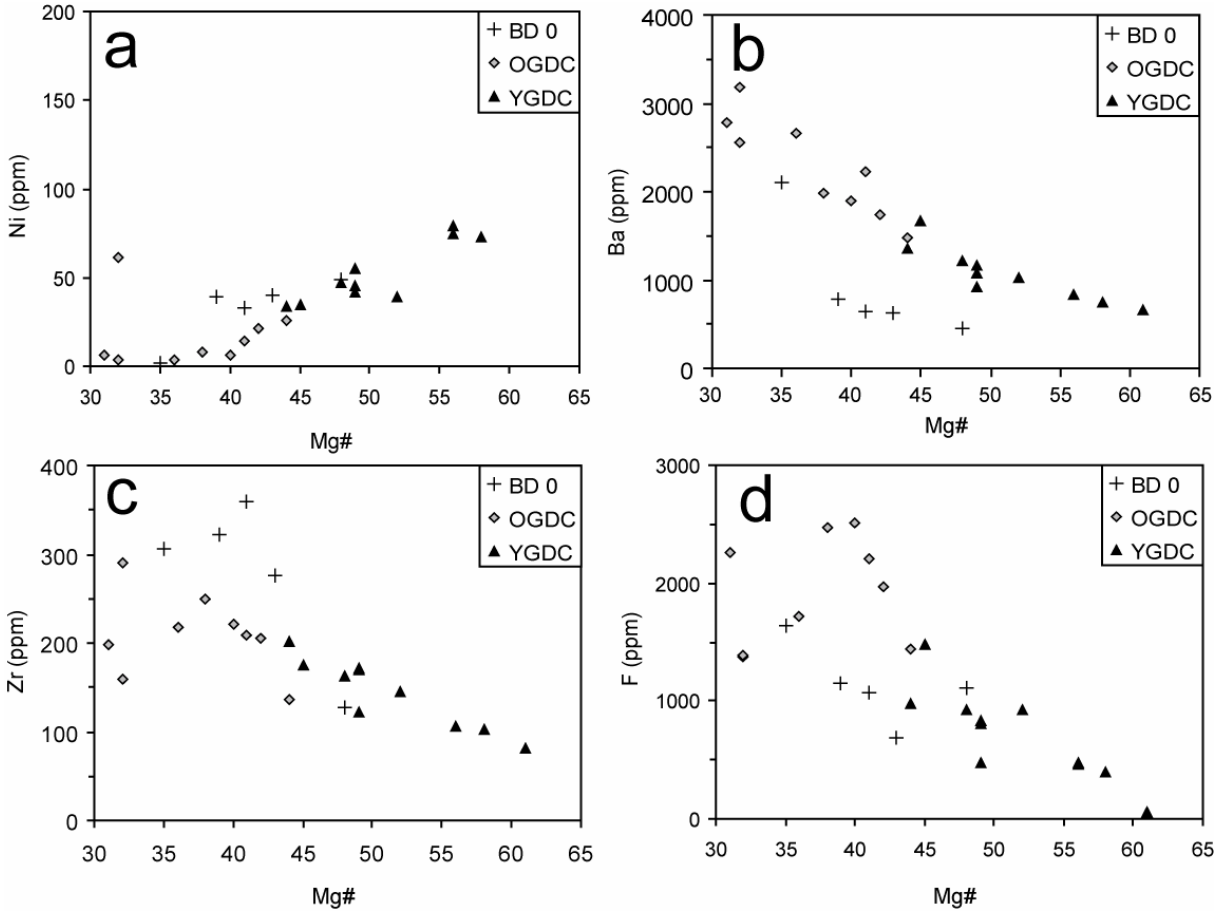

Figure 7 Chronological differences for Gardar dykes with Mg# = Mg/(Mg+Fe^{2+}) as fractionation index [BD 0 = Brown Dykes, 1.28 Ga; OGDC = Older Giant Dyke Complex, 1.18 Ga; YGDC = Younger Giant Dyke Complex, 1.16 Ga; Upton et al., 2003].

Pyrohydrolysis – Ion chromatography analyses

Sixteen representative samples were chosen for halogen determination (F, Cl and Br) using pyrohydrolysis extraction and ion chromatographic quantification (PHIC). In general, the fluorine contents range from 700 to 3900 ppm (Table 3) and chlorine contents vary from < 100 to 1200 ppm. Bromine contents are generally very low (< 2.1 ppm) and were only detectable by PHIC analysis (not by XRF). In order to compare the dykes with Gardar intrusions and fluid inclusion data, we also analysed mineral separates and whole rocks from the Ilímaussaq and Ivigtut intrusions. The whole rock halogen values for the Ilímaussaq rocks largely correspond to the analyses made by Bailey et al. (2001) and range from 1400 to 14000 ppm F, < 200 to > 25000 ppm Cl and from < 0.7 to 53 ppm Br (Table 3). Amphibole mineral separates from the kakortokites contain 5000 to 8000 ppm fluorine whereas the Cl content is

below 100 ppm. Br was not detected. One eudialyte sample contains 1450 ppm F, 13000 Cl and < 0.5 ppm Br. Granite whole rocks from Ivigtut have a high F content between 5000 and 16000 ppm whereas Cl is below 153 ppm. Br is below 0.7 ppm. The Cl/Br ratios are generally very high reaching up to 26000 in the eudialyte. The Cl/F (weight) ratios are generally low and range from <<0.1 to 0.5. Only the eudialyte and the naujaite whole rock (due to the presence of sodalite) reach Cl/F values of 10.

Table 3 Pyrohydrolysis-Ion-Chromatographic halogen results of samples analysed in this study. Cl/Br and Cl/F are weight ratios. n.d. = not detected: minimum values of Cl/Br ratios for these samples based on Cl content detected by ion-chromatography. Mineral samples from Ilímaussaq: ILM101: Eudialyte; all other samples amphiboles.

Dyke Samples	F (ppm)	Cl (ppm)	Br (ppm)	Cl/Br	Cl/F
40455	1180.8	109.5	n.d.	> 500	0.093
40583	734.3	75.9	< 0.7	> 700	0.103
85981	2655.9	1197.0	0.8	1596	0.451
101250	1979.2	231.8	< 0.7	> 500	0.117
101269	981.0	172.0	n.d.	> 1500	0.175
101318	1512.0	847.0	1.6	542	0.560
101337	691.6	147.7	< 0.7	571	0.213
101432	2136.4	1068.5	n.d.	> 6000	0.500
101438	1037.1	83.1	< 0.7	>300	0.080
GD02	1537.4	662.4	2.1	316	0.431
GD13	3535.9	143.1	n.d.	> 500	0.040
GD24	2704.1	1551.7	2.0	770	0.574
GD28	2353.9	176.5	1.2	150	0.075
GD31-A	2818.5	1057.6	0.7	1574	0.375
GD7	3928.3	158.5	n.d.	> 500	0.040
JS89	2353.0	1203.4	1.1	1136	0.511
Ilímaussaq	whole rocks				
1857-Augitsyenite	1397.0	392.0	< 0.7	891	0.281
1370-Naujaite	2399.6	25729.9	53.2	484	10.722
XL61-Kakortokite	7532.8	166.9	1.4	118	0.022
XL59-Kakortokite	14204.7	1225.9	1.8	677	0.086
Ilímaussaq	minerals				
ILM101-Eudialyte	1448.9	13156.1	< 0.7	> 25000	9.080
KK-0-2-S-Am	8705.3	36.6	n.d.	> 100	0.004
KK-8-2-S-Am	6331.9	39.2	n.d.	> 101	0.006
12-2-S-Am	6789.0	32.4	n.d.	> 102	0.005
KK-16-2-S-Am	8123.3	96.1	n.d.	> 103	0.012
KP3-Am	4983.8	42.8	n.d.	> 104	0.009
KP5-Am	5079.4	41.9	n.d.	> 105	0.008
Ivigtut	whole rocks				
1453-B	16440.4	38.2	< 0.7	> 100	0.002
1454	6886.9	152.6	< 0.7	313	0.022
1465	5216.9	123.7	< 0.7	> 300	0.024

Discussion

Evidence for fractional crystallisation

The dykes of the Gardar Province have been investigated by many authors in the past (e.g. Berthelsen & Henriksen, 1975; Upton & Emeleus, 1987; Pearce & Leng, 1996; Goodenough et al., 2002; Halama et al., 2007). Generally, all Gardar dykes describe clear fractionation trends, i.e. incompatible trace elements correlate negatively with Mg# whereas compatible elements commonly decrease with decreasing Mg#.

The positive correlation between Fe_2O_3-Mg#, TiO_2-Mg# (Fig. 6 a, b) and V-Mg# (not shown) indicates fractionation of Fe-Ti-oxides. CaO/Al_2O_3 decreases with decreasing Mg# which suggests fractionation of clinopyroxene (Fig. 6 c). However, this trend is not clearly defined within one single dyke region, but is evident for all Gardar dykes. The same holds true for the Sc-Mg# diagram (not shown). Mattsson & Oskarsson (2005) proposed Sc/Y against Mg# as another test for clinopyroxene fractionation. For the Gardar dykes, Sc/Y correlates positively with Mg# which further suggests a certain amount of clinopyroxene fractionation.

Fractionation of olivine is highly likely for Gardar dykes, because Ni correlates positively with Mg# (Fig. 6 d). A similar trend can be followed for Cr, Fe, Co and Zn vs. Mg# (Fig. 6 a, e). However, the dykes in the vicinity of Ilímaussaq-Narsaq-Motzfeldt describe a different trend for those elements which will be scrutinised in more detail below.

The Gardar dykes generally have a low P_2O_5 content which commonly does not exceed 2 wt%. However, due to their high abundance of volatiles (especially F), apatite saturation may have actually been attained (Watson, 1980). This is evidenced by the perfect correlation of F with P_2O_5 for the dykes in the Tugtutôq-Isortoq-Nunarssuit-Narsasuaq region (Fig. 9 b) which describes a normal fractionation trend. In contrast, more evolved dykes in the Ivigtut area are up to three times more F-enriched at the same P_2O_5 content than primitive ones. Therefore, the extraordinarily high F content in the Ivigtut area may not be explained by apatite fractionation. Possibly, apatite saturation was not achieved in these dykes (Watson, 1980) and therefore, fluorine became progressively enriched in more fractionated dykes.

The negative Eu-anomaly in chondrite-normalised (McDonough & Sun, 1995) REE patterns (Tab. 1) can be attributed to early-magmatic plagioclase fractionation as evidenced by the large occurrence of anorthosites underlying the Gardar Province (Blaxland & Upton, 1978; Upton, 1996; Halama et al., 2002; Schönenberger et al., 2008).

Late-stage enrichment of Ni, Cr, Fe, Zn, Co

The transition metals Ni, Cr, Fe, Zn and Co are positively correlated with Mg# for most Gardar dykes implying normal fractionation trends. However, all dykes in the region Narsaq-Ilímaussaq-Motzfeldt describe a concave trend with a minimum at Mg# values of ~30 (Fig. 6 a, d, e). This trend is most obvious for Ni, Cr and Zn and appears to be independent of the Mg#, because the same trends can be seen if plotted against MgO or SiO_2.

No mineral phase was observed in thin section which could account for the enrichment of these transition metals. It is doubtful that the metals were incorporated into sulphides, because they only show a weak (if any) correlation with sulphur. Spinels also appear to have played a minor role, because there are no strong correlations among the elements of the different (Fe-Al-Zn-Mn-) spinel group members. Only total Fe_2O_3 displays a positive trend with TiO_2 for all Gardar dykes suggesting that ulvøspinel may have fractionated.

Cr/Ni is positively correlated with Mg# even though the dykes in the Ilímaussaq-Narsaq-Motzfeldt area are restricted to lower Cr/Ni ratios and lower Mg# (Fig. 8 a). The overall positive correlation indicates that the Cr/Ni ratio is dependent on fractionation processes (Martin et al., 2005). In Fig. 8 b, the Gardar dyke compositions fall near, but largely above, a mixing line between a slab melt and a mantle peridotite (Drummond et al., 1996; Tsuchiya et al., 2005). A simple mixing process would result in a Ni decrease in the modified mantle (Tsuchiya et al., 2005), i.e. the dykes should lie below the mixing line. The higher Ni contents relative to Cr could result from interaction of a slab-derived adakitic melt with mantle peridotite. According to Kelemen (1995), this interaction would cause an increase in Ni content of the melt due to the dissolution of olivine and the formation of orthopyroxene (which incorporates less Ni relative to olivine). However, dissolution of olivine would not only increase the Mg/Fe ratio, but also the absolute MgO concentration which is both not observed for the dykes in the Ilímaussaq-Narsaq-Motzfeldt area. Hence, the interaction of an adakitic melt with the overlying mantle wedge cannot fully explain the high Ni contents at low Mg#.

The extraordinary trend of the transition metals may be attributed to changes in oxygen fugacity. Morse et al. (1991) showed that the fractionation of Ni in olivine depends on the oxygen fugacity. At low oxygen fugacities near the wüstite-magnetite buffer, about half of the total Ni content in the magma may be present as Ni^0. This part would be retained in the melt and not incorporated into olivine, but later fractionating minerals. Accordingly, Cr was most likely not incorporated into liquidus phases at such low oxygen fugacities and high temperatures (Shearer & Papike, 2005). Marks & Markl (2001) constrained very reduced

formation conditions (FMQ -4) for the augite syenite in the 1.16 Ga old (Krumrei et al., 2006) Ilímaussaq intrusion. The dykes from the Ilímaussaq area under discussion pre-date the Ilímaussaq complex. It is not unreasonable to assume that the dyke magma which preceded the Ilímaussaq one was also rather reduced. This is in accordance with results from Upton & Thomas (1980) who derived reducing conditions (FMQ down to -5) for the YGDC magma. On the other hand, Upton et al. (2006) assumed rather high oxygen fugacities for mela-aillikites from the Tugtutoq-Nugarmiut region (NW of Narsaq). Therefore, even if it is very likely that the oxygen fugacity played a major role for this peculiar trend, it is not possible to definitely constrain its underlying causes with the methods used.

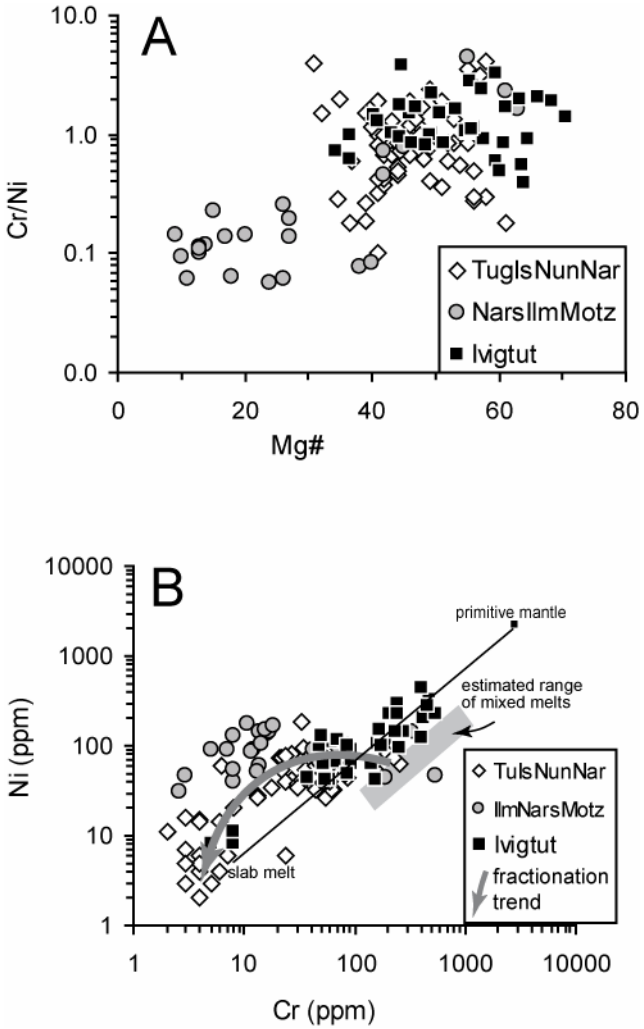

Figure 8 a-b. Peculiar trends for transition metals in the Ilímaussaq-Narsaq-Motzfeldt area. a) The dykes in this region are restricted to lower Cr/Ni ratios and Mg# compared to the rest. According to Martin et al. (2005), the overall positive correlation can be attributed to fractionation processes. b) Most dykes lie above the potential mixing line of the primitive mantle with a slab melt.

Crustal contamination

The lack of a positive Pb-anomaly in primitive mantle-normalised trace element patterns (Fig. 5) may suggest no or an insignificant upper crustal contamination and indicates negligible late-stage alteration (Le Roex et al., 2001). Assimilation of lower crustal rocks also seems to be insignificant for most of the Gardar dykes, because there is no obvious positive correlation

between Zr – Zr/Nb, K/Nb – Zr/Nb or K/Nb – SiO_2 (not shown). Zr/Nb ratios for the majority of dykes vary from 2 to 7. However, the dykes in the region of Isortoq and Nunarssuit (± Tugtutôq and Ivigtut) seem to be partly contaminated by lower crustal rocks, because their Zr/Nb ratio ranges from 10 to 29 consistent with Zr/Nb ratios of the continental crust (Taylor & McLennan, 1985). This is also in accordance with results from Halama et al. (2004) who showed that the Isortoq dykes assimilated up to 10% lower crustal Archaean gneisses. Thus, crustal contamination cannot be entirely ruled out as was also shown by Taylor & Upton (1993). The Pb isotopes they analysed in the Gardar complexes Kûngnât and Tugtutôq showed that the more evolved rocks have lower μ_1 resulting from increasing crustal control in the course of fractional crystallisation (Taylor & Upton, 1993).

Constraints on mantle source

Several studies dealt with the potential magma source of the Gardar melts. There is general consensus that the majority of melts was derived from a lithospheric mantle and that the melts were only little (if at all) affected by crustal contamination (Goodenough, 1997; Goodenough et al., 2002; Upton et al., 2003; Halama et al., 2004). This is evidenced by low $^{86}Sr/^{87}Sr$ ratios of 0.703 and initial ε_{Nd} values of +2 to +6 (Pearce & Leng, 1996; Andersen, 1997; Goodenough et al., 2002). However, temporal differences, i.e. differences in the course of the Gardar cycles, can be seen.

Although an OIB-source mantle was proposed by Halama et al. (2003), the Gardar basalts show trace element patterns which differ from OIB patterns and preclude an asthenospheric derivation (this study; Upton & Emeleus, 1987). An asthenospheric origin also appears improbable, because Older and Younger Gardar magmatism have geochemical and petrological affinities, despite being separated by 100 Ma or more when plate tectonics were active. Accordingly, these factors suggest that the sub-continental lithospheric mantle had a strong control on the magma compositions.

Hence, it can be assumed that the magmas formed by partial melting of sub-continental mantle lithosphere which had been metasomatised by subduction-related fluids rich in LILE and incompatible elements like K, Ba, P and LREE (Upton & Emeleus, 1987; Upton et al., 2003; Goodenough, 1997).

The decrease in Zr/Nb ratios in the interval between extrusion of the Eriksfjord Formation basalts and the emplacement of the OGDC, YGDC and subsequent smaller mafic dykes suggested that a metasomatic modification – involving an increase in Nb – affected the source mantle at some time in the Gardar before ~ 1180 Ma. Early- and mid-Gardar basalts and

hawaiites *and* those of Nunarssuit-Isortoq show strong Zr-Nb correlation with an average Zr/Nb ratio of about 18, whereas those of the Ilímaussaq-Narsaq-Motzfeldt area dykes are distinctly richer in Nb with Zr/Nb ratios generally between 2 and 7.

According to Upton & Emeleus (1987), the pronounced geochemical difference between the basaltic-hawaiitic magmas of the late Gardar dyke-swarm in the western part and those produced at other times and places in the Gardar Province may denote that the source rocks beneath this lineament had been affected by a metasomatic event by which the source rocks were differentially enriched in some incompatible elements, particularly K, Ba, P and LREE.

The enrichment of LREE over HREE may also reflect a mantle source which was metasomatised by subduction processes (e.g. Upton & Emeleus, 1987; see below). This is not only evidenced by the LREE enrichment in the dykes, but also in the Gardar intrusions and in the Ketilidian basement itself, i.e. the Julianehåb batholith (Garde et al., 2002).

To account for the ubiquitous high Al_2O_3/CaO contents of the Gardar mafic magmas (and the resultant cpx-poor, troctolitic products) Upton & Emeleus (1987) proposed that extensive melt extraction during the Ketilidian orogeny left a depleted, harzburgitic lithospheric mantle that was subsequently restored to fertility by metasomatism. If, as suggested, this was a garnet-bearing harzburgite, melt extraction would have been at depths >60 km.

Halogens in the Gardar Province

The general abundance of fluorite throughout the Province has been noted by Upton and Emeleus (1987). Fluorite is commonly associated with calcite and crystallised along joint and fault surfaces. It is a modal component in several of the syenite complexes, and it occurs as amygdale infillings and as a component of the cement in tuffs and diatreme breccias. Fluorite is also abundantly present in some of the carbonatites. Apatites, amphiboles and biotites in the Province are typically fluorine-rich varieties (e.g. Finch et al., 1995). Peralkaline granite sheets in the Kungnat Complex gave rise to fluorite-rich metasomatism in gabbroic wall-rocks (Macdonald et al., 1973) and high fluoride contents were inferred for ultramafic aillikite magmas in which cuspidine ($Ca_4Si_2O_7F_2$) crystallised (Upton et al., 2006). In the Ilímaussaq Complex, F-contents in the agpaitic magmas were high enough for fluorite to crystallise as a cumulus mineral in the layered kakortokites which are interpreted to be floor cumulates (e.g. Sørensen, 2001) and for villaumite (NaF) to form in the late-stage lujavrite magmas (Bondam and Ferguson, 1962). Chlorine was also important as evidenced by the occurrence of sodalite within the Older Giant Dyke Complex and the nepheline syenites of the plutons. There is also the spectacular and unique sodalite (var. hackmanite) flotation cumulate close to the roof of

the agpaitic intrusion at Ilímaussaq (Sørensen et al., 2006). This cumulate (naujaite), is ~ 500 m thick and is inferred to have extended across the entire intrusion with a total volume of ~ 60 km^3. Chlorine contents in the naujaite are in the range 2-3.5 wt% rising to an extreme of 4.6 wt% (Bailey et al., 2001). Bailey et al. (2001) and Krumrei et al. (2007) noted the presence of cryptic variation in the naujaite with the content of Br, I and B in the sodalites generally decreasing downwards.

The halogen contents of the dyke rocks can be used to obtain insight into the source of the abundant halogens (in particular F) of the Gardar Province and shed light on possible enrichment and/or depletion processes:

Potential source of fluorine

Smith et al. (1981) and Edgar et al. (1996) considered the various minerals in the upper mantle that could store volatiles (in particular F and Cl) in their crystal structure. They ruled out dry silicates like olivine, garnet or pyroxene and considered the 'hydrated' minerals like amphibole, phlogopite or apatite in which F substitutes for OH^-. However, recent experiments have shown that even nominally F-free minerals like olivine can incorporate remarkable amounts of F up to 0.45 wt% (Bromiley & Kohn, 2007), but it was not possible to quantify the amount of fluorine within such minerals with the methods applied. Furthermore, the good correlation of certain elements with fluorine suggests that this mechanism is only of subordinate importance in the investigated rocks.

Phlogopite

According to Smith et al. (1981), phlogopite occurs in all rock types of the upper mantle and is the main carrier of H_2O and alkalis. Kushiro et al. (1967) pointed out that F-phlogopite is more stable at higher temperatures than OH-phlogopite. Edgar & Arima (1985) concluded from experiments that F is rather partitioned into phlogopite than apatite making phlogopite a more likely source of F in the mantle. They further showed that the F-content in phlogopite is independent of pressure, but increases with decreasing temperature.

The analysed Gardar dykes only show a weak positive correlation between K_2O and F (Fig. 9 a). If the dykes were derived as partial melts from a phlogopite-bearing mantle source and if all F was stored in mica, the correlation should be more pronounced (Edgar et al., 1996).

Amphibole

The only amphibole species stable under mantle pressure and temperature conditions is K-richterite (ideally $K[NaCa]Mg_5Si_8O_{22}[OH,F]_2$) in which K substitutes for Na at high pressures (Harlow & Davies, 2004). K-amphiboles may be an important source for alkalis, water and/or trace elements in the mantle (Konzett et al., 1997). Harlow & Davies (2004) found a positive correlation between K and pressure which is in agreement with Konzett et al. (1997) who observed an increase in K/(K+Na) with increasing pressure. In contrast, F is negatively correlated with pressure, but positively with temperature. From the K-F relationship of the studied samples (Fig. 9 c), it is evident that not only primitive dykes with a lower K- and F-content, but also more evolved ones lie outside the richterite field (Deer et al., 1997 and references therein). Thus it can be assumed that K-richterite was an insignificant source of F in the Gardar mantle.

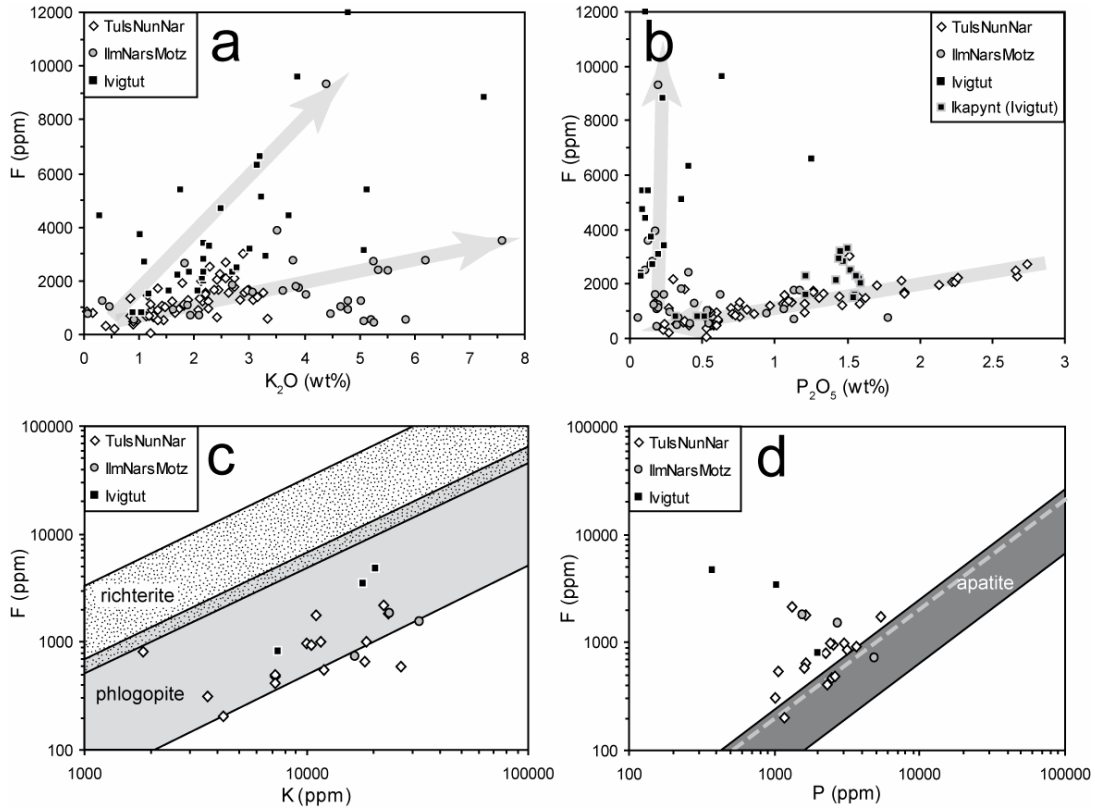

Figure 9 a-d. Diagrams constraining potential mineral reservoirs for F in mantle source. The good correlations between K_2O-F and P_2O_5-F (a, b) suggest F being derived from F-phlogopite and F-apatite, respectively. This is further evidenced by Figs. 9 c and d that show the typical F-K and F-P range for richterite, phlogopite and apatite, respectively (Hogarth, 1988; Boudreau et al., 1993; Campbell & Henderson, 1997; Deer et al., 1997 and references therein; O'Reilly & Griffin, 2000; Bühn et al., 2001; Chakhmouradian et al., 2002; Fleet, 2003 and references therein). Dashed line in d) refers to hypothetical fluorapatite with a P/F ratio of 4.89 (Smith et al., 1981; Sigvaldason & Óskarsson, 1986) [TulsNunNar = Tugtutôq-Isortoq-Nunarssuit-Narsarsuaq; IlmNarsMotz = Ilímaussaq-Narsaq-Motzfeldt].

Apatite

Smith et al. (1981) pointed out that Cl-bearing, F-rich apatite may be present in the source region of carbonatites derived from the upper mantle. It may thus play an important role in the Gardar Province since there are carbonatitic dykes/complexes (Upton et al., 2003). Some of the Gardar carbonatites (Qagssiasuk) are very apatite-rich (Stewart, 1970; Anderson 1997) and are associated with fluorite. Gardar carbonatite dykes described by Pearce et al. (1996) typically contain 1-2 vol% fluorite, in rare cases even nearly 50 vol%.

According to experiments by Watson (1980), the occurrence of residual apatite in magma source regions is generally precluded since as much as 3-4 wt% P_2O_5 (at 50 wt% SiO_2) are soluble in basic magmas. Therefore, even at low degrees of partial melting, apatite would not be a residual phase. According to that and taking into account the (relatively) high content of phosphorus in most primitive dykes, it can be assumed that apatite has been in the mantle source. This apatite was most likely removed from the mantle source region.

Brenan (1993) experimentally investigated the composition of apatite at high p and T (10-20 kbar, ~ 1000 °C). He found out that only low concentrations of F and Cl in an acidic (H_2O-HCl or CO_2-H_2O) fluid are required to achieve a high X_{FClAp}/X_{OHAp} in apatite. This ratio also rises with aqueous NaCl in direct proportion of F-concentration. Fluid inclusion studies in various Gardar intrusions have shown that the fluid is generally NaCl-dominated and that CO_2 can be a major component, too (Köhler et al., 2008; Graser et al., in press; Schönenberger & Markl, in press; Konnerup-Madsen et al., 1985; Konnerup-Madsen, 1984). Taken these considerations into account, we suggest that apatite must have been rather enriched in F.

To further constrain which mantle phases may have served as a F-reservoir, the range of K/F ratios in richterite (Deer et al., 1997 and references therein) and phlogopite (Fleet, 2003 and references therein) worldwide were compared to the K/F ratios in the most primitive dykes (Mg# > 50; Fig. 9 c). The large overlap of primitive dykes with the K/F-range of phlogopite is striking. Hence, it can be assumed that phlogopite played a crucial role for F-storage in the mantle and that richterite can be neglected. Fig. 9 c also illustrates that only few dykes fall off the phlogopite range suggesting an additional F-rich phase.

This may have been apatite, because some of those primitive dykes which fall off the phlogopite field do in fact lie within the apatite one (Hogarth, 1988; Boudreau et al., 1993; Campbell & Henderson, 1997; O'Reilly & Griffin, 2000; Bühn et al., 2001; Chakhmouradian et al., 2002; Fig. 9 d). Some primitive dykes from Tugtutôq-Isortoq-Nunarssuit-Narsarsuaq

actually coincide with the line defined by a hypothetical fluorapatite with a P/F ratio of 4.89 (Smith et al., 1981; Sigvaldason & Óskarsson, 1986).

Halogen ratios – evidence of fluid separation/evolution?

For the discussion of the halogen ratios, only those samples analysed with pyrohydrolysis-IC combination were taken into account. For these, all halogens (F, Cl and Br) were analysed in one run in order to assure internal consistency.

In the analysed dyke rocks, a high fluorine content is commonly linked to low chlorine and very low bromine contents. Accordingly, the Cl/Br ratio of the dyke rocks is usually > 300 and ranges from approx. 300 to > 1500. The Cl/Br ratio does not vary for different dyke generations and no correlation between the halogens and any other element (major or trace) can be observed.

In this context it is interesting to compare the data from the dykes with other halogen data available for Gardar magmatic rocks, mineral separates and fluid inclusions. In general, the Cl/Br ratios of the analysed whole rocks and mineral separates are comparable to the rather high values of the dykes (Tab. 2 and Krumrei et al., 2007; Bailey et al., 2001, 2006; Bailey, 2006). Ilímaussaq rocks have values > 200 reaching up to 1000 (Tab. 2 and Bailey et al., 2001, 2006). Krumrei et al. (2007) analysed the halogen contents of sodalite from the roof cumulates of the Ilímaussaq intrusion (naujaite) and obtained Cl/Br (weight) ratios from 500 to 1500. A late-stage eudialyte from the floor cumulates (kakortokites) has a Cl/Br ratio of > 25000 (Tab. 3). Granitic rocks from the Ivigtut intrusion also have Cl/Br ratios > 300.

However, the high Cl/Br ratios of minerals/rocks are in complete contrast to the constantly low Cl/Br ratios of fluid inclusions from different Gardar intrusions. Recent results of fluid inclusion studies from the Ilímaussaq, Motzfeldt and Ivigtut complexes (Graser et al., in press; Schönenberger & Markl, in press and Köhler et al., 2008) showed that the fluids are dominated by Na and Cl and commonly have a Cl/Br ratio of 100 (±30; by weight) which is much lower than the ratios of the corresponding whole rocks. These differences also apply if the analytical uncertainties are taken into account as the absolute content of bromine in the whole rock samples is extremely low (Tab. 2, < 2 ppm) compared to a rather high Cl content. The high whole rock Cl/Br (weight) ratios (mostly > 500) do not seem to be related to the halogen composition of known reservoirs (e.g. Burgess et al., 2002): Cl/Br in chondrite material (C1 chondrite) is believed to be similar to the primitive mantle with Cl/Br weight ratios of ~ 230 (Dreibus et al., 1979) while crustal and MORB ratios are 273 and 400, respectively (Newsom, 1995; Jambon et al., 1995).

Therefore, the most likely process to account for the highly differing ratios of the fluids and rocks is degassing or fluid unmixing as supported by (experimental) work of Bureau et al. (2000) and Bureau & Métrich (2003). They found that Br is preferentially partitioned into the fluid compared to the melt. A similar behaviour was also shown for fluid-halite partitioning (Foustoukos & Seyfried, 2007) where the low salinity fluid contained larger amounts of Br than halite. Following this argumentation, it may be assumed that the dyke rocks exsolved a fluid during their crystallisation which was subsequently lost (degassed). This fluid became enriched in Br relative to the melt yielding the observed high Cl/Br ratios in the residual magmas/rocks. The fluid inclusion Cl/Br data mentioned above are in agreement with such an interpretation. The whole system before degassing would accordingly have had a Cl/Br ratio between 100 and 500 in accordance with the known reservoir compositions named above.

Interestingly, Bureau & Métrich (2003) suggested that the high Cl/Br (weight) ratios of MORB of ~ 400 (Jambon et al., 1995) is related to the fact that these rocks were more strongly affected by degassing than the primitive mantle (Cl/Br 230; Dreibus et al., 1979). They also propose degassing for melt inclusions from Mount Vesuvius (Marianelli et al., 1999) which led to high Cl/Br ratios >> 300.

Further evidence for fluid unmixing/degassing processes may be obtained from the Cl/F ratios: The Cl/F (weight) ratios of the dykes roughly define two groups: One group has Cl/F ratios which scatter around 0.5 whereas the second group has values near or below 0.1 (partially < 0.05). As for the Cl/Br ratios, no correlation between regional occurrence, chemical composition or evolutionary stage of the dykes (e.g. Mg#) can be made.

However, comparison of dyke data with whole rocks, mineral separates and fluid inclusions from the Ilímaussaq and Ivigtut intrusions (Tab. 2 and Bailey et al., 2001; Graser et al., in press; Köhler et al., 2008) provides again further insights into associated processes. The fluid inclusions of the Ilímaussaq and Ivigtut complexes are dominated by Cl, hence the Cl/F ratios of the fluids are usually >> 10 (Graser et al., in press; Köhler et al., 2008). In contrast to these high fluid Cl/F ratios, the analysed whole rocks from the Ilímaussaq and Ivigtut intrusions have low ratios < 1 (Table 3). These contrasting datasets can be explained by the findings by Villemant & Boudon (1999) who assumed that F is not affected by magmatic degassing and the Cl/F ratio can accordingly serve as “degassing index”. A high Cl/F ratio in rocks would therefore represent a low degree of degassing and a low Cl/F ratio would represent a high degree of degassing. Accordingly, fluorine has a strong affinity for the melt and it is more compatible than Cl (and Br) (Villemant & Boudon, 1999). As a consequence, Cl (and Br) preferentially partitions into the fluid compared to F. This would explain the high Cl/F ratios

in the fluid even in intrusions which are generally characterised by extremely high F contents (e.g. the Ivigtut intrusion; Pauly & Bailey, 1999; Köhler et al., 2008).
The generally low Cl/F ratios of the whole rocks point to the fact that a fluid or volatile-rich melt with high Cl (and Br) content separated before the final crystallisation of the rocks. Accordingly, early-formed rocks which did not exsolve large amounts of a fluid phase would have rather high Cl/F ratios as possibly seen in the early Ilímaussaq augite syenite (Cl/F 0.3, e.g. Sørensen et al., 2006). This hypothesis may be transferred to the results from the dyke rocks. Low Cl/F ratios (< 0.1) would point to a fluid exsolution whereas higher values of ca. 0.5 may suggest that only small amounts of fluid were separated.

In summary, both the Cl/Br and Cl/F ratios lead to similar conclusions: The exsolution (loss) of a fluid phase from a magma leads to high Cl/Br and low Cl/F ratios in the remaining melt (rock). On the other hand, the exsolved fluid retains rather low Cl/Br and high Cl/F ratios. This can be easily explained by the decreasing affinity of the halogens to the melt in the order Br < Cl < F and a relative enrichment of the halogens in the fluid in the order Br > Cl > F. Hence, the halogen ratios from fluids, minerals and whole rocks can provide valuable information on the separation and evolution of a fluid phase associated with the former melt.

Mantle metasomatism

The largest part of the Gardar Province is situated within the 1855-1795 Ma old Ketilidian orogen (Fig. 1). This post-collisional belt is the result of the convergence between the Archaean craton and an oceanic plate subducting northward (Chadwick & Garde, 1996).
It is believed that subduction-related processes during the Ketilidian orogeny led to metasomatism of the mantle beneath Gardar resulting in an enrichment of LILE, LREE and other incompatible elements (Upton & Emeleus, 1987; Goodenough, 1997; Goodenough et al., 2002; Upton et al., 2003). The relation of Gardar magmas to subduction processes and the Ketilidian orogeny is also evidenced by Nd-model ages which basically range from 1850-1720 Ma (Schönenberger & Markl, in press; Marks et al., 2004; Goodenough et al., 2002) and largely correspond to the age of the Ketilidian orogen.
Generally, fluid influx can modify the mantle wedge during subduction processes (McCulloch & Gamble, 1991; Arculus, 1994) to produce a hybridised mantle from which calcalkaline rocks form (Green & Ringwood, 1972; Nicholls & Ringwood, 1973). McCulloch & Gamble (1991) and Kessler et al. (2005) demonstrated that HFSE and HREE largely remain immobile during slab-fluxing processes. In contrast, LILE (Rb, Cs, Ba, Sr, U, Pb) and LREE become

enriched due to their rock-melt incompatibility and high mobility (Tatsumi et al., 1986; Tatsumi & Nakamura, 1986).

Two potential processes can lead to mantle metasomatism: a) metasomatism through fluids expelled from the subducting slab or b) metasomatism by felsic-siliceous, slab-derived melts (e.g. Arculus, 1994; Yogodzinski et al., 1994). Both mechanisms are closely related and can hardly be distinguished. However, Wyllie (1984), Peacock (1990) and Peacock et al. (1994) showed that slab melting is restricted to a) young, hot subducting slab, b) slow subduction into a warm mantle wedge and/or c) highly oblique convergence. Moreover, slab melts which are in equilibrium with an eclogitic (grt + cpx) residue typically have La/Nb and Ba/Nb ratios of 7 and 186, respectively (Prouteau et al., 2001).

A special process in subduction zones was described by Klemme (2004). He observed fluoride-glass blebs in lherzolitic xenoliths and inferred fluoride-silicate unmixing in the upper mantle. This unmixing also implies element fractionation where the silicate melt becomes enriched in HREE, HFSE, Ti and Cs. In contrast, the fluoride melt preferably retains LREE, Sr and Ba thus exhibiting subduction-related trace element characteristics. Hence, if unequivocal petrographic evidence lacks, it will be impossible to distinguish if the signature was inherited from slab melts/fluids or if it reflects an unmixed fluoride melt fraction.

Little is known about subduction processes beneath the Gardar Province. Garde et al. (2002) noted lacking evidence of a continent-continent collision and Chadwick & Garde (1996) described the oblique convergence between the Archaean craton and an oceanic plate suggesting that slab melting may have occurred during the Ketilidian orogeny. In contrast, Rollinson & Tarney (2005) proposed that a magma source with near-constant K/Rb ratios must have been enriched by a fluid rather than melt. The great majority of Gardar dykes has almost constant K/Rb ratios between 350 and 450 suggesting that the mantle wedge was metasomatised by slab fluid-related processes which is also strengthened by both the very low La/Nb (< 1-3) and Ba/Nb (mean at 39) ratios. Former subduction processes are also supported by characteristic K/Ba and Ba/La ratios (Nelson, 1992).

Samples of this study do not show any evidence for a mantle fluoride-silicate melt immiscibility in the sense of Klemme (2004). The studied thin sections neither comprise any fluoride glass blebs along grain boundaries nor any melt pockets. However, if discussing such immiscibility, the Ivigtut cryolite deposit in the NW of the Gardar Province must be mentioned. The deposit hosts the most F-rich magmatic rocks worldwide and actually evolved from fluoride-silicate melt immiscibility (Pauly & Bailey, 1999). This unmixing did not take place in the mantle, but rather at shallow crustal levels and under hydrothermal conditions

(Pauly & Bailey, 1999; Köhler et al., 2008). Furthermore, recalculations assuming 25 ppm F in the primitive mantle (McDonough & Sun, 1994) and the fluorine content of the Ivigtut deposit (Pauly & Bailey, 1999) revealed that only ~ 14 km^3 primitive mantle material would be required to release enough fluorine to form the cryolite deposit at Ivigtut. However, considering the size of the whole Gardar Province (several hundreds of km^2 of outcropping intrusions/dykes), it can be assumed that the total volume of a fluoridic melt in the sense of Klemme (2004) would have been much higher. If such an unmixing process had occurred in the Gardar Province, the silicate melt would have been enriched in HREE and HFSE, but the opposite is the case for the dykes (Fig. 5).

Summary and Conclusions

The XRF analyses of dykes from across the Gardar Province confirmed their moderately to highly evolved nature. Even though they generally display normal fractionation trends, the dykes can be distinguished chronologically and spatially. Older dykes are higher fractionated than younger ones. Trace element distribution shows an enrichment in LILE and LREE while HREE, HFSE, Nb and Ti are depleted. These features together with the high contents of Sr and K_2O suggest subduction-related mantle metasomatism beneath the Gardar Province and reveal the dykes' strong affinity with shoshonites. The dykes show evidence for plagioclase, Fe-Ti oxide and olivine fractionation. In the Ilímaussaq-Narsaq-Motzfeldt area, the dykes describe a peculiar trend where the content of the transition metals Ni, Co, Fe, Zn and Cr suddenly increases at Mg# below 30. This may be attributed to the reduced nature of the magma source in which Ni is present as Ni^{2+} and Ni^0 with the latter being retained in the melt and not incorporated into minerals.

Generally, all dykes are rich in F and comparable to equally high F contents in Andean rocks (Morgan et al., 1989; Halter et al., 2004). Hence, it can be assumed that fluorine enrichment may be typical of subduction-related mantle metasomatism, irrespective if it is an active subduction (Andes) or a post-collisional setting (Gardar). In the Gardar Province, this feature can even be observed in dykes (and other rocks) having intruded the crust ~ 700 Ma after the subduction event. Within the Gardar Province, the dykes in the Ivigtut area have the highest content of F suggesting that the extreme F enrichment at the Ivigtut cryolite deposit was not (only) an effect of hydrothermal metasomatic processes, but can also be attributed to a heterogeneously F-enriched mantle. Within the magma source, F may have largely been incorporated into F-phlogopite and F-apatite. In general, the halogens and especially the

halogen ratios seem to record a degassing process leading to extremely high Cl/Br and low Cl/F ratios in the analysed dyke rocks. This is highly supported by comparing data from whole rocks and mineral separates from the Ivigtut and Ilímaussaq intrusions which also have high Cl/Br (up to 25000) and low Cl/F ratios (<< 1). On the other hand, fluid inclusions yield contrary results of low Cl/Br (ca. 100) and high Cl/F (> 10) in accordance with the degassing theory of Villemant and Boudon (1999). Therefore, the degassing or exsolution of a fluid phase leads to an enrichment of halogens in the fluid in the order: F < Cl < Br which are eventually lost from the rocks.

Acknowledgments

Michael Marks kindly provided dyke samples from the Ilímaussaq-Narsaq area. Heiner Taubald, Gisela Bartholomä and Bernd Steinhilber are thanked for the XRF analyses. Lotte Melchior Larsen from GEUS helped with sample maps and Bjørn Thomassen with GEUS archive material. Gerlind Dreibus gave valuable advice during the set-up of pyrohydrolysis extraction apparatus and Verena Krasz helped with the ion chromatography.. Thomas Wenzel improved an earlier version of the manuscript significantly. His help is greatly acknowledged.

References

Andersen, T., 1997. Age and petrogenesis of the Qassiarsuk carbonatite-alkaline silicate volcanic complex in the Gardar rift, South Greenland. Mineralogical Magazine 61, 499-514.

Arculus, R.J., 1994. Aspects of magma genesis in arcs. Lithos 33, 189-208.

Bailey, J.C., 1977. Fluorine in granitic rocks and melts: a review. Chemical Geology 19, 1-42.

Bailey, J.C., Gwozdz, R., Rose-Hansen, J., Sørensen, H., 2001. Geochemical overview of the Ilímaussaq alkaline complex, South Greenland. In: Sørensen, H. (Ed.), The Ilímaussaq Alkaline Complex, South Greenland, Status of Mineralogical Research with New Results. Geology of Greenland Survey Bulletin 190, 35-54.

Bailey, J.C., Sørensen, H., Andersen, T., Kogarko, L.N., Rose-Hansen, J., 2006. On the origin of microrhythmic layering in arfvedsonite lujavrite from the Ilímaussaq alkaline complex, South Greenland. Lithos 91, 301-318.

Bailey, J.C., 2006. Geochemistry of boron in the Ilímaussaq alkaline complex, South Greenland. Lithos 91, 319-330.

Berthelsen, A., Henriksen, N., 1975. Geological Map of Greenland 1:100,000. Ivigtut 61V.1.Syd. The orogenic and cratogenic geology of a Precambrian shield area. Descriptive text. Grønlands Geologiske Undersøgelse, Copenhagen.

Blaxland, A.B., van Breemen, O., Emeleus, C.H., Anderson, J.G., 1978. Age and origin of the major syenite centres in the Gardar Province of South Greenland: Rb-Sr studies. Geological Society American Bulletin 89, 231-244.

Blaxland, A.B, Upton, B.G.J. 1978. Rare-earth distribution in the Tugtutôq younger giant dyke complex: evidence bearing on alkaline magma genesis in south Greenland. Lithos, 11, 291-299.

Bondam, J., Ferguson, J., 1962. An occurrence of villiaumite in the Ilímaussaq intrusion south Greenland. Meddelelser om Grønland 172.

Bottomley, D.J., Clark, I.D., Battye, N., Kotzer, T., 2005. Geochemical and isotopic evidence for a genetic link between Canadian Shield brines, dolomitization in the Western Canada Sedimentary Basin, and Devonian calcium-chloridic seawater. Canadian Journal of Earth Sciences 42, 2059-2071.

Boudreau, A.E., Love, C., Hoatson, D.M., 1993. Variation in the composition of apatite in the Munni Munni Complex and associated intrusions of the Wet Pilbara Block, Western Australia. Geochimica et Cosmochimica Acta 57, 4467-4477.

Brenan, J.M., 1993. Partitioning of fluorine and chlorine between apatite and aqueous fluids at high pressure and temperature: implications for the F and Cl content of high P-T fluids. Earth and Planetary Science Letters 117, 251-263.

Bromiley, D.V., Kohn, S.C., 2007. Comparisons between fluoride and hydroxide incorporation in nominally anhydrous and fluorine-free mantle minerals. Geochimica et Cosmochimica Acta 71, Goldschmidt Conference Abstracts, A124.

Bureau, H., Métrich, N., 2003. An experimental study of bromine behaviour in water-saturated silicic melts. Geochimica et Cosmochimica Acta 67, 1689-1697.

Bureau, H., Keppler, H., Métrich, N., 2000. Volcanic degassing of bromine and iodine: experimental fluid/melt partitioning data and applications to stratospheric chemistr. Earth and Planetary Science Letters 183, 51-60.

Burgess, R., Layzelle, E., Turner, G., Harris, J.W., 2002. Constraints on the age and halogen composition of mantle fluids in Siberian coated diamonds. Earth and Planetary Science Letters 197, 193-203.

Bühn, B., Wall, F., Le Bas M.J., 2001. Rare-earth element systematics of carbonatitic fluorapatites, and their significance for carbonatite magma evolution. Contributions to Mineralogy and Petrology 141, 572-591.

Campbell, L.S., Henderson, P., 1997. Apatite paragenesis in the Bayan Obo REE-Nb-Fe ore deposit, Inner Mongolia, China. Lithos 42, 89-103.

Candela, P.A., 1986. Toward a thermodynamic model for the halogens in magmatic systems; an application to melt-vapor-apatite equilibria. Chemical Geology 57, 289-301.

Carmichael, I.S.E., Turner, F.J., Verhoogen, J., 1974. Igneous petrology. McGraw-Hill Books Co., New York. 739 p.

Carroll, M.R., Webster, J.D., 1994. Solubilities of sulfur, noble gases, nitrogen, chlorine, and fluorine in magmas. In: Carroll, M.R., Holloway, J.R. (Eds.), Volatiles in Magmas, Reviews in Mineralogy 30, Mineralogical Society of America.

Chadwick, B., Garde, A.A., 1996. Palaeoproterozoic oblique plate convergence in South Greenland: a re-appraisal of the Ketilidian orogen. From: Brewer, T.S., Atkin, B.P. (Eds), Precambrian crustal evolution in the North Atlantic Region. Geological Society of London, Special Publication 112, 179-196.

Chakhmouradian, A.R., Reguir, Ekatarina, Mitchell, R.H., 2002. Strontium-apatite: new occurrences, and the extent of Sr-FOR-Ca Substitution in apatite-group minerals. The Canadian Mineralogist 40, 121-136.

Coats, R.R., 1953. Geology of Buldir Island, Aleutian Islands, Alaska. U.S. Geological Survey Bulletin 989-A, 1-26.

Coats, R.R., Nelson, W.H., Lewis, R.Q., Powers, H.A., 1959. Geological reconnaissance of Kiska Island, Aleutian Islands, Alaska. U.S. Geological Service Bulletin 1028-R, 563-581.

Deer, W.A., Howie, R.A., Zussman, J., 1997. Rock-forming minerals. Volume 2B: Double-chain silicates. The Geological Society, London, 616-634.

Defant, M.J., Drummond, M.S., 1990. Derivation of some modern arc magmas by melting of young subducted lithosphere. Nature 347, 662-665.

Dolejš, D., Baker, R., 2007 a. Liquidus Equilibria in the System K_2O-Na_2O-Al_2O_3-SiO_2-F_2O_{-1}-H_2O to 100 Mpa: I. Silicate-Fluoride Liquid Immiscibility in Anhydrous Systems. Journal of Petrology 48, 785-806.

Dolejš, D., Baker, R., 2007 b. Liquidus Equilibria in the System K_2O-Na_2O-Al_2O_3-SiO_2-F_2O_{-1}-H_2O to 100 Mpa: II. Differentiation Paths of Fluorosilicic Magmas in Hydrous Systems. Journal of Petrology 48, 807-828.

Dreibus, G., Spettel, B., Wanke, H., 1979. Halogens in meteorites and their primordial abundances. In: Ahrens, L.H. (Ed.), Origin and Distribution of the Elements. Wiley, 33-38.

Drewes, H., Fraser, D.G., Snyder, G.L., Barnett, H.F., 1961. Geology of Unalaska Ilsand and adjacent insular shelf, Aleutian Islands, Alaska. U.S. Geological Survey Bulletin 1028-S, 583-676.

Drummond, M.S., Defant, M.J., Kepezhinskas, P.K., 1996. Petrogenesis of slab-derived trondhjemite-tonalite-dacite/adakite magmas. Transactions of the Royal Society of Edinburgh: Earth Sciences 87, 205-215.

Edgar, A.D., Arima, M., 1985. Fluorine and chlorine contents of phlogopite crystallized from ultrapotassic rock compositions in high pressure experiments: Implications for halogen reservoirs in source rocks. American Mineralogist 70, 529-536.

Edgar, A.D., Pizzolato, L.A., Sheen, J., 1996. Fluorine in igneous rocks and minerals with emphasis on ultrapotassic mafic and ultramafic magmas and their mantle source regions. Mineralogical Magazine 60, 243-257.

Escher, A., Watt, W.S., 1976. Geology of Greenland. Geological Survey of Greenland, Copenhagen, 603 p.

Finch, A.A., Parsons, I., Mingard, S.C., 1995. Biotites as Indicators of Fluorine Fugacities in Late-Stage Magmatic Fluids: the Gardar Province of South Greenland. Journal of Petrology 36, 1701-1728.

Fleet, M.E., 2003. Micas. In: Deer, W.A., Howie, R.A., Zussman, J. (Eds). Rock-forming minerals, Volume 2B. The Geological Society, London, 354-369.

Foustoukos D.I. and Seyfried W.E., Jr. (2007) Trace element partitioning between vapor, brine, and halite under extreme supercritical phase separation. Geochimica et Cosmochimica Acta, 71, 2056-2071.

Garde, A.A., Hamilton, M.A., Chadwick, B., Grocott, J., McCaffrey, K.J.W., 2002. The Ketilidian orogen of South Greenland: geochronology, tectonics, magmatism, and fore-arc accretion during Palaeoproterozoic oblique convergence. Canadian Journal of Earth Sciences 39, 765-793.

Govindaraju, K. 1994. Compilation of working values and sample description for 383 geostandards. Geostandards Newsletter 18, 158 p.

Graser, G., Potter, J., Köhler, J., Markl, G., in press. Isotopic, major, minor and trace element geochemistry of late-stage fluids in the peralkaline Ilímaussq intrusion, South Greenland, Lithos.

Green, T.H., Ringwood, A.E., 1972. Crystallization of garnet-bearing rhyodacite under high pressure hydrous conditions. Journal of the Geological Society of Australia 19, 203-212.

Goodenough, K.M., 1997. Geochemistry of Gardar Intrusions in the Ivigtut area, South Greenland. PhD thesis, Edinburgh.

Goodenough, K.M., Upton, B.G.J., Ellam, R.M., 2002. Long-term memory of subduction processes in the lithospheric mantle: evidence from the geochemistry of basic dykes in the Gardar Province of South Greenland. Journal of the Geological Society, London 159, 705-714.

Halama, R., Waight, T., Markl, G., 2002. Geochemical and isotopic zoning patterns of plagioclase megacrysts in gabbroic dykes from the Gardar Province, South Greenland; implications for crystallisation processes in anorthositic magmas. Contributions to Mineralogy and Petrology 144, 109-127.

Halama, R., Wenzel, T., Upton, B.G.J., Siebel, W., Markl, G. 2003. Reconstruction of an OIB signature in crustally contaminated rift-related basalts : a geochemical and Sr-Nd-O isotopic study of the Proterozoic Eriksfjord Basalts, Gardar Province, South Greenland. Mineralogical Magazine, 67, 831-854.

Halama, R., Marks, M., Brügmann, G., Siebel, W., Wenzel, T., Markl, G., 2004. Crustal contamination of mafic magmas; evidence from a petrological and Sr-Nd-Os-O isotopic study of the Proterozoic Isortoq dike swarm, South Greenland. Lithos 74, 3-4, 199-232.

Halama, R., Joron, J.-L., Villemant, B., Markl, G., Treuil, M., 2007. Trace element constraints on mantle sources during mid-Proterozoic magmatism: evidence for a link between the Gardar (South Greenland) and Abitibi (Canadian Shield) mafic rocks. Canadian Journal of Earth Sciences 44, 459-478.

Halter, W.E., Bain, N., Becker, K., Heinrich, C.A., Landtwing, M., VonQuadt, A., Clark, A.H., Sasso, A.M., Bissig, T., Tosdal, R. M., 2004. From andesitic volcansim to the formation of a porphyry Cu-Au mineralizing magma chamber : the Farallón Negro Volcanic Complex, northwestern Argentina. Journal of Volcanology and Geothermal Research 136, 1-30.

Harlow, G.E., Davies, R., 2004. Status report on stability of K-rich phases at mantle conditions. Lithos 77, 647-653.

Hogarth, D.D., 1988. Chemical composition of fluorapatite and associated minerals from skarn near Gatineau, Quebec. Mineralogical Magazine 52, 347-358.

Jambon, A., Déruelle, B., Dreibus, G., Pineau, F. 1995. Chlorine and bromine abundance in MORB: the contrasting behaviour of the Mid-Atlantic Ridge and East Pacific Rise and implications for the chlorine geodynamic cycle, Chemical Geology 126, 101-117.

Jochum, K.P., Nohl, U., Herwig, K., Lammel, E., Stoll, B., Hofmann, A.W., 2005. GeoReM: A New Geochemical Database for Reference Materials and Isotopic standards. Geostandards and Geoanalytical Research 29, 333-338.

Kelemen, P.B., 1995. Genesis of high Mg# andesites and the continental crust. Contributions to Mineralogy and Petrolog 120, 1-19.

Kessler, R., Schmidt, M.W., Ulmer, P., Pettke, T., 2005. Trace element signature of subduction-zone fluids, melts and supercritical liquids at 120-180 km depth. Nature 437, 724-727.

Klemme, S., 2004. Evidence for fluoride melts in Earth's mantle formed by liquid immiscibility. Geology 32, 441-444.

Kogarko, L.N., 1974. Role of Volatiles. In: Sørensen, H. (Ed.). The Alkaline Rocks. London: John Wiley & Sons., 474-487.

Kogarko, L.N., Ryabchikov, I.D., 1978. Volatile components in magmatic processes. Geochemistry International 15, 9-32.

Köhler, J., Konnerup-Madsen, J., Markl, G., 2008. Fluid geochemistry in the Ivigtut cryolite deposit, South Greenland. Lithos 103, 369-392.

Konnerup-Madsen, J., 1984. Compositions of fluid inclusions in granites and quartz syenites from the gardar continental rift province (South Greenland). Bulletin de Minéralogie 107, 327-340.

Konnerup-Madsen, J., Dubessy, J., Rose-Hansen, J., 1985. Combined Raman microprobe spectrometry and microthermometry of fluid inclusions in minerals from igneous rocks of the Gardar province (south Greenland). Lithos 18, 271-280.

Konzett, J., Sweeney, R.J., Thompson, A.B., Ulmer, P., 1997. Potassium Amphibole Stability in the Upper Mantle: an Experimental Study in a Peralkaline KNCMASH System to 8.5 GPa. Journal of Petrology 38, 537-568.

Krumrei, T.V., Villa, I.M., Marks, M., Markl, G., 2006. A 40Ar/39Ar and U/Pb isotopic study of the Ilímaussaq Complex, South Greeland; implications for the 40K decay constant and for the duration of magmatic activity in a peralkaline complex. Chemical Geology 227, 258-273.

Krumrei, T.V., Pernicka, E., Kaliwoda, M., Markl, G., 2007. Volatiles in a peralkaline system: Abiogenic hydrocarbons and F–Cl–Br systematics in the naujaite of the Ilímaussaq intrusion, South Greenland, Lithos 95, 298-314.

Kullerud, K., 1996. Chlorine-rich amphiboles: interplay between amphibole composition and an evolving fluid. European Journal of Mineralogy 8, 355-370.

Kushiro, I., Syono, Y., Akimoto, S., 1967. Stability of phlogopite at high pressures and possible presence of phlogopite in the Earth's upper mantle. Earth and Planetary Science Letters 3, 197-203.

Le Maitre, R.W., Bateman, P., Dudek, A., Keller, J., Lameyre Le Bas, M.J., Sabine, P.A., Schmid, R., Sørensen, H., Streckeisen, A., Woolley, A.R., Zanettin, B., 1989. A classification of igneous rocks and glossary of terms. Blackwell, Oxford.

Le Roex, A., Späth, A., Zartman, R.E., 2001. Lithospheric thickness beneath the southern Kenya Rift: implications from basalt geochemistry. Contribution to Mineralogy and Petrology 142, 89-106.

Lowenstern, J.B., 1994. Chlorine, fluid immiscibility, and degassing in peralkaline magmas from Pantelleria, Italy. American Mineralogist 79, 353-369.

Macdonald, R., Upton, B.G.J., Thomas, J.E. 1973. Potassium- and fluorine-rich hydrous phase coexisting with peralkaline granite in south Greenland. Earth Planet. Sci. Letts. 18, 217-222.

Marianelli, P., Métrich, N., Sbrana, A., 1999. Shallow and deep reservoirs involved in magma supply of the 1944 eruption of Vesuvius. Bulletin Volcanology 61, 48–63.

Markl, G., Schumacher, J.C., 1996. Spatial variations in temperature and composition of greisen-forming fluids; an example from the Variscan Triberg granite complex, Germany. Economic Geology and the Bulletin of the Society of Economic Geologists 91, 576-589.

Marks, M., Markl, G., 2001. Fractionation and Assimilation Processes in the Alkaline Augite Syenite Unit of the Ilímaussaq Intrusion, South Greenland, as Deduced from Phase Equilibria. Journal of Petrology 42, 1947-1969.

Marks, M., Vennemann, T., Siebel, W., Markl, G., 2004. Nd-, O-, and H-isotopic evidence for complex, closed-system fluid evolution of the peralkaline Ilímaussaq Intrusion, South Greenland. Geochimica Cosmochimica Acta 68, 3379-3395.

Martin, A.R., 1985. The Evolution of the Tugtutôq-Ilímaussaq Dyke Swarm, Southwest Greenland. PhD thesis, Edinburgh.

Martin, H., Smithies, R.H., Rapp, R., Moyen, J.-F., Champion, D., 2005. An overview of adakite, tonalite-trondhjemite-granodiorite (TTG), and sanukitoid: relationships and some implications for crustal evolution. Lithos 79, 1-24.

Mattsson, H.B., Oskarsson, N., 2005. Petrogenesis of alkaline basalts at the tip of a propragating rift: Evidence from the Heimaey volcanic centre, south Iceland. Journal of Volcanology and Geothermal Research 147, 245-267.

McCulloch, M.T., Gamble, J.A., 1991. Geochemical and geodynamic constraints on subduction zone magmatism. Earth and Planetary Science Letters 102, 358-374.

McDonough, W.F.M., Sun, S.S., 1995. The composition of the Earth. Chemical Geology 120, 223-253.

Metrich, N., Rutherford, M.J., 1992. Experimental study of chlorine behavior in hydrous silicic melts. Geochimica Cosmochimica Acta 56, 607-616.

Michel, A., Villemant, B., 2003. Determination of Halogens (F,Cl,Br,I), Sulfur and Water in Seventeen Geological Reference Materials. Geostandards Newsletters 27, 163-171.

Middlemost, E.A.K., 1989. Iron oxidation ratios, norms and the classification of volcanic rocks. Chemical Geology 77, 19-26.

Morgan, George, B. VI., London, D., Luedke, R.G., 1998. Petrochemistry of Late Miocene Peraluminous Silicic Volcanic Rocks from the Morococala Field, Bolivia. Journal of Petrology 39, 601-632.

Morse, S.A., Rhodes, J.M., Nolan, K.M., 1991. Redox effect on the partitioning of nickel in olivine. Geochimica et Cosmochimica Acta 55, 2373-2378.

Nelson, D.R., 1992. Isotopic characteristics of potassic rocks: evidence for the involvement of subducted sediments in magma genesis. Lithos 28, 403-420.

Newsom, H.E., 1995. Composition of the solar system, planets, meteorites, and major terrestrial reservoirs. In: Ahrens, T.J. (Ed.), Global Earth Physics, American Geophysical Union, Washington, DC, 159–189.

Nicholls, I.A., Ringwood, A.E., 1973. Effect of water on olivine stability in tholeiites and production of silica-saturated magmas in the island arc environment. Journal of Geology 81, 285-300.

Nijland, T.G., Jansen, J.B.H., Maijer, C., 1993. Halogen geochemistry of fluid during amphibolite-granulite metamorphism as indicated by apatite and hydrous silicates in basic rocks from the Bamble sector, South Norway. Lithos 30, 167-189.

Nye, C.J., Turner, D.L., 1990. Petrology, geochemistry and age of the Spurr Volcanic Complex, Eastern Aleutian Arc. Bulletin of Volcanology 52, 205-226.

O'Reilly, S.Y., Griffin, W.L., 2000. Apatite in the mantle: implications for metasomatic processes and high heat production in Phanerozoic mantle, Lithos 53, 217-232.

Pan, Y., Fleet, M.E., 1996. Rare element mobility during prograde granulite facies metamorphism: significance of fluorine. Contributions to Mineralogy and Petrology 123, 251-262.

Pauly, H., Bailey, J.C., 1999. Genesis and evolution of the Ivigtut cryolite deposit, SW Greenland. Meddelelser om Grønland, Geoscience 37, 60 p.

Peacock, S.M., 1990. Fluid processes in subduction zones. Science 248, 329-337.

Peacock, S.M., Rushmer, T., Thompson, A.B., 1994. Partial melting of subducting oceanic crust. Earth and Planetary Science Letters 121, 227-244.

Pearce, N.J.G., Leng, M.J., 1996. The origin of carbonatites and related rocks from the Igaliko Dyke Swarm, Gardar Province, South Greenland: field, geochemical and C-O-Sr-Nd isotope evidence. Lithos 39, 21-40.

Prouteau, G., Scaillet, B., Pichavant, M., Maury, R., 2001. Evidence for mantle metasomatism by hydrous silicic melts derived from subducted oceanic crust. Nature 410, 197-200.

Rollinson, H.R., Tarney, J., 2005 Adakites – the key to understanding LILE depletion in granulites. Lithos 79, 61-81.

Salvi, S., Fontan, F., Monchoux, P., Williams-Jones, A.E., Moine, B., 2000. Hydrothermal Mobilization of High Field Strength Elements in Alkaline Igneous Systems: Evidence from the Tamazeght Complex (Morocco). Economomic Geology 95, 559-576.

Schönenberger, J., Köhler, J., Markl, G., 2008. REE systematics of fluorides, calcite and siderite in peralkaline plutonic rocks from the Gardar Province, South Greenland. Chemical Geology 247, 16-35.

Schönenberger, J., Markl, G., in press. The magmatic and fluid evolution of the Motzfeldt intrusion in South Greenland: insights into the formation of agpaitic and miaskitic rocks. Journal of Petrology.

Shearer, C.K., Papike, J.J., 2005. Early crustal building processes on the Moon; models for the petrogenesis of the magnesian suite. Geochimica et Cosmochimica Acta 69, 3445-3461.

Sigvaldason, G.E., Óskarsson, N., 1986. Fluorine in basalts from Iceland. Contributions to Mineralogy and Petrology 94, 263-271.

Smith, J.V., Delaney, J.s., Hervig, R.L., Dawson, J.B., 1981. Storage of F and Cl in the upper mantle; geochemical implications. Lithos 2, 133-147.

Sørensen, H., 2001. Brief introduction to the geology of the Ilímaussaq alkaline complex, South Greenland, and its exploration history. In: Sørensen, H. (Ed.), The Ilímaussaq alkaline complex, South Greenland: status of mineralogical research with new results. Geology of Greenland Survey Bulletin, 190, 7–24.

Sørensen, H., Bohse, H., Bailey, J.C., 2006. The origin and mode of emplacement of lujavrites in the Ilimaussaq alkaline complex, South Greenland. Lithos 91, 286-300.

Stewart, J.W., 1970. Precambrian alkaline ultramafic/carbonatite volcanism at Qagssiarssuk, South Greenland. Bull. – Grønlands Geologiske Undersøgelse 84 (also Medd. Grønl. 186 (4), 70 pp.).

Tagirov, B., Schott, J., Harrichourry, J.C., Salvi, S., 2002. Experimental study of aluminum speciation in fluoride-rich supercritical fluids. Geochimica et Cosmochimica Acta 66, 2013-2024.

Tatsumi, Y., Hamilton, D.L., Nesbitt, R.W., 1986. Chemical characteristics of fluid phase from a subducted lithosphere and origin of arc magmas: evidence from high-pressure experiments and natural rocks, Journal of Volcanology and Geothermal Reasearch 29, 293-309.

Tatsumi, Y., Nakamura, N., 1986. Composition of aqueous fluid from serpentinite in the subducted slab. Geochemical Journal 30, 191-196.

Taylor, P.N., Upton, B.G.J., 1993. Contrasting Pb isotopic compositions in two intrusive complexes of the Gardar Magmatic Province of South Greenland. Chemical Geology 104, 261-268.

Taylor, S.R. & McLennan, S.M., 1985. The Continental Crust: its Composition and Evolution. Oxford: Blackwell Scientific, 312 p.

Tsuchiya, N., Suzuki, S., Kimura, J.-I., Kagami, H., 2005. Evidence for slab melt/mantle reaction: petrogenesis of Early Cretaceous and Eocene high-Mg andesites from the Kitakami Mountains, Japan. Lithos 79, 179-206.

Upton, B.G.J., 1962. Geology of Tugtutôq and neighbouring islands, South Greenland. Part I. Meddelelser om Grønland, Grønlands Geologiske Undersøgelse 169, p.60.

Upton, B.G.J., Thomas, J.E., 1980. The Tugtutôq Younger Giant Dyke Complex, South Greenland; fractional crystallization of transitional olivine basalt magma. Journal of Petrology 21, 167-198.

Upton, B.G.J., Stephenson, D., Martin, A.R., 1985. The Tugtutôq older giant dyke complex: mineralogy and geochemistry of an alkali gabbro-augite-syenite-foyaite association in the Gardar Province of South Greenland. Mineralogical Magazine 49, 623-642.

Upton, B.G.J., Emeleus, C.H., 1987. Mid-Proterozoic alkaline magmatism in southern Greenland: the Gardar province. From: Fitton, J.G. & Upton, B.G.J. (Eds), Alkaline Igneous Rocks. Geological Society Special Publication No. 30, 449-471.

Upton, B.G.J., 1996. Anorthosites and trocyolites of the Gardar magmatic province. *In* : Petrology and Geochemistry of Magmatic Suites of Rocks in Continental and Oceanic Crusts. A volume dedicated to Professor Jean Michot, D. Demaifffe (ed.), 19-34. Université Libre de Briuxelles, Royal Museum, for Central Africa (Tevuren).

Upton, B.G.J., Emeleus, C.H., Heaman, L.M., Goodenough, K.M, Finch, A.A., 2003. Magmatism of the mid-Proterozoic Gardar Province, South Greenland: chronology, petrogenesis and geological setting. Lithos 68, 43-65.

Upton, B.G.J., Craven, J.A., Kirstein, L.A., 2006. Crystallisation of mela-aillikites of the Narsaq region, Gardar alkaline province, south Greenland and relationships to other aillikitic–carbonatitic associations in the province. Lithos 92, 300-319.

Veksler, I., 2004. Liquid immiscibility and its role at the magmatic-hydrothermal transition: a summary of experimental studies. Chemical Geology 210, 7-31.

Villemant, B., Boudon, G., 1999. H_2O and halogen (F, Cl, Br) behaviour during shallow magma degassing processes. Earth and Planetary Science Letters 168, 271-286.

Villemant, B., Mouatt, J., Michel, A., 2008. Andesitic magma degassing investigated through H2O vapour–melt partitioning of halogens at Soufrière Hills Volcano, Montserrat (Lesser Antilles). Earth and Planetary Science Letters 269, 212-229.

Watson, E.B., 1980. Apatite and phosphorus in mantle source regions: an experimental study of apatite/melt equilibria at pressures to 25 kbar. Earth and Planetary Science Letters 51, 322-335.

Webster, J.D., 1990. Partitioning of F between H_2O and CO_2 fluids and topaz rhyolite melt. Implications for mineralizing magmatic-hydrothermal fluids in F-rich granitic systems. Contributions to Mineralogy and Petrology 104, 424-438.

Williams-Jones, A.E., Samson, I.M., Olivio, G.R., 2000. The genesis of hydrothermal fluorite-REE deposits in the Gallinas Mountains, New Mexico. Economic Geology and the Bulletin of the Society of Economic Geologists 95, 327-341.

Wood, S.A., 2003. The geochemistry of rare earth elements and ytttrium in geothermal waters. In: Simmons, S.F., Graham, I. (Eds.), Volcanic, geothermal, and ore-forming fluids; rules and witnesses of processes within the Earth. Special Publication (Society of Economic Geologists (U.S.) 10, 133-158.

Wyllie, P.J., 1984. Sources of granitoid magmas at convergent plate boundaries. Physics of The Earth and Planetary Interiors 35, 12-18.

Yogodzinski, G.M., Volynets, O.N., Koloskov, A.V., Seliverstov, N.I., Matvenkov, V.V., 1994. Magnesian andesites and the subduction component in a strong calc-alkaline series at Piip volcano, Far Western Aleutians. Journal of Petrology 35, 163-204.